Biotechnological production of aromatic amines and aromatic alcohols by recombinant *Escherichia coli* strains

Von der Fakultät Energie-, Verfahrens- und Biotechnik der Universität Stuttgart
zur Erlangung der Würde eines Doktors der Naturwissenschaften (Dr. rer. nat.)
genehmigte Abhandlung

Vorgelegt von
Behrouz Mohammadi Nargesi
aus Masjed-Soleiman, Iran

Hauptberichter: Prof. Dr. Georg A. Sprenger
Mitberichter: apl. Prof. Dr. Martin Siemann-Herzberg

Tag der mündlichen Prüfung: 01/02/2019

Institut für Mikrobiologie der Universität Stuttgart
2019

Dedicate to my family...

and…

Who give me love in my life…

“Two there are who are never satisfied — the lover of the world and the lover of knowledge.”

(Rumi)

This thesis is based on experimental work carried out under supervision of Prof. Dr. Georg A. Sprenger at the Institute of Microbiology, University of Stuttgart, Germany during the years 2014-2018.

Parts of this work have already been published:

Peer-reviewed publications

I. **Mohammadi Nargesi, B.**, Sprenger, G. A., & Youn, J.-W. (2019). Metabolic Engineering of *Escherichia coli* for para-Amino-Phenylethanol and para-Amino-Phenylacetic Acid Biosynthesis. Frontiers in Bioengineering and Biotechnology, 6, 201.

II. **Mohammadi Nargesi, B**., Trachtmann, N., Sprenger, G. A., & Youn, J.-W. (2018). Production of p-amino-l-phenylalanine (l-PAPA) from glycerol by metabolic grafting of *Escherichia coli*. Microbial Cell Factories, 17(1), 149.

Conference contributions - lectures

I. **Mohammadi Nargesi B,** Sprenger G, Youn J-W. Metabolic grafting of *Escherichia coli* for the biosynthesis of aromatic amines. Annual Conference VAAM 2018, 18 April 2018 , Wolfsburg, Germany.

II. **Mohammadi Nargesi B,** Youn J-W, Sprenger G. Biosynthesis of 2-Phenylethanol (rose-like odor) by pathway engineering in *Escherichia coli*. The 18th International and Iranian Congress of Microbiology, university of Tehran medicine, Tehran. 2017.

III. **Mohammadi Nargesi B,** Sprenger G, Youn J-W. Metabolic engineering of *Escherichia coli* for synthesis of 2-(4-AminoPhenyl) Ethanol (PAPE). Annual Conference 2017 of the Association for General and Applied Microbiology (VAAM), Wurzburg, Germany.

IV. Youn J-W, **Mohammadi Nargesi B,** Sprenger G. Metabolic engineering of *Escherichia coli* for production of p-Amino phenylalanine (PAPA). Annual Conference of the Association for General and Applied Microbiology (VAAM), 2016, Jena, Germany

Conference contributions - Posters

I. **Mohammadi Nargesi B**, Youn J-W, Sprenger G. Metabolic Grafting of *Escherichia coli* for the biosynthesis of aromatic amines. Metabolic Engineering 12 (AIChE), June 24-28, 2018, Munich, Germany.

Erklärung:

I hereby declare that I have written the submitted dissertation myself and in this process have used no other sources or materials than those indicated.

Hiermit erkläre ich, dass ich die beigefügte Dissertation selbständig verfasst und keine anderen als die angegebenen Hilfsmittel genutzt habe.

Stuttgart, 11 July 2018

Behrouz Mohammadi Nargesi

Acknowledgment

First and foremost, I would like to express my deepest thanks and appreciation to my supervisor (Doktorvater) Prof. Dr. Georg A. Sprenger, for giving me the opportunity to join his research group at Institute of Microbiology, University of Stuttgart, Germany. He is very kind, supportive, and expert with great knowledge in various research fields especially in Microbiology and Biotechnology (Metabolic engineering). His supervision was very beneficial to me and helped me to learn how to approach the purposes in my research study and managing a team research work. Many thanks for your helpful advices, extraordinary supervision, endless patience and kind support.

I am very much grateful to my closest co-author Dr. Jung-Won Youn who did the supervision of my research work in the lab. His excellent guidance and professional suggestions helped me to grow as a young researcher. Many thanks for all your support, ideas, guidance, patience and consultation during my PhD study.

I would like to express my deepest thanks to my co-examiner, apl. Prof. Dr. Martin Siemann-Herzberg at Institute for Biochemical Engineering, University of Stuttgart for his great suggestions and ideas never-ending friendly and helpful nature.

I would like to thank Prof. Dr.-Ing. Ralf Takors for his kind cooperation to carry out fed-batch cultivation (fermentation) at the Center of Bioprocess Engineering.

I am grateful to Prof. Dr. Bernhard Hauer at Institute of Biochemistry and Technical Biochemistry, University of Stuttgart for the inmost cooperation in LC-MS analysis.

A special thank goes to Dr. Hamid Rajabi Memari (Ph.D Committee in Iran) for his kind and outstanding advices and the being more than an advisor.

I would like to express my sincere thanks to Dr. Katrin Gottlieb and Dr. Natalie Trachtmann, for kindly providing me with the required strains and plasmids in my research work.

Special thanks for Dr. Bernd Nebel for his guidance in the experimental work on LC-MS analysis. Many thanks to Mr. Alexander Dietrich for his support in the planning and implementation of fed-batch fermentation at the Center of Bioprocess Engineering.

I would like to thank Dr. Jana Hoffmann at Institute of Industrial Genetics, University of Stuttgart for kindly providing *Saccharomyces cerevisiae W3118* strain. Special thanks to my dear friend Dr. Kambiz Morrabi for his helpful advices and guidance before and after stay in Germany, We have shared many discussions, debates, and incredible soccer times together.

I would like to thank all of the administrators and technical staff, Mrs. Kristina Kauffmann, Mrs. Simone Reinhardt, Mr. Olaf Dickel, Mr. Janosch Gröning, for all their kind support.

My warm gratitude goes also to my dear friends and colleagues, Jakob, Marcel, Florian, Emma, Tony, Erik, Wolf and Mathias for creating a lovely working atmosphere and for their valuable advices, delightful discussions, very enjoyable and informative conversations. Special thanks also to dear friend Matthias Schapfl for helping me in FPLC analysis and preparative isolation of PAPA.

I thank funding sources, scholarship program for study provided by the ministry of science, research and technology (IRAN) and Ministerium für Wissenschaft und Kunst (MWK), Baden-Württemberg, Germany.

In particular, I would like to thank my parents, Katayoun and Alinaz. I am grateful to you for what I have become and for your eternal love and care! Many thanks also go to my brothers and sister, Behnam, Iman and Sahar, and their families. You all bring happiness, wisdom in my life and, although life keeps us so busy all the time.

Last but not least, I thank my best friend and my everlasting love, Noushin (Banou), who supported me in all decisions with a lot of patience and has always given me strong backing! There are no words that could possibly explain your sacrifices through the tough times of my PhD study. Many thanks for proof-reading my thesis at the end. I am really lucky and happy to have you nearby!

Table of Contents

List of Figures

List of Tables

Symbols and Abbreviations

Symbols	Definition
4-APA	*para*-amino-phenylacetic acid
ADC	4-amino-4-deoxychorismic acid
ADP	*para*-amino-deoxy prephenate
AmpR	Ampicillin resistance
APP	*para*-amino-phenylpyruvate
AroB	DHQ synthase
AroF	DAHP synthase; inhibited by tyrosine
AroG	DAHP synthase; inhibited by phenylalanine
AroH	DAHP synthase; inhibited by tryptophan
AroL	Shikimate kinase
AspC	Aspartate aminotransferase
ATP	Adenosine triphosphate
Bp	Base pair
BSA	Bovine serum albumin
C.gl.	*Corynebacterium glutamicum*
° C	degrees Celsius (temperature unit)
Da	Dalton
DAHP	3-deoxy-D-arabino-heptulosonate-7-phosphate
DHQ	3-dehydroquinic acid (3-dehydroquinic acid)
DHS	3-dehydroshikimic acid
DMSO	Dimethyl sulfoxide
DTT	Dithiothreitol
E4P	Erythrose-4-phosphate
EDTA	Ethylenediaminetetraacetate
EntB	Isochorismatase from Escherichia coli
g	grams (mass unit)
h	hour (time unit)
HPLC	High performance / high pressure liquid chromatography
IPTG	Isopropyl β-D-1-thiogalactopyranoside
Kan	Kanamycin
KM	Michaelis constant (unit = [M])
LB	Luria-Bertani
L-PAPA	*para*-amino-L-phenylalanine
M	Molar
MM	Minimal medium
NAD	Nicotine-adenine dinucleotide (oxidized form)
NADH	Nicotine adenine dinucleotide (reduced form)
OD	Optical density at a specific wavelength
PABA	*para* -aminobenzoic acid
PabAB	4-amino-4-deoxychorismic acid (ADC) synthase
PAGE	polyacrylamide gel electrophoresis
PapB	4-amino-4-deoxy-chorismate mutase
PapC	4-amino-4-deoxyprephenate dehydrogenase
PAPE	*para* -amino-phenylethanol
PCR	Polymerase chain reaction
PEP	Phosphoenol pyruvate

Symbols	Definition
DAHP	3-deoxy-D-arabino-heptulosonate-7-phosphate
DHQ	3-dehydroquinic acid (3-dehydroquinic acid)
DHS	3-dehydroshikimic acid
DMSO	Dimethyl sulfoxide
DTT	Dithiothreitol
E4P	Erythrose-4-phosphate
EDTA	Ethylenediaminetetraacetate
EntB	Isochorismatase from Escherichia coli
pps	Phosphoenolpyruvate synthetase
RP	Reversed phase
S3P	Shikimic acid 3-phosphate
SDS	Sodium dodecyl sulfate
TAE	TRIS acetate EDTA
TEMED	Tetramethylethylenediamine
TFA	Trifluoroacetic acid
TyrA	chorismic acid mutase / prephenic acid dehydrogenase
TyrB	Tyrosine aminotransferase
pps	Phosphoenolpyruvate synthetase
RP	Reversed phase
S3P	Shikimic acid 3-phosphate
SDS	Sodium dodecyl sulfate
2-PE	2-Phenylethanol
Tyrosol	2-(4-Hydroxyphenyl)ethanol
Hydroxytyrosol	3,4-dihydroxyphenylethanol
4-HPA	4-Hydroxyphenyl acetic acid
3,4-DHPA	3,4-Dihydroxyphenyl acetic acid
PAL	Phenylacetaldehyde
PAAL	*para*-aminophenylacetaldehyde
PAPE	*para* -aminophenylethanol
4-APA	*para* -aminophenylacetic acid
4-ACA	4-amino cinnamic acid
4-HACA	4-amino hydroxycinnamic acid
PP	Phenylpyruvate
Aro10	ThDP-Ketoacid decarboxylase
FeaB	Phenylacetaldehyde dehyrogenase
YahK	Aldehyde reductase
CmR	Chloramphenicol resistance
Kan R	Kanamycine resiatnace
PPP	Penthose phosphate pathway
DNA	Deoxyribonucleic acid
ESI	Electrospray ionization
et al.	*et alia*
FPLC	Fast protein liquid chromatography
F6P	Fructose 6-phosphate
G6p	Glucose 6 phispahte
FBP	Fructose 1,6 bisphosphate
Glu	Glucose
Gly	Glycerol
HPLC	High-performance liquid chromatography

Symbols	Definition
m/z	mass-to-charge ratio
NAD^+	Nicotinamide adenine dinucleotide
$NADP^+$	Nicotinamide adenine dinucleotide phosphate
MS	mass spectrometry
OD_{600nm}	Optical density at a wavelength of 600 nm.
2D-gel	Two-Dimensional Gel Electrophoresis
PCR	Polymerase chain reaction
PEP	Phosphoenolpyruvate
E4P	Erythrose 4-phosphate
PO2	Oxygen
PTS	phosphotransferase system
RT	Room temperature
SDS	Sodium dodecyl sulfate
TAE-Buffer	Tris, Acetate, EDTA buffer
UV	Ultraviolet
V/V	Volume per Volume
g	gram
mg	miligram
mM	milimolar
%	Percentage
Y	Yield
$g\ l^{-1}$	gram per liter
l	liter
EMP Pathway	Embden–Meyerhof–Parnas
EDP Pathway	Entner-Doudoroff pathway
C source	Carbon source
DHAP	dihydroxyacetone phosphate
GA3P	glyceraldehyde-3-phosphate
TCA	tricarboxylic acid cycle
acetyl-CoA	Acetyl coenzyme A
L-Trp	L-tryptophan
L-Tyr	L-tyrosine
L-Phe	L-phenylalanine
L-Asp	L-aspartic acid
4-HPP	4-hydroxyphenylpyruvate
3,4-DHPP	3,4-Dihydroxyphenylpyruvate
3,4-DPAL	3,4-Dihydroxyphenyacetaldehyde
TyrR	Transcriptional regulatory protein TyrR
TrpR	Tryptophan operon repressor

Summary

Aromatic amine (AA) are an important group of industrial chemicals which are widely used for technical and pharmaceutical applications and described as the building block of drugs (Bedair et al. 2006; Jobdevairakkam and Velladurai 2009; Sacco and Bientinesi 2016), antibiotics, plastics and aromatic polymers (Arora 2015; Masuo et al. 2016; Tsuge et al. 2016; Kawasaki et al. 2018). In addition, aromatic alcohols, as other valuable compounds, are widely used in manufacturers of perfumes, cosmetics, and foods, and pharmaceutical industry (Etschmann et al. 2002; Miró-Casas et al. 2003; Bai et al. 2014). Most of the AAs and aromatic alcohols are chemically synthesized from petroleum sources and considered as "unnatural", which are inappropriate to make cosmetic, drugs or food ingredient, thereby natural microbial biosynthesis of these valuable compounds in *E.coli* would be an alternative approach.

In the first part of this study, a de-novo biosynthesis pathway was established for high titer production of three aromatic amines, *para*-amino-L-phenylalanine (L-PAPA), *para*-amino-phenylethanol (PAPE) and *para*-amino-phenylacetic acid (4-APA) from glucose/glycerol via genetic modification of the shikimate pathway in recombinant *E. coli* (Mohammadi et al. 2018 and 2019). To generate a platform strain for L-PAPA production from shikimate pathway, the genes *pabAB* from *Corynebacterium glutamicum* (Kozak 2006), *papB* and *papC* from *Streptomyces venezuelae* (Blanc et al. 1997; He et al. 2001; Mehl et al. 2003) were heterologously overexpressed from plasmid in *E. coli* FUS4.7R (Gottlieb et al. 2014). Then, the metabolic flux was directed to PAPE and 4-APA production via overexpression of *aro10* from *Saccharomyces cerevisiae* (Kneen et al. 2011; Vuralhan et al. 2003 and 2005) and both *aro10* and *feaB* in *E. coli* FUS4BCR, respectively. The engineered *E. coli* strains were cultured in the shake-flasks with fed batch condition and investigated for L-PAPA, PAPE and 4-APA production by HPLC and LC-MS. In the simple shake flask experiments, the plasmid based strain produced L-PAPA as high as 0.534 ± 0.024 g l^{-1} from 5 ± 0.24 g l^{-1} glycerol. Also, introduction of *aro10* and *yahK* in L-PAPA producing strain resulted in 0.526 ± 0.025 g l^{-1} PAPE. Furthermore, by introducing *feaB* into the PAPE- producing strain, 4-APA was obtained with a titer of 0.458 ± 0.014 g l^{-1}. Last but not least, by further strain improvement and optimizing growth condition via glucose/glycerol feed strategy, an increasing titer of L-PAPA, PAPE and 4-APA approximately 5.5 ± 0.4 g l^{-1}, 2.5 ± 0.15 g l^{-1} and 3.4 ± 0.3 g l^{-1} were obtained, respectively. In subsequent fed-batch cultivation with a final volume of 12.2 l and the carbon

sources glycerol, a final L-PAPA-titer of 16.8 g l^{-1} was obtained. This equals a yield of 0.13 L-PAPA / glycerol (g g^{-1}) and a space-time-yield of 0.22 g l^{-1} h^{-1} L-PAPA formation over the whole process.

Furthermore, a de-novo biosynthesis pathway for the production of 2-Phenylethanol (2-PE)/tyrosol from glucose with genetically engineered *E. coli* strains without additional L-phenylalanine/ L-tyrosine as supplement was demonstrated. Starting from chorismate, which is the direct precursor of phenylpyruvate (PP)/ 4-Hydroxyphenylpyruvate (4-HPP), an artificial Ehrlich biosynthesis pathway was created (Etschmann et al. 2002) toward 2-PE or tyrosol. To generate a platform strain for production of 2-PE and tyrosol from shikimate pathway, the genes *pheA* or *tyrA* encoding proteins chorismate mutase/prephenate dehydratase or prephenate dehydrogenase (feedback resistance variant, Rüffer et al. 2004; Gottlieb et al. 2014), respectively, were cloned and subsequently overexpressed from plasmid in *E. coli*. In the next step, the metabolic flux was directed to 2-PE and tyrosol production via overexpression of *aro10* encoding phenylpyruvate decarboxylase from *S. cerevisiae*. Furthermore, in order to enhance the flux toward downstream 2-PE/tyrosol pathway, the relevant genes of three rate limiting steps including *aroF*, *aroB* and *aroL* were subcloned and overexpressed from plasmid. Upon simple batch cultivation, these strains separately yielded 369 ± 25 mg l^{-1} 2-PE and 437 ± 33 mg l^{-1} tyrosol from 4.5 ± 0.21 g l^{-1} glucose. Final titer in the shake flask was further improved through glucose fed-batch fermentation to 1.75 ± 0.12 g l^{-1} 2-PE and 1.68 ± 0.19 g l^{-1} tyrosol. The subsequent significant enhancement of 2-PE/tyrosol production occurred through employing in situ product removal (ISPR) techniques including two-phase extraction by different organic compounds (Etschmann et al. 2002; Rüffer et al. 2004; Schügerl and Hubbuch 2005; Hu and Xu 2011; Chreptowicz et al. 2018). In subsequent glucose-limited fed-batch cultivation with a benchtop bioreactor system (0.75 l), a final 2-PE and tyrosol-titer of 3.1 g l^{-1} and 3.6 g l^{-1} reached with a yield and a space-time-yield of 0.07 g g^{-1} and 0.03 g l^{-1} h^{-1} for 2-PE and 0.08 g g^{-1} and 0.04 g l^{-1} h^{-1} for tyrosol, respectively. These works have successfully demonstrated the possibility of synthesizing of several invaluable fine chemicals in whole-cell system using plasmid based-*E.coli* strains. In addition, the titter and yield previously reported in the biosynthesis of aromatic amines (L-PAPA, PAPE or 4-APA) or even aromatic alcohols (2-PE or tyrosol) have been significantly improved in this study.

Zusammenfassung

Aromatische Amine (AA) sind eine wichtige Gruppe von Industriechemikalien, die für viele technische und pharmazeutische Anwendungen genutzt werden. Diese können als Bausteine für die Herstellung von Medikamenten (Bedair et al. 2006; Jobdevairakkam und Velladurai 2009; Sacco und Bientinesi 2016), Antibiotika, Kunststoffen und aromatischen Polymeren genutzt werden (Arora 2015; Masuo et al., 2016; Tsuge et al . 2016; Kawasaki et al. 2018).

Darüber hinaus werden aromatische Alkohole; in Parfums, Kosmetika, Nahrungsmitteln und Pharmazeutika verwendet (Etschmann et al. 2002; Miró-Casas et al. 2003; Bai et al. 2014). Die meisten AA und aromatischen Alkohole werden chemisch aus erdölbasierten Rohstoffen synthetisiert. Diese AA sind ungünstig für die Herstellung von Kosmetika, Arzneimitteln oder Nahrungsmittelbestandteilen. Daher ist eine natürliche mikrobielle Biosynthese dieser wertvollen Verbindungen mit *E. coli* ein attraktiver Ansatz. Im ersten Teil dieser Arbeit wurde ein *De-novo*-Biosyntheseweg für die Produktion von drei aromatischen Aminen, *para*-Aminophenylalanin (L-PAPA), *para*-Aminophenylethanol (PAPE) und 4-Aminophenylessigsäure (4-APA) aus Glukose/Glyzerin durch genetische Modifikation in rekombinanten *E. coli* etabliert (Mohammadi et al. 2018 and 2019). Zur Erzeugung eines Plattformstamms für die L-PAPA-Produktion wurden die Gene *pabAB* aus *Corynebacterium glutamicum* (Kozak 2006; Stolz et al. 2007), *papB* und *papC* aus *Streptomyces venezuelae* (Blanc et al. 1997; He et al. 2001; Mehl et al. 2003) in *E. coli* FUS4.7R heterolog mittels Plasmiden überexprimiert (Gottlieb et al. 2014). In *E. coli* FUS4BCR wurde anschließend der metabolische Fluss durch Überexpression der Phenylpyruvat-Decarboxylase (*aro10)* aus *Saccharomyces cerevisiae* (Vuralhan et al. 2003 und 2005; Kneen et al. 2011) oder durch *aro10* mit *feaB* (Phenylacetaldehyd-Dehydrogenase) zur Produktion von PAPE und 4-APA optimiert. Die gentechnisch veränderten *E. coli*-Stämme wurden in Schüttelkolben mit Fed-Batch-Bedingungen kultiviert und mittels HPLC und LC-MS auf l-PAPA, PAPE und 4-APA-Produktion untersucht. In den einfachen Schüttelkolben-Experimenten erzeugte der l-PAPA produzierende Stamm 0,534 ± 0,024 g l^{-1} l-PAPA aus 5 ± 0,24 g l^{-1} Glyzerin. Außerdem führte die zusätzliche Einführung von *aro10* und *yahK* (Aldehyd-Reduktase) in den l-PAPA-produzierenden Stamm zu 0,526 ± 0,025 g l^{-1} PAPE. Darüber hinaus wurde durch die Überexpression von *feaB* in den PAPE-produzierenden Stamm ein Titer von 0,458 ± 0,014 g l^{-1} 4-APA ermöglicht. Schließlich wurde durch weitere Stammverbesserungen und Optimierungen der Wachstumsbedingungen mit Glukose/Glyzerol- Zufütterung der Titer

von l-PAPA, PAPE und 4-APA auf etwa 5,5 ± 0,4 g l^{-1}, 2,5 ± 0,15 g l^{-1} und 3,4 ± 0,3 g l^{-1} erhöht. Bei anschließender Fed-Batch-Kultivierung mit einem Endvolumen von 12,2 L mit Glyzerin als Kohlenstoffquelle wurde ein End-Titer von 16,7 g l^{-1} l-PAPA erhalten. Dies entspricht einer Ausbeute von 0,13 l-PAPA / Glycerin (g g^{-1}) und einer Raum-Zeit-Ausbeute von 0,22 g l^{-1} h^{-1} l-PAPA über den gesamten Prozess.

Darüber hinaus wurde ein *De-novo* Biosyntheseweg für die Produktion von 2-Phenylethanol (2-PE)/Tyrosol aus Glucose mit gentechnisch veränderten *E. coli*-Stämmen basierend auf der Plasmidexpression konstruiert. Ausgehend von Chorismat, dem direkten Vorläufer von Phenylpyruvat (PP)/ 4-Hydroxyphenylpyruvat (4-HPP), wurde ein künstlicher Ehrlich-Biosyntheseweg in Richtung 2-PE oder Tyrosol generiert (Etschmann et al. 2002). Um einen Plattformstamm für die Produktion von 2-PE und Tyrosol aus dem Shikimatweg zu erzeugen, wurde die Gene *pheA* oder *tyrA* kodierende Proteine Chorismatmutase/Prephenatdehydratase oder Prephenatdehydrogenase (Rüffer et al. 2004; Gottlieb et al. 2014) zusätzlich in *E. coli* überexprimiert. Im nächsten Schritt wurde der metabolische Fluss durch die Überexpression von *aro10* in die 2-PE- und Tyrosol-Produktion gelenkt. Um den Fluss in Richtung des stromaufwärts gelegenen 2-PE/Tyrosol-weges zu erhöhen, wurden die relevanten Gene der drei geschwindigkeitsbegrenzenden Schritte im Shikimatweg *aroF*, *aroB* und *aroL*, überexprimiert. Nach Batch-Kultivierung ergaben diese Stämme 369 ± 25 mg l^{-1} 2-PE und 437 ± 33 mg l^{-1} Tyrosol aus 4,5 ± 0,21 g l^{-1} Glukose. Der Endtiter im Schüttelkolben wurde durch eine Glukose-Fed-Batch-Fermentation auf 1,75 ± 0,12 g l^{-1} 2-PE und 1,68 ± 0,19 g l^{-1} Tyrosol erhöht. Eine anschließende signifikante Steigerung der 2-PE / Tyrosol-Produktion erfolgte durch Anwendung eines *In-situ*-Verfahrens zur Produktentfernung (ISPR). Diese Zweiphasenextraktion wurde mit verschiedenen organischen Verbindungen untersucht (Etschmann et 2002; Schügerl und Hubbuch 2005; Astumi et al. 2008; Hu und Xu 2011). In einer anschließenden Glucose-limitierten Fed-Batch-Kultivierung in einem Benchtop-Bioreaktorsystem (0,75 l) wurde ein Endtiter von 3,1 g l^{-1} 2-PE und 3,6 g l^{-1} Tyrosol mit einer Ausbeute und einem Raum-Zeit-Verhältnis von 0,07 g g^{-1} und 0,03 g 1^{-1} h^{-1} für 2-PE bzw. 0,08 g g^{-1} bzw. 0,04 g l^{-1} h^{-1} für Tyrosol erreicht. Diese Arbeit zeigt, dass die Synthese (im Gramm-Maßstab) von aromatischen Aminen (bzw. l-PAPA, PAPE oder 4-APA) und aromatischen Alkoholen (bzw. 2-PE oder Tyrosol) mit rekombinanten *E. coli* Stämmen möglich ist.

1. Introduction

1.1 Introduction to metabolic engineering

Synthetic biology (Hobom 1980), as part of modern biology with great potential application is expected to bring fundamental changes to the world around us, such as environmental conservation, high-quality production, and human and medical health issues (Yeh and Lim 2007; Andrianantoandro et al. 2006; Benner and Sismour 2008). Briefly, synthetic biology as a powerful tool improves abilities to design, build or redesign natural biological systems using molecular biology tools (Serrano 2007; Kirschner 2007; Benner and Sismour 2008). Metabolic engineering (Bailey 1991), as part of Synthetic biology, is not only the introduction and transfer of several genes into a cell, but also plays an important role in balancing processes such as how the genes are regulated, overexpressed or under expressed in the new pathway (Khosla and Keasling 2003). In addition, metabolic engineering involves diverse concerns such as the directing flux from central metabolic pathways to the downstream and biosynthetic pathway for the target product. As such, the control of recombinant gene expression, and metabolic flux balances, both within the heterologous metabolic pathway and between the pathway and the host's native metabolism is a very important issue in the metabolic engineering process (Bailey 1991; Khosla and Keasling 2003; Witze 2013). These innovations have offered a variety of applications in metabolic engineering microorganisms aiming to give them new abilities which are not inherent to the microorganism (Bailey 1991). Today, many studies have been conducted on the most commonly known microorganisms, such as *Escherichia coli, Corynebacterium glutamicum* and *Saccharomyces cerevisiae* and modified them for production various components such as aromatic amino acids from renewable resources (Ikeda 2006; Sprenger 2007a; Patnaik et al. 2008; Khamduang et al. 2009; Santos et al. 2012; Juminaga et al. 2012; Wang et al. 2013; Gottlieb et al. 2014; Liu et al. 2014; Weiner et al. 2014; Doroshenko et al. 2015; Lee and Wendisch 2016), biofuels from renewable resources (Kalscheuer et al. 2006; Antoni et al. 2007; Atsumi et al. 2008a; Fortman et al. 2008; Yim et al. 2011; Buijs et al. 2013; Burgard et al. 2014), the conversion of raw materials into bulk and fine chemicals (Koma et al. 2012; Cheng and Tao 2012; Baumgärtner et al. 2013 a and b; Kim et al. 2014 a,b and c; Gottlieb et al. 2014; Li et al. 2018), therapeutically useful products such as antimalarial drug precursor artemisinic acid, amorphadiene (Ro et al. 2006; Tsuruta et al. 2009; Paddon and

Keasling 2014; Wang et al. 2014), Taxol (Huang et al. 2001; Engels et al. 2008; Ajikumar et al. 2011), Levodopa (Min et al. 2015), Vitamin E compound δ-Tocotrienol (Albermann et al. 2008; Ghanegaonkar et al. 2013) and antitumor drugs violacein and deoxyviolacein (Rodriguez et al. 2012; Rodriguez et al. 2013; Fang et al. 2015). Also, "metabolic grafting" has been proposed instead of metabolic engineering (Sprenger 2007b), which refers to an ancient horticultural technique which can be traced back before 2000 BC to ancient China. In this technique, one or more stems of plant with leaf buds are joined on a single mother plant to grow as a unit plant (Meng et al. 2012). Relying on this definition, therefore, transferring a part of the pathway from natural host to heterologous host to achieve a recombinant target is also a kind of grafting in microbes. The examples given above are just a few of the research that show the implementation of "metabolic grafting" (metabolic engineering) and demonstrate the ability of synthetic biology to provide an alternative to traditional methods in heterologous hosts such as *E. coli* or *S. cerevisiae*.

1.2 *Escherichia coli (E. coli)* as host

Escherichia coli (E. coli) is a gram-negative, rod-shaped, facultative anaerobic and coliform bacterium belonging to the Enterobacteriaceae family (Madigan et al. 2012). *E. coli* K12 strains (Blattner et al. 1997) are frequently employed in molecular biology as both a tool and a model organism due to easy and fast growing, well-characterized genome, comprehensive systemic understanding of the metabolism and availability of tools for genetic manipulation, and therefore are of particular interest (Blattner et al. 1997; Hayashi et al. 2006). *E. coli* is undemanding and is characterized by rapid growth on complex nutrient media (Swartz 1996). As a facultative anaerobic bacterium, *E. coli* can grow under aerobic and anaerobic conditions (Lin 1976). Because of these properties and the molecular genetic methods available, *E. coli* is among the most frequently used bacterial hosts for biotechnological production of pharmaceuticals and fine chemicals (Huang et al. 2012). The majority of fine chemicals are produced from fossil resources through costly and non-environmentally friendly technologies. Today, due to concerns about negative environmental impacts of fossil-based resources, biotechnological based production become as a potential alternative to overcome these issues (Bozell and Petersen 2010). Microbial production provides unique advantages and is increasingly being used to produce fine and bulk chemicals for the food, pharmaceutical or energy sources (Liese and Villela1999; Schmid et al.

2001; Ishige et al. 2005; Tao and Xu 2009). Several molecules industrially produced by employing recombinant *Escherichia coli* such as insulin (FDA Drug Bull. 1982), growth hormone (GH), glucagon, Interferon (Jozala et al. 2016; Swartz 1996), 1,3-propanediol (Tong and Cameron 1992; Nakamura and Whited 2003), 1,4- Butanediol (Burgard et al. 2014) and amino acids (Lee et al. 2007; Gottlieb et al. 2014; Weiner et al. 2014; Chen and Zeng 2017). There is a wide and growing global biotechnology market which has risen from 54 billion USD in 1999 to 500 billion USD in 2011 (Bruschi et al. 2011) and is expected to reach 727.1 billion USD by 2025 with a growth rate of 7.4% (Grand View Research, Inc 2017).

1.3 Transport and metabolism of glycerol/glucose in *E. coli*

Glucose is a preferred carbon source for *E. coli* and is one of the sugars that are transported and phosphorylated via the PEP-dependent phosphotransferase system (PTS) (Postma et al. 1993). The glucose uptake is coupled to the phosphorylation of the substrate. The phosphate group is derived from phosphoenolpyruvate (PEP) and is transferred to the glucose molecule through a coupled enzymatic cascade. The activated molecule glucose-6-phosphate (G6P) can be diverted into the hexose monophosphate pathway for the production of NADPH and ribose-5-phosphate, or glycolysis pathway (Embden–Meyerhof–Parnas (EMP pathway)) (Figure **1-1**). The degradation of glucose can occur via three different degradation pathways. The most important is the Embden-Meyerhof-Parnas pathway (EMP), followed by the hexose monophosphate pathway (or Pentose Phosphate Pathway (PPP)) and the Entner-Doudoroff pathway (EDP) (Kim and Gadd 2011). For EDP, however, it has been shown that this pathway is usually not active on glucose as a C source in *E. coli* (Wang et al. 1958). In glycolysis or EMP, G6P is first isomerized to fructose-6-phosphate (F6P) which is then phosphorylated with adenosine triphosphate (ATP) to yield fructose-1,6-bisphosphate (FBP). FBP is then cleaved via the aldolase into dihydroxyacetone phosphate (DHAP) and glyceraldehyde-3-phosphate (GA3P), which is further metabolized to PEP and pyruvate in several steps and then into the TCA cycle via oxaloacetate and acetyl-CoA Cycle (Figure **1-1**) (Kim and Gadd 2011). PPP is important for the delivery of intermediates (erythrose-4-phosphate (E4P) and ribose-5-phosphate) and redox cofactors (NADPH) for the synthesis of biomolecules. *E. coli,* like many other bacteria, prefers glucose as carbon and energy source due to supporting faster growth rate compared to other sugars (Bren et al. 2016). Glucose as ideal carbon source is widely used in the microbial production of several

fine chemicals in *E.coli* (Atsumi et al. 2008b; Koma et al. 2012; Satoh et al. 2012b; Kim et al. 2014b; Masuo et al. 2016; Tateyama et al. 2016; Li et al. 2018; Liu et al. 2018). Glycerol on the other hand, has become a favorable carbon source for the production of most valuable fine chemicals (da Silva et al. 2009; Almeida et al. 2012; Khanna et al. 2012; Gottlieb et al. 2014; Weiner et al. 2014; Sprenger 2017). Glycerol like other uncharged small molecules can enter the cell either by passive diffusion (Richey and Lin 1972) or through *E.coli* glycerol facilitator, GlpF (Heller et al. 1980). In the *E. coli*, there are two independent pathways in the glycerol metabolism leading synthesis of DHAP, subsequently can enter into central metabolism pathway (Figure **1-1**). Glycerol can be utilized by *E.coli* through phosphorylation (by ATP-dependent glycerol kinase (encoded by *glpK*; Zwaig et al. 1970) to glycerol-3-phosphate (G3P). G3P can then be oxidized to dihydroxyacetone phosphate (DHAP) either by an aerobic glycerol-3-phosphate dehydrogenase encoded by *glpD* (Weiner and Heppel 1972) or by an anaerobic glycerol-3-phosphate dehydrogenase encoded by *glpA* (Cole et al. 1988). Under anaerobic condition another pathway may be present (Gonzalez et al., 2008) (Figure **1-1**, Blue arrow). In this case, the glycerol can be first oxidized to dihydroxyacetone (DHA) by the NAD^+-dependent glycerol dehydrogenase (encoded by *gldA*) (Tang et al. 1979) and then be phosphorylated by the PEP-dependent dihydroxyacetone kinase (encoded by *dhaKLM*) to DHAP (Jin and Lin 1984). In contrast to glucose, when using glycerol as the C source, however, several gluconeogenesis reactions must occur. This is necessary to get a substantial flow in direction of the PPP (Figure **1-1**). Glycerol has no competing application in the food industry and it appears as a byproduct during biodiesel production (da Silva et al. 2009; Almeida et al. 2012; Weiner et al. 2014; Sprenger 2017). The advantage of using glycerol instead of glucose is that glycerol has a higher reduction potential compared to glucose which can result in higher biomass and product formation. Furthermore, unlike glucose which requires phosphoenolpyruvate (PEP) for its uptake into *E.coli* (PTS dependent glucose uptake), no phosphoenolpyruvate (PEP) is required for glycerol uptake into *E .coli* (Andersen and von Meyenburg 1980; Yazdani and Gonzalez 2007; Gonzalez et al. 2008; Ahn et al. 2008; Gottlieb et al. 2014). Being cost-effective of glycerol (Yang et al. 2012; Sprenger 2017 (11 cents per Kg)) has recently extended application ranges, including bio-based production of bulk chemicals or fine chemicals (da Silva et al. 2009) such as lactic acid (Mazumdar et al. 2013), succinic acid (Blankschien et al. 2010), propionic acid (Barbirato et al. 1997), citric acid (Papanikolaou et al. 2002), aromatic compounds (Weiner et al.

2014; Gottlieb et al. 2014; Khamduang et al. 2009; Thongchuang et al. 2012) and etc. (Silva et al. 2009; Martínez-Gómez et al. 2012).

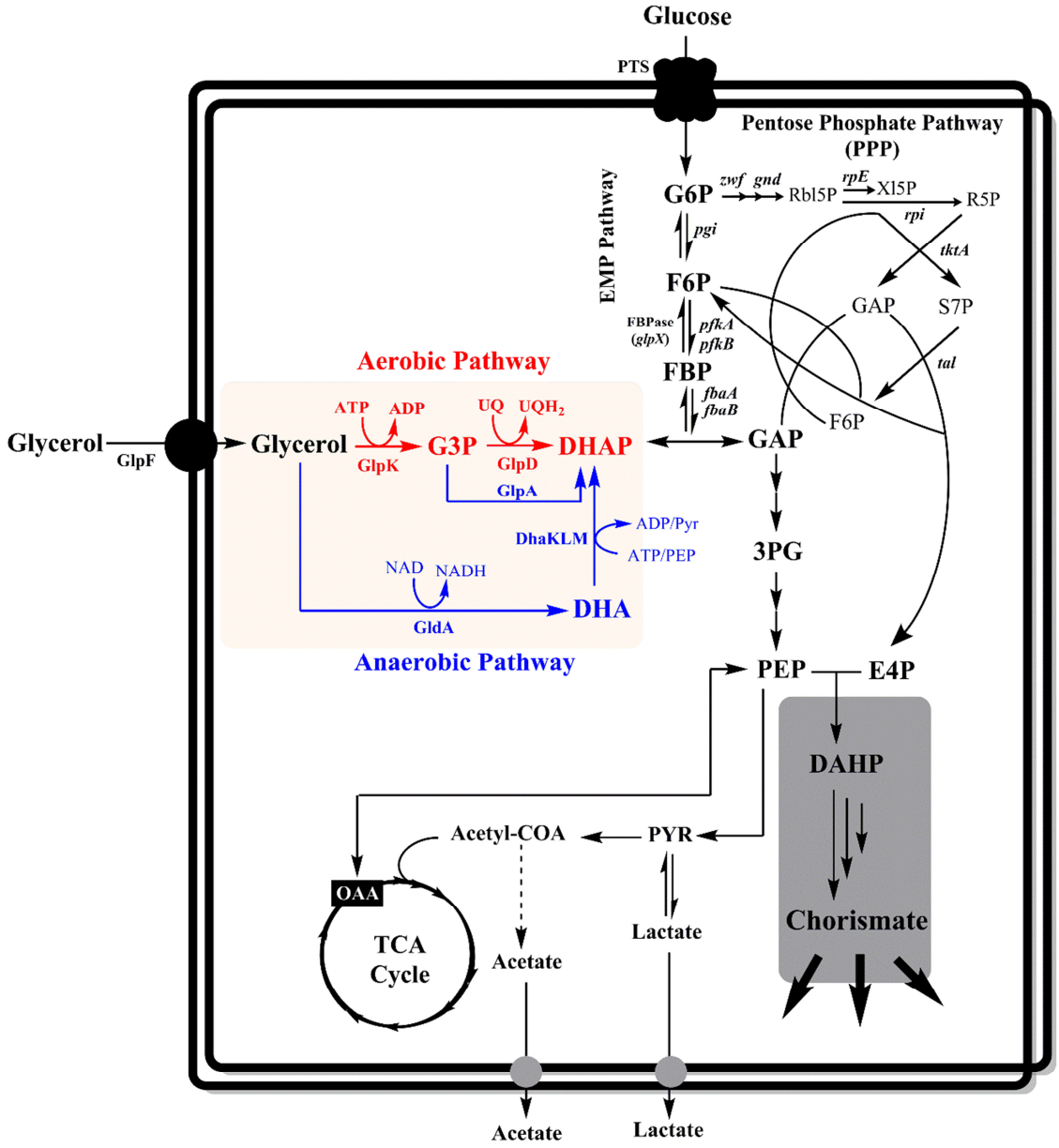

Figure 1-1 Schematic represent the metabolic pathways from glucose or glycerol in *E. coli*: Abbreviations: G6P, glucose-6-phosphate; F6P-fructose-6-phosphate; F1,6-BP, Fructose-1, 6-bisphosphate; G3P , Glycerol-3-phosphate; DHA-dihydroxyacetone; DHAP, Dihydroxyacetone phosphate; GAP-glyceraldehyde-3-phosphate; 3PG-3-phosphoglycerate; PEP-phosphoenolpyruvate; TCA, Tricarboxylic acid cycle; PPP, pentose phosphate pathway; RbI5P, Ribulose 5-phosphate; Xl5P, Xylulose-5- phosphate; R5P, Ribose 5-phosphate; S7P, Sedoheptulose 7-phosphate; OAA, oxaloacetate; PYR, Pyruvate; DAHP, 3-Deoxy-D-arabinoheptulosonate 7-phosphate; E4P, Erythrose 4-phosphate; *zwf*, Glucose 6-phosphate dehydrogenase; *gnd*, Gluconate 6-phosphate dehydrogenase; *rpE*, Ribulose-phosphate 3-epimerase; *rpi*, Ribose-5-phosphate isomerase; *pgi*, Phosphoglucose isomerase; *pfkA/B*,

Fructose-6-phosphate Kinase; *fbaA/B*, fructose 1,6-diphosphate aldolase; FBPase (*glpX*), Fructose-1,6-bisphosphatase; GlpK, Glycerol kinase; GlpD, aerobic glycerol-3-phosphate dehydrogenase; GlpA, anaerobic glycerol-3-phosphate dehydrogenase; GldA, glycerol-dehydrogenase; DhaKLM, PEP-dependent dihydroxyacetone kinase; *tktA*, transketolase; *tal*, transaldolase. The information presented in this figure is from EcoCyc database (Karp et al. 2002). The glycerol metabolism pathway is taken from the Gottlieb K dissertation (2011, Ph.D. Dissertation).

1.4 Aromatic amino acid compounds

Aromatic amino acids are being produced in large scale of several thousand metric tons by fermentations or biotransformation with genetically modified microorganisms like *E. coli* or *Corynebacterium glutamicum* (Ikeda 2006; Sprenger 2007a; Juminaga et al. 2012; Gottlieb et al. 2014; Rodriguez et al. 2014; Lee and Wendisch 2016). Aromatic compounds find many applications in biotechnology, nutrition and medicine. L-Phe is mainly used for the synthesis of the low calorie sweetener aspartame (L-aspartyl- L-phenylalanine methyl ester) while L-Trp is used as precursors of antitumor drugs violacein and deoxyviolacein and animal feed (Ikeda 2006; Sprenger 2007a; Rodriguez et al. 2012; Rodriguez et al. 2013; Fang et al. 2015). L-Tyr is used as dietary supplement in phenylketonuria and is a precursor in the synthesis of Levodopa (L-3, 4-dihydroxyphenylalanine) which is used in Parkinson´s disease treatment (Munoz et al. 2011; Min et al. 2015).

1.4.1 Aromatic amino acids pathway in *E. coli*

The synthesis of aromatic amino acids occurs in plants, fungi and bacteria through shikimate pathway. The shikimate pathway offers an interesting starting point for the synthesis of natural product and drug synthesis, fungicides, antibiotics and fine chemicals (Haslam 1974; Herrmann 1995; Floss 1996; Herrmann and Entus 2001). The aromatic amino acids as well as a variety of promising aromatic metabolites are formed starting from the synthetic building block chorismic acid (Figure 1-2). Chorismic acid is formed in *E. coli* by the shikimic acid pathway (Pittard 1996; Pittard and Yang 2008). An overview of this metabolic pathway and the individual enzymes in the different organisms is provided by numerous reviews (Lingens 1968; Herrmann 1995; Pittard 1996; Herrmann and Weaver 1999; Macheroux et al. 1999; Sprenger 2007a; Sprenger 2007b; Pittard and Yang 2008). First committed step of this pathway consists of the synthesis of 3-deoxy-arabinoheptulosonate-7-phosphate (DAHP) from phosphoenolpyruvate (PEP) and erythrose 4-phosphate (E4P) by different isomer types of DAHP synthase (Figure 1-

2); PEP is a key intermediate in glycolysis and E4P, a key intermediate in pentose phosphate pathway (PPP). This reaction is achieved via the DAHP synthase enzymes AroG, AroF and AroH which are feedback sensitive to L-Phe, L-Tyr, and L-Trp, respectively (Herrmann 1995; Pittard 1996; Sprenger 2007a). In three further biosynthesis steps shikimic acid is formed, which became the name of this biosynthetic pathway (Haslam 1974; Sprenger 2007a and b). Subsequently, by ATP-dependent phosphorylation of shikimic acid and addition of another PEP molecule 5-enolpyruvylshikimate-3-phosphate (EPSP) and subsequently chorismic acid is formed. From chorismic acid, L-Trp is formed in several steps via anthranilate. L-Tyr and L-Phe are formed via prephenate and then converted to phenylpyruvate (PP), or 4-hydroxyphenylpyruvate (4-HPP) (Figure 1-2; Pittard 1996; Sprenger 2007a; Ikeda 2006). In addition to the aromatic amino acids, chorismic acid is a branching point for biosynthesis of *para*-aminobenzoic acid, folic acid, menaquinone and other aromatic compounds (Figure **1-3**; Pittard 1996). Biosynthesis of aromatics amino acids are highly regulated in *E.coli* by several regulatory systems (Neidhardt et al. 1992; Pittard 1996), DNA level either by attenuation or repression and end-product inhibition of enzymes (Frost and Draths 1995; Pittard 1996). In the transcription repression, the aromatic amino acids (when they are present) form a complex with their DNA-binding transcriptional regulator (TyrR for L-Phe, L-Tyr and L-Trp, TrpR only for L-Trp) and then bind to a certain recognition target sequence (bind to "weak TyrR boxes" in the presence of aromatic amino acid and bind to "strong TyrR boxes" in the absence of aromatic amino acid) near the transcriptional promoter region of the genes *aroF*, *aroG*, and *aroH* (Pittard et al. 2004). The presence of the DNA-binding protein complex either through exclusion of RNA polymerase from promotor or interferes with the proper binding site of RNA polymerase leads to transcription inhibition (Pittard 1996; Pittard et al. 2004). In addition to the repression, TyrR also activates transcription when bound at appropriate site near the C-terminal region of alpha-subunit of RNA polymerase (Pittard et al. 2004). It has also been shown that several genes involved in the aromatics biosynthesis including *aroL, tyrP, mtr, aroP, tyrB, aroG* are down regulated (transcription) by activation of the TyrR regulon (Pittard et al. 2004). In addition, the proteins themselves are regulated via allosteric enzyme inhibition. There are the two most important regulatory points, the first committed step reaction, which is catalyzed by three different isoenzymes of DAHP synthase (AroF, AroG and AroH), and the reactions starting from chorismate. Each of the three isoenzymes is specifically inhibited by an aromatic amino acid

(Pittard 1996; Sprenger 2007a and b; Ikeda 2006). L-Phe and L-Tyr inhibits 95% the activity of AroG and AroF, respectively, while AroH might be inhibited up to 60% by L-Trp (Camakaris and Pittard 1974; Schoner and Herrmann 1976; McCandliss et al. 1978; Pittard 1996).

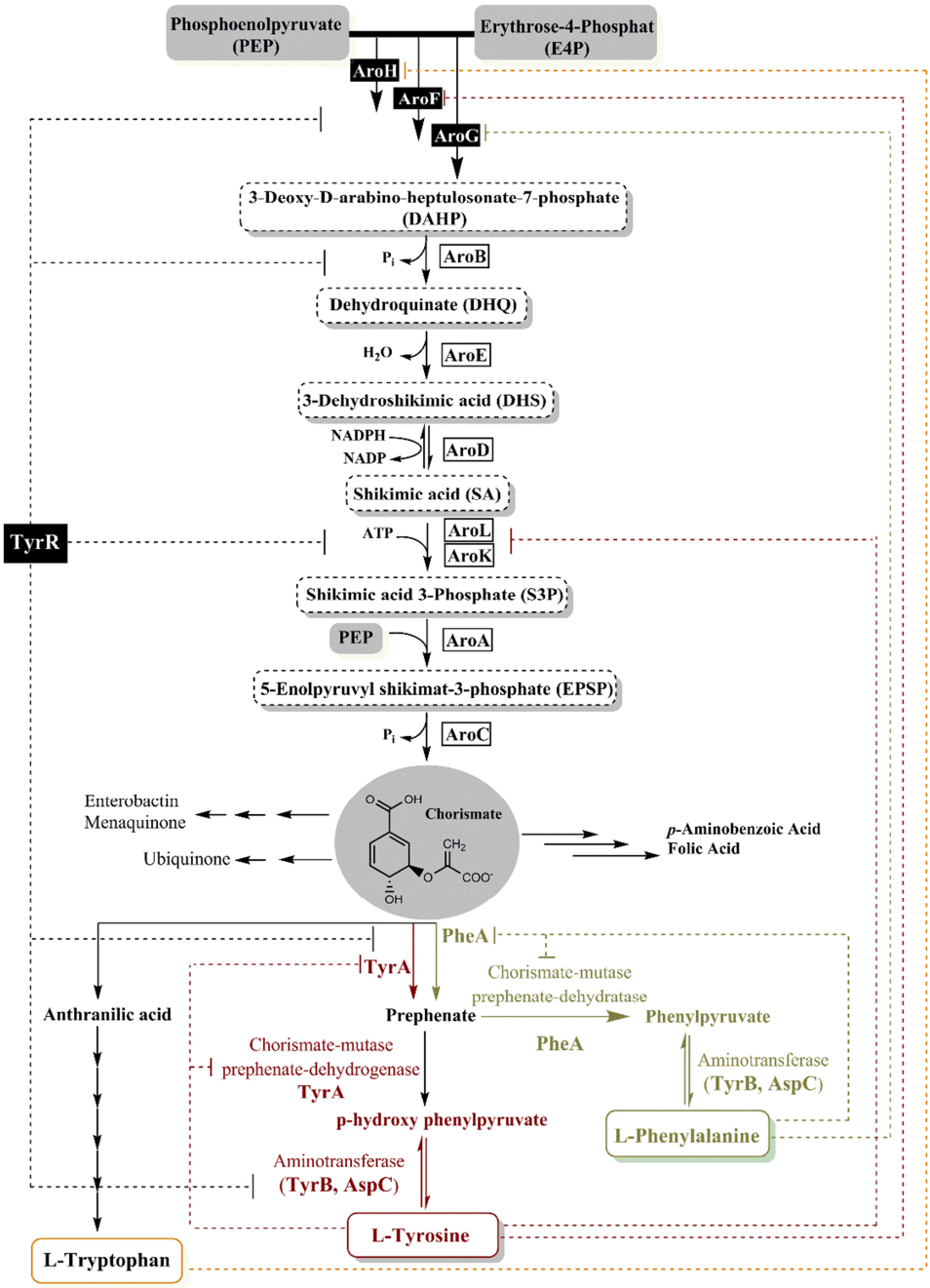

Figure 1-2 the shikimic acid pathway in *Escherichia coli* and involved genes. Starting from phosphoenolpyruvate (PEP) and erythrose-4-phosphate (E4P), chorismic acid is formed in the end of shikimic acid pathway; Explanation of the enzymes involved: DAHP synthases AroF, AroG and AroH; 3-dehydroquinate synthase AroB; 3-dehydroquinate dehydratase AroD; shikimate dehydrogenase AroE;

shikimate kinases AroL and AroK; EPSP synthase AroA; chorismate synthase AroC; chorismate mutase/prephenate dehydratase PheA; chorismate mutase/prephenate dehydrogenase TyrA; transcriptional regulatory protein TyrR; aspartic aminotransferase AspC and aromatic amino transferase TyrB. The information presented in this figure is from EcoCyc database (Karp et al. 2002) and previous works (Sprenger 2007b; Gottlieb 2011, Ph.D. Dissertation).

Interestingly, the shikimate pathway is not completely inhibited even at high concentrations of all three aromatic amino acids due to partial inhibition of AroH by L-Trp. 80% of the total activity of all DAHP synthases in *E. coli* is from AroG (Tribe et al. 1976; Pittard 1996). Studies on the efflux transporters indicated five aromatic amino acid transporters in *E.coli*, a general transport protein AroP and four specific proteins including two tryptophan-specific proteins (Mtr and TnaB), a tyrosine-specific protein (TyrP), and a phenylalanine-specific permease (PheP) (Sarsero et al. 1991; Pi et al. 1991; Heatwole and Somerville 1991; Whipp and Pittard 1977; Wookey and Pittard 1988; Pittard 1996). Among them, *pheP* is constitutively expressed while *aroP*, *tyrP* and *mtr* genes are under the control of the TyrR regulon (Pittard 1996; Pittard et al. 2004). Studies on the flux through the shikimic acid pathway indicated several rate-limiting reactions in enhancement of aromatic amino acids such as 3-dehydroquinate synthase (AroB), SHK kinase II (AroL), EPSP synthase (AroA) and chorismate synthase (AroC) (Snell et al. 1996; Pittard 1996; Yi et al. 2002; Dell and Frost 1993; Oldiges et al. 2004). After eliminating these limitations, the flux toward the shikimic acid pathway can be enhanced by increasing availability of the two starting compounds PEP and E4P (Draths and Frost 1990; Patnaik et al. 1995). This can be achieved by protein overexpression of transketolase A (*tktA*) and/or transaldolase (*tal*) (Patnaik et al. 1995; Sprenger et al. 1995; Sprenger et al. 1998), *glpX* in case of glycerol as carbon source (Gottlieb et al. 2014) or by deletion/overexpression of individual genes using PEP from the central metabolism pathway (Patnaik and Liao 1994; Chandran et al. 2003; Zhu and Shimizu 2005; Gosset 2009; Noda et al. 2016).

1.4.2 Chorismate, a central branch point in shikimate pathway

The shikimate pathway has been intensively investigated in the last decade due to providing valuable intermediate of compounds for preparation of bulk chemicals, natural product and drug synthesis (Sprenger 2007b; Rodriguez et al. 2014; Bongaerts et al. 2001; Ikeda 2006; Bongaerts et al. 2011; Jiang and Zhang 2016). As example, oseltamivir phosphate (GS-4104-02, Tamiflu ™), an anti-influenza drug derivate from shikimate or quinate (Krämer et al. 2003; Martínez et

al. 2015). Chorismic acid is one of the most interesting building blocks of the shikimate pathway (Gibson 1963). From there, various biosynthetic pathways can be derived towards many aromatic compounds (Figure **1-3**). Among them are three proteinogenic aromatic amino acids, L-phenylalanine (L-Phe), L-tyrosine (L-Tyr), and L-tryptophan (L-Trp) (Gibson 1963; Bongaerts et al. 2001 and 2011; Ikeda 2006; Sprenger 2007a and b; Gosset et al. 2009; Koma et al. 2012; Gottlieb et al 2014; Rodriguez et al. 2014; Doroshenko et al. 2015).

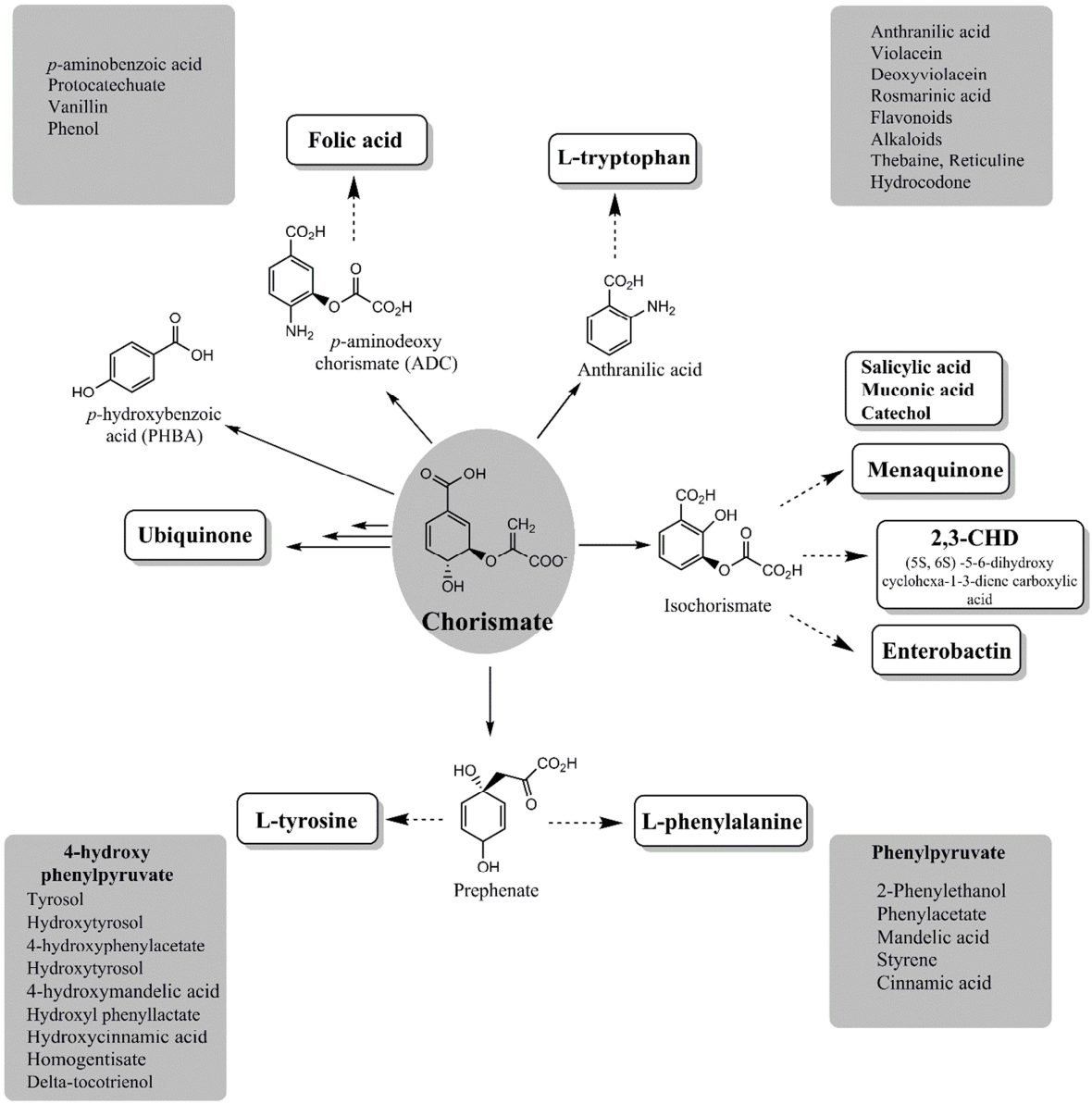

Figure 1-3 Chorismic acid as a central branch point metabolite in production of various aromatic compounds. The information inside of picture is taken from several publications (listed in the above text,

see section 1.4.2), but the plan of figure is derived from Sprenger (2007b) and Kozac S (2011, Ph.D. Dissertation).

Other important chorismic acid derivatives are *p*-hydroxybenzoic acid (Barker and Frost 2001; Pugh et al. 2014), benzyl alcohol (Pugh et al. 2015), *p*-aminobenzoic acid (Koma et al. 2014), protocatechuate and catechol (Pugh et al. 2014), vanillin (Li and Frost 1998; Kunjapur et al. 2014), anthranilic acid (Balderas-Hernandez et al. 2009), δ-tocotrienol (a vitamin E, Albermann et al. 2008; Ghanegaonkar et al. 2013), phenol (Kim et al. 2014b; Miao et al. 2015; Thompson et al. 2016), *S*- and *R*- mandelic acid (Sun et al. 2011), 4-hydroxymandelic acid (Li et al. 2016), salicylic acid and muconic acid (Lin et al. 2014), styrene, cinnamic acid and hydroxylated derivatives thereof (Sariaslani 2007; McKenna and Nielsen 2011; Koma et al. 2012; Vargas-Tah et al. 2015), 2-phenylethanol (Etschmann et al. 2002; Koma et al. 2012; Kang et al. 2014), 4-hydroxyphenylacetate and tyrosol (Koma et al. 2012; Satoh et al. 2012 a and b; Bai et al. 2014), hydroxytyrosol (Li et al. 2018), hydroxyphenyllactic acid, tyramine and other L-Phe or L-Tyr-derived compounds (Koma et al. 2012), rosmarinic acid and flavonoids (Bloch and Schmidt-Dannert 2014; Jiang and Zhang 2016), antitumor drugs like violacein and deoxyviolacein (Rodrigues et al. 2013), several plant alkaloids (Nakagawa et al. 2011), or even opiates like thebaine, reticuline or hydrocodone (Nakagawa et al. 2016). Various secondary metabolites such as phenylpropanoids (Wang et al. 2015; Bloch 2014) and some antibiotics (chloramphenicol, pristinamycin and others) in *Streptomycetes* are also derived from the aromatic pathway (He et al. 2001; Blank et al. 1997; Floss 1996). However, due to instability, lack of availability in pure form and the high price (1395 €/100 mg/80% purity, from Sigma-Aldrich (on 21th May 2018)) the synthesis of chorismic acid through microbial fermentation so far was low (Kozak 2006). For the reasons mentioned above and due to the importance of chorismate in industry, many studies concerning chorismate-derived compounds production have been conducted within the past years (as mentioned above), resulting in new and impressive research for its biotechnological production using microorganisms (Bongaerts et al. 2011; Rodriguez et al. 2014; Martínez et al. 2015; Jiang and Zhang 2016).

1.5 Aromatic amine (AA) compounds

1.5.1 General information (current status, and future perspective)

Aromatic amines are aromatic hydrocarbon molecules containing at least a benzene ring and an amino group (Stellman 1989; Arora 2015). Aromatic amines are an important group of industrial chemicals of which several have been characterized and are widely used as building blocks for manufacturing of dyes, pesticides, drugs, antibiotics, rubbers, high performance plastics and semi conductive or conductive polymers, and other industrial products (Stellman 1989; Sousa et al. 2013; Arora 2015; Tsuge et al. 2016; Masuo et al. 2016; Kawasaki et al. 2018).

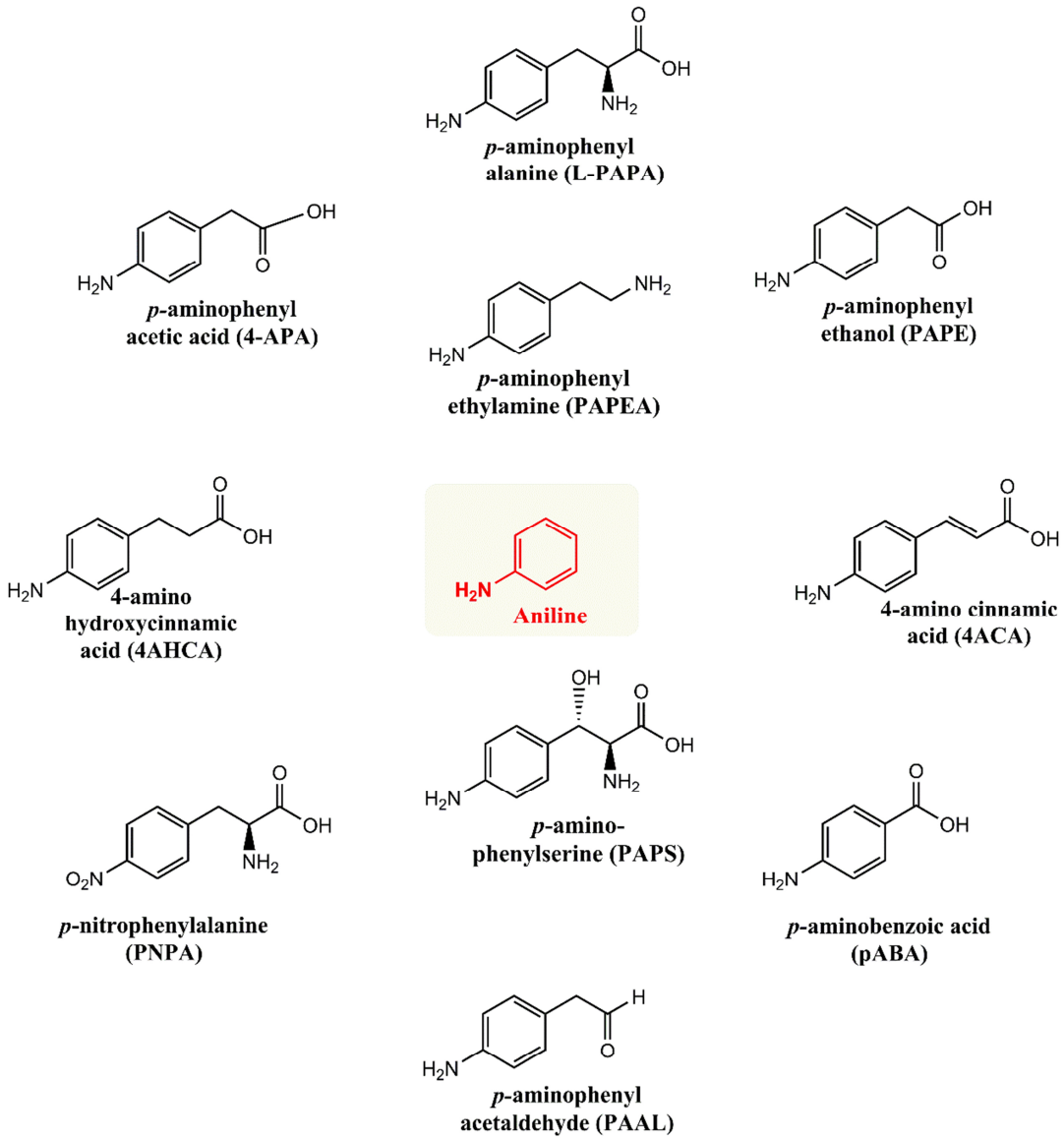

Figure 1-4 Example of Aromatic Amines (AA) comounds

In recent years much attention has been paid to aromatic amines as a high-valuable building blocks for the synthesis of high-performance artificial plastics (polymer), which have unique properties such as ultraviolet absorbance, high thermal and mechanical resistance (Suvannasara et al. 2014; Tsuge et al. 2016; Kawasaki et al. 2018). It has been recently reported that two “bio” monoamines ("bio" refers to microbial production of aromatic monomers) (Figure 1 4), 4-amino-cinnamic acid (4-ACA) and 4-amino hydroxyl-cinnamic acid (4-AHCA) can be used in synthesis of high performance bio based polymers such as functional polyimide film (Suvannasara et al. 2014); ultra-strong, transparent polytruxillamides (Tateyama et al. 2016) and Poly 4-aminocinamic acid (Poly-4AHCA) (Kawasaki et al. 2018). It was shown that 4-ACA (Suvannasara et al. 2014; Tateyama et al. 2016; Kawasaki et al. 2018) and 4-AHCA (Kawasaki et al. 2018) can be produced by bioconversion of non-proteinogenic aromatic amino acid, *para*-amino-L-phenylalanine (L-PAPA) using recombinant *E. coli*. Several aromatic amines addressed in microorganisms (Figure **1-4**), *para*-aminobenzoic acid (PABA) is an intermediate of the folate biosynthesis pathway (Koma et al. 2014), *para*-nitrophenylalanine (PNPA) is an intermediate in obafluorin biosynthesis pathway (Herbert and Knaggs 1988; Schaffer et al. 2017), *para*-amino-phenylserine (PAPS) and *para*-amino-L-phenylalanine (L-PAPA) are an important building block for biosynthesis of several antibiotics like chloramphenicol (Chang et al. 2001; He et al, 2001; Fernández-Martínez et al, 2014) or pristinamycin (Blanc et al. 1997). Recently, L-PAPA has been prepared from biomass using recombinant *E.coli* (Masuo et al. 2016; Tateyama et al. 2016). Other aromatic amines (Figure **1-4**), *para*-aminophenylethanol (PAPE), *para*-aminophenyl actetic acid (4-APA), *para*-aminophenyl ethylamine (PAPEA), *p*-aminophenyl acetaldehyde (PAAL), whereas recombinantly are produced in *E. coli*, but no evidence was found for natural synthesis (Masuo et al. 2016). The rare, non-proteinogenic aromatic amino acid, *para*-amino-L-phenylalanine (L-PAPA) is involved as the building block (diamine) in the synthesis of aromatic polyamides (Masuo et al. 2016; Tateyama et al. 2016). Not only L-PAPA is an essential and valuable precursor to plastics, it is also used as an important precursor to technical and pharmaceutical applications (Yamaguchi et al. 2007; Suvannasara et al. 2014; Kumar et al. 2016; Masuo et al. 2016) and has been described as a building block of the anticancer drug Melphalan® (Bergel and Stock 1954; Jobdevairakkam and Velladurai 2013). In nature, L-PAPA was identified as an important component for seed defense against two important pests (bruchid beetle) of *Vigna* and *Phaseolus* crops (Dardenne et al. 1975, Birch et al. 1986), and as an

intermediate of the chloramphenicol, pristinamycin and obafluorin biosynthesis pathways in *Streptomyces venezuelae, S. pristinaespiralis* and *Pseudomonas fluorescens,* respectively (Herbert and Knaggs 1988; Brown et al. 1996; Blanc et al. 1997; He et al, 2001; Chang et al. 2001; Yanai et al. 2004; Mast et al. 2011). Two aromatic amines, PAPE and 4-APA have not been well-described as compared to L-PAPA. These can be considered as building blocks in fine chemical industries for the synthesis of aromatic polyamides (Masuo et al. 2016), polymers or copolymer (Li et al. 1999; Xu et al. 2008) and surface functionalization of graphene (Yadav and Cho 2013). PAPE can be also used (research) for the synthesis of Myrbetriq® precursor (Sacco and Bientinesi 2016). Due to the good transparency and very high stability in high temperatures (glass transition temperature more than 200˚C), they possibly can be used as potential building blocks in synthesis of aromatic amines polymers and super engineering plastics (SEP) (Maekawa et al. 2015; Tsuge et al. 2016). Due to the fast-growing demand for aromatic amines polymers and super-engineered plastics (Masuo et al. 2016), L-PAPA, PAPE, 4-APA and other aromatic amines have become promising monomers for synthesis of SEPs. Engineering plastics (SEPs) are a good alternative to traditional materials such as wood, ceramic and metal material or even would be considered as new material for novel technological applications. Today, apart from the advantages of these types of plastics in mechanical/thermal and other properties (Maekawa et al. 2015; Tsuge et al. 2016), they are much easier to form, even in complex shapes. Super engineer plastic has also the potential to be used in the future for a variety of devices such as smart phones, tablet, computers, home electrical appliances, automobile, medical instruments, airplanes, industrial machines, cooking ware, and etc. In 2014, the global engineering plastics market was valued at $57.2 billion and was expected to reach nearly $ 100 billion by 2020 (Suvannasara et al. 2014; Masuo et al. 2016; Gupta 2017). Currently, global demand for engineering plastics is growing fast, and several engineering plastic manufacturing companies such as BASF und DowDuPont are consistently considering developing and expanding products that can be used for new applications (Gupta 2017). Currently, L-PAPA is obtained in a three-step chemical synthesis from *para*-nitrotoluene (Mattocks and Hartung 1946) or from D-/L-phenylalanine (Jobdevairakkam and Velladurai 2013). However, due to the high-value and industrial importance of aromatic amines, attempts have been made to produce aromatic amines such as PABA (Koma et al. 2014), L-PAPA (Mehl et al. 2003; Masuo et al. 2016; Tateyama et al. 2016), 4-ACA (Suvannasara et al. 2014; Tateyama et al. 2016; Kawasaki et al. 2018),

4AHCA (Kawasaki et al. 2018), 4-APA and PAPE (Masuo et al. 2016) in bacteria. Based on the biosynthesis pathway, metabolic grafting provides an alternative approach to produce these valuable aromatic amines via extensive pathway engineering in microbes.

1.5.2 Heterologous production of AAs from simple carbon source (glucose/glycerol)

It was clear that various secondary metabolites with different biological activities are produced by microorganisms, and scientists have always tried to use some of these compounds as drugs for humans or animals, industrial and agricultural chemicals and etc (Fujita et al. 2013; Liu et al. 2015; Kawaguchi et al. 2017). However, some of these compounds may not be directly used and further modification needs to be made to improve biological activity of them. Amino groups are generally known as one of the most unique functional groups in biology, which plays a predominant role in biological activity of aminoglycosides (Mingeot-Leclercq et al. 1999) and are easily modified by other functional groups because of their high reactivity. Naturally regiospecific amination can occur through addition an amino group into para-position of benzene ring. However, substances which can be a substrate for this reaction are limited, and few enzymes have been known to transfer an amino group to a benzene ring (Kaplan and Nichols 1983; Kaplan et al. 1985; Slock et al.1990; Green and Nichols 1991; Brown et al. 1996; Kozak 2006; Stolz et al. 2007). In addition to enzymatic methods, a conventional chemical method for modifying a certain substance with amino/nitro groups is available. On the other hand, this is very difficult to introduce an amino/nitro group specifically in the *para*-position of benzene ring using the chemical method. However, in chemical procedure, it is necessary to modify first a benzene ring with a nitro group (Jobdevairakkam and Velladurai 2013), and then a nitro group can be reduced to an amino group. The nitrobenzene reactant is very unreactive and extremely difficult, so rather harsh reaction conditions should be used to introduction of the nitro group into the benzene ring. Accordingly, an alternative biological approach to introduce an amino group specifically in the *para*-position of benzene ring may allow production of new aromatic amino components that have unique properties with significant potential for pharmaceutical or industrial applications (Bergel and Stock 1954; Jobdevairakkam and Velladurai 2013).

The first step of most *E. coli* metabolic engineering studies to produce recombinant compounds is creating a completely, or partially, synthetic pathway according to the pathways existing in the *E. coli*. Therefore, the sustainable synthesis of these aromatic compounds by transferring genes

associated with heterologous pathways involving several enzymes which is usually challenging. To do this, several methods have been developed which can be used for transferring DNA into chromosome (CRISPR-Cas9 system, λ Red recombinase system) or plasmid (Datsenko and Warnner 2000; Jones et al. 2000; Albermann et al. 2010; Li et al. 2015; Jiang et al. 2015). Here, a plasmid-based method for the biosynthesis of aromatic amines and aromatic alcohols in *E. coli* will be described.

1.5.2.1 Microbial biosynthesis of L-PAPA

L-PAPA synthesis starts from chorismate by enzymes that are involved in the conversion chorismic acid to *para*-aminophenylpyruvic acid (APA) as summarized in the following (Figure **1-5**) (Blanc et al. 1997): 4-amino-4-deoxychorismic acid (ADC) synthase (Kaplan and Nichols 1983; Nichols et al. 1989; Green and Nichols 1991; Goncharoff and Nichols 1984; Viswanathan et al. 1995), 4-amino-4-deoxychorismic acid mutase, and 4-amino-4-deoxyprephenic acid dehydrogenase (Brown et al. 1996; He et al. 2001). In the first step (Figure **1-5**), glutamine- or ammonia-dependent 4-amino-4-deoxychorismate synthase (ADC synthase) acts on chorismic acid to produce 4-amino-4-deoxychorismate (ADC) (Teng et al. 1985; Nichols et al. 1989; Green and Nichols 1991). The ADC synthase as a part of the *para*-aminobenzoate (pABA) biosynthesis pathway is found in a wide variety of organisms such as *Escherichia coli* (Kaplan and Nichols 1983; Goncharoff and Nichols 1984; Walsh et al. 1987; Green and Nichols, 1991; Parsons et al. 2002), *Bacillus subtilis* (Slock et al.1990), *Klebsiella pneumoniae* (Kaplan et al. 1985; Goncharoff and Nichols 1988), *Corynebacterium glutamicum* (Stolz et al. 2007; Kubota et al. 2016) and *Saccharomyces cerevisiae* (encoded by *ABZ1*, Edman et al. 1993) or as part of pristinamycin/chloramphenicol/obafluorin biosynthesis pathways in *Streptomyces pristinaespiralis* (Blanc et al. 1997), *Streptomyces venezuelae* (Brown et al. 1996; He et al. 2001) and *Pseudomonas fluorescens* (Herbert and Knaggs 1988). ADC synthase generally classified into two main types, two separate genes (*pabA* and *pabB)* which is not organized in an operon such as in *E. coli* (Nichols et al. 1989; Parsons et al. 2002), *Bacillus subtilis* (Slock et al.1990), *Klebsiella pneumoniae* (Goncharoff and Nichols 1988) or composed of one fused-gene, *pabAB* in *Corynebacterium glutamicum* (Kozak 2006; Stolz et al. 2007; Kubota et al. 2016). The N-terminal part of PabAB is similar to PabA (*E. coli*), while the C-terminal part has sequence similarity to PabB (*E. coli*). These two parts are connected in the $PabAB_{C.gl.}$ by a linker sequence consisting of the 5 amino acid residues alanine, arginine,

threonine, tyrosine and arginine. In *E. coli* in the absence of PabA and glutamine, PabB converts ammonia and chorismate into 4-amino-4-deoxychorismate (in the presence of Mg^{2+}). PabA converts glutamine into glutamate only in the presence of stoichiometric amounts of PabB (Viswanathan et al. 1995).

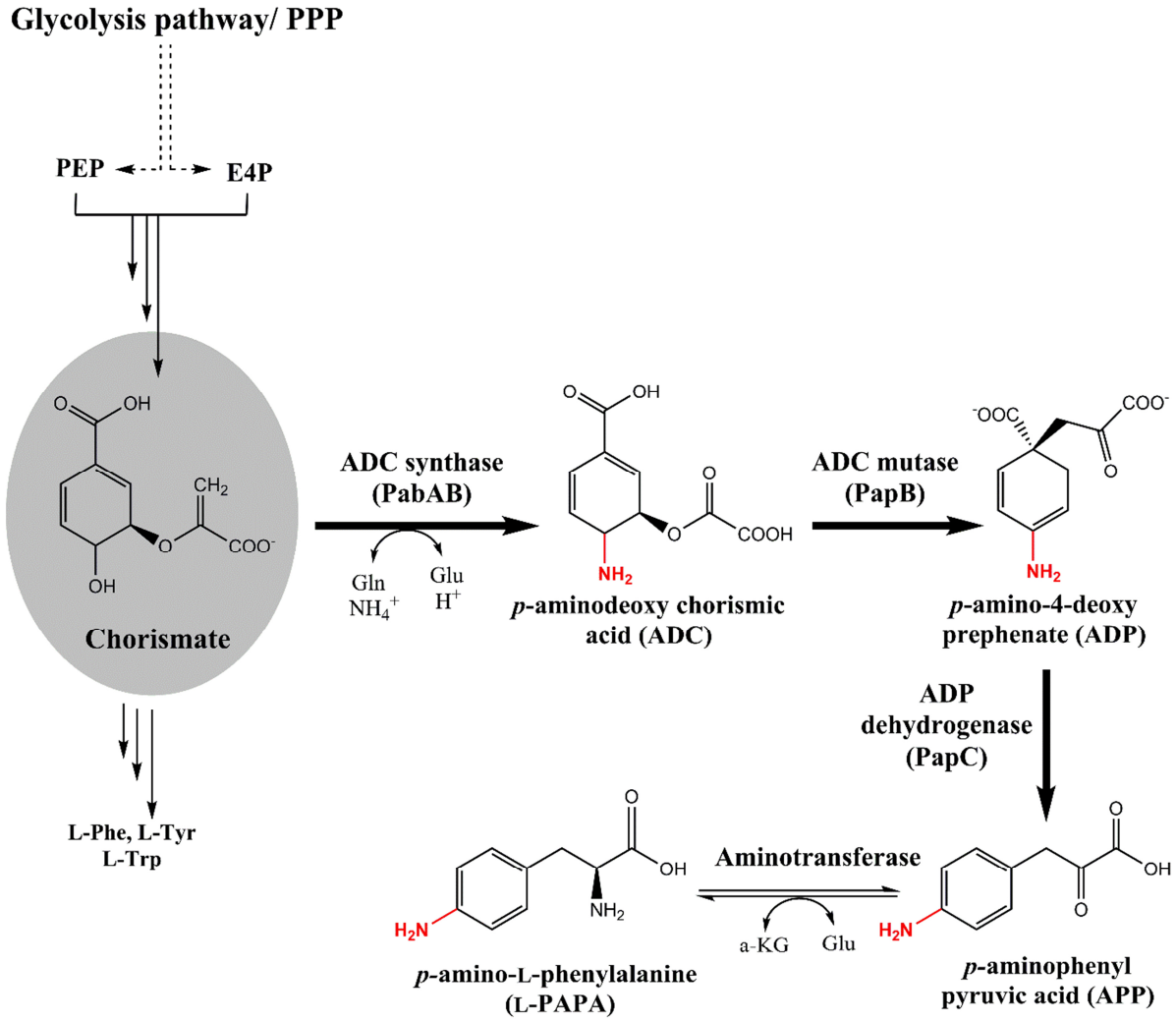

Figure 1-5 Microbial biosynthesis of L-PAPA. Starting from chorismic acid, L-PAPA is formed via the three intermediates ADC, ADP and APP. The amino group donor in first reaction is glutamine. Pathway presented here is the part of chloramphenicol biosynthesis pathway in *Streptomyces venezuelae* (He et al. 2001) and has also been investigated in the *E. coli* by the Schultz group (Mehl et al. 2003) and recently by Takaya Group ("Masuo et al. 2016").

The second enzyme in pABA biosynthesis pathway is 4-amino-4-deoxychorismate lyase (PabC in *E.coli*), a pyridoxal phosphate-dependent enzyme that catalyzes formation pABA by elimination of pyruvate from ADC (Nichols et al. 1989; Ye et al. 1990; Parsons 2002). The

second specific reaction in pristinamycin I /chloramphenicol biosynthesis is catalyzed by a 4-amino-4-deoxychorismic acid mutase, encoded by *papB* in *S.pristinaespiralis* (76% homology with *cmlD* in *S. venezuelae*). The 4-amino-4-deoxyprephenic acid formed in the reaction is channeled towards the formation of *para*-aminophenylpyruvate (APP) by a monofunctional prephenate dehydrogenase named 4-amino-4-deoxyprephenic acid dehydrogenase encoded by *papC* in *S.pristinaespiralis* (96% homology with *cmlC,* in *S. venezuelae*) (Blanc et al. 1997; He et al. 2001). More specifically, these two enzymes PapB/PapC are analogous of bifunctional enzyme chorismate mutase/prephenate dehydrogenase (TyrA) that catalyzes a similar primary metabolic reaction in tyrosine biosynthesis pathway in *E.coli* (Pittard 1996). Apart from *Streptomyces pristinaespiralis* and *Streptomyces venezuelae* which are typically known as source of PapB/PapC, other organisms such as *Streptomyces loidensis* that produces Vernamycin B (Bodanszky and Ondetti 1963; Cocito 1979) and *Corynebacterium hydrocarboclastus* that produce Corynecin (Nakano et al. 1976) can be considered as other sources of these two genes for further studies (Yanai et al. 2004). In the end, aminotransferases form L-PAPA from APP and serves then as intermediate for the synthesis of several antibiotics (Figure **1-5**). *E. coli* is not a natural producer of L-PAPA but it was known that the *E. coli* aminotransferases (Pittard 1996; Fotheringham et al. 1986; Inoue et al. 1988; Hayashi et al. 1993; Onuffer et al. 1995) can convert *para*-aminophenylpyruvate (APP) into L-PAPA (Mehl et al. 2003; Masuo et al. 2016; Tateyama et al. 2016). Recently, *papA,B,C* homolog genes from *Pseudomonas fluorescens* have been successfully cloned and expressed to establish a recombinant aromatic amine platform in *E. coli* (Masuo et al. 2016; Tateyama et al. 2016). Earlier, L-PAPA formation in *E. coli* was studied by the group of Peter Schultz who showed that L-PAPA can be recombinantly produced from glucose and incorporated as a non-natural amino acid ("21st amino acid") into proteins in specifically engineered *E. coli* strains (Mehl et al. 2003).

1.5.2.2 Microbial biosynthesis of PAPE and 4-APA

An important intermediate in L-PAPA pathway is APP, a para-amino ketoacid analog to phenylpyruvate (PP). APP can be decarboxylated to *para*-amino phenyl acetaldehyde (PAAL) by α-ketoacid decarboxylase and subsequently depending on the redox status of the cells either reduced to *para*-aminophenylethanol (PAPE) by alcohol dehydrogenases or oxidized to the *para*-aminophenylacetic acid (4-APA) by aldehyde dehydrogenases (Figure **1-6**) (Masuo et al.

2016). A critical enzyme in this pathway is thiamine diphosphate (ThDP)-dependent keto acid decarboxylase, which is common in plants, yeasts and fungi but less in bacteria (Konig et al. 1998). It was shown that there are five candidate enzymes in *Saccharomyces cerevisiae* (Hohmann and Meacock 1998; Vuralhan et al. 2005) catalyzing decarboxylase reaction in the Ehrlich pathway (Etschmann et al. 2002). Three of them (PDC1, PDC5 and PDC6) are specifically identified as pyruvate-dependent decarboxylase, although they also have phenylpyruvate decarboxylase activity (Hohmann and Cederberg 1990). THI3 and Aro10 encode Ketoacid decarboxylase and likely contribute to branched-chain amino acids catabolism (Dickinson et al. 2000). Moreover, it has been shown that *aro10* gene encodes a ThDP-dependent phenylpyruvate decarboxylase with a broad substrate specificity (Vuralhan et al. 2003; Vuralhan et al. 2005; Kneen et al. 2011) and play a key role in the catabolism of aromatic amino acids as well as branched-chain amino acids through the Ehrlich pathway in yeast (Kneen et al. 2011). Apart from Aro10, many studies have also reported different kinds of α-ketoacid decarboxylase in the different species of bacteria and fungi such as benzoylformate decarboxylase (BFDC1) from *Pseudomonas putida* (Polovnikova et al. 2003; Yep et al. 2008), alpha-ketoisovalerate decarboxylase (KivD) from *Lactococcus lactis* (Delaplaza et al. 2004), phenylpyruvate decarboxylase (PDC) from *Pichia pastoris* (Kuberl et al. 2011), pyruvate decarboxylase (ZmPDC) from *Zymomonas mobilis* (Siegert et al. 2005), 2-keto acid decarboxylase (KdcA) from *Lactococcus lactis* (Yep et al. 2006) and *Acetobacter pasteurianus* (Chandra et al. 2001) as well as α-ketoacid decarboxylase (PpdA) from *Aspergillus oryzae* (Masuo et al. 2015). Unlike Aro10, some of the keto acid decarboxylases such as BFDC1 and ZmPDC are more specific and limited to unbranched aliphatic and aromatic substrates (Sprenger and Pohl 1999). In addition, Aro10 as a high-potency candidate enzyme has been successfully applied in the recombinant production of various fine chemicals in the *E. coli* such as PAPE, 4-APA (Masuo et al. 2016), 1-butanol (Atsumi et al. 2008 a and b), 1-Propanol, Isobutanol (Atsumi et al. 2008b), 2-phenylethanol (Atsumi et al. 2008b; Kang et al. 2014), Salidroside (Bai et al. 2014), tyrosol (Bai et al. 2014; Li et al. 2018) and hydroxytyrosol (Li et al. 2018). As already mentioned (Figure **1-5**), the second step in the Ehrlich pathway depending on the redox state of the cell (Vuralhan et al. 2003), phenyl acetaldehyde (or *para*-aminophenylacetaldehyde (PAAL)) can be reduced to phenyl ethanol (or *para*-aminophenylethanol (PAPE)) by alcohol dehydrogenase or reductases (Figure **1-6**). They are commonly found in many organisms

including human, plants, yeasts, fungi and different species of bacteria (Jornvall et al. 1987). In yeast, there are various alcohol dehydrogenases (ADH1, ADH2, ADH3, ADH4, and ADH5) and a formaldehyde dehydrogenases (Sfa1) which can catalyze the last step of the Ehrlich pathway to generate aromatic alcohols (Dickinson et al. 2003). Among these, ADH1 and ADH2 are known to have a major role in the Ehrlich pathway. In addition in several studies, ADH2 has been used as a candidate enzyme for the production of diverse range of aromatic alcohols such as PAPE (Masuo et al. 2016), 1-butanol (Atsumi et al. 2008 a and b), 1-Propanol (Atsumi et al. 2008b), Isobutanol (Atsumi et al. 2008b; Atsumi et al. 2010), 2-phenylethanol (Atsumi et al. 2008b; Kim et al. 2014 a and c). Apart from yeast, *E. coli* has also 13 known endogenous aldehyde reductase or alcohol dehydrogenase (AdhE, YqhD, AdhP, EutG, YiaY, YjgB, FucO, BetA, YahK, DkgA (YqhE), YbbO, GldA, and YghA) which are associated with metabolism of different components (Atsumi et al. 2010; Rodriguez and Atsumi 2014). Of these, YahK and YqhD have been shown as strictly NADH dependent with broad aldehyde reductase activity (Perez et al. 2008; Koma et al. 2012; Pick et al. 2013; Rodriguez and Atsumi 2014). It has been reported that YqhD is involved in enhanced resistance to reactive oxygen species in *E.coli* and has a critical role in response to compounds that generate membrane lipid peroxidation (Perez et al. 2008). It was also shown that YahK has broad substrate activity, such as acetaldehyde, isobutyraldehyde, hexanal (Pick et al. 2013), octanal, decanal (Rodriguez and Atsumi 2014), phenyl acetaldehyde and hydroxyl phenyl acetaldehyde (Koma et al. 2012). Several studies showed different applications of YahK and YqhD for microbial production of fine chemicals such as isobutanol (Atsumi et al. 2008b; Atsumi et al. 2010), 1-propanol, 1-butanol (Atsumi et al. 2008b), 1,2-propanediol (Clomburg and Gonzalez 2011), 1,3-propanediol (Tang et al. 2009), 2-phenylethanol and tyrosol (Koma et al. 2012).

On the other hand, phenyl acetaldehyde (or *para*-aminophenylacetaldehyde (PAAL)) may be oxidized to phenyl acetic acid (or *para*-aminophenylacetic acid (4-APA)) by aldehyde dehydrogenases (ALDHs) (Figure **1-6**). These are also found in a variety of living organisms from single cells to complex organisms (Jackson et al. 2011). Generally, most of them are common in functional activity, and are known as “aldehyde scavenger’, in response to a wide range of environmental and chemical stresses including dehydration and ultraviolet radiation (Singh et al. 2014). The third step in the upper pathway, that is, the oxidation of the *para*-aminophenylacetaldehyde (or PAL) generated by Aro10 to 4-APA (PA), is catalyzed by a phenyl

acetaldehyde dehydrogenase encoded by *padA* gene in *E. coli* W (Ferrnandez et al. 1997) or the homologous *feaB* gene in *E. coli* K-12 (Hanlon et al. 1997). It has been shown that *E.coli K-12* can use 2-phenylethylamine as the sole carbon and energy source through 2-phenylethylamine catabolism pathway (Parrott et al. 1987; Hanlon et al. 1997). In this pathway, two major enzymes are involved, an amine oxidase that converts 2-phenylethylamine into phenyl acetaldehyde, and a NAD^+-phenyl acetaldehyde dehydrogenase (FeaB (PadA)) that oxidizes the latter to phenyl acetic acid (Parrott et al. 1987; Hanlon et al. 1997; Ferrandez et al. 1997).

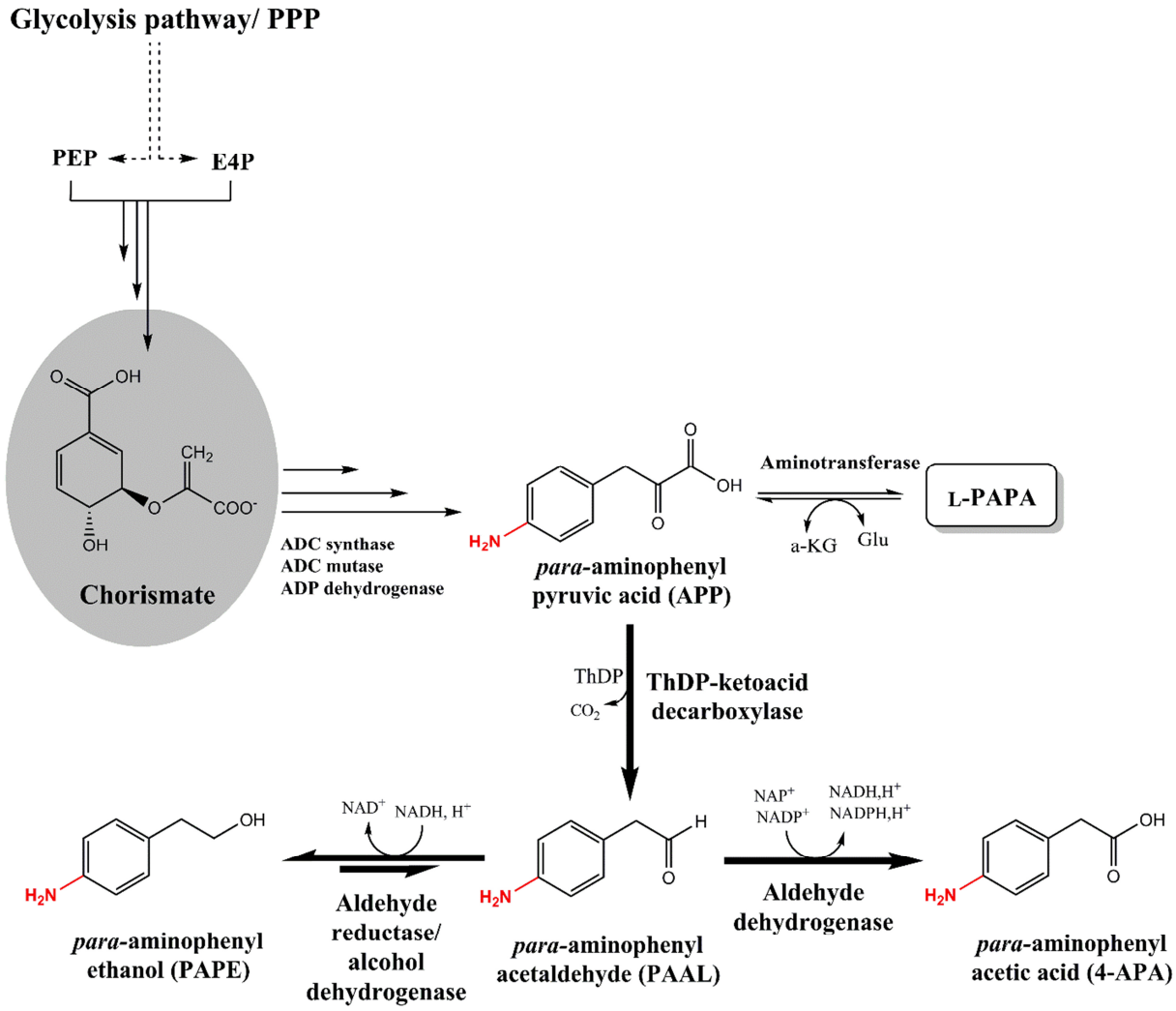

Figure 1-6 Microbial biosynthesis of PAPE and 4-APA from glucose in *E. coli*. Starting from chorismic acid, APP is formed via the two intermediates ADC and ADP which are already described in Figure **1-5**. Followed by decarboxylation of APP to PAAL by ThDP-ketoacid decarboxylase and subsequently PAAL either reduce to PAPE by alcohol dehydrogenase/aldehyde reductase or oxidized to 4-APA by aldehyde dehydrogenase. The information presented has been reported by Takaya Group ("Masuo et al. 2016").

It was previously reported that FeaB, AldB and AldH from *E. coli* act as aldehyde dehydrogenase almost equally well on phenyl acetaldehyde, 4-hydroxyphenylacetaldehyde, dihydroxyphenyl acetaldehyde, phenyl propionaldehyde or benzaldehyde (Ferrandez et al. 1997, Ho and Weiner 2005; Jo et al. 2008; Koma et al. 2012; Zhang et al. 2017). Also, in yeast at least six aldehyde dehydrogenases (ALD2, ALD3, and ALD6, ALD4, ALD5, and HFD1) with different subcellular gene expression level were observed. It was also shown that ALD4 and ALD6 are mainly involved in acetate formation from acetaldehyde, whereas ALD2 and ALD3 are involved in β-alanine production from 3-aminopropanal (Wang et al. 1998; White et al. 2003). In a recent investigation, Masuo et al. (2016) have used ALD2 and ALD3 for whole cell biotransformation of 4-APA from PAPA, according to the obtained results the ALD2 in combination with Aro10 showed better effect on 4-APA production compared to ALD1.

1.6 Aromatic alcohol compounds

1.6.1 General information (State of art, microbial biosynthesis, applications)

Alcohols are classified as aliphatic alcohols and aromatic alcohols. Aromatic alcohols are an important distinct class of aromatic compounds containing an alcoholic hydroxyl group attached directly to an aromatic hydrocarbon group (Rabinowitz and Vogel 2009; Mainguet and Liao 2010). Aromatic alcohol was originally named because of its fragrant properties. Among them, several have an odor (like 2-PE), however, there are some compounds that are chemically aromatic alcohol, but do not have a distinct smell. Aromatic alcohols are widely applied in range of cosmetics, fragrances, food additive (baking and winemaking), precursors in pharmaceuticals and fine chemical industry (Atsumi et al. 2008b; Hua and Xu 2011; González et al. 2018). It was found that an oily phase from beer containing several aromatic higher alcohols (such as tryptophol, tyrosol and phenyl ethanol) can be produced by the yeast during fermentation (Webb and Ingraham 1963; Szlavko 1973; Ghosh et al. 2013). Whereas these are naturally found in plants, bacteria and fungi, the vast majority of them are synthesized from petroleum-based benzene (by hydroxyalkylation of benzene with ethylene and propylene oxides (Mamedov 2006)) and petroleum by-products. Most aromatic alcohols are naturally derived from catabolism of aromatic amino acids (phenylalanine, tyrosine, and tryptophan) through the Ehrlich pathway (Etschmann et al. 2002; Hazelwood et al. 2008), which was first described more

than a century ago in yeast (Ehrlich 1907). This pathway consists of three enzymatic steps (Etschmann et al. 2002; Wittmann et al. 2002; Hazelwood et al. 2008): as the first intermediate in the Ehrlich pathway, an amino acid is transaminated to from an α-keto acid, then the α-keto acid is decarboxylated to form an aldehyde and reduced to form its corresponding alcohol (Figure 1-3; Figure 1-6) (Hazelwood et al. 2008). One of the most important aromatic alcohols is 2-phenylethanol (2-PE, rose-like odour), which is widely used as fragrance compound in a variety of consumer products such as colognes, cosmetic soaps, detergents and fine chemical industries (Hua and Xu 2011; Kim et al. 2014 a and c; Kang et al. 2014). 2-PE as a higher alcohol (higher alcohol containing C4 and C5, such as 1-butanol, isobutanol, 2-methyl-1-butanol or 3-methyl- 1-butanol) can also be used as a promising biofuel due to its higher energy density which is not found in lower alcohols (C1 and C2) such as ethanol, methanol (Atsumi et al. 2008b; Atsumi et al. 2010; Mainguet and Liao 2010). Tyrosol (2-(4-hydroxyphenyl) ethanol) and hydroxytyrosol (3, 4-dihydroxyphenylethanol) as another attractive aromatic alcohols are found mainly in the fruit and leaf of the olive (Tsimidou et al. 1992). During the past decades, several interesting aspects of tyrosol and hydroxytyrosol have been shown for human health (Miró-Casas et al. 2003; Covas et al. 2003; Rodríguez-Morató et al. 2016). For instance, tyrosol as an effective substance (antioxidant properties) can play a role in the inhibition of cholesterol oxidation in LDL (Caruso et al. 1999), cardiovascular diseases (di Benedetto et al. 2007) and anti-inflammatory activity (LPS-TNF inhibitor) (Giovannini et al. 2002). In addition, tyrosol with potent industrial value can be used as precursor in the synthesis of salidroside (Bai et al. 2014; Chung et al. 2017) and two selective β1 receptor blockers drugs betaxolol (Ippolito and Vigmond 1988) and metoprolol (Yoo 1982), which are effective in the treatment of hypertension, glaucoma, high blood pressure, heart failure, and migraines (Borchard 1998; Satoh et al. 2012). In contrast, several studies mostly in vitro assays have indicated higher antioxidant activity of hydroxytyrosol than tyrosol due to ortho-diphenolic structure of hydroxytyrosol (Giovannini et al, 1999; Takeda et al. 2014; Anter et al. 2014). It has been shown that hydroxytyrosol can reduce the levels of oxidized-LDL which can lead to the protection of blood lipids against oxidative damage (Raederstorff 2009), protection against DNA damage (Deiana et al, 1999) and anti-inflammatory (Takeda et al. 2014) as well as anticarcinogenic effect on human tumoral cell line HL60 (Anter et al. 2014). These aromatic alcohols, most importantly 2-PE, can be extracted from essential oils of certain flowers mostly rose petals (Kovacheva et al. 2010)

with a global production equaling about 0.5 tons/year (Etschmann et al. 2002), whereas tyrosol and hydroxytyrosol extract from olive oil. This extraction processes have several drawbacks including complex and high cost isolation processes, low recovery yields (1.9 mg/kg tyrosol and 2.6 mg/Kg hydroxytyrosol from olive oil; Servili et al. 2002), and time-consuming (Achmon and Fishman 2015). Therefore conventional method cannot meet the large and fast growing demands of aromatic alcohols compared to chemically synthesized 2-PE, tyrosol or hydroxtyrosol. For instance, 2-PE costs labelled with "natural" (non-chemical) was estimated around US$ 1000/ kg (Etschmann et al. 2002; Hua and Xu, 2011), whereas "unnatural" 2-PE was available on a scale of US$ 5/ kg (Hua and Xu 2011). For industrial purposes, the majority of 2-PE, tyrosol and hydroxytyrosol are produced by chemical synthesis (Etschmann et al. 2002).The chemical synthesis of tyrosol and hydroxytyrosol can be developed from analogs such as the 2-phenylethanol (Sysolyatin et al. 2015) and tyrosol (Bovicelli et al. 2007) as starting materials, respectively. The majority of 2-PE is synthesized from benzene or styrene via a Friedel–Craft reaction (Etschmann et al. 2002; Suastegui and Shao 2016), with a world's annual production approximately 10,000 ton/year (Hua and Xu, 2011; Chreptowicz et al. 2016). 2-PE global market size is estimated to reach US $700 million by 2019 (Pandal 2014; Suastegui and Shao 2016). However, large-scale chemical manufacturing is often associated with such problems such as technical difficulties, increased fire danger, undesired by-products, and higher purification costs as well as the processes require protection and deprotection steps (Etschmann et al. 2002; Hua and Xu 2011; Achmon and Fishman 2015; Sysolyatin et al. 2015). Also, a chemical process may have negative impacts on the environment and products are legally considered as "unnatural", which are prohibited from being used in some application especially in food industries and cosmetics (Xu et al. 2007). Due to increasing concern about chemical process, there is a need for developing a new method for production of these components. Microbial production or bioconversions of natural precursors using either microbial cells or enzymes could be a competitive alternative and environmentally friendly approach with obvious advantages and great potential for production of 2-PE, tyrosol and hydroxytyrosol (Espín et al. 2001; Etschmann et al. 2002; Allouche et al. 2004; Bouallagui et al. 2006; Brooks et al. 2006; Hua and Xu 2011; Satoh et al. 2012a and b; Yin et al. 2015; Li et al. 2018). Hence based on the FDA regulation and European legislation, products obtained by biotechnological approach can be considered as

"natural", if the substrates for the process are of natural origin (Hua et al. 2007a; Hua et al. 2007b).

1.6.2 Heterologous production of aromatic alcohol from a simple carbon source (glucose)

1.6.2.1 Microbial biosynthesis of 2-PE

In the past decades, microbial biotechnology has emerged as the leading method for biosynthesis of some aromatic compounds, such as phenol (Kim et al. 2014; Miao et al. 2015), vanillin (Hu et al. 2007a; Hu et al. 2010), benzaldehyde (Krings et al. 1998; Serra et al. 2005), benzyl alcohol (Pugh et al. 2005), phenylacetic acid (Etschmann et al. 2005; Koma et al. 2012; Guo et al. 2018), tyrosol (Satoh et al. 2012a; Bai et al. 2014; Li et al. 2018), hydroxytyrosol (Satoh et al. 2012b; Li et al. 2018) and 2-phenylethanol (Etschmann et al. 2005; Koma et al. 2012; Kim et al. 2014; Kang et al. 2014; Yin et al. 2015; Machas et al. 2017; Li et al. 2018; Liu et al. 2018; Guo et al. 2018). In the past decades, several microbial species such as yeast (Kim et al. 2014; Yin et al. 2015), *Aspergillus* (Lomascolo et al. 2001; Masuo et al. 215), *Microbacterium sp.* (Jollivet et al. 1992) and *Enterobacter* sp. (Zhang et al. 2014) have been reported with 2-PE production capacity. Yeast, such as *Saccharomyces cerevisiae* (Kim et al. 2014a) and *Kluyveromyces marxianus* (Kim et al. 2014c), can synthesize 2-phenylethanol through the Ehrlich pathway (Etschmann et al. 2002; Wittmann et al. 2002). Details of the Ehrlich pathway and involved enzymes has already described in section 1.5.2.2 (and Figure 1-7). Furthermore, although yeasts are known as good candidate for 2-PE synthesis, the efficiency is quite low; so many attempts were made to enhance efficiency such as optimization process, screening of stress-tolerant strain and metabolic engineering of related pathways (Etschmann and Schrader 2003; Etschmann and Schrader 2006; Hua and Xu 2011; Kim et al. 2014; Chreptowicz et al. 2016; Suastegui and Shao 2016). Previous studies have reported *E. coli* as a potential candidate for production of aromatic alcohols, particularly for 2-PE (Koma et al. 2012; Kang et al. 2014; Machas et al. 2017). Accordingly, it was shown that a phenylalanine overproducer *E. coli* strain through overexpression of phenylpyruvate decarboxylase gene (*ipdC*) from *Azospirillum brasilense* and aldehyde reductase gene (*yahK*) from *E. coli* can produce 7.7 mM (941 mg l^{-1}) of 2-PE from 51.7 mM glucose (yield~ 0.10 g g^{-1}) (Koma et al. 2012). In another example, a recombinant 2-PE biosynthesis pathway composed of *adh1* (encoding alcohol dehydrogenase) and *kdc* (encoding phenylpyruvate decarboxylase) from *Saccharomyces cerevisiae S288c* and *Pichia pastoris*

GS115 were heterologously expressed in *E. coli* resulting in 285 mg l^{-1} of 2-PE from 20 g l^{-1} glucose (yield~ 0.01 g g^{-1}) (Kang et al. 2014). Considering that a few attempts have been made on recombinant production of 2-PE in *E. coli* (Koma et al. 2012; Kang et al. 2014), hence a new platform in *E. coli* was constructed that can produce 2-PE yield and titer more efficiently (Figure 1-7).

1.6.2.2 Microbial biosynthesis of tyrosol and hydroxytyrosol

In recent years more attention has been paid into the microbial production of tyrosol and hydroxytyrosol due to their potential biological activities and beneficial health effects (Satoh et al. 2012 a and b; Bai et al. 2014; Rodríguez-Morató et al. 2016; Lee et al. 2018; Liu et al. 2018). The metabolic engineering have been investigated as a possible tool for the microbial production of these valuable substances by reconstituting natural pathways or even designing artificial pathways (Sun et al. 2015; Liu et al. 2018). Naturally tyrosol, like 2-PE, is synthesized in *Saccharomyces cerevisiae* through Ehrlich pathway from 4-hydroxyphenylpyruvate (4-HPP) through the sequential catalysis of phenylpyruvate decarboxylase, and alcohol dehydrogenase (Figure 1-7) (Sentheshanmuganathan and Elsden 1958; Hazelwood et al. 2008). In addition, it has been demonstrated that tyrosol can be recombinantly synthesized through three pathways in *E. coli*: Shortly in the first pathway, tyrosine decarboxylase catalyzes conversion L-Tyr to tyramine, and then tyramine oxidase and alcohol dehydrogenase convert tyramine to 4-hydroxyphenylacetaldehyde and tyrosol, consecutively (Satoh et al. 2012b). It has been also shown that tyrosol can be synthesized from tyrosine by using enzymes involved in the Ehrlich pathway from *Saccharomyces cerevisiae* (Bai et al. 2014; Li et al. 2018). Here the key intermediate, 4-hydroxyphenylpyruvate (4-HPP), is derived from L-Tyr by transamination and then decarboxylated to 4-hydroxyphenylacetaldehyde (4-HPAA) by pyruvate decarboxylase (Aro10) and finally reduced to tyrosol by alcohol dehydrogenase (ADHs). The third pathway utilized different AAs genes encoding aromatic aldehyde synthases from *Arabidopsis thaliana*, *Petunia hybrid*, and *Petroselinum crispum* converts tyrosine to 4-hydroxyphenylacetaldehyde (4-HPAL) and then 4-HPAL was reduced to tyrosol by different alcohol dehydrogenase (Chung et al. 2017). It was previously reported that recombinant *E. coli* can produce tyrosol, but the pathway efficiency is still low and needs to be further improved for economical production of tyrosol. In contrast, hydroxytyrosol can be produced from tyrosol via whole cell bioconversion

of *E.coli* (Brooks et al. 2005) *or Pseudomonas aeruginosa* (Allouche et al. 2004) immobilized resting cells by only one step reaction catalysis by 4-hydroxyphenylacetate 3-hydroxylase (HpaBC). So far, two pathways are reported for hydroxytyrosol biosynthesis in *E. coli*. The first pathway starts from tyrosine and subsequently tyrosine is converted to hydroxytyrosol by tyrosine hydroxylase (TH), l-DOPA decarboxylase, tyramine oxidase, and alcohol dehydrogenases, consecutively (Satoh et al. 2012a).

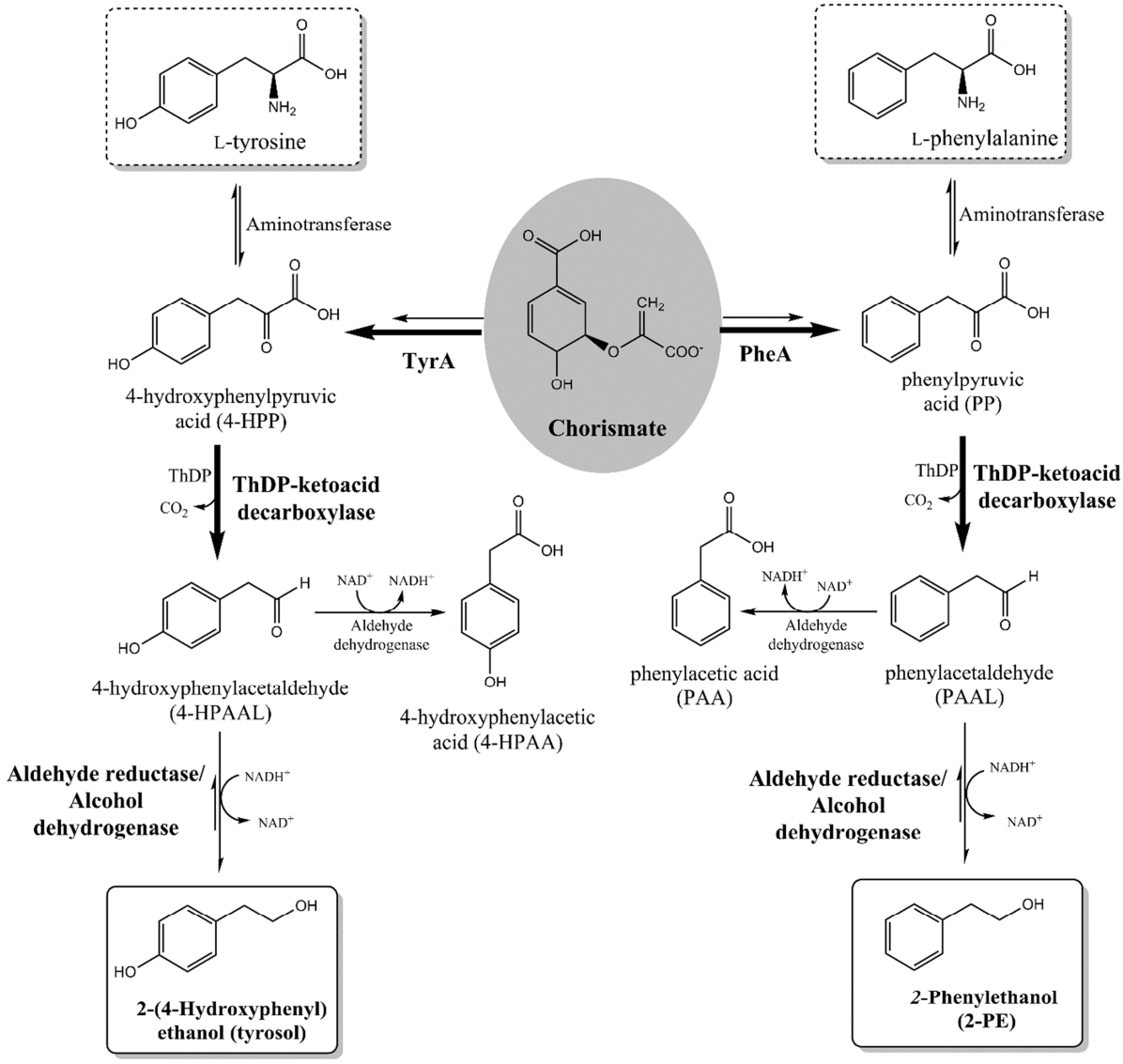

Figure 1-7 Mmicrobial biosynthesis of 2-PE and tyrosol through Ehrlich pathway. Starting from chorismic acid, PP or 4-HPP is formed via PheA/ TyrA. Following by decarboxylation of PP to PAL or 4-HPP to 4-HPAL by ThDP-ketoacid decarboxylase and subsequently PAAL/4-HPAAL either reduce to 2-PE/tyrosol by alcohol dehydrogenase/aldehyde reductase or oxidized to PAA/4-HPAA by aldehyde dehydrogenase. Tyrosol pathway provided here is from YMDB: the Yeast Metabolome

Database (Jewison et al. 2012) and 2-PE pathway from Etschmann et al. 2002.

More recently, an artificial biosynthesis pathway for hydroxytyrosol production in *E.coli* through tyrosol was established (Li et al. 2018). A recombinant tyrosol biosynthetic pathway by overexpression of Aro10 was constructed to covert 4-hydroxyphenylpyruvate to 4-hydroxyphenylacetaldehyde and then by alcohol dehydrogenase (ADH) further improved tyrosol production. The artificial pathway was further extended for hydroxytyrosol production by overexpressing *E. coli* native hydroxylase HpaBC (Li et al. 2018).

1.7 Problem definition of the current study

Since only a few aromatic amines (AAs) in nature have been found so far (section 1.5.1), this study shall open up new perspectives in the development of biomass-derived AAs. Microbial production of the aromatic "bio-monomers" (L-PAPA, PAPE, 4-APA) enables the construction of various aromatic polyamide/imide derivatives with different physical properties (Suvannasara et al. 2014; Tateyama et al. 2016; Tsuge et al. 2016; Kawasaki et al. 2018). On the other hand, considering importance of these higher-value compounds in the chemical and pharmaceutical industry, the microbial production of these compounds as an alternative and inexpensive method is still negligible (Koma et al. 2012; Kang et al. 2014; Masou et al. 2016; Li et al. 2018; Liu et al. 2018). However, since aromatic amines/aromatic alcohols occur naturally in low concentrations (1.5.1 and 1.6.1), chemical syntheses cannot be carried out inexpensively due to the required protective group chemistry, detrimental impacts on the environment, low product yields or high substrate costs (sections 1.5.2 and 1.6.2). In addition, the microbial production of these aromatic amines/aromatic alcohols have so far been performed for only a few studies on a small scale and obtained results are still far from industrial scale production (Koma et al. 2012; Suvannasara et al. 2014; Kang et al. 2014; Masuo et al. 2016; Tateyama et al. 2016; Machas et al. 2017; Kawasaki et al. 2018; Li et al. 2018). In order to achieve a more economical production, it can be deemed affordable to convert the raw materials glycerol/glucose into higher-value products. Since *E. coli* is able to utilize glycerol/glucose as C sources, a microbial conversion into more valuable fine chemicals is conceivable. Furthermore it is a core issue to maximize the efficiency of *E. coli* "chassis' strain to the best performs production of these higher-value components. As previously mentioned, the number of aromatic amines/aromatic alcohols compounds engineered from renewable resources remains limited (Masuo et al. 2016; Tateyama et al. 2016; Kawasaki et

al. 2018), and thus the focus of this work will be on the biosynthetic production of higher-value compounds derived from chorismic acid (Figure **1-8**).

1.8 Objectives of the current study

The one aim of this study is metabolic engineering of *E. coli* for construction of a de novo platform for microbial biosynthesis of five interesting aromatic amines and aromatic alcohols component, which are derived from the last common metabolite of shikimate pathway, chorismic acid (Figure **1-8**). Steps in the metabolic engineering to achieve the desired goals are given in the following flowchart.

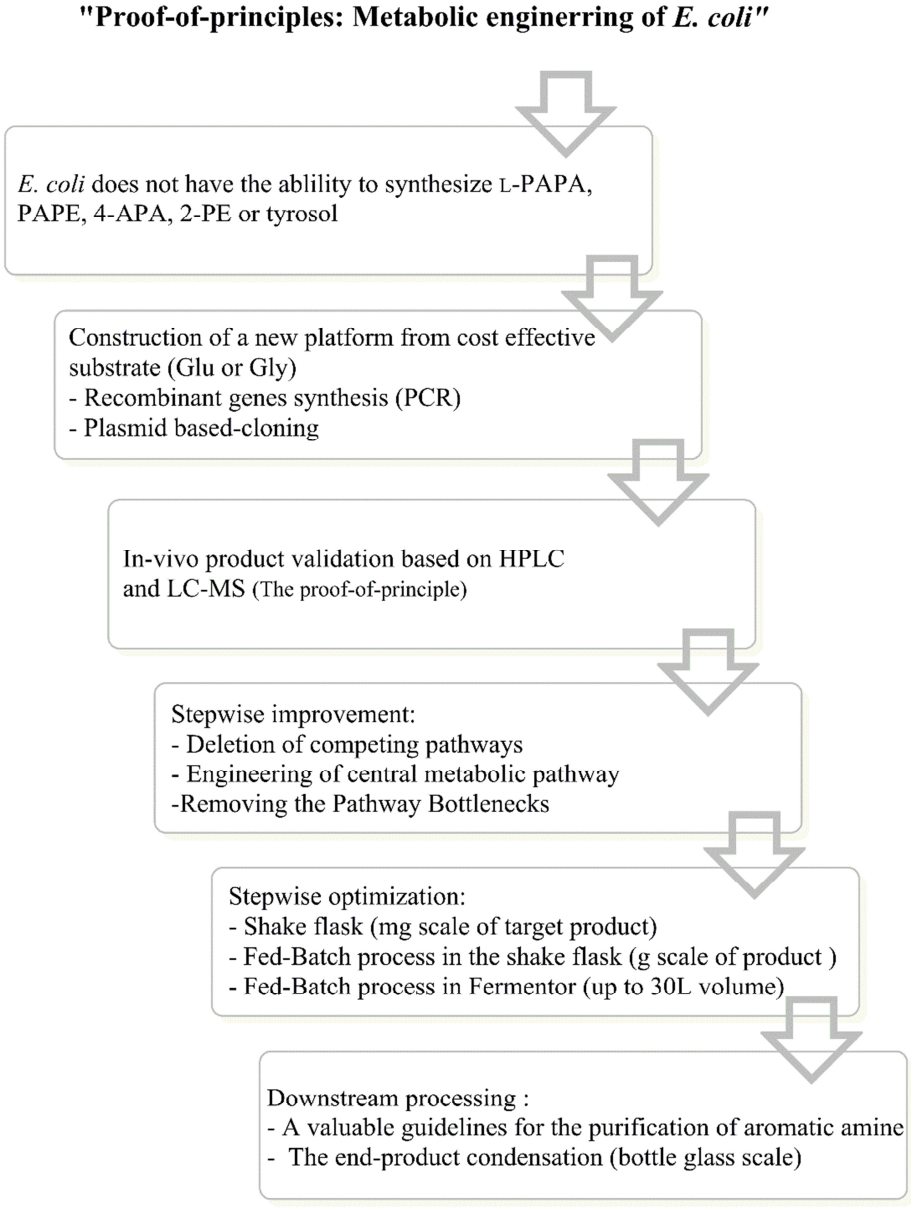

The aromatic amines/aromatic alcohols compounds can be found in such groups of plants, bacteria (*S. venezuelae, S. pristinaespiralis* and *P. fluorescens*) and yeast (*S. cerevisiae* and *K. marxianus*), but *E. coli* does not have the ability to naturally synthesize these compounds (Brown et al. 1996; Blanc et al. 1997; Herbert and Knaggs 1988; Giovannini et al. 1999; He et al. 2001; Etschmann et al. 2002). Since these compounds may inhibit the cell growth of *E. coli*, their effect on cell growth are studied and considered in our metabolic engineering approach. The biosynthesis of all five target components was studied with recombinant *E. coli* strains, starting from the renewable resource glycerol or glucose (Figure **1-8**). In this regard, microbial biosynthesis of these target compounds should be possible in principle if suitable enzymes for the conversion of chorismic acid (as main precursor) to target metabolite are found and overexpressed. An effective microbial synthesis of aromatic amines component (L-PAPA, PAPE and 4-APA) and aromatic alcohol (2-PE, tyrosol) should be made possible by the following proof-of-principles.

The first step required in the biosynthesis of these three interesting aromatic amines, is conversion of chorismic acid to ADC (Figure **1-8**) through substitution of the *para*-hydroxy group in chorismic acid by an amino group. This reaction has been previously described several times in *E. coli* (Walsh et al. 1987; Green and Nichols 1991; Viswanathan et al. 1995; Parsons et al. 2002) and *Corynebacterium glutamicum* (Kozak 2006; Stolz et al. 2007; Kubota et al. 2016). In this study a *pabAB* gene from folate biosynthesis pathway in *Corynebacterium glutamicum* was preferred over the two separate genes *pabA* and *pabB* which reside in the *E. coli* chromosome. In addition, it was shown that combination of *pabA* and *pabB* genes from *E.coli* lead to a less active enzyme (Kozak 2006). Therefore, the enzymes that catalyze this reaction, PabAB $_{C.glu}$, can be plasmid overexpressed or alternatively integrated into host's chromosome in order to direct flux from chorismic acid to ADC. The second and third steps are the microbial conversion of ADC to ADP and APP (Figure **1-8**) which are not physiological for *E. coli*. Therefore, the two enzymes PapB and PapC from chloramphenicol biosynthesis pathway in *Streptomyces venezuelae* can be plasmid overexpressed to possibly convert ADC to ADP and then APP, consecutively. It has already shown that PapB and PapC have an activity in L-PAPA production in *E. coli* (Mehl et al. 2003). From here onwards, two pathways are possible, APP can be transaminated to L-PAPA by aminotransferase enzyme (TyrB, AspC) which are physiological function in *E.coli* or decarboxylated to APAAL by phenylpyruvate decarboxylase (Figure **1-8**).

Since this decarboxylation reaction is not physiological in *E. coli*, thus it was preferred to overexpress the Aro10 from *S. cerevisiae* (Kneen et al. 2011; Vuralhan et al. 2003 and 2005) with diverse range of substrate spectrum. The Last step in PAPE and 4-APA pathway is reduction of APAAL to PAPE by YahK (aldehyde reductase) or oxidation to 4-APA by FeaB (aldehyde dehydrogenase) (Figure **1-8**). By combined protein overexpression of PabAB together with PapB and PapC, L-PAPA should then be microbial synthesized. Furthermore, the simultaneous expression of Aro10 and YahK or FeaB together with PabAB, PapB and PapC, should lead to the microbial biosynthesis of PAPE or 4-APA in *E. coli*, respectively. Moreover, effective conversion of chorismate to these three aromatic amines requires the stepwise optimization of central metabolism and shikimate pathway which are involved (i) elimination of competing pathway, (ii) elimination of tyrosine repression (TyrR), (iii) removing the bottleneck by overexpression of rate limiting steps in shikimate pathway/downstream pathway and (i) overexpression of genes involved in the central metabolism pathway (*tktA, glpX*) (Sprenger 2007b; Gottlieb et al. 2014). It has been reported that aromatic amino acids can pass through the cell membrane. Considering structure similarity of aromatic amines to aromatic amino acid, therefore, it can be assumed that aromatic amines can also pass through the cell membrane and detect in the culture supernatant (Figure **1-8**). Apart from plasmid-based overexpression that was applied in this study, several chromosomal integration strategies (Datsenko and Wanner 2000; Albermann et al. 2010; Li et al. 2015; Jiang et al. 2015) have been also developed to overcome problems of expression stability in plasmid-based system. It should be taken into consideration that chromosomal integration methods have also some disadvantages such as, integration process is labor-intensive and time-consuming and production rate is low (one copy of target gene) compared to plasmid-base system (Palomares et al. 2004).

In addition, the cultivation experiments was performed initially in the conventional shake flask, which is a very common and useful tool that allows a large number of experiments on the laboratory scale simultaneously. The shake flask is a suitable laboratory tool for researchers to obtain requires data and knowledge at the beginning of research. However, this method has disadvantages such as less regulation and controlling possibilities or limitations in oxygen supply and feed strategy (Winkler and Socher 2014). To overcome these issues, Fed-batch operation in a closed fermenter can be applied. Finally, a high-performance method can be introduced for the product isolation.

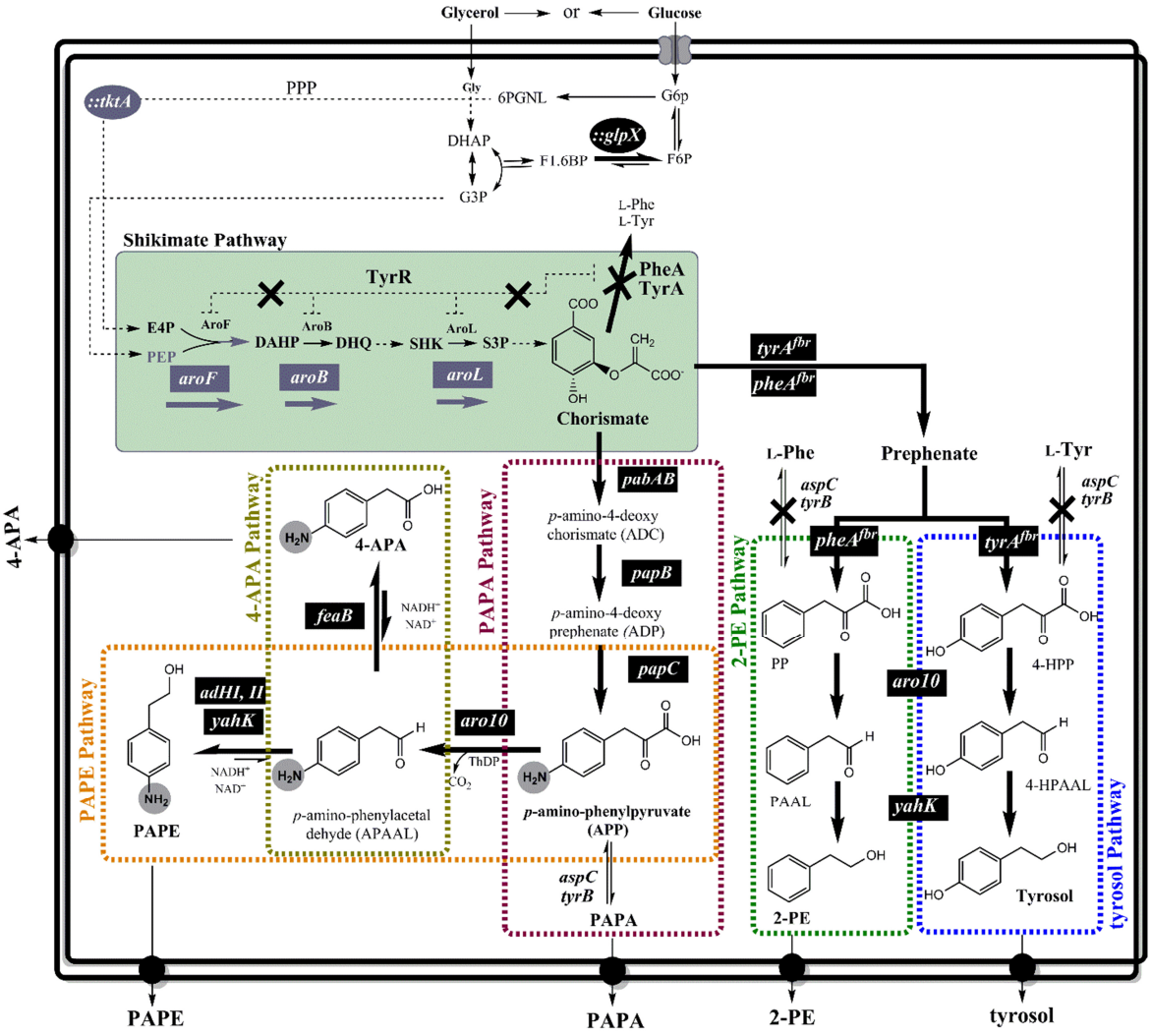

Figure 1-8 Schematic diagram depicting the study objectives. The aim of this study was microbial biosynthesis of aromatic amine components (L-PAPA, PAPE or 4-APA) and aromatic alcohols (2-PE or tyrosol) from simple carbon source by pathway engineering in *E. coli*. Enzymes and molecules are abbreviated as follows : G6p, Glucose 6-phosphate; F6p, fructose 6 phosphate; G3P, Glyceraldehyde 3-phosphate; PPP, Pentose phosphate pathways; E4P, Erythrose 4 phosphate; PEP, Phosphoenolpyruvic acid; DAHP,3-Deoxy-D-arabinoheptulosonate 7-phosphate; DHQ, Dehydroquinate; SHIK, Shikimate; S3P, Shikimate 3- phosphate; TktA, transketolase A; AroF, AroG and AroH, DAHP synthase; AroB, Dehydroquinate synthase; AroL, Shikimate Kinase; PabAB, 4-Amino-4-deoxychorismate synthase (ADC synthase); PapB, 4-amino-4-deoxychorismate mutase; PapC, 4-amino, 4-deoxyprephenate dehydrogenase; Aro10, phenylpyruvate decarboxylase; YahK, Aldehyde reductase; FeaB, phenyl acetaldehyde dehydrogenase; ADHI, II, alcohol dehydrogenase I and II; $PheA^{fbr}$, chorismate mutase/prephenate dehydratase (feedback resistance); $TyrA^{fbr}$, chorismate mutase/prephenate dehydrogenase (feedback resistance); AspC, aspartic aminotransferase and TyrB, aromatic aminotransferase . (Gottlieb et al. 2014; Masou et al. 2016; Kang et al. 2014; Li et al. 2018).

In the second part of this study, a de novo platform for production of aromatic alcohols in *E. coli* was established. Two physiological pathways, phenylalanine and tyrosine were extended to biosynthesis of 2-PE and tyrosol in *E.coli*, respectively (Figure **1-8**). Here a de-novo recombinant biosynthesis pathway for more efficient and high titer 2-PE and tyrosol production in *E. coli* directly from glucose as inexpensive carbon source was demonstrated (Figure **1-8**). To improve L-Phe/L-Tyr production, several efforts were made by engineering shikimate pathway in *E.coli* through overexpression of four genes composed of *aroF*, *aroB*, *aroL* and $PheA^{fbr}$/$TyrA^{fbr}$ encoding bifunctional enzyme chorismate mutase-prephenate dehydratase/dehydrogenase (feedback inhibition resistant), which catalyzes the necessary reaction of chorismate conversion to phenylpyruvate (PP) or 4-hydroxyphenylpyruvate (4-HPP) in *E. coli*. In addition, two aminotransferase genes (*tyrB* and *aspC*) as well as *tyrR* as the negative regulator in *E. coli* were deleted (Figure **1-8**). Phenylpyruvate (PP) or 4-hydroxyphenylpyruvate (4-HPP) are converted to phenylacetaldehyde (PAAL) or 4-hydroxyphenylacetahldehyde (4-HPAAL) by the enzyme phenylpyruvate decarboxylase (Aro10) from *Saccharomyces cerevisiae*, followed by endogenous reduction of PAAL/4-HPAAL to 2-Phenylethanol (2-PE) or tyrosol by aldehyde reductase (*yahK, yqhD, yjgB*) (Koma et al. 2012). In addition, product inhibition may limit the high-titer production of 2-PE/tyrosol using recombinant *E.coli*, thus in situ product removal (ISPR) techniques including two-phase extraction by different organic components were applied (Etschmann et al. 2002; Kim et al. 2014; Hua et al 2010; Li et al. 2015). The production process was performed both under batch and fed-batch modes in the shake flask and fermenter. The products isolation through a combination of centrifugation and two-phase extraction was performed.

So far, however, synthesis of aromatic amine (AA) with glycerol as C source has not been considered in detail. For this reason, another aim of this is to investigate the potential of using glycerol as the renewable carbon substrate to produce valuable aromatic amines by Recombinant *E. coli* Strains. In this work, therefore, it should not only be investigated whether the use of glycerol in comparison to glucose is possible in principle for Aromatic amines or Aromatic alcohols synthesis. It should also be examined whether the production in engineered *E. coli* strains can be further enhanced by means of pathway engineering and process optimization? and can production strains be efficiently converted glycerol (as the major byproduct of biodiesel) into higher-value products?

2. Materials and Methods

2.1 Chemicals and Reagents

The chemicals used in this study are listed in the Table **2-1**, *para*-amino-L-phenylalanine hydrochloride (L-PAPA), *para*-amino phenylethanol (PAPE), 2-phenylethanol, tyrosol and hydroxytyrosol were purchased from Sigma-Aldrich Chemie GmbH (Taufkirchen, Germany), *para*-amino phenylacetic acid (4-APA) from Merck KGaA (Darmstadt, Germany) and all other chemical were either from Carl Roth GmbH (Karlsruhe, Germany), Fluka (Taufkirchen, Germany) or Merck KGaA (Darmstadt, Germany) and were of the highest available purity. All restriction enzymes and T4 DNA ligase were purchased from New England Biolabs (Ipswich, USA). KOD Hot Start DNA Polymerase for gene amplification was from Novagen, Merck KGaA (Darmstadt, Germany), Taq DNA polymerase used for screening-PCR was from Genaxxon Bioscience GmbH (Ulm, Germany). Plasmid preparation and gel extraction kits were obtained from Macherey-Nagel (Düren, Germany) and DNA sequencing services were provided by GATC Biotech (Constance, Germany).

Table 2-1 Substances and reagents used in this study

Name of chemiclas	Company	Purity
2-(4-Aminophenyl) ethanol	Sigma-Aldrich (Taufkirchen, Germany)	≥ 98.0%
2-(4-Hydroxyphenyl)ethanol (tyrosol)	Sigma-Aldrich (Taufkirchen, Germany)	98%
2-Phenylethanol	Sigma-Aldrich (Taufkirchen, Germany)	99%
3,4-dihydroxyphenylethanol (Hydroxytyrosol)	Sigma-Aldrich (Taufkirchen, Germany)	≥ 98.0%
4-Amino-L-phenylalanine hydrochloride	Sigma-Aldrich (Taufkirchen, Germany)	96
4-Aminophenylacetic acid	Merck KGaA (Darmstadt, Germany)	98%
Acetonitril	Carl Roth GmbH (Karlsruhe, Germany)	≥99,9 %
Acetone	Carl Roth GmbH (Karlsruhe, Germany)	≥99,9 %
Agar powder	Carl Roth GmbH (Karlsruhe, Germany)	
Agarose powder	Bio-Rad (Munich, Germany)	
Ammonium sulfate	Sigma-Aldrich (Taufkirchen, Germany)	≥99.5
Ampicillin Sodium salt	Carl Roth GmbH (Karlsruhe, Germany)	≥97 %
Ammonium persulfate (APS)	Carl Roth GmbH (Karlsruhe, Germany)	≥ 98%
L-Arabinose	Sigma-Aldrich (Taufkirchen, Germany)	≥ 99%
Bradford -Reagent (5X)	Carl Roth GmbH (Karlsruhe, Germany)	

Name of chemicals	Company	Purity
Calcium chloride dihydrate	Carl Roth GmbH (Karlsruhe, Germany)	≥99 %
CHAPS	GERBU Biotechnik GmbH	≥98%
Bromophenol blue	Carl Roth GmbH (Karlsruhe, Germany)	
Chloramphenicol	Carl Roth GmbH (Karlsruhe, Germany)	≥98.5
Coomassie Brilliant Blue G250	Carl Roth GmbH (Karlsruhe, Germany)	
Coomassie Brilliant Blue R250	Carl Roth GmbH (Karlsruhe, Germany)	
Diammonium hydrogen phosphate	Carl Roth GmbH (Karlsruhe, Germany)	≥98 %
Dipotassium hydrogen phosphate	Carl Roth GmbH (Karlsruhe, Germany)	≥98 %
Dodecane	Merck KGaA (Darmstadt, Germany)	≥99%
Sodium sulphate anhydrous	Carl Roth GmbH (Karlsruhe, Germany)	≥99 %
Dithiothreitol (DTT)	GERBU Biotechnik GmbH	≥99%
EDTA disodium salt	Carl Roth GmbH (Karlsruhe, Germany)	≥99 %
Ethanol	Carl Roth GmbH (Karlsruhe, Germany)	≥99.8 %
Ethyl acetate	Carl Roth GmbH (Karlsruhe, Germany)	≥99.5 %
Formic acid	Carl Roth GmbH (Karlsruhe, Germany)	98%%
Glucose monohydrate	Carl Roth GmbH (Karlsruhe, Germany)	≥99.5%
Glycerol	Carl Roth GmbH (Karlsruhe, Germany)	≥98%
Glycine	Carl Roth GmbH (Karlsruhe, Germany)	≥99%
Hydrochloric acid (HCL)	Carl Roth GmbH (Karlsruhe, Germany)	≥37%
Iron(II) Sulfate Heptahydrate	Carl Roth GmbH (Karlsruhe, Germany)	≥99%
Isopropyl β-D-1-thiogalactopyranoside (IPTG)	Carl Roth GmbH (Karlsruhe, Germany)	≥99%
Kanamycin	Carl Roth GmbH (Karlsruhe, Germany)	≥750 I.U.mg^{-1}
L-Aspartic acid sodium salt monohydrate	Honeywell Fluka™ (Taufkirchen, Germany)	≥99 %
L-Phenylalanine	Sigma-Aldrich (Taufkirchen, Germany)	≥98%
L-Tyrosine	Sigma-Aldrich (Taufkirchen, Germany)	≥98%
MacConkey-Agar Base (Difco)	Otto Nordwald (Hamburg)	
Magnesium sulfate Heptahydrate	Carl Roth GmbH (Karlsruhe, Germany)	≥99 %
Magnesium sulfate Monohydrate	Merck KGaA (Darmstadt, Germany)	≥99 %
Methanesulfonic acid	Carl Roth GmbH (Karlsruhe, Germany)	≥98%
2-Mercaptoethanol	Sigma-Aldrich (Taufkirchen, Germany)	≥99.0%
Methanol	Carl Roth GmbH (Karlsruhe, Germany)	≥99 %
Pharmalyte pH 3-10	Pharmacia Biotech Inc	
Phosphoric acid (85%)	Carl Roth GmbH (Karlsruhe, Germany)	≥85%
Polypropylene glycol 1200 (PPG)	Sigma-Aldrich (Steinheim, Germany)	≥97%
Polyethylene glycol 400, 2000 (PPG)	Sigma-Aldrich (Steinheim, Germany)	-
Potassium dihydrogen phosphate	Carl Roth GmbH (Karlsruhe, Germany)	≥99 %
Rotiphorese® Gel 30 (37,5:1)	Carl Roth GmbH (Karlsruhe, Germany)	
Sodium Acetate	Carl Roth GmbH (Karlsruhe, Germany)	≥99 %
Sodium chloride	Carl Roth GmbH (Karlsruhe, Germany)	≥99.8
Sodium dodecyl sulfate (SDS)	Carl Roth GmbH (Karlsruhe, Germany)	≥99 %
Sodium sulphate	Carl Roth GmbH (Karlsruhe, Germany)	≥99 %

Name of chemiclas	Company	Purity
Sulfuric acid	Merck KGaA (Darmstadt, Germany)	≥95-97%
TEMED	Honeywell Fluka™ (Taufkirchen, Germany)	
Tetrahydrofuran (THF)	Carl Roth GmbH (Karlsruhe, Germany)	≥99.5 %
Thiamine hydrochloride	Honeywell Fluka™ (Taufkirchen, Germany)	≥99 %
Thiourea	Sigma-Aldrich (Taufkirchen, Germany)	
Tributyrin	Carl Roth GmbH (Karlsruhe, Germany)	≥97.5 %
Trifluoroacetic acid	Carl Roth GmbH (Karlsruhe, Germany)	≥99,9 %
Tris	Carl Roth GmbH (Karlsruhe, Germany)	≥99 %
Trisodium citrate	Carl Roth GmbH (Karlsruhe, Germany)	≥99
Tryptone	Carl Roth GmbH (Karlsruhe, Germany)	
Urea	Carl Roth GmbH (Karlsruhe, Germany)	≥99,5 %
Yeast extract	Carl Roth GmbH (Karlsruhe, Germany)	
Alkaline Phosphatase	New England Biolabs (Ipswich, USA)	
BlueStar Plus Prestained Protein Marker	Nippon Genetics (Duren, Germany)	
Bovine Serum Albumins (BSA)	Sigma-Aldrich (Taufkirchen, Germany)	
GeneRuler DNA Ladder Mix 10kb	Thermo Fisher Scientific (Braunschweig)	
Immobiline DryStrip pH 3-10 L, 7 cm	GE Healthcare Life Sciences, Co	
KOD Hot Start DNA Polymerase	Novagen, Merck KGaA (Darmstadt, Germany)	
PCR clean-up, gel extraction	Macherey-Nagel (Düren, Germany)	
Plasmid DNA isolation Miniprep kit	Macherey-Nagel (Düren, Germany)	
T4 DNA ligase	New England Biolabs (Ipswich, USA)	
Taq DNA polymerase	Genaxxon Bioscience GmbH (Ulm, Germany)	

2.2 Bacterial strains and Plasmids

2.2.1 Bacterial strains

The bacterial strains used throughout this study are listed in Table 2.2. *E. coli* DH5α was used for cloning experiments. LJ110 is an *E. coli* wild-type strain, employed in this study as a parental host.

Table 2-2 Bacterial strains used in this study

Bacterial strains	Genotype	References
Escherichia coli		
BW25113	*lac*Iq *rrn*BT14 _*lac*ZWJWJ16 *hsdR514*_*ara*BADAH33 _*rha*BADLD78	(Datsenko und Wanner 2000)
BL21(DE3)	*F⁻ ompT hsdS$_B$ (rB⁻ mb⁻) gal dcm (DE3)* exprimiert T7-RNA-Polymerase	Novagen,Schwalbach

Bacterial strain	Genotype	References
LJ110 (W3110)	Wildtype W3110 *(F−, λ−, IN (rrnD-rrnE) 1, rph-1)*	(Bachmann 1972) (Zeppenfeld et al. 2000)
DH5α	*supE44 Δlac*U169 *(Φ80lacZ_*M15*), hsd*R17 *rec*A1 *end*A1 *gyrA*96 *thi-1 rel*A1	(Hanahan 1983)
FUS4	*LJ110 Δ(pheA tyrA aroF) Δlac::Ptac::aroFBL*	(Gottlieb et al. 2014)
FUS4.7	*FUS4 Δ rbs::Ptac::glpX Δ gal::Ptac::tktA-cat*	(Gottlieb et al. 2014)
FUS4.7-*tyrR*-cat	*FUS4 tyrA::cat-FRT*	(Mohammadi et al. 2018)
FUS4.7R	*FUS4.7 Δ tyrR::FRT*	(Mohammadi et al. 2018)
FUS4BC-cat	*FUS4 tyrB::cat-FRT, aspC ::cat-FRT*	(Mohammadi et al. 2019)
FUSBC	*FUS4 ΔtyrB, ΔaspC ::FRT*	(Mohammadi et al. 2019)
FUSBC-*tyrR-cat*	*FUS4BC tyrA::cat-FRT*	(Mohammadi et al. 2019)
FUSBCR	*FUS4BC ΔtyrR::FRT*	(Mohammadi et al. 2019)
Saccharomyces cerevisiae		
W3118	ATCC*:* MYA-423, MATa*, his3, trp1, leu2::* pLEU2 *lexAop6, ura3-52::*URA3-*lexAop8-lacZ*	(Van den Hazel et al. 1992)

2.2.2 Plasmids

The plasmids used in this study are shown in Table **2-3**.

Table 2-3 Plasmids used in this study

Plasmid Name	Description	References
pJNT522	*Kan*^{R}, RBS, *lac* I, *ori*	(Mohammadi et al. 2018)
pJNT*aroFBL*	pJNT Ptac::*aroF aroB aroL* from *E.coli*	(Mohammadi et al. 2018)
pJeM2	*rha*R *rha*S *rha*PBAD ,eGFP, mob *Kan*^{R}	(Jeske and Altenbuchner 2010)
pKD46	Red disruption system (γ, β, exo unter Kontrolle von *ara*Bp), AmpR, *ori* R101	(Datsenko und Wanner 2000)
pCP20	FLP$^+$, λ cI 857$^+$, λ ρR repA101$_{(ts)}$, Ap^R, Cm^R	(Cherepanov und Wackernagel 1995)
pCO1kanFRT	Amp^R FRT-*Km*^{R}-FRT	(U. Degner and G. Sprenger, unpublished, Gottlieb et al. 2014)
pCO1catFRT	Amp^R FRT-*cat*^{R}-FRT	(U. Degner and G. Sprenger, unpublished, Gottlieb et al. 2014)
pJF119EH	P_{tac}, RBS, Amp^R, *lac I, ori* colE1	(Fürste et al. 1986)
pC53	pJF119EH-*pabAB*; *pabAB* from *Corynebacterium glutamicum* (ATCC 13032); Cloned with BamHI	(Kozak S 2006, Ph.D. dissertation, Uni Stuttgart)
pF81	P$_{tac}$::*aroF, pheA*^{fbr} *, aroB, aroL* Amp^R, lacI	(Rüffer et al. 2004; Sprenger 2007 and Gottlieb et al. 2014)

Plasmid Name	Description	References
pMK-*papBC*	Cloning vector including the synthetic codon optimized genes of *papBC* $^{S.v.}$, Kan^R	Thermo Fisher, Geneart
pC53BC	pJF119EH *pabAB* $_{C.glu}$–*papB* and *papC* from *Streptomyces venezuelae*	(Mohammadi et al. 2018)
pBluescript SK	Amp^R, cloning vector, f1 *ori*	Thermo Fisher, Geneart
pBSK-*aro10*	pBluescript SK, *aro10* from *Saccharomyces cerevisiae*	This study
pBSK-*adHI*	pBluescript SK, *adHI* from *Saccharomyces cerevisiae*	This study
pBSK-*adHII*	pBluescript SK, *adHII* from *Saccharomyces cerevisiae*	This study
pBSK-*yahK*	pBluescript SK, *yahK* from *E.coli BW25113*	This study
pBSK-*feaB*	pBluescript SK, *feaB* from *E.coli BW25113*	This study
pC53BCA	pC53BC, *aro10* from *Saccharomyces cerevisiae*	(Mohammadi et al. 2019)
pC53BCAHI	pC53BC, *aro10* and adHI from *Saccharomyces cerevisiae*	(Mohammadi et al. 2019)
pC53BCAHII	pC53BC, *aro10* and adHII from *Saccharomyces cerevisiae*	(Mohammadi et al. 2019)
pC53BCAY	pC53BC, *aro10* from *Saccharomyces cerevisiae* and *yahK* from *E.coli BW25113*	(Mohammadi et al. 2019)
pC53BCAF	pC53BC, *aro10* from *Saccharomyces cerevisiae* and *feaB* from *E.coli BW25113*	(Mohammadi et al. 2019)
pJFA10	pJF119EH, *aro10* from *Saccharomyces cerevisiae*	(Mohammadi et al. 2019)
pJFA10F	pJF119EH, *aro10* from *Saccharomyces cerevisiae* and *feaB* from *E.coli BW25113*	(Mohammadi et al. 2019)
pFABL	pJNT522, *Ptac*::*aroF, pheA* ^{fbr}, *aroB, aroL,* Kan^R, lacI	(Mohammadi et al. 2019)
pJFA119-tyrA	pJF119EH, *tyrA* encoding feedback resistance variant	(N.Trachtmann, unpublished)
pBSK-tyrA	pBluescript SK, *tyrA* from pJFA119- *tyrA*	This study
pJFT	pJF119EH, *tyrA* from pBSK *tyrA*	This study
pJFTA10	pJFT, *aro10* from *Saccharomyces cerevisiae*	This study
pJNT*aroFBL-yahK*	pJNTaroFBL, *yahK* from *E.coli BW25113*	This study
pJNT*aroFBL-feaB*	pJNTaroFBL, *feaB* from *E.coli BW25113*	This study

2.2.3 Plasmids construction

2.2.3.1 Plasmid construction for L-PAPA production

For the overexpression of the genes $pabAB_{C.g}$ and $papBC_{S.v.}$, plasmid pC53BC was constructed (Mohammadi et al. 2018). The genes *papB* and *papC* from *S. venezuelae* (He et al. 2001; Piraee et al. 2001) were custom synthesized (Thermo Fisher, Geneart Regensburg) and codon optimized for *E. coli* to give pMK-*papBC* (see Table **2-3**); this plasmid was then restricted with BglII and BamHI. The resulting fragment containing *papBC* was isolated and then cloned as an BglII/BamHI fragment front the *pabAB* gene in plasmid pC53 (Kozak 2006), which was digested with BglII/BamHI, resulting in plasmid pC53BC (See Table **2-3**). The recombinant genes are

under the control of the P*tac* promoter in pC53, a vector which is based on pJF119EH (Fürste et al. 1986).

2.2.3.2 Plasmid construction for PAPE and 4-APA production

Recombinant plasmids pC53BCAY and pC53BCAF were constructed by subsequent insertion of the *aro10* and *yahK* or *feaB* genes downstream of *pabAB-papBC* genes the plasmid pC53BC (Mohammadi et al. 2019). First, the phenylpyruvate decarboxylase gene *aro10* (NCBI Gene ID: 851987, Appendix) was amplified from genomic DNA of *Saccharomyces cerevisiae W3118* (Vuralhan et al 2003; Kneen et al 2011) by using the primer pairs *aro10*-Fw/Rw (Table **2-13**). The *aro10* fragment (1.9 Kba) was first introduced into an EcoRV blunt-end restricted cloning vector pBluescript KS to generate pBSK-*aro10* and then sequence-verified before continuing with the construction process. The *aro10* fragment was then isolated by BamHI-XbaI restriction which was ligated to a BamHI/XbaI restricted pJF119EH and pC53BC subsequently to yield pJFA10 and pC53BCA (Table **2-13**), respectively. Two alcohol dehydrogenase genes *adHI* (NCBI Gene ID: 854068, Appendix) and *adHII* (NCBI Gene ID: 855349, Appendix) from *Saccharomyces cerevisiae* W3118, an aldehyde reductase gene (*yahK*, NCBI Gene ID: 944975, Appendix) and a phenylacetaldehyde dehydrogenase (*feaB,* NCBI Gene ID: 945933, Appendix) from *Escherichia coli BW25113* were PCR amplified from genomic DNA using primer pairs *adHI*-Fw/-Rw, *adHII*-Fw/-Rw, *yahK*-Fw/-Rw and *feaB*-Fw/Rw (Table **2-13**). The obtained PCR fragments, *adHI* (1.1 Kba), *adHII* (1.1 Kba), *yahK* (1.1 Kba) and *feaB* (1.5 Kba) were ligated blunt end into an EcoRV restricted pBluescript-KS (cloning vector) to generate pBSK-*adHI*, pBSK-*adHII*, pBSK-*yahK* and pBSK-*feaB*, respectively. The sequences were then verified by sequencing (GATC, Konstanz, Germany). The obtained fragments *adHI, adHII, yahK* and *feaB* were digested with SphI/SbfI and then ligated into pC53BCA previously digested with SphI/SbfI enzyme, to generate plasmids pC53BCAHI, pC53BCAHII, pC53BCAY and pC53BCAF, respectively. Additionally, the *yahK* and *feaB* fragments from BSK-*yahK* and pBSK-*feaB* were digested with SmaI/KpnI and ligated into pJNT*aroFBL*, yielding pJNT*aroFBL-yahK* and pJNT*aroFBL-feaB*, respectively (Table **2-3**). Constructs were confirmed by various digest screens and DNA sequencing. Ribosome binding site sequences were introduced directly by designing into primers. A list of plasmids and strains used in this study are listed in Table **2-3**.

2.2.3.3 Construction of L-Phe/2-PE production plasmids

For L-phenylalanine overproduction the plasmid pF81 was used (Rüffer et al. 2004). Recombinant plasmid pFABL (*kan*^{R}) was constructed by exchange of the ampicillin resistance gene of pF81 (Rüffer et al. 2004) by a kanamycin resistance gene from pJNT*aroFBL* (Mohammadi et al. 2018). Plasmid pJNT*aroFBL* possesses the features of vector pJNT522 (Mohammadi et al. 2018) which is derived from pJeM2 (Jeske and Altenbuchner 2010) and pJF119EH (Fürste et al. 1986). First, plasmid pJNT*aroFBL* was digested by restriction enzyme BamHI/SspI and then obtained fragments *aroB-aroL-kan*^{R} ligated into plasmid pF81 previously digested by BamHI/SspI (yielded P*tac-aroF-pheA*^{fbr}) to yield recombinant plasmid pFABL (kan^R). Plasmid pFABL contains the expression cassettes *aroF, aroB, aroL* and *pheA* (PheA (fbr)) encoding 3-deoxy-D-arabino-heptulosonate 7-phosphate (DAHP) synthase, dehydroquinate synthase, shikimate kinase I and chorismate mutase/prephenate dehydratase (feedback-resistance version), respectively. Additionally, for the conversion of L-phenylalanine to 2-PE, pJFA10 plasmid harboring *aro10* gene was used (Table **2-3**). The resulting recombinant plasmids pFABL and pFABL/pJFA10 were then transformed with *E.coli* strains for the overproduction L-phenylalanine and 2-PE, respectively.

2.2.3.4 Construction of L-Tyr/tyrosol production plasmids

For construction of L-Tyr overproducing plasmid, plasmid pBSK-*tyrA*^{fbr} (fbr : feed-back inhibition resistance) was first constructed by ligating a 1.2 kb EcoRI/HindIII fragment from pJF119-*tyrA*^{fbr} (Natalie Trachtman, unpublished) into pBluescript KS previously digested with EcoRI/HindIII. Then *tyrA* fragment from pBSK-*tyrA*^{fbr} was digested with EcoRI/KpnI and subsequently ligated into pJF119EH previously digested with EcoRI/KpnI to generate plasmid pJFT (Table **2-3**). Finally *aro10* fragment (1.9 Kba) was digested by KpnI/XbaI from pBSK-*aro10* plasmid (Table **2-3**) and then ligated downstream *tyrA* into pJFT previously digested with KpnI/XbaI to yield pJFTA10.

2.3 Media

2.3.1 Complex Media

Luria-Bertani (LB) medium (Bertani 1951) was used as a standard medium for the cultivation of *E. coli* in shake flasks or on agar plates (Table **2-4**). By adding 1.8 % agar to the medium,

solid nutrient medium was obtained (Sambrook and Russell 2001). Liquid cultures were incubated in a rotary shaker at 37°C- 150 rpm. For strains harboring plasmids which derived from pFJ119EH, pKD46 and pBluescript KS the medium was additionally supplemented with 100 μg ml^{-1} Ampicillin. In case of strains contain plasmids derived from pJNT522, the medium was supplemented with 50 μg ml^{-1} Kanamycin. To induce gene expression on plasmid derivatives of pFJ119EH and pJNT522, the LB medium was supplemented with 0.5 mM IPTG (final concentration) after culture has reached to OD_{600nm}~0.5-0.6. For the cultivation of the *E. coli* in liquid medium, Erlenmeyer flasks were used which were filled with a maximum of 10% of the total volume. For volumes up to 5 ml, test tubes (maximum filling volume 1 ml) were used.

Table 2-4 LB- media component

Component	Concentration
tryptone	10 g l^{-1}
Yeast extract	5 g l^{-1}
NaCl	10 g l^{-1}
Agar (1.8%)	18 g l^{-1}
Adjust the pH to ~ 7.0	
sterilized by autoclaving	

Super optimized broth (SOB, Table **2-5**) is a complex media that can be used during electro-transformation to help competent cells recover and ultimately result in better transformation efficiency. SOC is exactly the same as SOB, but SOC also contains 20mM glucose (3.603 g) (Hanahan 1983).

Table 2-5 SOB media component

Component	Concentration
tryptone	20 g l^{-1}
Yeast extract	5 g l^{-1}
NaCl	0.5 g l^{-1}
KCl	0.186 g l^{-1}
Adjust the pH to ~ 7.0	
990 ml with dH2O sterilized by autoclaving	
MgCl2	0.96 g l^{-1}
10 ml filter sterilized 1 M MgCl2	

To make SOC from SOB, after autoclaving 20 ml filter sterilized 1 M glucose was added to SOB media.

2.3.2 Minimal medium

The mineral medium used for synthesis of aromatic amines and aromatic alcohols in the batch/fed batch cultivations in the shake-flasks or fermenter was from Gerhardt (1984) with some modification as shown in Table **2-6**.

Table 2-6 Gerhardt minimal medium components [a]

Component	Concentration	Component	Concentration
KH_2PO_4	3 g l^{-1}	$MgSO_4*7H_2O$	0.3 g l^{-1}
K_2HPO_4	12 g l^{-1}	$FeSO_4*7H_2O$	0.112 g l^{-1}
		Na Citrate (15ml stock solution/ L medium)	1.5 g l^{-1}
$(NH4)_2SO_4$	5 g l^{-1}	$CaCl_2*2H_2O$	0.015 g l^{-1}
NaCl	0.1 g l^{-1}	Thiamine. HCL	0.0075 g l^{-1}
L-Phe and L-Tyr		0.04 mg ml^{-1} (0.22-0.24 mM)	
Glucose or glycerol	4.5-5 g l^{-1}		

[a] (Gerhardt et al. 1984)

For the synthesis of L-PAPA in 30 l bioreactor system, minimal medium from Gerhardt (1984) was modified by 1.5 times (50%) increasing concentration all compounds as listed in Table **2-7**. For all growth experiments with FUS4, FUS4.7 and FUS4.7R strains in minimal medium (MM), the untransformed *E.coli* cells were prepared from freshly-streaked agar plate. Subsequently, the transformation was carried out with the recombinant plasmids according to the procedure described in section 2.4.10. For selection, the cells were then plated on LB-Ampicillin, LB-Kanamycin or both of them. Subsequently, the transformed cells were adapted to growth on minimal medium by streaking on minimal medium agar plates plus ampicillin or kanamycin and the corresponding carbon source.

Table 2-7 Composition of the modified Gerhardt medium for the synthesis of L-PAPA in 30 l bioreactor

Component	Concentration	Component	Concentration
KH_2PO_4	4.5 g l^{-1}	$MgSO_4*7H_2O$	0.45 g l^{-1}
K_2HPO_4	18 g l^{-1}	$FeSO_4*7H_2O$	0.168 g l^{-1}
		Na Citrate (15ml stock solution /l medium)	2.25 g l^{-1}
$(NH4)_2SO_4$	7.5 g l^{-1}	$CaCl_2*2H_2O$	0.0225 g l^{-1}
NaCl	0.15 g l^{-1}	Thiamine. HCL	0.0125 g l^{-1}
L-Phe and L-Tyr		0.06 mg ml^{-1}	
Glycerol	8.1 g l^{-1}		

The plates were incubated for 24-48 hour at 37 °C and then used for the growth experiments. Since the cells carried a recombinant plasmid, antibiotic was always added to the medium. The *E.coli* wild type (LJ110) was also prepared from freshly-streaked agar plate for the growth experiments and then adapted to the growth on minimal medium with the appropriate carbon source on minimal medium agar plates. For the growth experiments, an initial pre-culture was prepared in a total volume of 10 ml of minimal media. The main culture was inoculated to OD_{600nm} ~ 0.06-0.08. For the experiments in shake flasks, 250 ml flasks were always used, which were filled with 20 ml of minimal medium (See 2.3.2). The experiments were performed with a 4.5-5 g l^{-1} carbon source (glucose/glycerol). The cells induced with 0.5 mM IPTG at the beginning of the growth exponential phase (OD_{600nm}~0.5-0.6) and cultured at 30°C in the batch and fed batch condition.

2.3.3 Media supplements

The strains based on FUS4 (FUS4.7, FUS4.7R, FUS4BC and FUSBCR) are auxotrophic for both L-Tyr and L-Phe, hence these two amino acids were added to the minimal media as supplementary (Gottlieb, K 2011; PhD dissertation, University of Stuttgart). After IPTG induction, additional L-Tyr (0.24 mM) and L-Phe (0.22 mM) were also added for more cell growth. Apart from L-Tyr and L-Phe, L-Asp was also added to the minimal medium at a concentration of 22.5 mM in case of auxotrophic for L-Asp (FUSBC and FUSBCR strains). If necessary, antibiotics and IPTG were added in the minimal medium as well (Table **2-8**).

Table 2-8 Media supplements used in this study [a]

Supplements	Stock solution	Final concentration	Solvent
L-Tyr	100 mM	0.24 mM	H_2O (titer with 37% HCL)
L-Phe	100 mM	0.22 mM	H_2O (titer with 5N NaOH)
L-Asp	1 M	22.5 mM	H_2O
Kanamycin	50 mg ml^{-1}	50 µg ml^{-1}	H_2O
Ampicillin	100 mg ml^{-1}	100 µg ml^{-1}	H_2O
IPTG	1 M	0.5 mM	H_2O

[a] (Gottlieb 2011, Ph.D Dissertation).

2.4 Molecular biology methods

Standard molecular biology methods were carried out according to Sambrook and Russell (2001). When using the commercial products described in the following sections, the methods described by the manufacturer were followed unless otherwise specified.

2.4.1 Polymerase chain reaction (PCR)

To amplify linear DNA from plasmids or chromosomal DNA, polymerase chain reaction (PCR) was used (Mullis and Faloona 1987). The standard PCR was performed in a thermal cycler from Analytik Jena AG (Jena, Germany). The annealing temperature and elongation time were adjusted according to primers (Table **2-13**) and expected fragment length.

Table 2-9 Standard PCR Reaction [a]

Component	50 µl reaction	Final Concentration
10X Standard Taq Reaction Buffer	5 µl	1X
10 mM dNTPs	1 µl	0.2 mM
10 µM of Forward Primer	1 µl	0.2 µM (0.05–1 µM)
10 µM of Reverse Primer	1µl	0.2 µM (0.05–1 µM)
Template (DNA, Plasmid)	1 µl	<1,000 ng DNA
Nuclease-free water	to 50 µl	-
Taq DNA Polymerase	1 µl	1 units/50µl PCR

[a] Method described by the manufacturer (Genaxxon Bioscience GmbH, Ulm, Germany)

In this work, Taq DNA polymerase (Table **2-9**) or KOD Hot Start DNA Polymerase (Table **2-11**) was used for PCR reactions depending on the reaction type. A standard PCR program is shown in the following Table (Table **2-10**).

Table 2-10 Standard PCR Program

Steps	Temperature	Time
Denaturation	95°C	5 min
1-Denature	94°C	30 seconds
2-Annealing	[a]	45 seconds*
3-Extension	72°C	60-120 seconds [b]
Repeat steps 1-3 for 30-35 cycle		
Final Extension	72°C	10 minutes
Hold	4-10°C	pause

[a] 10 °C lower than Melting Temperature (Tm) of primers
Tm= 4 (G+C) + 2 (A+T)
[b] Taq DNA Polymerase amplifies 1000 bp per 60 second

KOD Hot Start DNA Polymerase (Table **2-11** and Table **2-12**) with proof-reading activity according to manufacture procedure was used for the accurate PCR amplification of long strand DNA sequences (to minimize mutations in the amplifications) which were to be used for further cloning works.

Table 2-11 KOD Hot Start DNA polymerase Protocol [a]

Components	Volume	Final Concentration
10X Buffer for KOD Hot Start	5 µl	1X
25 mM MgSO4	3 µl	1.5 mM
dNTPs (2 mM each)	5 µl	0.2 mM
PCR Grade Water	(X=31) µl	-
Sense (5') Primer (10 µM)	1.5 µl	0.3 µM
Anti-Sense (3') Primer (10 µM)	1.5 µl	0.3 µM
Template DNA	(Y=2) µl	100 ng genomic DNA/ 10 ng plasmid DNA
KOD Hot Start Polymerase (1 U/µl)	1 µl	0.02 U/µl
Total reaction volume	50 µl	-

[a] Method described by the manufacturer (Novagen, Merck KGaA (Darmstadt, Germany))

For the amplification of target genes from chromosomal DNA, the primers were chosen to introduce restriction enzyme recognition sequences (underlined) outside the reading frame to facilitate later use for the construction of expression vectors (Table **2-13**).

Table 2-12 Cycling Conditions of KOD Hot Start DNA polymerase [a]

	Target size			
Step	< 500 bp	500–1000 bp	1000–3000 bp	> 3000 bp
Polymerase activation	95°C for 2 min			
1-Denature	95°C for 20 s			
2-Annealing	Lowest Primer T_m (ºC) for 10 s			
3-Extension	70°C for 10 s/kb	70°C for 15 s/kb	70°C for 20 s/kb	70°C for 25 s/kb
Repeat steps 1-3 for 30 (plasmid) or 35 cycle (genomic DNA)				

[a] Method described by the manufacturer (Novagen, Merck KGaA (Darmstadt, Germany))

The program of the amplification was carried out according to the 3-step PCR method of the manufacturer's instructions of the KOD Hot Start DNA Polymerase (Table **2-12**), whereby only the region homologous to the template was taken into account for the calculation of the melting temperature of the primers (Table **2-13**).

Table 2-13 Primer Sequences uses in this study

Primer names	Sequences (5'->3')
from *Saccharomyces cerevisiae*	
aro10-Fw	TAAGCGGATCCTAAGGAGGAACAATATGGCACCTGTTACAATTGA
aro10-Rw	TCCGCTCTAGACTATTTTTTATTTCTTTTAAGTGCCGCTGC
adHI-Fw	CTCACCTGCAGGAAGGAGGATATACATATGTCTATCCCAGAAACAAAAAGGT GT
adHI-Rw	TCGC GCATGCTTATTTAGAAGTGTCAACAACGTATCTACCA
adHII-Fw	ACACACCTGCAGGTAAGGAGGAACAATATGTCTATTCCAGAAACTCA
adHII-Rw	TCCGCGCATGCTTATTTAGAAGTGTCAACAACG

Primer names	Sequences (5'->3')
from *E. coli* BW25113	
yahK-Fw	CACACCTGCAGGAAGGAGGATATACATATGAAGATCAAAGCTGTT GGTG
yahK-Rw	TTTTGCATGCTCAGTCTGTTAGTGTGCG
feaB-Fw	AGTGCCTGCAGGAAGGAGGATATACATATGACAGAGCCGCATGT AGCAG
feaB-Rw	AGAGCATGCTTAATACCGTACACACACCGA
primers for inactivation of *tyrR*	
Del- *tyrR* -Fw	ATCATCATATTAATTGTTCTTTTTTCAGGTGAAGGTTCCCTGTGTA GGCTGGAGCTGCTTCG
Del - *tyrR* -Rw	AATATGCCTGATGGTGTTGCACCATCAGGCATATTCGCGCCATAT GAATATCCTCCTTAG
Ko-*tyrR*- Fw	TGACGGCACGACTCGGGATTAAAG
Ko-*tyrR*- Rw	AACAACGTTATCACCCTC TCCACT

The PCR products were then separated by agarose gel electrophoresis (section 2.4.4) and purified by NucleoSpin® Gel and PCR Clean-Up Kit (section 2.4.5), depending on the intended use.

2.4.2 Plasmid DNA isolation

Isolation of plasmid DNA was performed in accordance to the methods given in the NucleoSpin plasmid kit (Macherey-Nagel, Düren). Thereby DNA plasmids with high purity were obtained. The DNA plasmids were stored at -28 ˚C prior to use.

2.4.3 DNA cleavage by restriction enzymes

DNA cleavage by restriction endonucleases was carried out according to the manufacturer's instructions (New England Biolabs, Frankfurt a. M.). For this approach, approximately 500 ng of DNA was digested in 20µl corresponding buffer. 2-3 units of the restriction enzymes per µg of the DNA were used to achieve complete DNA digestion. The digestion was carried out for 1 to 2 hours (with PCR products) at the optimum temperature according to the manufacturer's instructions (New England Biolabs, Frankfurt a. M.).

2.4.4 Separation and visualization of DNA

Agarose gel electrophoresis was used to visualize and separate DNA fragments according to their size. The agarose concentration was 0.5-1.5% depending on the size of the DNA fragments. The DNA samples were admixed with 1/10 volume of 6X loading buffer (Thermo Fisher Scientific, Braunschweig) before loading to the agarose gel. Gel electrophoresis was carried out in TAE buffer (Table 2-14) and, depending on the gel size, at 80-120 V. 5 µl of GeneRuler DNA

Ladder Mix 100 bp - 10 kb (Thermo Fisher Scientific, Braunschweig) was used as standard Ladder. After electrophoresis, the gel was stained for 15 minutes in an ethidium bromide solution (Ethidium bromide solution (10 mg ml^{-1})) to make the DNA visible and document under UV light at 365 nm (Kozak S 2006; Gottlieb 2011).

Table 2-14 50X TAE buffer

Components	Concentration
Tris base	242.2 g
EDTA	100 ml (0.5M)
Acetic acid	57.1 ml
Adjust the pH to ~ 8.3	

→ Fill to 1l with dH_2O

2.4.5 Extraction of DNA fragments from agarose gels

For the purification of DNA fragments from agarose gels, the "NucleoSpin® Gel and PCR Clean-Up Kit" (Macherey-Nagel, Düren) was used according to the manufacturer's instructions.

2.4.6 DNA-Sequencing

The verification of nucleic acid sequences was carried out by sequence analysis in Clone Manager 7 (Sci Ed Software, USA) after custom sequencing by GATC Biotech (Konstanz, Germany).

2.4.7 Ligation of DNA fragments

The following procedure was used for ligation of the digested fragment into the linearized vector by bacteriophage T4 DNA ligase ligases (according to the manufacturer's instructions, New England Biolabs, Frankfurt a. M.).

- The following reaction in a micro-centrifuge tube was placed on ice.

Component	20 µl reaction
10X T4 DNA Ligase Buffer	2 µl
Vector DNA[1]	50 ng
Insert DNA	37.5 ng
Nuclease-free water	to 20 µl
T4 DNA Ligase	1 µl (20 U $µl^{-1}$)

[1] Above table shows a ligation using a molar ratio of 1:3 plasmid to insert (used of NEBio Calculator to calculate molar ratios). (ng of vector × kb size of insert) / kb size of vector × molar ratio of insert (3 insert:1 vector) = ng of insert

- After mixing by pipetting up and down, samples were incubated at room temperature for 1-2 hours (single strand overhangs) or overnight at 16 ° C (blunt-end). Then, chilled on ice and transformed 5 µl of the reaction into 200 µl competent cells by electroporation or heat shock.

2.4.8 Preparation of chemically competent *E. coli* cells (Cohen et al. 1972)

The calcium chloride method described below briefly (Cohen et al. 1972). The untransformed *E.coli* cells were prepared from freshly-streaked agar plate and transferred it into 10 ml of LB in sterile 100-ml polypropylene tube. Then, the culture was incubated overnight at 37°C (150 rpm).

The procedure is detailed below:

- 500 µl of pre- culture was inoculated into 50 ml of LB in a sterile 500-ml flask.
- The culture was incubated for 3-4 hour at 37 °C with shaking (150 rpm) until the OD_{600nm} reached 0.6-0.8 (< 10^8 cells ml).
- The cells was transferred to the sterile, ice-cold 50-ml falcon tube and chilled on ice for 10 min and followed by centrifugation at 6000 g for 10 min at 4 °C.
- The supernatant was discarded and then cell pellets was resuspended in 10 ml of ice-cold 0.1 M $CaCl_2$.
- Followed by centrifugation at 6000 g for 10 min at 4 °C.
- The supernatant was discarded once more and then cell pellets was resuspended in 2 ml of filter-sterilized ice-cold 0.1 M $CaCl_2$ and stored on ice.
- Finally, 200 µl aliquots was transferred in a sterile microfuge tubes and continued to transformation or snap freeze immediately in liquid nitrogen and stored at –70 °C.

2.4.9 Preparation of electro competent *E. coli* cells (Dower et al. 1988)

In order to obtain electrocompetent cells, an overnight culture of the cells was first inoculated in LB medium and then incubated at 37°C (150 rpm). On the next day, 500 µl of the overnight culture were transferred to 50 ml of LB medium. After reaching OD_{600nm}~0.6, the cells were removed by centrifugation (6000 g for 10 min at 4 °C) and resuspended in 10 ml of ice-cold 10% glycerol. The cells were then centrifuged once more and resuspended again in 10 ml of ice-cold

10% glycerol. After a final centrifugation (6000 g for 10 min at 4 °C), the cells were then resuspended in 2 ml ice-cold 10% glycerol and immediately used for the electroporation.

2.4.10 Transformation of competent *E. coli* cells

2.4.10.1 Transforming chemically competent *E. coli* cells using heat shock (Sambrook et al. 2001)

The following procedure was used to transform competent *E. coli* cells by heat shock:

- 200 µl of freshly or frozen of competent *E.coli* cells was placed on ice.
- Target DNA (50-100 ng of PCR product or plasmid) was added to the competent *E.coli* cells and then their mixture incubated on ice for 30 mins.
- Then, tube was placed at 42º C for 60-90 seconds to allow uptake of DNA into cells, followed by return on ice for 2 min.
- 1 ml of LB was added to each tube and then incubated at 37ºC for 45-60 mins in a rotary shaking incubator to let the cells recover from the heat shock and start growing again.
- The incubated cells were streaked onto agar plates with the Amp/Kan antibiotic. When blue/white selection was used, the plates were coated with 40 µl of 2% X-gal in DMSO and IPTG (0.1mM) at least one hour before streaking the bacteria.
- Usually two plates were streaked for each transformation. On one plate 100 µl of the 1 ml cell mixture was streaked and on the other one, remaining (900 µl) were streaked onto agar plates after the spin-down (14,000 rpm for 30 seconds).
- The inverted plates were incubated at 37ºC overnight and transformed colonies appeared after 12-16 hours.

2.4.10.2 Transforming electrocompetent *E. coli* cells using electroporation

For the transformation of linear PCR product in the chromosomal inactivation of genes (see 2.4.11) Datsenko and Wanner (Datsenko and Wanner, 2000) method was used. The *E.coli* cells were first made electrocompetent with the following protocol:

- 500 µl of pre- culture was inoculated into 50 ml of SOB (Table **2-5**) in a sterile 500-ml flask.

- The culture was incubated for 3-4 hour at 37 °C with shaking (150 rpm) until the OD_{600nm} reached 0.6-0.8 (< 10^8 cells ml).
- The cells were transferred to the sterile, ice-cold 50-ml falcon tube followed by centrifugation at 6000 g for 10 min at 4 °C.
- The supernatant was discarded and then cell pellet was resuspended in 10% ice-cold glycerol.
- The supernatant was discarded once more and then cell pellets was resuspended in 200 µl of filter-sterilized 10% ice-cold glycerol.
- Finally, 60 µl aliquots was transferred in a sterile microfuge tubes and continued to electroporation.

During the transformation, 20 µl PCR products (100-200ng) were added to 60 µl of cells on ice. Electroporation was performed under the following conditions with the Gene Pulser® II (Bio-Rad): 200 Ω, 25 µF, 1.95 kV for 4-5.5 milliseconds, followed by immediate mixing of the batch with 1 ml of SOC medium and incubation in a 1.5 ml of reaction tube overnight at 30 °C and 90 rpm. On the following day, the batches were in 250 µl portions spread onto LB agar plates with the appropriate antibiotic and incubated at 30 °C until colonies appeared.

2.4.11 Chromosomal inactivation of genes

The inactivation of *tyrR* was carried out according to the instructions of Datsenko and Wanner (2000) using PCR primers as given in Table **2-13**. The pCO1*cat*FRT plasmid (Gottlieb et al. 2014; Rodrigues et al. 2013) containing chloramphenicol resistance flanked by FRT sequences. This segment was amplified using specific primers with partially overlapping to the FRT cassette flanking around chloramphenicol resistance gene (20-22 nucleotides marked in underlined), and partially overlapping to the area around the *tyrR* gene in the *E. coli* genome (del-*tyrR*–Fw/del-*tyrR*-Rw, Table **2-13**). The pKD46 plasmid containing the *λ*-Red recombinase gene under a promoter induced by L-arabinose was transformed into the *E. coli* FUS4.7 strain (Gottlieb et al. 2014). Then the linear PCR product (chloramphenicol resistance flanked by FRT sequences) was transformed by electroporation into *E. coli* FUS4.7. The selections of positive clones were carried out for the introduced antibiotic marker and by colony PCR. Using test primers included (Table **2-13**): Ko-*tyrR*-Fw (~250-300 bp upstream of *tyrR*) and Ko-*tyrR*-Rw (~250-300bp downstream of *tyrR*), a fragment 1600bp long is to be expected if deletion is done correctly and

successfully. Otherwise, a fragment 2100 bp long will be amplified which means deletion was failed. After successful knockout of the *tyrR*, the altered cells were transformed with the plasmid pCP20 (Cherepanov und Wackernagel 1995), which carries the gene for the FLP recombinase and allow removing the chloramphenicol resistance cassette from the chromosome (Datsenko and Wanner 2000). To verify whether that the antibiotic resistance has been removed, PCR amplifications using upstream and downstream primers (Ko-*tyrR*-Rw and -Fw) were performed. The remarkable note here is that after removing the antibiotic resistance gene, FLP sites remain in the host chromosome. Finally the Red and FLP helper plasmids can be simply cured by growth at 37°-42°C because they are temperature-sensitive replicons (Datsenko and Wanner 2000). In addition, two aminotransferase (*tyrB* and *aspC*) in FUS4 strain were deleted by knocking out the *E. coli* chromosomal genes *tyrB* and *aspC* followed by deletion *tyrR* created FUSBCR (Dr. Youn Jung-Won, unpublished).

2.5 Biochemical methods for protein analysis

2.5.1 Ultrasonic cell disruption

For expression analysis and detection of enzyme activities in cell-free extracts, cells were disrupted by sonication (procedure was from Florian Baumgärtner 2016; Ph.D thesis, University Stuttgart). For this purpose, seed cultures were initially prepared in 10 ml LB medium with the appropriate antibiotic for selection on the expression plasmid. For inoculation, 1/50 of the total volume of the main culture was used and incubated at 30°C, 150 rpm. Recombinant gene expression was induced at OD_{600nm} ~ 0.6 by the addition of 0.5 mM IPTG and the culture was cultured on the shaker at least for another 6 hours at 30°C. Suspensions of induced and non-induced *E. coli* were harvested by centrifugation for 15 min at 6000 x g, 4°C. The resultant pellets were washed twice with ice-cold 50 mM Tris/HCl buffer or 100 mM potassium phosphate buffer (Table **2-15**) followed by centrifugation (15 min, 4 °C, 6000 g), then cell pellet was resuspended in 2 ml of the corresponding buffer or Lysis Buffer (Table **2-16**) for 2D- gel electrophoresis and then sonicated under ice cooling in 4 cycles with 30 ultrasound pulses each at 200 W and 20 kHz (Bandelin Sonopuls HD 200, BANDELIN electronic, Berlin) amplitude 55%; 30 seconds between the individual pulses. In order to cool the cell suspension, incubation was carried out on ice for 15 sec for each of the 4 cycles. The cell debris was then separated by

centrifugation for 60 min at 22,000 x g, 4˚C and then the soluble fractions (as cell-free extracts) were used for further works or stored at -70 °C until use.

Table 2-15 washing Buffer

Component	Concentration
Tris buffer Adjust pH to 7.5 with HCL	50 mM
Potassium Phosphate buffer Adjust pH to 7.5	100mM

Table 2-16 Lysis Buffer

Component	Concentration
Tris	40 mM
Urea	8 M
CHAPS	4 % (w/v)
Dithiothreitol	65 mM (made on day of use)
stored at -28ºC	

2.5.2 Determination of the protein concentration according to Bradford (Bradford 1976)

Total protein concentrations in the samples were determined using the Bradford protein assay protocol (Bradford 1976). A calibration curve with bovine serum albumin (BSA, Serva, Heidelberg) in concentrations of 0.05, 0.1, 0.15, 0.2 and 0.3 mg ml^{-1} was used as a standard for protein content (Figure **2-1**). Samples were diluted and then 50 µl was added to cuvettes, followed by 1ml Bradford reagent (Table **2-17**). The mixtures were then vortexed for 10s and incubated at room temperature in the dark for 10 min before measuring the optical density (OD) at 595 nm using UV cuvettes and a Varian Cary 50 Bio UV/Vis Spectrophotometer.

Table 2-17 Composition of the Bradford reagent [a]

Component	Concentration
Coomassie Brilliant Blue G-250	100 mg
Ethanol (96 %)	50 ml
H_3PO4 (85 %)	100 ml
H_2O	850 ml
Reagent after collection and incubation at RT was stored and protected from light at 4 °C.	
[a] (Bradford 1976)	

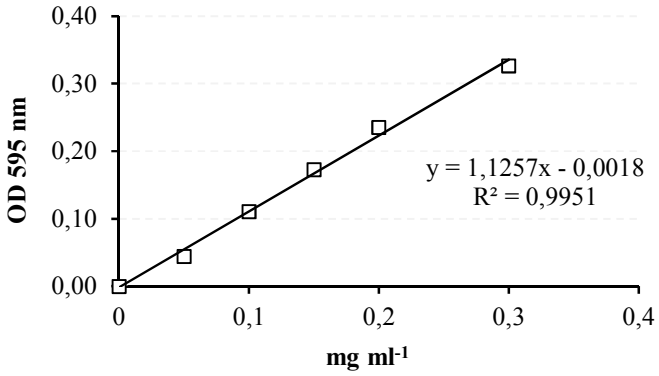

Figure 2-1 the example of Bradford calibration curve for estimation of protein concentration. The equation obtained from the regression line (y=1.1257x-0.0018) was later used as a guide to protein concentration.

2.5.3 SDS-polyacrylamide gel electrophoresis

2.5.3.1 SDS-polyacrylamide gel electrophoresis (1D-PAGE)

SDS-polyacrylamide gel electrophoresis (SDS-PAGE) was performed under denaturing conditions in the discontinuous gel system according to procedure described by Laemmli (Laemmli 1970). For this purpose, appropriate amount of 10-12% resolving gel solution (Table **2-18**) and 5% stacking gel (Table **2-19**) were prepared based on the molecular weight range of proteins (10-200KDa).

Table 2-18 12% resolving gel (data apply to 20 ml gel solution) [a]

Component	Concentration
30 % Acrylamid:Bisacrylamid (37.5:1)	8 ml
Tris-HCL (1.5 M, pH 8.8)	5 ml
Aqua dest.	6.6 ml
Added in this order:	
10 % SDS solution	200 µl
10 % Ammonia persulphate	200 µl (freshly)
TEMED (avoid bubbles)	20 µl
Pour gel immediately and overlay with isopropanol	

[a] (manufacturer's instructions Carl Roth GmbH; Gottlieb 2011, Ph.D Dissertation)

Table 2-19 5% Stacking gel (data applied to 5 ml gel solution) [a]

Component	Concentration
30 % Acrylamid:Bisacrylamid (37.5:1)	0.83 ml
Tris-HCL (1.0 M, pH 6.8)	0.63 ml
Aqua dest.	3.4 ml
Added in this order:	
10 % SDS solution	50 µl
10 % Ammonia persulphate	50 µl (freshly)
TEMED (avoid bubbles)	5 µl
pour gel immediately and then comb was inserted	

[a] (manufacturer's instructions Carl Roth GmbH; Gottlieb K 2011, Ph.D Dissertation)

For denaturation and preparation, 2-10µg of protein extracts were mixed with 0.5 sample volumes of the 2X SDS loading buffer (Table **2-20**) for an uniform negative load, followed by

heat- denaturation at 105 °C (heater) for 5 min. The prepared sample was loaded into wells of stacking gel and then filled the tank with 1X SDS running buffer (Table **2-21**). Then, the resolving gel can be run at 20 mA for 30 min followed by 1.5-2 hour in 30 mA (120V voltage) on resolving gel. For size comparison, 5 µl of the protein standard BlueStar Prestained Protein Marker (Nippon Genetics, Düren) were applied into the first lane.

Table 2-20 SDS loading buffer (3X) [a]

Component	Concentration
Glycerol	129 g l^{-1}
SDS solution	30 g l^{-1}
Bromphenolblau in H2O	0.75 g l^{-1}
β-Mercaptoethanol	5 g l^{-1}

[a] (Baumgärtner 2016, Ph.D Dissertation)

Table 2-21 SDS Running Buffer (10X) [b]

Component	Concentration
Glycerol	188 g
Tris-base	30.2 g
SDS	10 g

[b] (Gottlieb 2011, Ph.D Dissertation)

The protein bands were made visible by staining in the dye Commassie Brilliant Blue Buffer (Table **2-22**), which binds nonspecifically to the cationic and hydrophobic side chains of the protein. The gel was incubated for 1-2 hour at room temperature in the Coomassie staining solution and then washed in destaining buffer I (Table **2-23**) for 30 min followed by several washing steps with destaining buffer II (Table **2-23**) until the background was removed.

Table 2-22 Commassie Brilliant Blue Buffer [a]

Component	Concentration
Coomassie Brilliant blue R250	0,1%
Methanol	40%
Acetic acid	10%

[a] (Gottlieb 2011, Ph.D Dissertation)

Table 2-23 SDS Destaining Buffer I and II[b]

Component	Concentration
SDS Destaining **Buffer I**	
Ethanol	70 %
Acetic acid	10 %
SDS Destaining **Buffer II**	
Ethanol	40 %
Acetic acid	10 %

[b] (Baumgärtner 2016, Ph.D Dissertation)

2.5.4 2D-SDS polyacrylamide gel electrophoresis

2D PAGE is an effective method for analyzing complex protein mixtures according to two independent properties (molecular weights and isoelectric points). Two-dimensional (2D) PAGE separates proteins based on net charges by isoelectric focusing (IEF) and in the second dimension by SDS-PAGE according to proteins molecular masses (O'Farrell 1975; Klose 1975).

2.5.4.1 Isoelectric focusing: the first dimension of two-dimensional gel electrophoresis

Isoelectric focusing (Bjellqvist et al. 1982; Righetti 1984) was performed on immobilised pH gradient (IPG) strips (pH Gradient, 7 cm; GE Healthcare Life Sciences, Co) with linearly increasing focusing ranges (pH 3-10) accordingly to manufacture advice (GE Healthcare Life Sciences, Co).

Sample preparation and Rehydration of IPG stripes

125 µl (Table **2-24**) of rehydration buffer (Table **2-25**) added to 50µg of extracted protein samples (2.5.1) and incubated at room temperature for 1 hour according to manufacture advice (GE Healthcare Life Sciences, Co). The incubated samples were placed in well of re-swelling tray over complete length of stripe. The IPG strips were laid with the gel side down into the channel, avoiding any bubbles. The strip was then overlaid with mineral oil and the tray was placed in the IEF focusing cell (Bio-Rad, Hertfordshire, UK) for active rehydration according to manufacturers' protocol (Ready StripTM IPG strip instruction manual) for 12-16 hours.

Table 2-24 Rehydration solution volume [a]

Immobiline DryStrip	Suitable sample load (µg)	
	Coomassie	Silver
7cm 3–11 L	25-60	3-6
Immobiline DryStrip	Rehydration volume (µl)	
7 cm	125	

[a] (GE Healthcare Life Sciences, Co)

Table 2-25 Rehydration Buffer [b]

Component	Concentration
Urea	7 M
Thiourea	2 M
CHAPS	2%
Bromophenol blue	0.002% (1% Stock)
DTT	10 mM (day of use)
Pharmalyte pH 3-10	2% (made on the day of use)
stored at -28ºC	

[b] (Gottlieb 2011, Ph.D Dissertation)

Isoelectric focusing run

Following rehydration, the IPG strips are taken out of the channel using forceps and were put on wet tissue paper and then placed on a clean glass plate of the focusing tray. The IPG strips were laid with the gel side up into the channel. Then two filter paper wicks saturated with water

(5 µl) were placed on each electrode, underneath the strip (Take care that electrode stripes are in good contact with gel stripe). The strips were then overlaid with mineral oil and followed by focusing the IPG strips at a cool (20C) Multiphor II Electrophoresis System (Pharmacia Biotech) under the following conditions: 200 V, 5W, 10 mA for 10 min (stage I), 3500 V, 25W, 30 mA for 90 min (stage II) and 3500 V, 25W, 30 mA for 60 min (stage III). In the end, the IPG strips were removed from the focusing tray and were then either equilibrated and used immediately for the 2nd dimension or stored at -80°C for future use.

Equilibration of the IPG strips

Following isoelectric focusing, the IPG strips were equilibrated by placing them in a Falcon tube and immersed in 10 ml of SDS-equilibration buffer (Table **2-26**) for 15 min at room temperature in the shaker.

Table 2-26 SDS-equilibration Buffer

Component	Concentration
SDS	4% (w/v)
Tris	50 mM
Urea	6 M
Glycerol	30 % (v/v)
Bromophenol blue	0.002%
PH 8.8 with HCL, stored at -28C	
DTT	10 mM (day of use)

[a] (Gottlieb K 2011, Ph.D Dissertation)

2.5.4.2 SDS-PAGE electrophoresis: the second dimension of two dimensional gel electrophoresis

Casting of gels

The resolving gel (12%, Table **2-27**) was polymerized by freshly adding 10% (w/v) ammonium persulphate (APS) solution and tetramethylethylenediamine (TEMED) followed by addition of 2 ml isopropanol (2-propanol) to remove all bubbles and to make an uniform surface of gel.

Table 2-27 SDS Gel (12%)

Component	Concentration
30 % Acrylamid:Bisacrylamid (37.5:1)	8 ml
Tris-HCL 1.5mM- pH 8.8	7.5 ml
H2o	4.2 ml
SDS (10%)	200 ml
APS 10 % (freshly use)	200 ml
TEMED	20 µl
Agarose 0.5% for top	

Electrophoresis

Once equilibrated, all liquid was removed by tissue paper before IPG stripe was placed on top of the SDS-Gel. The IPG strip was inserted between the glass plates ensuring uniform contact with the gel surface (Note the orientation (+) end of the strip). In order to fix the strip, the gel was covered with 0.5% agarose (avoiding the air bubbles between of gel and stripe). Then two filter paper wicks saturated with protein marker (8 µl) were placed on each side of the strip. When the agarose gel became solid, the gel was run in 1X running buffer (Table **2-21**) for 1.5-2 hours at 100 V (30mA).

Staining and destaining of gels

Proteins were visualized by staining in Colloidal Coomassie staining buffer (Table **2-28**) overnight in room temperature. To destaining gel, tap water (several times change of dH_2O) was used to eliminate the background stain until optimum differentiation of protein spots was obtained.

Table 2-28 Colloidal Coomassie staining buffer [a]

Component	Concentration
Phosphoric acid	400 ml
Ammonium Sulphat	40 g
Coomassie G250 (5% in dH2O)	8 ml
Methanol (1:4)	100 ml (day of use)
stored at -28˚C	

[a] (Gottlieb 2011, Ph.D Dissertation)

Evaluation and Analysis

The gel image was archived and recorded using a HP scanner and then imported into Delta 2D Version 3.2 (Decodon GmbH). Then marked and annotated at least 3 known reference proteins (Table **2-29**) with molecular weight and pI to distinguish the location of other proteins of interest (Table **2-30**).

Table 2-29 Molecular weight and pI of 3 known reference proteins in *E.coli* (data from EcoCyc)

Name of Protein	pI	KDa
DnaK	4.8	68.8
Ef-TU	5.3	44.6
PstS	6.9	35.4

Table 2-30 Expected Molecular weight and pI of target proteins

Name of Protein	pI	KDa
PabAB	4.8-5.03	67.2
PapB	6.1	11.9
PapC	5.98	32.9
AroF	5.3-5.4	38.8-38.8
AroB	5.6-5.8	37.7-38.9
AroL	4.5-4.7	19.1

2.5.5 Determinations of specific activity of crude extracts

2.5.5.1 Preparation of cell free extracts

Single colonies of the *E. coli* DH5a harboring the pJF119EH and pJFA10 were cultivated in 10 ml LB medium containing 100 mg l^{-1} Ampicillin at 30°C for 12h. 1 ml of these preculture was subsequently used to inoculate 50 ml of the same medium. Cells were grown at 30°C at 150 rpm, until reaching an OD_{600nm} of~0.6, at which time point each was induced by the addition of IPTG to a final concentration of 0.5 mM. After 5-6 h, the cells were harvested and washed with 100 mM potassium phosphate buffer, pH~ 7.0. Aliquots of washed cells were frozen at -28°C for later use. Crude extracts was prepared by sonication immediately before use. The cell pellet from 50 ml of cultivation was resuspended in 2 ml 100 mM potassium phosphate buffer pH 7.0, and subjected to sonication (amplitude 55%; 4 cycles, 30 s bursts with 15 s rests). The lysate was centrifuged for 60 min at 22,000 g, 4°C to pellet cell debris. The cell free extract was used for specific activity determination. The protein concentration of the crude extracts was determined according to Bradford (Bradford 1976) by using bovine serum albumin as a standard (See section 2.5.2).

2.5.5.2 Specific activity assay (crude extract) of ThDP-Ketoacid decarboxylase (Aro10)

The decarboxylation of phenylpyruvate was measured at 30 ºC using a modified coupled enzymatic assay previously described for benzoylformate decarboxylase activity (Yep et al. 2006; Kneen et al. 2011)**.** The reaction mixture contained (in 1 ml): 100 mM potassium phosphate buffer (pH ~7.0); 1 mM $MgSO_4$; 0.5 mM thiamine diphosphate ; 0.2 mM NADH; 0.05–0.25 U yeast alcohol dehydrogenase (NADH dependent) and varying amount of crude extract (2- 100 µg) in a total volume of 1 ml. The reaction was initiated by adding 100 µl of 20 mM substrate, PH~ 7 (phenylpyruvic acid (sodium salt) as 2-keto acid-final concentration 2mM), and the consumption of NADH was monitored at 340 nm with a spectrophotometer. The

decrease in $\Delta A_{340\,nm}$ was recorded for approximately 20 min. Stock solutions (20 mM) of the phenylpyruvic acid (sodium salt) were usually prepared in assay buffer (100 mM potassium phosphate buffer (pH ~7.0), 1 mM $MgSO_4$, and 0.5 mM ThDP). A molar extinction coefficient of 6220 M^{-1} cm^{-1} and a 1 cm path length was used to establish crude activity in terms of U mg^{-1} protein. To correct for non-specific NADH oxidation, control assay was run using an assay mixture with cell free extract of empty plasmid (pJF119EH). To measure the specific activity of crude extract, varying concentration of crude extract (5, 10, 20, 40, 80 and 120 µg ml^{-1}) were applied. One unit (U) is defined as the amount of enzyme that catalyzes the decarboxylation of 1µmol of phenylpyruvate per minute at 30 ºC under standard conditions (Kneen et al. 2011). Specific activity was determined with the following formula:

$$\text{Specific activity} = \frac{\Delta A(340\text{nm}) \cdot V}{\varepsilon NADH \cdot l} = \frac{\Delta E(340\text{nm}) \cdot 0.001\text{L}}{6220 \frac{\text{L}}{\text{mol. cm}} \cdot 1\text{cm}} \times 10^6 = \frac{\frac{\mu\text{mol}}{\text{min}}}{\text{mg of crude extract}}$$

2.6 Cultivation of *E.coli*

2.6.1 *E. coli* susceptibility to aromatic amines and aromatic alcohols

Aromatic amines and aromatic alcohols susceptibility on *E. coli* wild type LJ110 strain were determined at various concentrations of aromatic amines or aromatic alcohols by measuring the OD_{600nm} (Cary 50 Bio, Varian). The cultures were grown at 37°C overnight in 10 ml minimal medium supplemented with a glucose or glycerol (0.5 %). The overnight culture was used to inoculate the minimal media (OD_{600nm} of 0.08-0.1) supplemented with various concentrations of aromatic amines or aromatic alcohols, and was then grown at 37°C for 48h. The optical density (OD) at 600 nm was monitored every 2h to investigate negative effects those aromatic compounds on cellular growth of the *E. coli*.

2.6.2 Synthesis of aromatic amines in shake flasks

2.6.2.1 Whole cell biotransformation of *E. coli* for production PAPE and 4-APA

The biotransformation was performed by whole-cell biocatalysts, consisting of *E. coli* LJ110 carrying pJFA10 plasmid for PAPE production and pJFA10F plasmid for 4-APA production. At first, seed cultures were initially prepared in 5 ml LB medium with the appropriate antibiotic and then incubated overnight at 37°C. For inoculation, 1/50 of the total volume of the culture was

used to inoculate 50 ml LB media to reach an OD_{600nm} of 0.1 and incubated at 37°C, 150 rpm. At an OD600nm of about 0.6, IPTG was added to the culture (final concentration 0.5 mM). After 4-6 h incubation (OD_{600nm} ~5) the cells were collected by centrifugation (6,000 g, RT and 10 min), washed twice with potassium phosphate buffer (200 mM, pH~7.0) and resuspended in a reaction mixture (10 ml) containing 5.5 mM "bio"- L-PAPA (~1 g l^{-1}), 200 mM potassium phosphate buffer (pH~7.0) and 0.25 mM thiamine diphosphate to start the biotransformation with an OD600 ~ 16. It was incubated in a rotary shaking incubator at 110 rpm and 30 °C. L-PAPA consumption and PAPE or 4-APA production were determined (based on HPLC, see section 2.7.2.2) by taking samples at 2 hour intervals over a period of 10 h. These experiments were done in triplicate to provide estimates of standard error.

2.6.2.2 Batch cultivation of *E. coli* for production of L-PAPA, PAPE and 4-APA

E. coli strains were grown in in 250 ml shake flasks filled with 20 ml of minimal medium (Table **2-6**) supplemented with L-Phe, L-Tyr and L-aspartic acid (If required, Table **2-8**) at 37°C and with a 150-rpm agitation. The initial glycerol/glucose concentration was 4.5-5 g l^{-1}. Overnight cultures were used as inocula (1% v/v). Induction was with 0.5 mM isopropyl-β-d-thiogalactopyranoside (IPTG) at OD_{600nm} ~ 0.6 and then shaking flasks were transferred from 37°C to 30°C. Samples were taken and centrifuged at 22,000 g for 10 min. The supernatant was removed gently by pipetting and then stored at -28°C until use. Experiments were performed in triplicate to provide estimates of standard error.

2.6.2.3 Fed-Batch cultivation *E. coli* for production of L-PAPA, PAPE and 4-APA

The glycerol/glucose fed-batch cultivation was performed in 250 ml shake flasks with 20 ml minimal media (Table **2-6**). The initial glycerol/glucose concentration was 4.5-5 g l^{-1}. Cultures were inoculated with an overnight grown culture. After 24h of cultivation, 0.5 mM IPTG (final concentration) was added to the culture and the shake flasks were transferred from 37°C to 30°C before giving pulses of glucose (~ 4.5g l^{-1}) or glycerol (~ 5 g l^{-1}) every 12h until 84-144h. In order to determine the proper feeding time during fed-batch cultivations, the concentration of glucose or glycerol was measured at specific intervals (every 6h) on the HPLC. Thus, when the concentration reached less than 0.5 g l^{-1}, additional pulses of glucose (~ 4.5g l^{-1}) or glycerol (~ 5 g l^{-1}) were added to the culture. Furthermore, every 24h, 2.5 g l^{-1} sodium bicarbonate was added to adjust the pH and 2 g l^{-1} ammonium sulfate was given as ammonium source. Samples were

taken and centrifuged at 22,000 g for 10 min. The supernatant was removed and stored at -28°C until use. These experiments were done in triplicate to provide estimates of standard error.

2.6.3 Synthesis of aromatic alcohols in shake flasks

2.6.3.1 Whole cell biotransformation of *E. coli* for production of 2-PE, tyrosol and hydroxytyrosol

Whole cell biotransformation was carried out by resting cells of *E. coli* wild type LJ110 harboring pJFA10 plasmid. At first, three single colonies were selected from the transformant pool and three seed cultures were grown in 10 ml LB broth with appropriate antibiotic at 30 °C while shaking at 150 rpm overnight. Each seed culture was used to inoculate 100 ml LB supplemented with appropriate antibiotics in a 1l shake flasks. Upon reaching an optical density at 600 nm (OD_{600nm}) of ~0.5-0.6, cultures were induced by addition of 0.5 mM IPTG (final concentration). Cultivation was continued for 4-6h before cells were harvested by centrifugation at 6,000 g, washed twice with pH~7.0 potassium phosphate buffer (200mM), and re-suspended in 10 ml potassium phosphate buffer and 0.25 mM thiamine diphosphate (ThDP) (final concentration) as cofactor supplemented with 10 mM (~1.65 g l^{-1}) L-phenylalanine for 2-PE production, 10 mM (~1.81 g l^{-1}) L-tyrosine for tyrosol production and 12.8 mM (~2.5 g l^{-1}) L-3,4-dihydroxyphenylalanine (L-DOPA) for hydroxytyrosol production. Subsequently cultures were incubated at 30°C (110 rpm) while levels of each of L-Phe/2-PE, L-Tyr/tyrosol and L-DOPA/hydroxytyrosol were monitored in the media for the next 24 h by periodic sampling for high performance liquid chromatography (HPLC) analysis. These experiments were done in triplicate to provide estimates of standard error.

2.6.3.2 Batch cultivation of *E.coli* for production of 2-PE and tyrosol

The engineered *E.coli* strains containing the recombinant plasmids were inoculated into 20 ml of minimal media (as described in Section 2.1.3) supplemented with 0.04 mg ml^{-1} L-Phe, 0.04 mg ml^{-1} L-Tyr, 4.5 g l^{-1} glucose and 3 g l^{-1} L-Asp, if necessary, in a 250 ml shaking flask (Adjusted initial OD_{600nm} was 0.1), followed by cultivation with vigorous agitation at 150 rpm at 37 °C. After 6~8 h incubation (OD_{600nm} ~0.6) cells were induced by adding 0.5mM IPTG (final conc.), and then the temperature was set to 30°C for next 72h. Samples were taken at different

time points (0,2,4,6,8,12, 24, 36, 48, 60, 72, 84 and 96 h) during cultivation and centrifuged at 22,000 g for 10 min and used for analysis by HPLC and LC-MS. Cell densities were determined by spectrophotometer OD_{600nm} (Cary 50 Bio, Varian). These experiments were done in triplicate to provide estimates of standard error.

2.6.3.3 Fed-batch cultivation *E.coli* for production of 2-PE and tyrosol

Fed-batch cultivation experiments were carried out in 250 ml Erlenmeyer flasks containing 20 ml of minimal medium. The cultures were grown at 37 °C with a stirring speed of 150 rpm for 24h and then cells were induced by adding 0.5mM IPTG (final conc.) and the temperature was shifted to 30°C followed by cultivation for an additional 72-120 h, whereupon the fed-batch cultivation was started through continuous feeding of glucose (4.5 g l^{-1}, every 12h). Furthermore, every 24h, 2.5 g l^{-1} sodium bicarbonate was added to adjust the pH. Samples were taken at indicated time points and centrifuged at 22,000 g for 10 min to determine OD_{600nm}, glucose, L-Phe and 2-PE concentration. These experiments were done in triplicate to provide estimates of standard error.

2.6.3.4 Two phase fed-batch cultivation *E.coli* for production of 2-PE and tyrosol

Two-phase cultivation was performed with the same initial setup used for the fed-batch cultivation. Cells were grown in 37°C until the stationary growth phase (~24h) in 250 ml Erlenmeyer flasks containing 20 ml of minimal media and varying concentration of organic solvents (Table 2-31; 10, 30, 40 and 50%) and were then shifted to 30°C along IPTG induction (0.5mM, final conc.), followed by the same glucose feeding strategy as the fed batch cultivation for next 72-120h. phase between aqueous culture media, and the organic phase was separated by centrifugation (22,000 g for 10 min) and the 2-PE or tyrosol concentrations was determined separately in each phase by HPLC. 2-PE or tyrosol content in aqueous phase was analyzed directly by HPLC, the organic phase was further diluted with MeOH (1:10) and then analyzed by HPLC. OD600nm was measured by re-suspending cell pellet in minimal medium, since cell growth occurs only in the aqueous medium phase. The final titer was calculated based on the volume of culture media (Titer = $(C_{aqu} \times V_{aqu} + C_{org} \times V_{org})/V_{aqu}$) (Kim et al. 2014b). C_{aqu}: concentration of 2-PE/tyrosol in aqueous phase; C_{org}: concentration of 2-PE/tyrosol in organic phase; V_{aqu}; volume of aqueous phase and V_{org}: volume of organic phase.

Table 2-31 List of organic solvents used in this study

Organic solvents	Company	Purity
Dodecane	Merck KGaA (Darmstadt, Germany)	≥99%
Polypropylene glycol 1200 (PPG)	Sigma-Aldrich (Steinheim, Germany)	≥97 %
Tributyrin	Carl Roth GmbH (Karlsruhe, Germany)	≥97.5 %
Polyethylene Glycol 400 and 2000 (PEG)	Sigma-Aldrich (Steinheim, Germany)	≥96%-

2.6.4 Fed-Batch cultivation in Bioreactor

2.6.4.1 Synthesis of L-PAPA

To scale up the L-PAPA production, the strain *E. coli* FUS4.7R pC53BC/pJNT-*aroFBL* was used. The cultivation was performed in modified Gerhardt medium (Table **2-6**) and glycerol as carbon source in a 30 l stirred-tank reactor (Bioengineering, Wald, Switzerland) at the Institute of Biochemical Engineering of the University of Stuttgart with a batch volume of 8 l and a final volume of 12.25 l. Fermentation culture for the production of L-PAPA was the same as minimal medium was employed for shake flask experiment, except that the concentration of compounds increased by 50% (See Table **2-7**). Culture medium at the beginning of the experiments was supplemented with 0.06 mg ml^{-1} L-Phe, 0.06 mg ml^{-1} L-Tyr and the required amount of antibiotics (100 mg l^{-1} Ampicillin and 50 mg l^{-1} kanamycin) based on the actual volume of fermenter. The working conditions were pH 7.0 (controlled by the addition of 15 % ammonia solution), 30 % oxygen saturation with a reactor pressure of 500 hPa above atmospheric pressure (starting with pO2 ~100 % at 350 rpm with an aeration rate of 4 l min^{-1}, when reaching 30 % the stirring rate was adjusted). An exponentially growing preculture (CDW ~0.18 g l^{-1}) was used to initiate the fermentation with 1.2 l of an overnight preculture with using the same medium as for the fermentation at 37°C. The initial glycerol concentration was about 8.1 g l^{-1}. The antifoam agent used was Struktol J647 from Schill Seilacher (Hamburg). After consumption of the glycerol initially introduced (11.7 h), indicated by an oxygen saturation increasing to the initial value, the expression of the recombinant genes was induced by the addition of 0.5 mM IPTG (Final concentration was calculated based on the actual volume of fermenter) and the feeds were started. The feeds consisted of a glycerol feed and an ammonium source feed. In addition, the temperature was shifted from 37°C to 30°C. Glycerol was fed to maintain a concentration between 0.6 - 1.0 g l^{-1} during fed batch cultivation. Since *E. coli* growth was controlled by

limiting factors L-Phe and L-Tyr, when the growth was constant, an additional pulse of L-Phe and L-Tyr (as described below) was added to allow biomass formation. Apart from the initial amount of L-Phe and L-Tyr (0.06 mg ml^{-1}) at the beginning of the experiment, L-Phe and L-Tyr were added in three additional pulses (0.06, 0.1 and 0.06 mg ml^{-1} L-Phe and L-Tyr) based on the actual volume of fermenter were added to the fermenter at 24, 34 and 56 h after inoculation, respectively. The cell densities were measured by optical density at 600nm (OD_{600nm}). The determination of the concentration of glycerol and final product was performed by HPLC. The biomass concentration during the process was determined at six time points and was otherwise calculated from the OD600 with a dry biomass to OD_{600nm} correlation factor of 0.368 g l^{-1}. The parameters selected for the fermentation are shown in Table **2-32**.

Table 2-32 Overview of the parameters selected for fermentation of L-PAPA in 30L fermenter

Parameters	Condition
Media	minimal medium (1.5X) + 0.06 mg ml^{-1} (fermentation volume) L-Phe and L-Tyr
Working volume/final volume	8 l/12.24 l
Start-OD_{600nm}	0.5
End OD_{600nm}	58 (controlled by phenylalanine and tyrosine addition)
Initial concentration of glycerol	8.1 g l^{-1}, feed started after induction (after 11.75h)
Glycerol Feeding	0.6 - 1.0 g l^{-1}, started after induction (after 11.75h)
L-Phe and L-Tyr feeding	Added in three pulses (0.06, 0.1 and 0.06 mg ml^{-1} L-Phe and L-Tyr were added to the actual volume fermenter)
Temperature	37°C, shifted to 30°C after induction (after 11.75h)
pH value	7.0 (automatically regulated with 15% Ammonia solution)
Oxygen saturation	30-80% (measured online and automatically regulated via stirrer speed)
Stirrer speed	400rpm, measured online and automatically increase to 1000 rpm via oxygen saturation and air-flow
Air flow	4 l min^{-1}, measured online and automatically regulated
Induction	0.5 mM IPTG (calculated based on the actual volume of fermenter), after consumption of the glycerol initially introduced (OD_{600nm} of 9.9)
Antifoam	Struktol J647, If required
Antibiotic	Ampicillin 100 mg l^{-1} + Kanamycin 50 mg l^{-1}, at the beginning of experiment

2.6.4.2 Synthesis of PAPE and 4-APA

To scale up the PAPE and 4-APA production the recombinant strains *E. coli* FUSBCR pC53BCAY/pJNT-*aroFBL-yahK* and *E. coli* FUS4BCR pC53BCAF/pJNT-*aroFBL-feaB,* respectively, were cultivated in a benchtop bioreactor system (Multifors 2, Infors AG, Switzerland) with a total volume of 0.75 l and a working volume of 0.5 l. The preculture was grown in a volume of 50 ml in a 0.5 l shaking flask by using the same medium (See Table **2-6**) as for the fermentation at 37°C. The working conditions had pH ~7.0 (controlled by the addition of

10 % ammonia solution) and 30 % oxygen saturation at ambient pressure (starting with pO2 ~ 100 % at 400 rpm with an aeration rate of 0.1-1 l min^{-1}, when reaching 30% the stirring rate was adjusted). An exponential growth preculture was used to initiate the fermentation at an OD_{600nm} of 0.25. Culture medium (Table 2-6) at the beginning of the experiments was supplemented with 0.044 mg ml^{-1} L-Phe, 0.046 mg ml^{-1} L-Tyr and the required antibiotics (100 mg l^{-1} Ampicillin and 50 mg l^{-1} kanamycin). After reaching OD_{600nm} of 3.0, IPTG (0.5 mM, final conc.), additional L-Tyr (0.044 mg ml^{-1}) and L-Phe (0.040 mg ml^{-1}) were added based on the actual volume of fermenter and then temperature was shifted from 37°C to 30°C. The initial glucose concentration was about 5 g l^{-1}. The glucose feed was started after the initial glucose was depleted to maintain a concentration between 0.4-8.0 g l^{-1} during cultivation.Glucose concentration was monitored by using Glucose Medi-Test stripes (Macherey Nagel, Düren, Germany) and by HPLC on an Organic acid column (See section 2.7.2.1). Antifoam (polypropylene glycol PPG 2000, Sigma-Aldrich, was diluted 1:10 with pure Ethanol) was added as required. The cell densities were measured by optical density at 600. The determination of the concentration of glucose and final product was performed by HPLC. The parameters selected for the fermentation are shown in Table **2-33**.

Table 2-33 Overview of the parameters selected for fermentation of PAPE and 4-APA

Parameters	Condition
Media	minimal medium (1X) + 0.04 mg ml^{-1} L-Phe and 0.044 mg ml^{-1} L-Tyr
Working volume/final volume	0.25 l/0.5 l
Start OD_{600nm}	0.22
End OD_{600nm}	18 (controlled by tyrosine addition)
Initial concentration of glucose	5 g l^{-1}, feed started after induction
Carbon source Feeding	0.4 - 0.8 g l^{-1}, started after induction
Temperature	37°C, shifted to 30°C after induction
pH value	7.0 (measured online and automatically regulated with 10 % Ammonia solution)
Oxygen saturation	30-80% (measured online and automatically regulated via stirrer speed)
Stirrer speed	400rpm, measured online and automatically increase to 1200 rpm via oxygen saturation and air-flow
Air flow	0.1-1 l min^{-1}, measured online and automatically regulated (increase to 1.0) via oxygen saturation and stirrer speed
Induction	0.5 mM IPTG (calculated based on the actual volume of fermenter), after consumption of the glucose initially introduced (OD_{600nm} of 3.0)
Antifoam	PPG 2000:Ethanol (1:10), If required
Antibiotic	Ampicillin 100 mg l^{-1} + Kanamycin 50 mg l^{-1}, , at the beginning of experiment

2.6.4.3 Synthesis of 2-PE and tyrosol

To the scale up of 2-PE and tyrosol, a two phase fed batch cultivation with *E. coli* FUS4.7R pJFA10/pFABL and *E. coli* FUS4.7R pJFA10T/pJNT*aroFBL* were carried out at a benchtop bioreactor system (Multifors 2, Infors AG, Switzerland), respectively. Inoculation cultivation was performed in a stirred tank reactor (0.75 l) with 175 ml Gerhardt medium (Table **2-6**) supplemented with 0.04 mg ml^{-1} L-Phe and 0.044 mg ml^{-1} L-Tyr and 5 g l^{-1} glucose as a carbon source and an inoculation volume of 10 ml, resulting in a OD_{600nm} of 0.25 at the beginning of the process. During the batch process, the temperature was controlled at 37 °C and pH was adjusted to 7.0 by the addition of ammonia solution (10% v/v). The oxygen saturation (pO_2) was maintained above 30% by the aeration rate and stirrer speed (400-1200 rpm). The antifoam (polypropylene glycol PPG 2000, Sigma-Aldrich, was diluted 1:10 with pure Ethanol) was added as required. After consumption of the glucose initially introduced (9.9 h after reaching OD_{600nm} of 4.1), indicated by an oxygen saturation increasing to the initial value, the expression of the recombinant genes was induced by the addition of IPTG (0.5 mM, final concentration was calculated based on the actual volume of fermenter) and the feeds were started. Glucose was fed to maintain a concentration between 0.4-0.8 g l^{-1} during cultivation.

Table 2-34 Overview of the parameters selected for two phase fermentation of 2-PE and tyrosol

Parameters	Condition
Media	Minimal Medium (1X) + 0.04 mg ml^{-1} L-Phe and L-Tyr
Working volume/final volume	0.175 l/ 0.45 l
Start-OD600	0.25
End OD600	6.5 (2-PE) and 23 (tyrosol)
Initial concentration of glucose	5 g l^{-1}, feed started after induction (9.9h)
Carbon source Feeding	0.4 – 0.8 g l^{-1}, started after induction (9.9h)
Temperature	37°C, shifted to 30°C after induction(9.9h)
Organic solvent	30% Polypropylene glycol 1200 (75ml), added after induction (9.9h), PPG 1200 is non-volatile, non-flammable and also non-toxic to humans
pH value	7.0 (measured online and automatically regulated with 10 % Ammonia solution)
Oxygen saturation	30-80% (measured online and automatically regulated via stirrer speed)
Stirrer speed	400rpm, measured online and automatically increase to 1200 rpm via oxygen saturation and air-flow
Air flow	0.1-1 l min^{-1}, measured online and automatically regulated (increase to 1.0) via oxygen saturation and stirrer speed
Induction	0.5 mM IPTG, after consumption of the glucose initially introduced (after 9.9h, OD 600 of 4.1)
Antifoam	PPG 2000:Ethanol (1:10), If required
Antibiotic	Ampicillin 100 mg l^{-1} + Kanamycin 50 mg l^{-1}

Afterwards, an additional pulse of L-Phe (0.04 mg ml^{-1}), L-Tyr (0.044 mg ml^{-1}) and 75 ml filter-sterilized Polypropylene glycol 1200 (30%, final conc.) as organic solvent (non-volatile, non-

flammable and also non-toxic to humans) based on the actual volume of fermenter was added and the temperature was reduced from 37°C to 30°C. Phase between aqueous culture media, and organic phase was separated by centrifugation (22,000 g for 10 min) and the 2-PE or tyrosol concentrations was determined separately in each phase by HPLC. 2-PE or tyrosol content in aqueous phase was analyzed directly by HPLC, organic phase was further diluted with MeOH (1:10) and then analyzed by HPLC. The total 2-PE/tyrosol titer was calculated based on the following equation (Kim et al. 2014). The total 2-PE/tyrosol titer = $(C_{aqu} \cdot V_{aqu} + C_{org} \cdot V_{org})/V_{aqu}$, where C_{aqu} and C_{org} are the 2-PE/tyrosol titer in the aqueous and PPG 1200 phase, respectively, and V_{aqu} and V_{org} are the volumes of the aqueous and PPG 1200 phase, respectively. OD600nm was measured by re-suspending cell pellet in minimal medium; since cell growth occurs only in the aqueous medium phase.The parameters selected for the fermentation are shown in Table **2-34**.

2.7 Analytical methods

2.7.1 Cell density determination

The density (cell growth) of bacterial cultures was measured by a photometer (Cary 50 Bio, Varian) at a wavelength of 600 nm (~OD_{600nm}). A free bacteria medium (LB or minimal medium) as blank test was used. When the samples obtained an extinction value greater than 0.3, the measured value of the sample was appropriately diluted with medium.

2.7.2 HPLC Analysis

The identification and direct determination of the concentrations of substrate (glycerol and glucose), metabolites (lactate and acetate), aromatic amines (L-PAPA, PAPE and 4-APA) and aromatic alcohols (2-PE, tyrsosl and hydroxytyrosol) were performed with HPLC. The substances contained in the tested samples were identified and quantified based on the calibration measurements.

2.7.2.1 Detection of glycerol, glucose, acetate and lactate concentration using High Performance Liquid Chromatography (HPLC)

Identification of substrates (glycerol and glucose) and metabolites (lactate and acetate) was performed with high pressure liquid chromatograph (Agilent Technologies Series 1200 system, Agilent, USA) with Chemstation for LC 3D Systems software, column oven, QuatPump, RI-71

refractive index detector (Showa Denko, Japan) fitted with an organic acid resin column, 300 × 8 mm (Chromatography service GmbH, Langerwehe, Germany). The column was heated constantly at 40°C for 20 min with flow rate 0.6 ml min^{-1}. 5 mM sulfuric acid was used as mobile phase and the components (glucose, glycerol, lactate and acetate) were detected with a Refractive Index Detector (RID). Under such condition, glucose (6.8 min), glycerol (8.4 min), acetate (10.31 min) and lactate (12.33 min) were eluted with acceptable separation within the 15 min run time.

2.7.2.2 Determination of L-PAPA, PAPE and 4-APA concentration by HPLC

To analyze L-PAPA, PAPE and 4-APA the samples were centrifuged at 22000 g for 10 min. The supernatant was transferred to a new tube and frozen at -28°C until use. The analysis was carried out with a symmetry C18 silica column reversed-phase HPLC column (Prontosil, 250 mm× 4 mm, CS Chromatography service GmbH) with a precolumn on an Agilent HPLC system (Agilent Technologies Series 1200 system, Agilent, USA) equipped with a diode array detector (1260 Infinity series, Agilent Technologies). 40 mM Na_2SO_4 (adjust pH ~2.67 with Methanesulfonic acid) was used as the mobile phase at a flow rate of 1 ml min^{-1} at 40°C. Absorption was detected at 210 nm. Under such conditions, L-PAPA (RT~2.24 min), PAPE (RT~5.99 min) and 4-APA (RT~6.5 min) were eluted with acceptable separation. The compounds were quantified using standard calibration curves of the respective commercial chemicals.

2.7.2.3 Determination of aromatic alcohols (2-PE, tyrosol and hydroxytyrosol) and aromatic amino acids (L-Phe, L-Tyr and L-DOPA) concentration by HPLC

For analyzing L-Phe, L-Tyr and L-DOPA, 1 mL of cell culture was centrifuged (22,000 g for 10 min) and the supernatant was then filtered with a 0.22 μm syringe filter for analysis. For 2-PE, tyrosol and hydroxytyrosol analysis, samples taken during cultivation period and supernatant were stored at -28°C for subsequent analysis. Organic and aqueous phase were separated easily by centrifuging at 22,000 g for 10 min and the organic phase was diluted with 10-fold with methanol before injection. All components were analyzed using high-performance liquid chromatography (HPLC, 1260 Infinity series, Agilent Technologies) equipped with a diode array detector (1260 Infinity series, Agilent Technologies) and a symmetry C18 silica column (Lichrospher 100 RP, 250 mm× 4 mm, chromatography service GmbH) with a precolumn of the same material. A gradient method comprising 0.1% (vol/vol) trifluoroacetic acid in

Water/Acetonitrile was applied with the following setup: 0–5 min 80/20, 10 min 20/80, 15 min 20/80 and 20 min 80/20 at a flow rate of 0.4 ml min-1 at 40°C, at UV detection wavelength of 210-290 nm. All compounds were calibrated with external standards in quantification experiments. Under such conditions, l-Phe (4.55 min, 210nm) and 2-PE (6.80 min, 210nm) together, l-Tyr (4.05 min, 280nm) and tyrosol (4.48 min, 280nm) together as well as L-DOPA (3.86 min, 280nm) and hydroxytyrosl (4.12 min, 280nm) were eluted with acceptable separation. The compounds were quantified using standard calibration curves of the respective commercial chemicals.

2.7.3 Product identification by LC-MS Analysis

HPLC-MS was performed at the Institute of Technical Biochemistry of the University of Stuttgart (Dr. Bernd Nebel) on Agilent 1260 system with 1260 Infinity UV detector and an Agilent 6130 mass spectrometer (Agilent Technologies Waldbronn, Germany) with LC/MSD Chemstation software and the Prontosil C18 (2) reversed-phase column already used in Section 2.7.2.2 examined. For the analysis of all components, the HPLC conditions used were as follows: Millipore water (0.1% Formic Acid) was used as mobile phase with a flow rate of 1 ml min^{-1}. The optical analysis was carried out at a wavelength of 210-280 nm and the mass-to-charge ratios (m/z) were recorded with an Agilent 6130 quadrupole mass spectrometer (Agilent Technologies, Waldbronn) in positive and negative scan mode (m/z 50-1000) at Dry gas flow of 10 l min^{-1} with a temperature of 330 ° C, a capillary voltage of 3000 V, a nebulization pressure of 2.76 bar and a fragmentor voltage of 7 V.

2.8 Downstream processing (extraction of aromatic amines and aromatic alcohols)

2.8.1 Sample preparation

The extraction procedure was carried out either according to liquid-liquid extraction with organic solvents (Chreptowicz et al. 2016; Konishi et al. 2016 US patent) with some modifications or FPLC chromatography. For this purpose, the fermentation culture supernatants were used, while cell pellet was removed by centrifugation for 30 min at 6, 000 g. The obtained supernatant was then passed through filter (0.2 μm) and used for next extraction steps as described on the following sections 2.8.2 and 2.8.3.

2.8.2 Aromatic alcohols (2-PE and tyrosol) extraction with ethyl acetate (modified from Chreptowicz et al. 2016)

The 2-PE/tyrosol isolation from culture broth was carried out according to the method as described previously by Chreptowicz et al. 2016 with some modifications. In brief, the obtained supernatant was mixed with a fresh (two months old) ethyl acetate 99.5% (100 ml for every 200 ml of the supernatant at the first extraction stage, then 50 ml for second and third extraction stages) in a separating Funnel glass. A mixing by hand at room temperature for 5 min followed by precipitation resulted in two distinct layers, the organic phase was collected and then centrifuged at 6,000g for 10 min to separate the remaining water phase. The collected organic phases were combined and subsequently treated with 25 g l^{-1} potassium carbonate as drying agent followed by incubation at room temperature for maximum 6h. At the next step, drying agent was removed by filtration followed by ethyl acetate distillation using a rotary evaporator VV2000 with WB2000 water bath (Heidolph Instruments, Schwabach), RK20 thermostat (Lauda, Lauda-Königshofen) and M2-C2 vacuum pump (Vacuubrand, Wertheim) at 60°C and 100-200 mbar. End product (condensed white-yellow liquid, See Figure **3-47** (c) and Figure **3-48** (c)) was separated and analyzed using HPLC according to procedure described in section 2.7.2.3.

2.8.3 Aromatic amine (L-PAPA) extraction with tetrahydrofuran (THF) or acetone (modified from Konishi et al. 2016)

The obtained supernatant (2.25 l in total, pH adjusted to 1 by hydrogen chloride 37%) was mixed with fresh Acetone (99.9%) or THF (99.5%) (250 mL for every 250 ml of the supernatant at the first extraction stage, then 100 ml for second and third stages) in a separating Funnel glass. Then the mixture was gently shaken by hand for 3 min and left for few minutes while the layers separate out and settle down. After 15 min, a brown phase (lower phase) was formed at the bottom and yellow water/organic phase (upper phase) was formed in the top of separating Funnel. Next, the organic water/organic phase passed through folded filter paper (150 mm) and poured into the flask while the lower phase was returned to the separation funnel and extracted again as described (minimum 2 times). The collected upper phases were combined and subsequently added to the rotary evaporator VV2000 with WB2000 water bath (Heidolph Instruments, Schwabach), RK20 thermostat (Lauda, Lauda-Königshofen) and M2-C2 vacuum pump (Vacuubrand, Wertheim) 55 °C and 150-300 mbar. Finally, the remaining residual

water/solvents were freeze-dried at below 5 mbar with the Alpha I-5 freeze-drying plant (Christ freeze drying plants, Osterode am Harz) with DUO 5 M pump (Pfeiffer Vacuum, Aßlar) and for product analysis by HPLC or further product purification by FPLC used (2.8.4).

2.8.4 FPLC (ÄKTA) for L-PAPA Purification

Another method used to purify L-PAPA was adsorption chromatography with FLPC (ÄKTA) on a lab-scale. For this purpose, the culture supernatants were used with prior modifications (See 2.8.1) and then 10 g of NaCl was added to 100 ml of supernatant. The pH of the suspension was then adjusted to 1 by hydrogen chloride (37%) and then sample was concentrated by freezes drying. Next, 10 ml water/0.1% Formic acid was added to the sample and followed by centrifugation (4°C, 5,000 rpm for 30 min) and filtration (0.2 µm). The concentrated sample was then fed into a Luna column (Phenomenex, C18 (2), 250 mm × 21.20 mm 5 micron) packed with silica gel on a ÄKTA purifier (Amersham Bioscience / GE Healthcare, Munich) with P-900 pump, Frac-950 fraction collector, pH /C-900 analytical unit, UV-900 spectrophotometer and Unicorn 5.11 software. A gradient method comprising 0.1% (vol vol^{-1}) formic acid in Water/Methanol was applied with a flow rate of 8 ml min^{-1} (Table 2-32). Upon column chromatography, fraction containing L-PAPA were selected, and then verified purity by HPLC analysis (See 2.7.2.2). Finally to obtain gram scale of L-PAPA, selected fraction collected together and concentrated by deep-freezing at below 5 mbar with the Alpha I-5 freeze-drying plant (Christ freeze drying plants, Osterode am Harz) with DUO 5 M pump (Pfeiffer Vacuum, Aßlar) to obtain gram scale end-product L-PAPA (Brown yellow powder, See Figure **3-31** (c)).

FPLC condition:

- Column: Luna (C18 (2), Phenomenex, 5 µm, 250 mm * 21.20 mm)
- Buffer condition: A: water with 0.1% FA , B: methanol with 0.1% FA
- Injection volume: 1.2 ml, Flow: 8 ml min^{-1}, Fraction size: 2 ml

Table 2-35 Gradient method used for FPLC

Time [min]	A [%]	B [%]
0	10	90
8	70	30
8	70	30
6	10	90
4	10	90
4	10	90

3. Results

This chapter contains the results of microbial synthesis (plasmid construction, de-novo pathway construction, whole cell biosynthesis and biotransformation), strain improvement, shake flask cultivation, Scale-up production (fermenter), downstream processing (extraction and purification) and analytical results of various aromatic compounds. The results are classified according to the syntheses of aromatic amines (part I) and syntheses of aromatic alcohols (part II). A brief overview of what are presented is shown in Figure 3-1.

3.1 Part I: Biosynthesis of Aromatic Amines

In this chapter, *E. coli* susceptibility on three aromatic amines is initially investigated and then the metabolic pathways for L-PAPA and PAPE or 4-APA based on expression plasmids are provided. The efficiency of the recombinant pathway is evaluated by whole cell biotransformation and then the de-novo platform from renewable substrate (glucose or glycerol) is established. The results of the HPLC and LC-MS analysis are presented to evaluate and verify the final products. Furthermore, the expression patterns of the plasmid-coded recombinant proteins on 2D gel are examined. This chapter also describes the application of metabolic engineering tools in optimizing the aromatic amines production including (i) elimination of competing pathway and negative regulator, (ii) remove of the bottleneck by overexpression of rate limited steps and (iii) overexpression of genes involved in the central metabolism pathway (*tktA, glpX*). Finally, results of fed batch cultivation in the shake flasks and fermenter (0.5-30 l) are presented. This chapter concludes with creating a valuable procedure for L-PAPA purification from the culture broth (Figure 3-1). Importantly here, both carbon sources (glucose and glycerol) are used in microbial biosynthesis of all three aromatic amines, whereas better L-PAPA results are obtained with glycerol as carbon source but for PAPE and 4-APA better results are observed on glucose (data not shown).

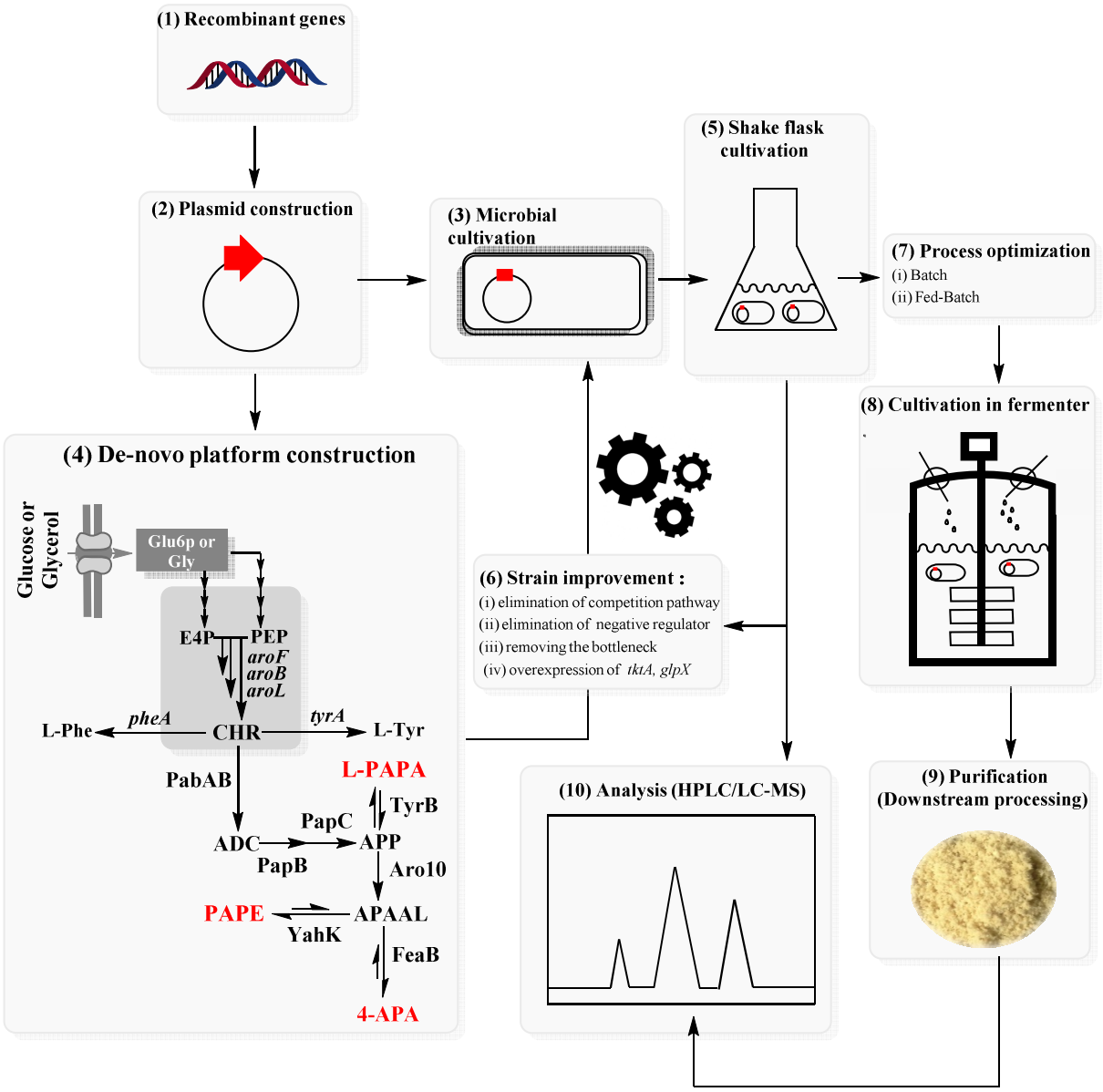

Figure 3-1 A brief overview of results

3.1.1 Metabolic engineering of *E. coli* for biosynthesis of *para*-amino phenylalanine (L-PAPA)

3.1.1.1 L-PAPA susceptibility on *E. coli* LJ110 growth

In order to evaluate the potential toxic effects of L-PAPA, as well as to estimate future limits on achievable titers in *E. coli*, the cell growth was measured in the presence of varying exogenous L-PAPA concentrations (0, 4, 6, 8 and 33 mM L-PAPA). An overnight culture grown in minimal media with 5 g l^{-1} glycerol was used to inoculate the media with an initial OD_{600nm} of 0.1. The growth rate in the presence of 4, 6 and 8 mM L-PAPA was slightly reduced compared to the absence of L-PAPA (0 mM L-PAPA) the same optical density (OD_{600nm} values) was reached after 24h of incubation (Figure **3-2**). At a concentration of 33 mM L-PAPA (~ 6 g l^{-1}), however, the formation of biomass and the growth rate were reduced. From this, the susceptibility limit of L-PAPA against *E. coli* wild-type (LJ110) was estimated to be 6 g l^{-1}. This was a particularly relevant concern in this study that further L-PAPA accumulation in the culture may contribute to the observed reduction in the biomass. Thus, based on these observations, it can be considered that L-PAPA could be proceeded in recombinant *E. coli* strains without severe toxicity to the producer cells (Mohammadi et al. 2018).

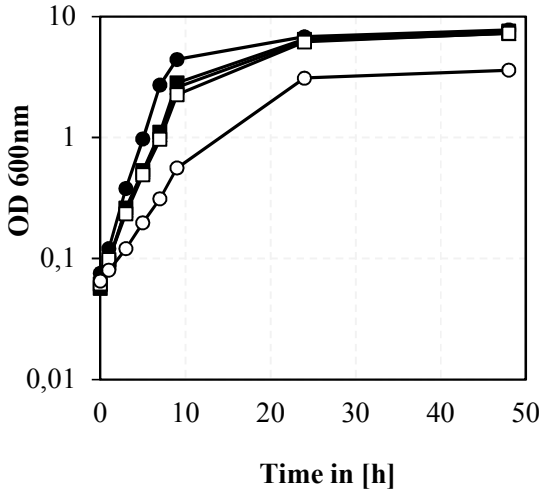

Figure 3-2 Growth experiment of *E. coli* LJ110 in minimal media (Gerhardt) with 5 g l^{-1} glycerol and different concentration of L-PAPA. The cells were cultivated at 37 °C in the absence of L-PAPA (●, filled circles) and in the presence of L-PAPA, 4 mM (■, filled squares), 6 mM (▲, filled triangles), 8 mM (□, open squares) and 33 mM L-PAPA (○, open circles). The cultivations were performed in duplicate and the mean values are given.

3.1.1.2 Construction of a de novo L-PAPA biosynthesis pathway in *E. coli*

De-novo L-PAPA biosynthesis pathway based on extended shikimate pathway in *E.coli* which carries the genes from different donor organisms was constructed (Figure **1-5**). The first step in the microbial biosynthesis of L-PAPA is the amination of chorismic acid to 4-amino-4-deoxychorismate (ADC) by ADC synthase (Figure **1-5**). Naturally, this reaction is part of the folic acid biosynthesis pathway in *E. coli*, which is catalyzed by two enzymes PabA and PabB (Nichols et al.1989; Parsons et al. 2002). Kozak (2006) reported that conversion of chorismic acid to ADC either by in-vivo test activity of separate proteins (PabA and PabB) or by fusion of two separate proteins (PabA and PabB fusion proteins) in the crude cell extract of *E. coli* could not be detected. Besides, instead of the two separate enzymes PabA and PabB, there is only one enzyme in *Streptomyces* and *Corynebacterium*, PabAB, which catalyzes this reaction (Brown et al. 1996; Chang et al. 2001). However, since the DNA sequence of the *pabAB* gene from *Streptomyces* is very GC-rich (GC content about 70% (Ikeda et al. 2003) and contains many rare codons for *E. coli*, thus a *pabAB* gene encoding 4-amino-4-deoxychorismate synthase from the PABA biosynthesis pathway in *C. glutamicum* (Kozak 2006; Stolz et al. 2007) was preferred to others. For this purpose an already described vector pC53 was used which is harboring $pabAB_{C.gl}$ in recombinant form and under the control of an IPTG-inducible P*tac* promoter (Kozak 2006). To complete the intended L-PAPA pathway, genes *papB* and *papC* with codon optimization for expression in *E. coli* were custom synthesized based on the gene sequences of *S. venezuelae* (*papB,* 4-amino-4-deoxy-chorismate mutase; *papC,* 4-amino-4-deoxyprephenate dehydrogenase) (He et al. 2001; Piraee et al. 2004). The synthetic DNA was digested with the restriction enzymes (BglII/BamHI) and then ligated into the digested (BglII/BamHI) plasmid pC53 to yield plasmid pC53BC (Mohammadi et al. 2018). The constructed plasmid pC53BC was introduced into *E. coli* LJ110 as host strain and then used for L-PAPA production. The proposed biosynthetic pathway for L-PAPA is schematically shown in Figure **1-5**.

3.1.1.3 Microbial biosynthesis of L-PAPA with *E. coli* LJ110 /pC53BC

The first step of the L-PAPA production was investigation of protein expression of all candidate enzymes as part of the L-PAPA pathway via 2D-SDS-PAGE. Differences in the protein composition of the two *E. coli* strains harboring full vector (pC53BC) or empty vector (pJF119EH), respectively, can be seen in Figure **3-3**. For the detection of individual protein

spots, 2D-SDS Gels of *E. coli* pC53BC (green spot) were compared with 2D-SDS gels from *E. coli* pJF119EH (empty plasmid as control, red spot). As labeled in Figure **3-3**, predicted spots presumably related to PabAB (63 KDa, pI~5.15), PapB (11 KDa, pI~6.01) and PapC (32 KDa, pI~6.1) are recognizable in 2D-SDS Gels of *E. coli* pC53BC (green spots). In contrast these protein spots are absent in 2D-SDS gels from *E. coli* pJF119EH (empty plasmid as control, red spots). Moreover three known protein spots for DnaK, PstS and Ef-Tu were also labeled in both gels (Figure **3-3**). Based on these results, it was assumed that plasmid-coded proteins are present in soluble form. Mass spectrometry analysis is required to further prove that these soluble spots are related to the desired recombinant proteins.

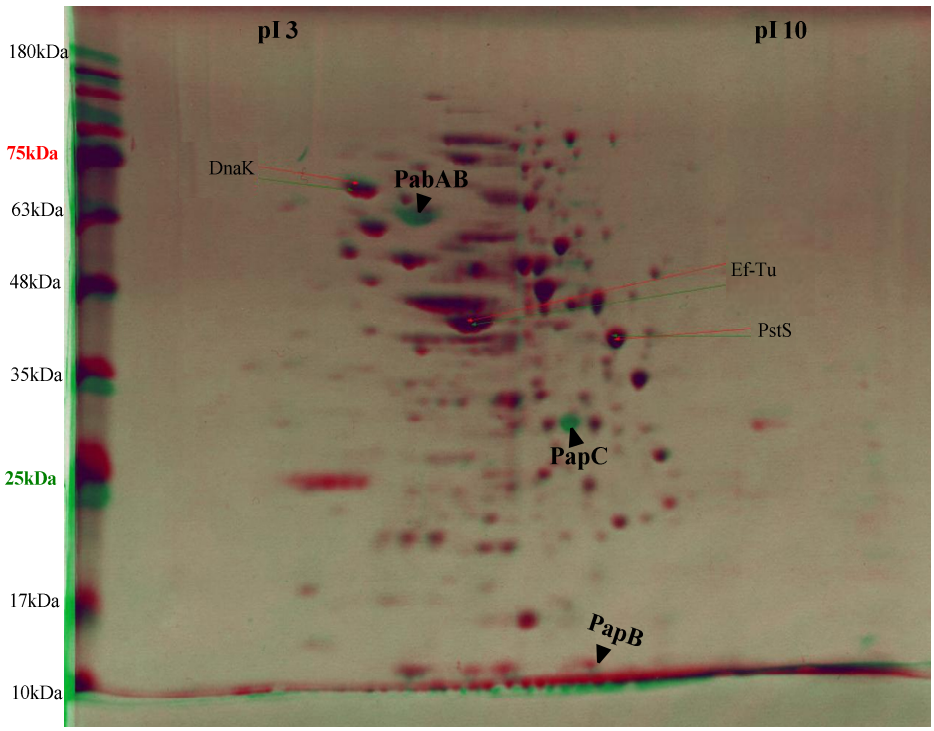

Figure 3-3 Comparison of 2D-SDS gel electrophoresis of *E. coli* harboring pC53BC (48h, green) vs. *E. coli* harboring pJF119EH (as control-red). For evaluation the software Delta2D Version 3.2 (Decodon GmbH) was used. Protein spots presumably related to PabAB, PapC and PapB are visible (labeled with black arrow). The identification of the spots was performed by pI and size comparison of the individual spots. Possible spots for PabAB (63kDa, 5.15), PapC (32kDa, 6.1) and PapB (11kDa, 6.01) were identified by comparison with control (pJF119- red).

The second step was investigation of in vivo functional activity of the recombinant protein. For this purpose, *E. coli* LJ110 pC53 was cultivated in the shake flask containing minimal medium and glycerol as carbon source (5 g l^{-1}). This strain was induced with IPTG (OD600nm~0.6, 0.5

mM). After induction the cultures are incubated at 37˚C for 48h and the supernatant was assayed by RP-HPLC for the presence of new peak (ADC or L-PAPA). A new unknown peak (RT=8.32 min) could be detected in HPLC chromatogram of *E. coli* LJ110 pC53 (Figure 3-4 (b)) compared to control (*E. coli* LJ110 pJF119, Figure 3-4 (a)), which is presumably related to ADC or pABA (*para*-aminobenzoic acid).

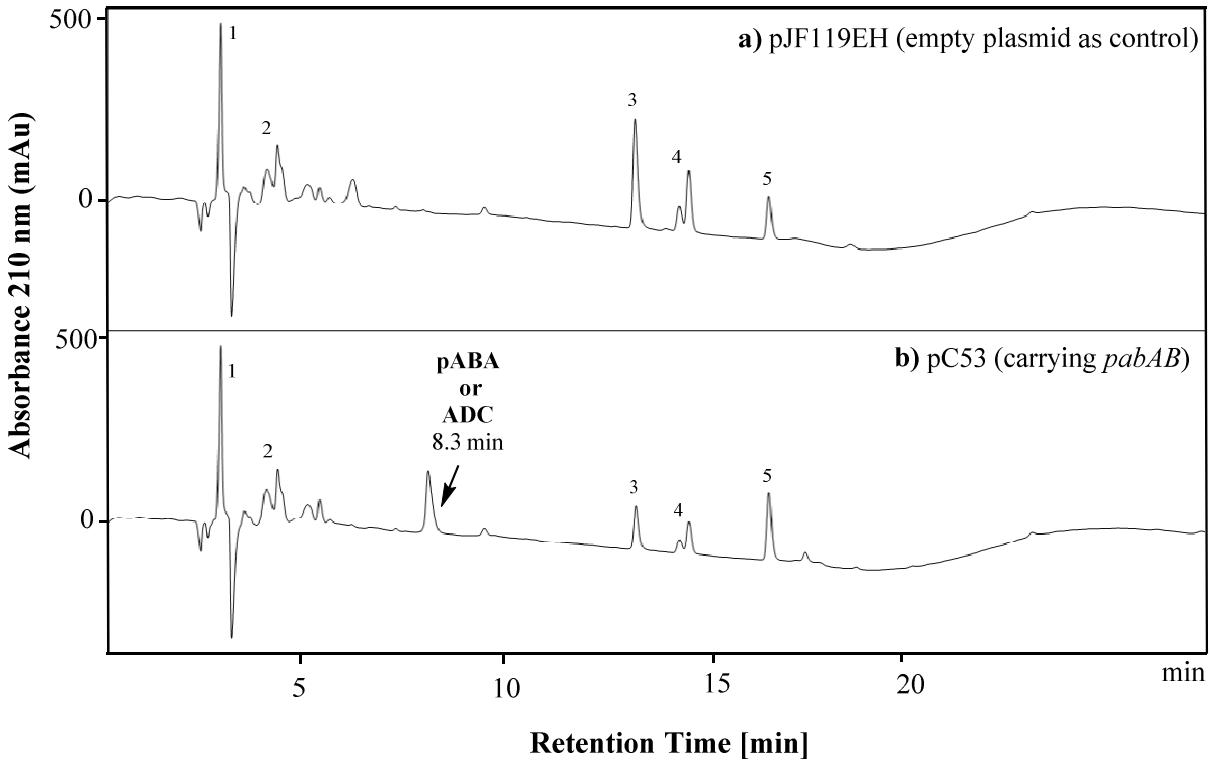

Figure 3-4 HPLC chromatograms represent the supernatant (after 48h) from the culture broth of *E. coli* LJ110 pJF119 (a) and *E. coli* LJ110 pC53 (b). An unknown peak (RT=8.32 min) which is likely related to ADC or pABA is labeled. The HPLC system was equipped with a symmetry C18 silica column (Lichrospher 100 RP, 250 mm× 4 mm, chromatography service GmbH) and a UV detector operating at a wavelength of 210 nm. Labeled peaks [1, 2, 3, 4 and 5] are from minimal medium components (phosphorus,..).

In addition, the constructed pC53BC was transformed into the strain *E. coli* LJ110 and the shake flask experiment in the minimal medium was carried out. After IPTG induction (Fin. Con. 0.5 mM) a new peak (L-PAPA, Figure **3-5** (b)) compared to the control (Figure **3-5** (a)) was found. Furthermore as seen in the Figure **3-5**, the supernatant of fermentation broth was analyzed by RP-HPLC, and L-PAPA was identified on the basis of the retention time with spike test with standard (Figure **3-5** (c)) and the LC–MS analysis (Figure **3-5** (d)).

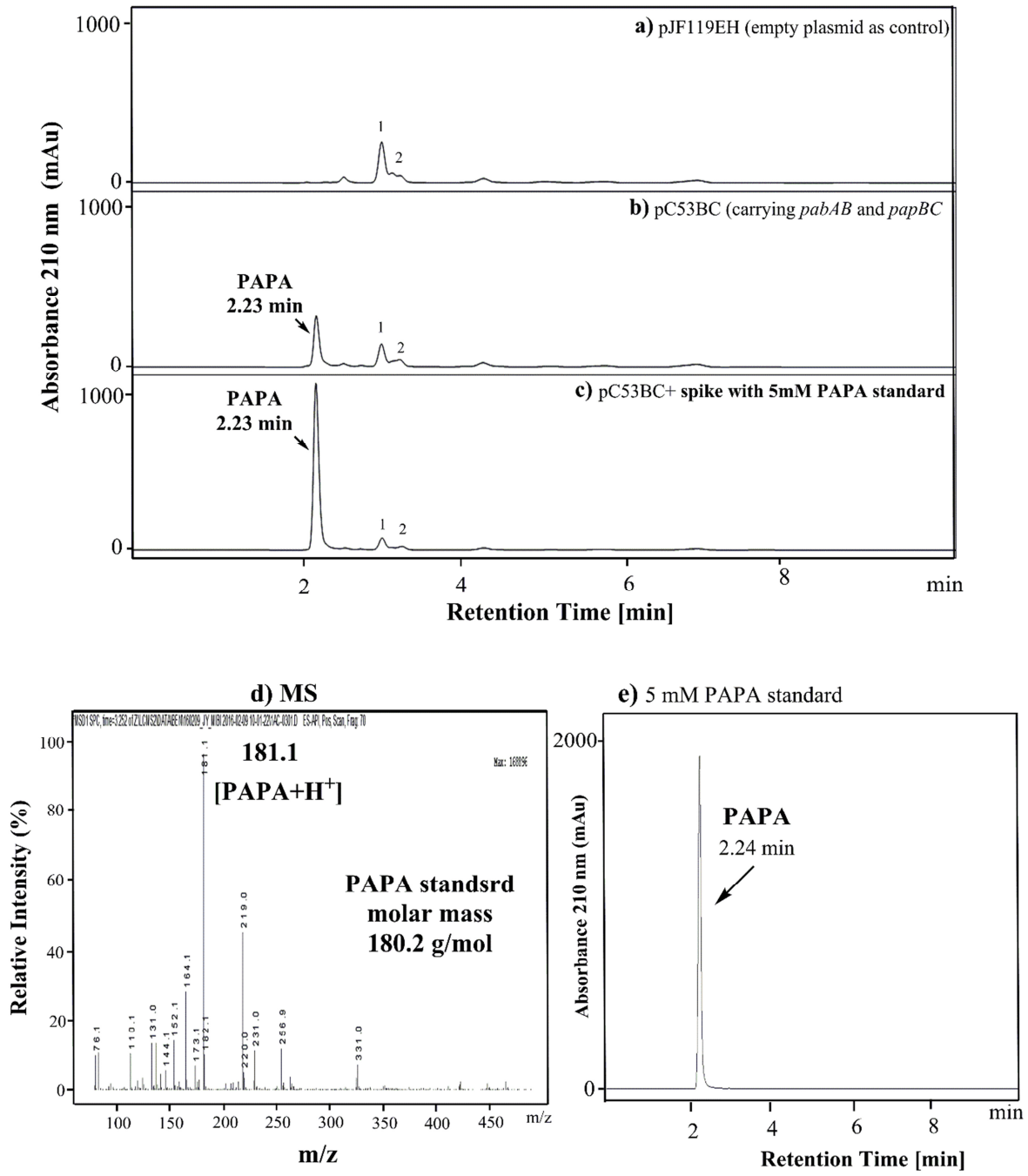

Figure 3-5 Reversed phase HPLC analysis and LC-MS analysis of PAPA. The chromatograms display; **(a)** An extract (after 48h) from the culture broth of *E. coli* LJ110 pJF119EH (as control); **(b)** an extract (after 48h) from the culture broth of *E. coli* LJ110 pC53BC; **(c)** spike test, 5 mM PAPA standard was added to a supernatant from the culture broth of *E. coli* LJ110 pC53BC; **(d)** LC-MS spectrum of PAPA from the culture broth of *E. coli* LJ110 pC53BC and **(e)** 5mM PAPA standard. The HPLC system was equipped with a symmetry C18 silica column (Prontosil, 250 mm× 4 mm, CS chromatography service GmbH) and a UV detector operating at a wavelength of 210 nm. Retention time: 2.24 minutes represent L-PAPA; absorption maximum at 210 nm; plotted as absorbance unit [mAU] versus time [min]. Labeled

peaks [1and 2] are from the media. Presumably peaks related to ADP, APP, ADC or pABA were not detectable. PAPA standard has a molar mass 180.207 g/mol (Appendix A1.).

As shown in Figure **3-5** (b), *E. coli* LJ110 strain carrying pC53BC plasmid produced a major product that has identical retention time (2.23 min and an absorption maximum at 210 nm) and yields identical $[M+H]^+$ ions to standard PAPA (Appendix-A1, detection was carried out spectrophotometrically in a wavelength range of 200-400 nm). The primary ion fragment at m/z 181.1 ($[M+H]^+$) corresponds to PAPA with molecular weight of 182.1 (Figure **3-5** (c)). These data confirmed the in vivo functionality of the constructed pathway in the biosynthesis of PAPA via plasmid based expression of *pabAB*, *papB* and *papC* genes in *E. coli.* A typical shake flask cultivation of *E. coli* LJ110/pC53BC in minimal medium was carried out and then after reaching OD_{600nm} ~ 0.6 expressions of recombinant genes for L-PAPA production was induced by adding IPTG (0.5 mM, red dotted line). After 48 h, a maximal L-PAPA concentration of 43 ± 1.8 mg l^{-1} in the supernatant (Figure **3-6** (b)) was measured, whereas in the *E. coli* LJ110 carrying empty plasmid (pJF119EH) no L-PAPA was detected. This proved that the recombinant genes were functionally expressed in *E. coli* which is compatible with former observations (Mehl et al. 2003; Masuo et al. 2016).

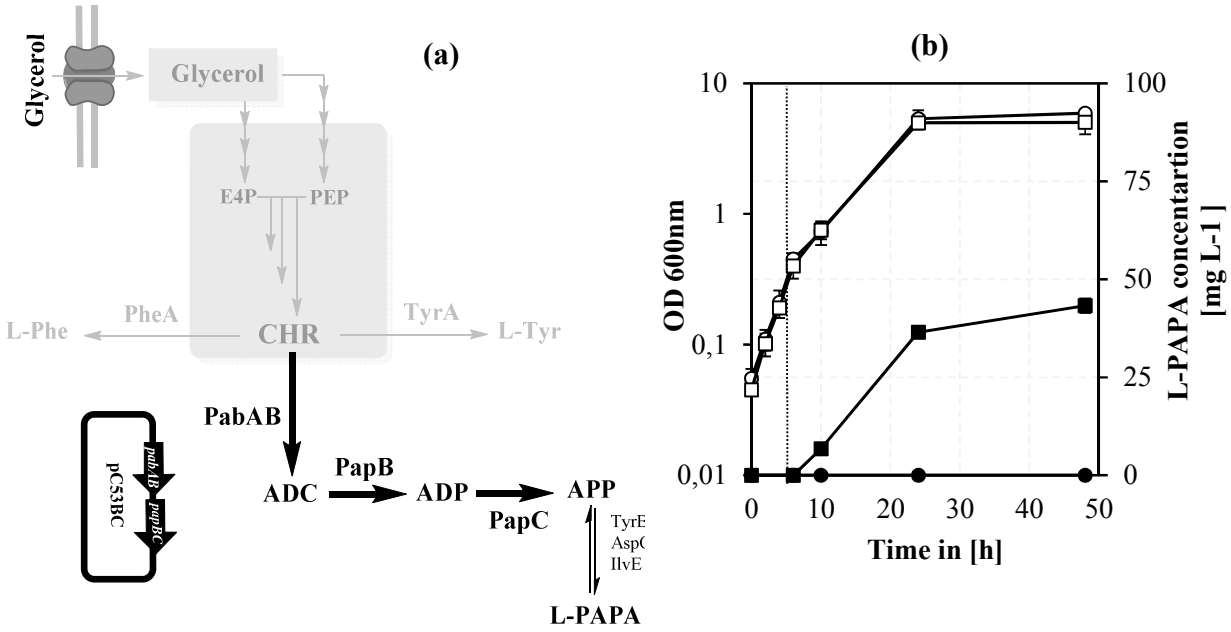

Figure 3-6 a) Proposal of a biosynthesis pathway for production of L-PAPA from glycerol in *E. coli* wild-type. **b)** Glycerol batch cultivation of *E. coli* LJ110 /pC53BC and *E. coli* LJ110 /pJF119EH (empty vector) in shake flasks. The initial glycerol concentration was 5 g l^{-1}. After reaching OD_{600nm}~ 0.6, the cultures was induced with 0.5 mM IPTG (final concentration, red dotted line). The concentrations of L-PAPA in *E.coli* LJ110/pC53BC (■, filled squares); in *E. coli* LJ110/pJF119 (●, filled circles) were

determined by HPLC and OD_{600nm} is presented as empty squares (□) in *E. coli* LJ110/pC53BC and empty circle (○) in *E. coli* LJ110/pJF119. The cultivations were performed in quadruplicate and the mean values are given. ADP, APP, ADC or pABA were not detectable in culture medium.

3.1.2 Metabolic engineering of *E. coli* for biosynthesis of *para*-amino phenylethanol (PAPE)

3.1.2.1 PAPE susceptibility on *E. coli* LJ110 growth

The tolerance of *E. coli* to PAPE was first studied to test whether PAPE is a suitable compound to be produced by *E. coli.* It is known that 2-phenylethanol (2-PE), an analog of PAPE, is toxic to *E. coli* at doses above 1–1.5 g l^{-1} (Masker and Eberle 1972; Lucchini et al. 1993; Kang et al. 2012). The PAPE toxicity was tested by monitoring the growth behavior of *E. coli* wild-type strain LJ110 in minimal medium supplemented with glucose (4.5 g l^{-1}) and varying PAPE concentrations of 0, 7.5, 15, 30, 40, and 50 mM (Figure **3-7**). Almost no or only a negligible effect of PAPE was observed up to a concentration of 30 mM. Although cells were able to grow until 40 mM of PAPE was present, the growth rate was severely reduced (≥ 60 %) compared to the control (without PAPE). Eventually, a complete growth inhibition was observed at a PAPE concentration of 50 mM (6.8 g l^{-1} PAPE) (Figure **3-7**), suggesting that the toxicity limit lies between 30-50 mM PAPE. These observations suggest that PAPE is compounds to be produced with recombinant *E. coli* strains without extreme toxicity to the producer cells.

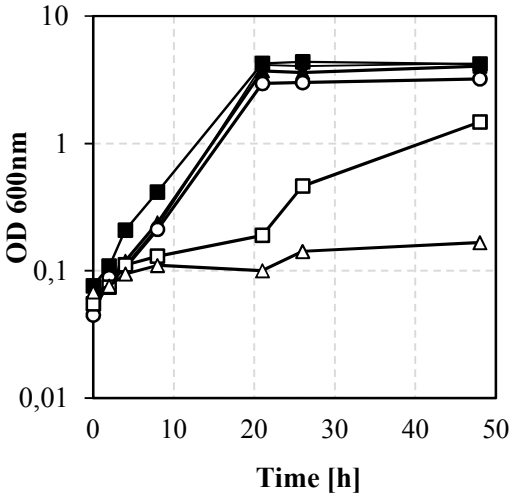

Figure 3-7 Growth experiment of *E. coli* LJ110 in minimal medium with 4.5 g l^{-1} glucose in the presence of varying PAPE concentrations. The growth was determined by measuring the OD_{600nm} (Cary 50 UV-Vis, Varian). The concentrations of PAPE were added to the medium as follows: 0 mM (filled square, ■); 7.5 mM (filled circle, ●); 15 mM (filled triangle, ▲); 30 mM (empty circle, ○); 40 mM (Empty Square, □) or 50 mM (empty triangle, Δ). The cultivations were performed in duplicate and the mean values are given.

3.1.2.2 Construction of a de novo PAPE biosynthesis pathway in *E. coli*

A de-novo PAPE pathway similar to the Ehrlich pathway which is part of the phenylalanine catabolism to form 2-PE in yeast (Etschmann et al. 2002) was constructed. For this purpose pC53BC (see Table **2-3**) was used as starting vector. *E. coli* lacks a gene for decarboxylation of phenylpyruvate or 4-hydroxyphenylpyruvate to phenylacetaldehyde or 4-hdroxyphenylacetaldehyde (Koma et al. 2012), respectively. Thus construction of a PAPE biosynthesis pathway based on L-PAPA required an exogenous decarboxylase enzyme. Subsequent reduction of the aldehyde would be by an endogenous alcohol dehydrogenase or aldehyde reductase. It has been demonstrated previously that the Aro10 from *Saccharomyces cerevisiae* is able to decarboxylate several keto acids as substrate (Vuralhan et al. 2003 and Kneen et al. 2001; Chung et al. 2017; Li et al. 2018). These enzymes are also able to catalyze the decarboxylation of *para*-amino phenylpyruvate (APP) to PAPE (Masuo et al. 2016). This activity would make it a suitable enzyme for the first step of the PAPE biosynthetic pathway. Thus *aro10* gene (1.9 Kbp) from *Saccharomyces cerevisiae* was PCR amplified and then cloned into BamHI/XbaI digested pJF119EH and pC53BC. The resulting plasmids carrying the *aro10* gene were designated pJFA10 and pC53BCA (Table **2-3**). Moreover, all genes were equipped with an optimized ribosomal binding site for *E. coli.* To complete the PAPE pathway, APAAL has to be reduced to PAPE by the endogenous alcohol dehydrogenases or aldehyde reductases in *E. coli* (Figure **1-8**).

3.1.2.3 Whole cell biotransformation of PAPE from L-PAPA for pathway function verification

First it was studied whether overexpression of *aro10* can lead to PAPE production by investigating the conversion of exogenously supplied *para*-amino-L-phenylalanine (L-PAPA) by *E. coli* LJ110 pJFA10 resting cells (Figure 3-8 (a)). As shown in Figure 3-8 (b), the concentration of L-PAPA was reduced in *E. coli* LJ110 pJF119EH from 1 ± 0.027 g l^{-1} L-PAPA to 0.82 ± 0.078 g l^{-1} but no APP or PAPE was detectable after 8h. The entire ~1± 0.029 g l^{-1} of initial L-PAPA was consumed within the first 8 h of the experiment with *E.coli* LJ110 pJFA10 cells. As L-PAPA was consumed, PAPE began to accumulate, doing so at similar initial rates. After 8 h, however, PAPE accumulation slowed down, reaching a maximum titer of 0.69 ± 0.034 g l^{-1}. A total conversion of 90.2% C mol mol^{-1} (~ 69 % mg mg^{-1}) at 8 h in *E. coli* LJ110 pJFA10 was obtained. In vivo conversion of L-PAPA to PAPE proved the functional expression of this

recombinant Aro10 in *E. coli*. In addition, although APP was not recognizable, 0.128 ± 0.027 g l^{-1} para-amino phenylacetic acid (4-APA) as a side product was detected after 8h in *E. coli* LJ110 pJFA10.

(a)

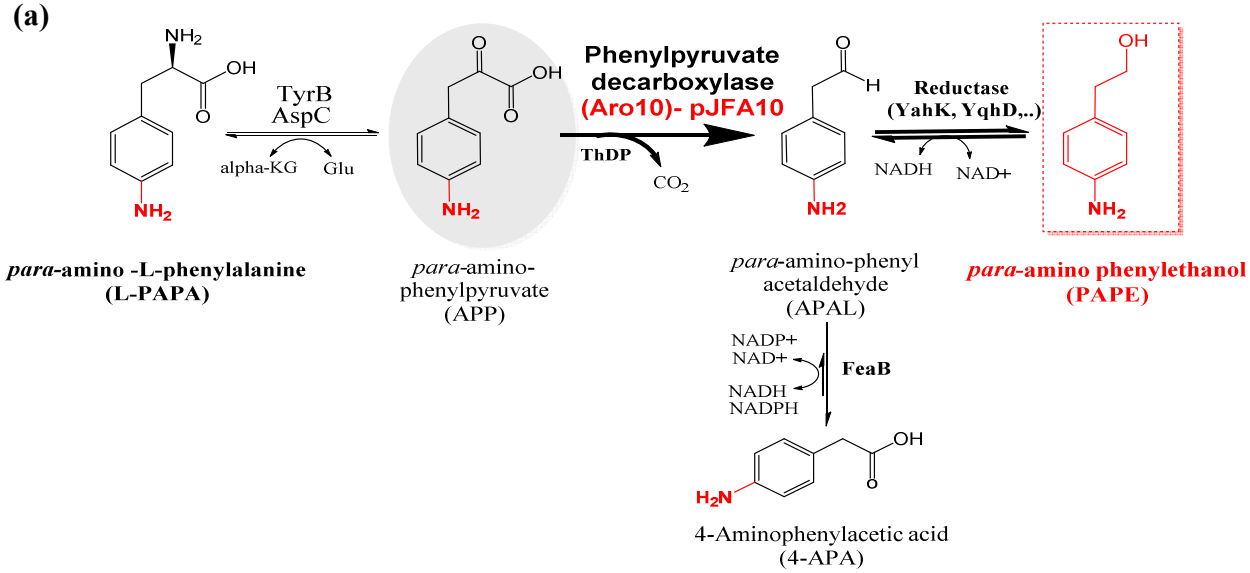

***para*-amino -L-phenylalanine (L-PAPA)**

para-amino-phenylpyruvate (APP)

para-amino-phenyl acetaldehyde (APAL)

***para*-amino phenylethanol (PAPE)**

4-Aminophenylacetic acid (4-APA)

(b)

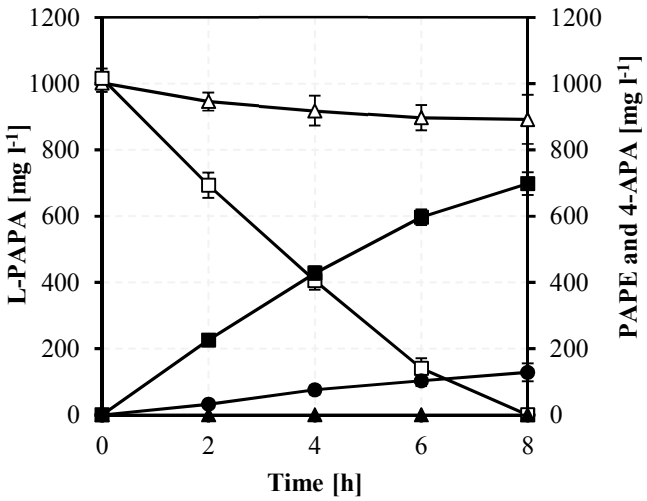

	Products			
	PAPE		**4-APA**	
	mg l^{-1}	yield (% mg mg^{-1})	mg l^{-1}	yield (%mg mg^{-1})
pJF119EH	n.d.	-	n.d.	-
pJFA10	698.3± 34	69	128.4± 27	13

Figure 3-8 Proposed pathway for whole cell biotransformation of *para*-amino-L-phenylethanol (PAPE) from *para*-amino-L-phenylalanine (L-PAPA) in *E.coli* LJ110 (**a**). Biological conversion 1 g l^{-1} exogenous L-PAPA by resting cell *E. coli* LJ110 pJF119EH (as control) and pJFA10 over the course of 8 h **(b).** *E. coli* cells were initially grown at 37C until reach OD600nm 0.6. Afterwards, 0.5mM IPTG (final conc.) was added and incubated at 30°C for 4-6h (OD_{600nm} ~5). The collected cells were resuspended in the 10 ml potassium buffer (pH~ 7) and followed by incubation in 30°C-110 rpm with start OD_{600nm} ~16. Concentrations of L-PAPA and PAPE were analyzed by HPLC. Filled triangle (▲), L-PAPA concentration in *E. coli* LJ110 pJF119EH (empty plasmid as control); Filled Square (■), L-PAPA concentration in *E. coli* LJ110 pJFA10; Empty triangle (Δ), PAPE production in *E. coli* LJ110 pJF119 (empty plasmid as control), Empty Square (□), PAPE production in *E. coli* LJ110 pJFA10 and filled circle (●), 4-APA concentration in *E. coli* LJ110 pJFA10. APP was not detected in HPLC chromatogram. The data represent the mean and standard deviations (± SD) from measurements of three biological replicates. [n.d.] stands for Not Detectable and [-], stands for not calculable.

Furthermore protein expression was monitored by SDS-PAGE from crude extracts of IPTG-induced *E.coli* DH5α cells carrying pJFA10. As negative controls, *E. coli* DH5α cell carrying the empty expression vector (pJF119EH) was used. As can be seen in Figure **3-9,** a strong band (labeled with **) likely related to Aro10 approximately 66 KDa (Kneen et al. 2011) was found as soluble protein in the crude extract from *E. coli* DH5α pJFA10. In contrast, a weak-narrow bound likely related to Aro10 was observed in the cell pellet from *E. coli* DH5α pJFA10, meaning most of recombinant Aro10 is presented in soluble form in crude extract. Moreover, this 66-kDa band (likely Aro10) was not observed in the crude extract as well cell pellet from *E. coli* DH5α carrying the empty expression vector (Figure **3-9**). These results imply that Aro10 probably generates a 66-kDa band mostly soluble in the crude extract. To investigate the specific activity of Aro10 in crude extract, a coupled enzyme assay was applied as previously described for benzoylformate decarboxylase activity (Yep et al. 2006; Kneen et al. 2011). Briefly, the two plasmids pJF119EH (empty plasmid as control) and pJFA10 were individually transformed into *E. coli* DH5α (cultivated at 30°C, OD_{600nm}~ 0.5, 0.5mM IPTG) and then crude extract was used for specific activity of Aro10. The specific crude extracts activity of Aro10 in the presence of phenylpyruvate (PP) as substrate coupled with yeast alcohol dehydrogenase (decrease in $NADH^+$ content) was investigated by incubating varying concentration of crude extract (5-120 µg ml^{-1}). In presence of phenylpyruvate (PP) as a substrate and ThDP (0.25 mM) as the cofactor, Aro10 may decarboxylate PP, generating Phenylacetaldehyde (PAAL) and CO_2. Subsequently, PAAL produced during this reaction can be reduced to 2-Phenylethanol by alcohol dehydrogenase, resulting in oxidation of NADH. Therefore, the spectrophotometry measurement of NADH levels can be used to monitor the decarboxylation activity of Aro10. For cell free extracts of *E.*

coli expressing the pJFA10 specific crude extract activity of phenylpyruvate decarboxylase (Aro10) was measured 107 ± 9 nmol min^{-1} mg^{-1} of proteins (Table **3-1**). This may demonstrate the presence of phenylpyruvate decarboxylase activity in *E. coli* expressing the pJFA10. Conversely, no or less remarkably background activity (2 ± 1.5 nmol min^{-1} mg^{-1}) was measured in cell extracts from *E. coli* harboring empty plasmid pJF119EH.

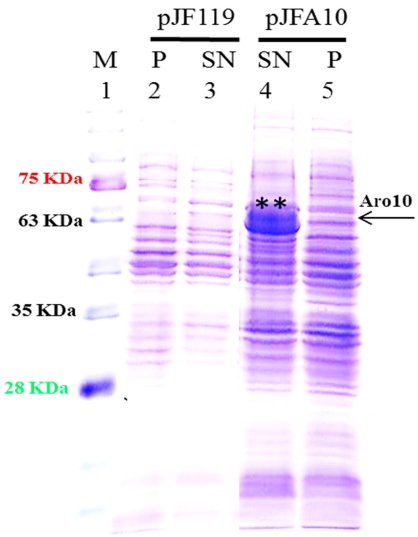

Figure 3-9 SDS-PAGE (12%) analysis of Aro10 expression (**) in crude extract and cell pellet from the *E. coli* DH5α harboring pJF119EH and pJFA10. Lane 1; prestained protein ladder [kDa], Lane 2; 5 µg protein from pellet of *E. coli* DH5α pJF119, Lane 3; 5 µg protein from crude extract of *E. coli* DH5a pJF119, Lane 4;10 µg protein from crude extract of *E. coli* DH5α pJFA10 and Lane 5; 10 µg protein from pellet of *E. coli* DH5α pJFA10. After reaching OD600nm~0.5-0.6, 0.5mM IPTG (final conc.) was added and was incubated at 30°C for 4-6h induction. Protein size of Aro10 was approximately 66 kDa (Kneen et al. 2011). SN, represent soluble crude extract and P, represent insoluble pellet.

Table 3-1 The specific crude extracts activity of Aro10 [a] in the presence of phenylpyruvate (PP) as substrate coupled with NADH oxidation (ΔE_{340nm}) by yeast alcohol dehydrogenase in cell free extract of *E. coli* pJFA10

Name of crude extract	**Crude extract activity (nmol min^{-1} mg^{-1}protein)**
pJFA10	107 ± 9

[a] Crude extract activity with three replicates were perfomed at 30°C (See section 2.5.5.2)

3.1.2.4 Microbial biosynthesis of PAPE from simple carbon source (glucose)

To test the in vivo activity of the overexpressed protein, *E. coli* LJ110 was transformed with pC53BCA. Since this strain has been successfully used for the microbial synthesis of L-PAPA (Figure **3-6**), thus a PAPE formation can be expected. In the shake flask, this strain was first incubated at 37°C until OD_{600nm} 0.5 and then gene expression was induced by the addition of 0.5 mM IPTG (final conc.).

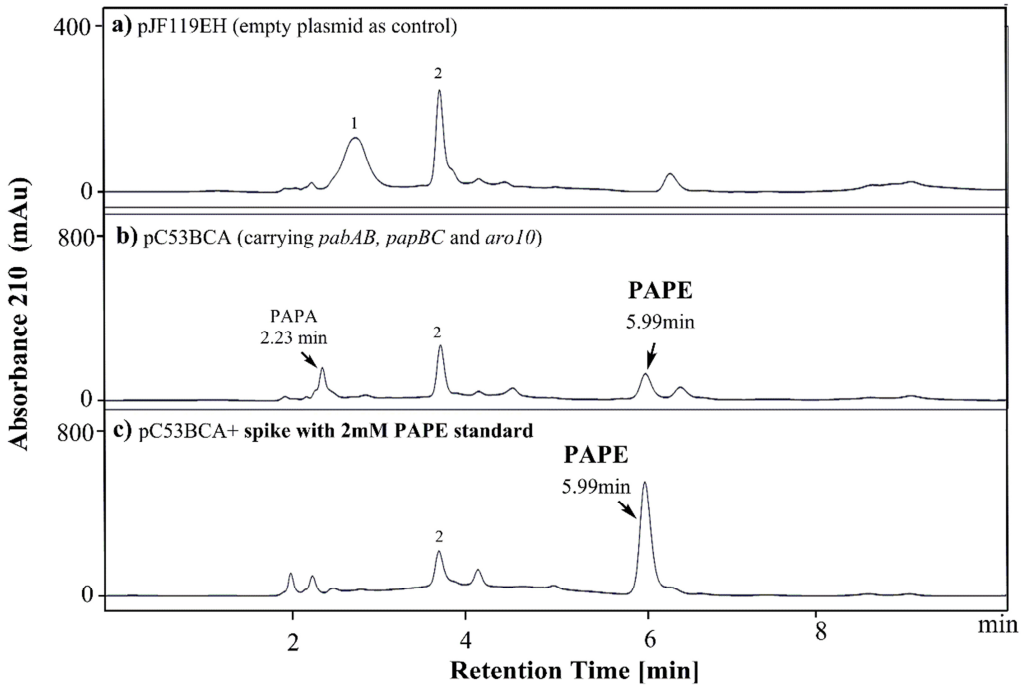

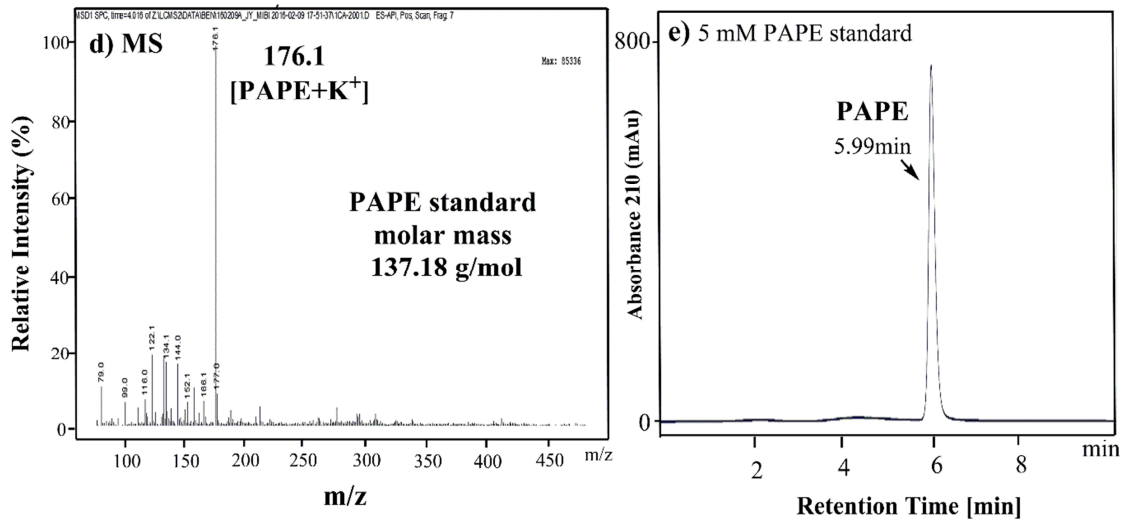

Figure 3-10 Reversed phase HPLC analysis and LC-MS analysis of PAPE. The chromatograms display; **(a)** An extract (after 48h) from the culture broth of *E. coli* LJ110 pJF119 (control); **(b)** an extract (after 48h) from the culture broth of *E. coli* LJ110 pC53BCA; **(c)** spike test, 2 mM PAPE standard was added to a supernatant from the culture broth of *E. coli* LJ110 pC53BCA; **(d)** LC-MS spectrum of PAPE and **(e)** 5mM PAPE standard. The HPLC system was equipped with a symmetry C18 silica column (Prontosil, 250 mm× 4 mm, CS Chromatography Service GmbH) and a UV detector operating at a wavelength of 210 nm. Retention time: 5.99 minutes represent PAPE; absorption maximum at 210 nm; plotted as absorbance unit [mAU] versus time [min]. Labeled peaks [1 and 2] are presumably from minimal media components (phosphorus,..). Presumably peaks related to APAAL, APP, ADC or pABA were not detectable. PAPE standard has a molar mass 137.17 g/mol (Appendix A2.).

The supernatant was assayed (Figure 3-10) for a new peak by comparing the HPLC-peak areas obtained for the PAPE standard and samples (Figure 3-10 (c and e)) and the LC–MS analysis (Figure 3-10(d), Appendix-A2). Comparison of the retention times of supernatant to those of analytical standards showed that the peak of PAPE with RT~5.9 min (Figure 3-10, (e)) was only observed in the HPLC chromatogram with the sample from the extract of the recombinant *E. coli* LJ110/pC53BCA (Figure 3-10, (b)), but not for the control (Figure 3-10, (a)). This means that L-PAPA and PAPE are formed in *E. coli*. Presumably peaks related to APAAL, APP, ADC or pABA were not detectable. As shown in Figure 3-10 (b), *E. coli* LJ110 pC53BCA produced a new product that has identical retention time 5.99 min and an absorption maximum at 210 nm (Figure 3-10 (b)).

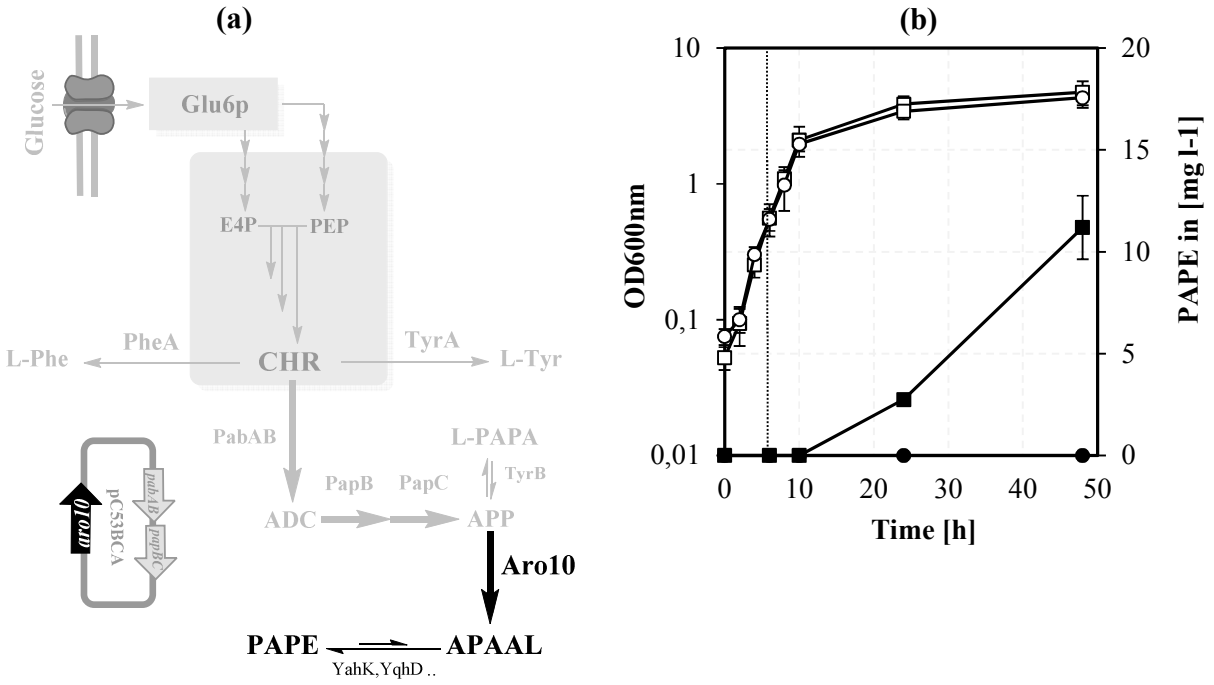

Figure 3-11 (a), Schematic represents PAPE biosynthesis pathway from glucose in *E. coli* LJ110 harboring single plasmid pC53BCA (A). **(b),** Glucose batch cultivation of *E. coli* LJ110/pC53BCA and *E. coli* LJ110/pJF119EH (empty vector) in the shake flasks. The initial glucose concentration was 4.5 g l^{-1}. After 10h of cultivation the cultures were induced with 0.5 mM IPTG (final concentration). PAPE concentration in *E. coli* LJ110 /pC53BCA (■, filled squares); in *E. coli* LJ110/ pJF119EH (●, filled circles) were determined by HPLC and OD600 is presented as empty squares (□) in *E. coli* LJ110/pC53BCA and empty circle (○) in *E. coli* LJ110 / pJF119EH. The data represent the mean and standard deviations (± SD) from measurements of three biological replicates

Both samples from standard PAPE and *E. coli* LJ110 pC53BCA showed a fragment ion m/z at 176.1 (M+ K^+) (Figure 3-10 (e)). The LC-MS data suggest that PAPE produced by recombinant *E. coli* LJ110 pC53BCA is very similar in ionization pattern to PAPE standard (Appendix-A2). Moreover, For PAPE produced by the established biosynthetic pathway one major peak corresponding to peak of the PAPE standard was found. The PAPE obtained was relatively low 11.2 ± 1.56 mg l^{-1} (Figure 3-11 (b)) compared to the produced L-PAPA (43 ± 1.8 mg l^{-1} (Figure **3-6** (b)), suggesting part of the carbon flux from upstream pathway was probably not directed toward PAPE production. Therefore, providing different genetic approaches via pathway engineering to direct more carbon flux toward APA production and consequently more PAPE production is necessary (See section 3.1.4).

3.1.3 Metabolic engineering of *E. coli* for biosynthesis of *para*-amino phenyl acetic acid (4-APA)

3.1.3.1 Assaying 4-APA toxicity on *E. coli*

To verify if *E. coli* would indeed be a suitable host for *para*-amino phenyl acetic acid (4-APA) production, 4-APA (98%) was fed to the cell culture of *E. coli* LJ110 immediately after inoculation to final concentrations ranging from 0 to 50 mM. As illustrated in Figure **3-12**, growth rate was reduced as a function of 4-APA concentration. Growth of *E. coli* was still possible up to 30mM. The cell growth of *E.coli* LJ110 was significantly inhibited at concentration of 40 mM. The final OD_{600nm} at 40 mM of 4-APA was about 50% of that control. At 50 mM, however, no growth was observed following 4-APA addition, suggesting that susceptibility limit of 4-APA against *E. coli* wild-type lies between 30-50 mM. Importantly with regard to the 4-APA toxicity level, it can be said that 4-APA accumulation at a significant level is at least possible in *E.coli.* Additionally, the accumulation of impurities from concentrated 4-APA (with only 98% purity) may contribute to the observed results.

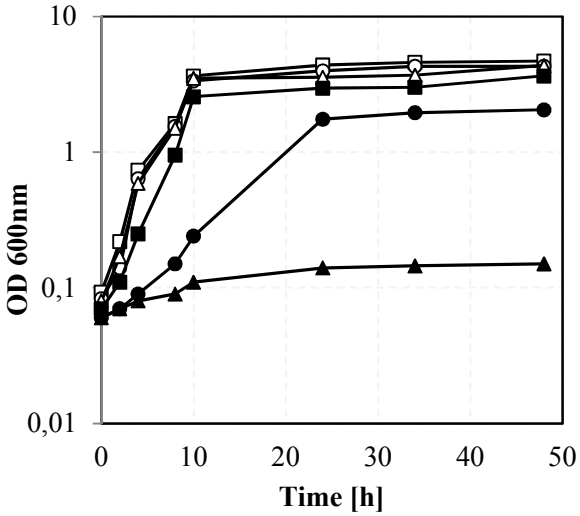

Figure 3-12 Inhibitory effect of exogenous 4-APA on cell growth of *E. coli* LJ110 in minimal medium with 4.5 g l^{-1} glucose. The growth was determined by measuring the OD_{600nm} (Cary 50 UV-Vis, Varian). The concentrations of 4-APA were added to the medium as follows: 0 mM (empty square, □); 10 mM (empty circle,○); 20 mM (empty triangle, Δ); 30 mM (filled square, ■); 40 mM (filled circle, ●) or 50 mM (filled triangle, ▲). The data represent the mean and standard deviations (± SD) from measurements of three biological replicates

3.1.3.2 Construction of a de novo 4-APA biosynthesis pathway in *E. coli*

A biosynthetic route that makes 4-APA through one enzymatic reaction via the intermediate *para*-aminophenyl acetaldehyde (APAAL, Figure **1-6**) was aimed. Previously it was reported that an endogenous *feaB* encoding phenyl acetaldehyde dehydrogenase in *E. coli* (Díaz et al. 2001; Ikeda 2006), can mediate conversion of phenyl acetaldehyde to phenyl acetate (Koma et al. 2014; Zhang et al. 2017). Therefore, it was investigated whether FeaB, which catalyzes the oxidation of phenyl acetaldehyde to phenyl acetic acid, is also able to convert APAAL to 4-APA. For this purpose, pC53BCAF vector which encoded all required genes for production 4-APA was constructed. Hence, the *feaB* gene (1.5 Kbp) from *E. coli* was PCR amplified and cloned into SphI/SbfI-digested the vectors pJFA10 and pC53BCA, yielding plasmids pJFA10F and pC53BCAF, respectively. Additionally, *feaB* gene was equipped with an optimized ribosomal binding site for *E. coli*.

3.1.3.3 Whole cell biotransformation of 4-APA from bio L-PAPA

To test whether native phenyl acetaldehyde dehydrogenase (FeaB) from *E. coli* has broad substrate activity and is sufficient to oxidize APAAL to 4-APA, the conversion of exogenously

supplied *para*-amino-L-phenylalanine (L-PAPA) by *E. coli* LJ110 pJFA10F resting cells was investigated. No 4-APA production was detected indicating that *E. coli* LJJ10 carrying empty plasmid pJF119EH did not have the ability to convert L-PAPA into detectable amounts of 4-APA (Figure 3-13 (b)).

(a)

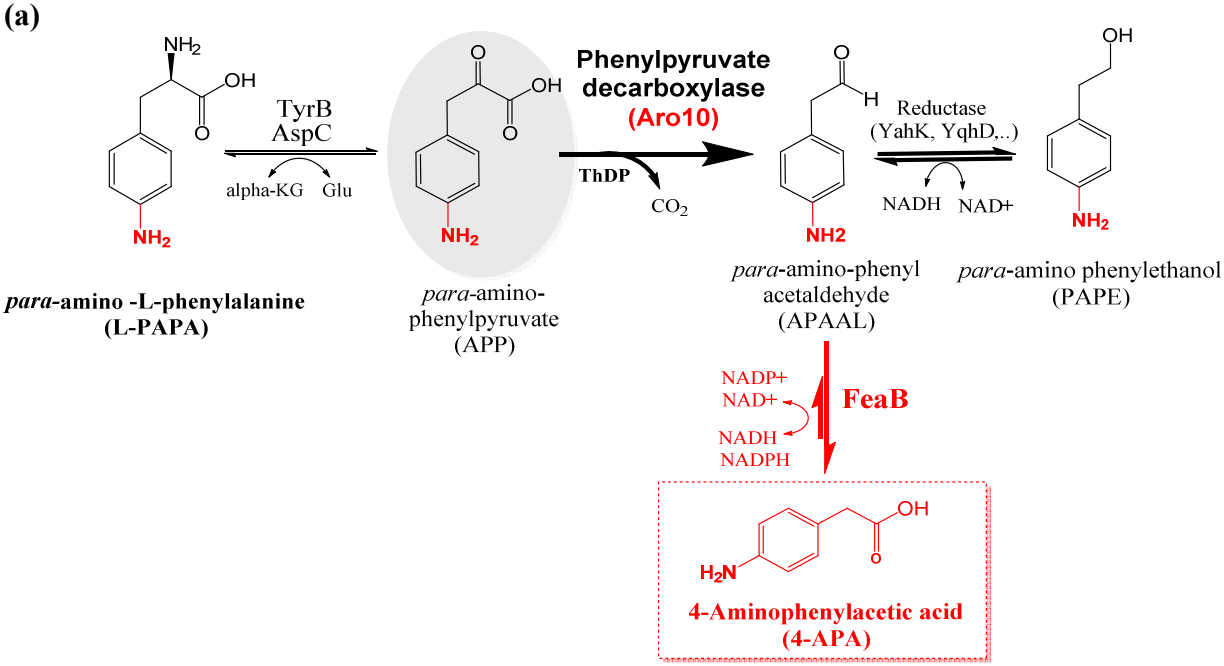

(b)

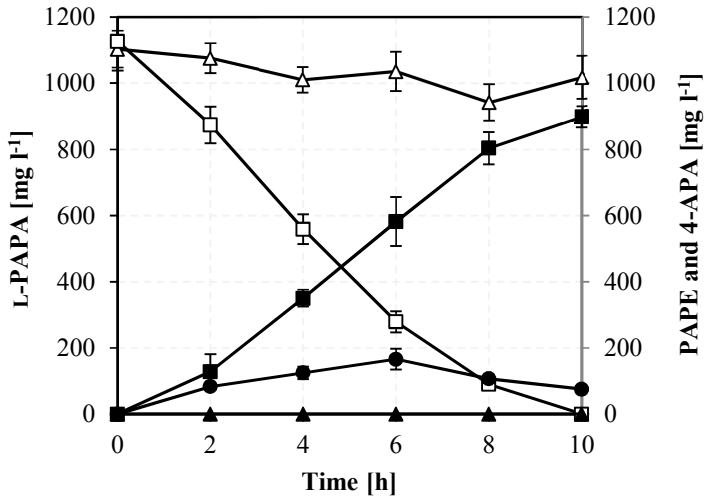

	Products			
	4-APA		**PAPE**	
	mg l^{-1}	yield (%, mg mg^{-1})	mg l^{-1}	yield (%,mg mg^{-1})
pJF119EH	n.d.	-	n.d.	-
pJFA10F	899 ± 32.1	80	75.5 ± 5.5	7

[n.d.] stands for Not Detectable and [-], stands for not calculable.

Figure 3-13 Whole cell biotransformation of 4-APA from L-PAPA in *E. coli* LJ110/pJA10F and pJF119EH. **(a)** Proposed pathway for bioconversion L-PAPA to 4-APA in *E. coli* wild type harboring pJFA10F plasmid (*aro10* and *feaB*). **(b)** Biological conversion of exogenous 1.12 ± 0.088 g l^{-1} L-PAPA by resting cell *E. coli* LJ110/pJA10F and pJF119EH (as control) over the course of 10 h. *E. coli* cells were initially grown at 37˚C until reach OD_{600nm} 0.6. Afterwards, 0.5mM IPTG (final conc.) was added and incubated at 30°C for 4-6h (OD600nm ~5). The collected cells were resuspended in the 10 ml potassium buffer (pH~ 7) and followed by incubation in 30°C-110 rpm with start OD_{600nm} ~16. Biotransformation was carried out on a rotary shaker with 110 rpm at 30°C. Concentrations of L-PAPA, 4-APA and PAPE were analyzed by HPLC. (Δ), L-PAPA concentration in *E. coli* LJ110 pJF119EH (empty plasmid as control); (□), L-PAPA concentration in *E. coli* LJ110 pJFA10F; (▲), 4-APA production in *E. coli* LJ110 pJF119EH (empty plasmid as control), (■), 4-APA production in *E. coli* LJ110 pJFA10F and (●), PAPE production in *E. coli* LJ110 pJFA10F. Triplicate assays were performed and the error bars indicated standard deviations (±SD).

In comparison, the strain *E. coli* LJ110 pJFA10F (simultaneously expressed *aro10* and *feaB*) produced 899 ± 32.1 mg l^{-1} 4-APA with a total conversion molar yield of 96.2% (80 % mg mg^{-1}, Figure 3-13) while concentration of L-PAPA was reduced from 1126 ± 88.5 mg l^{-1} to 90 ± 7.5 mg l^{-1} after 8 hours and was eventually fully consumed after 10 hours. Simultaneously, accumulation of PAPE was observed reaching a maximum titer of 166 ± 31.2 mg l^{-1}after 6h and then reduced to 75 ± 5.5 mg l^{-1} after 10 h in *E. coli* LJ110 pJFA10F. This was most likely due to the presence of an endogenous aldehyde reductase in *E.coli* (Rodriguez and Atsumi 2012). In vivo conversion of L-PAPA to 4-APA and PAPE proved the functional expression of recombinant *aro10* and *feaB* in *E.coli*.

3.1.3.4 Microbial biosynthesis of 4-APA from glucose

After the bioconversion results confirmed the efficient production of 4-APA from L-PAPA, the de-novo production of 4-APA from glucose was further investigated (Figure **3-15** (a)). For this purpose, batch cultivations of *E.coli* LJ110/ pC53BCAF in minimal medium supplemented with 4.5 g l^{-1} glucose were performed in shake flasks. After 48 h of cultivation, supernatant of cultures were analyzed for the presence of a new peak (4-APA) by HPLC. In addition, 4-APA validation

was performed by 4-APA standard addition (Figure 3-14 (c and e)) and by LC–MS analysis (Figure 3-14 (d)).

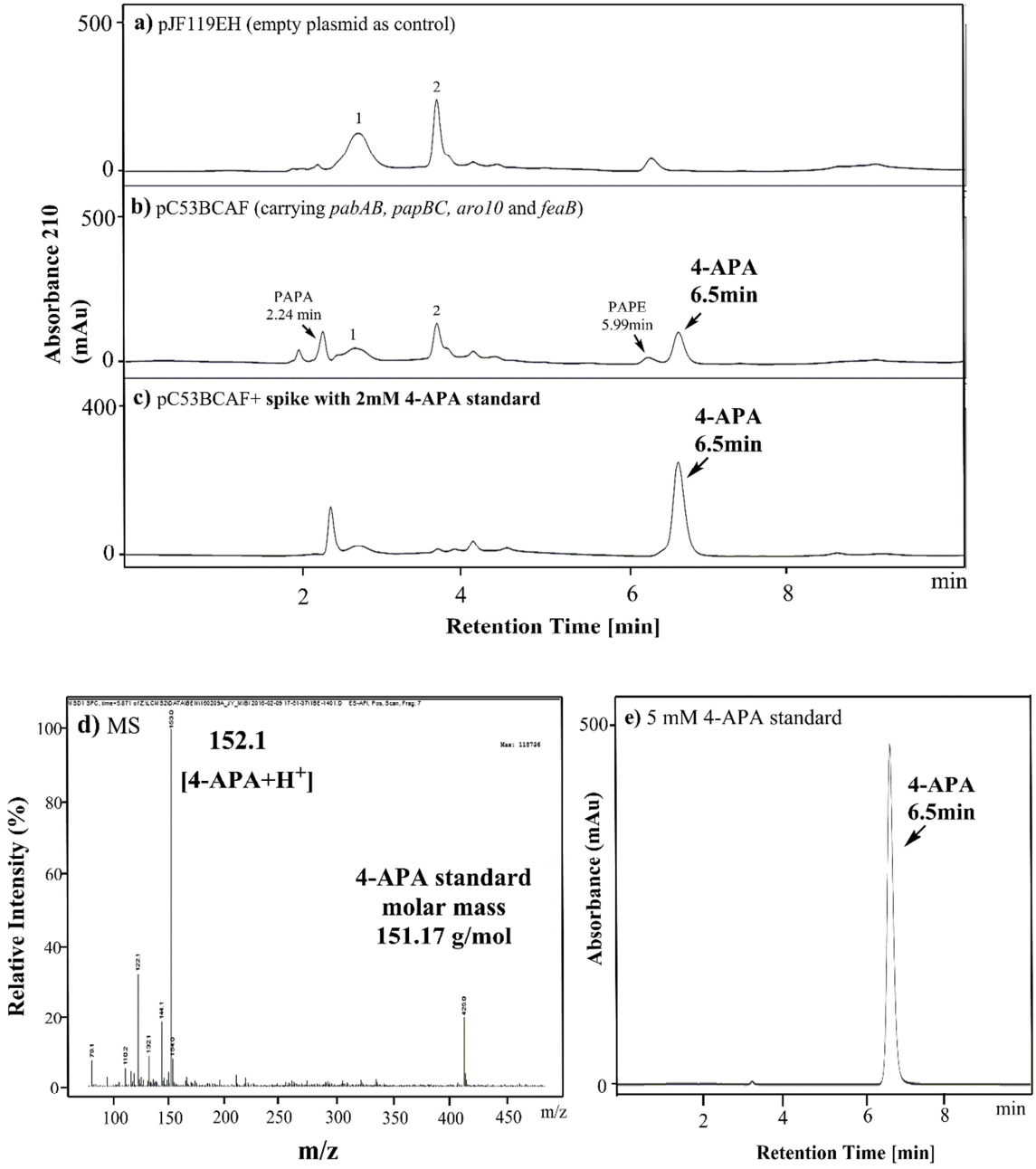

Figure 3-14 Reversed phase HPLC analysis and LC-MS analysis of 4-APA. The chromatograms display supernatant (after 48h) from the culture broth of *E. coli* LJ110 pJF119 (control **(a)**) and *E. coli* LJ110 pC53BCAF **(b)**; spike test, 2 mM 4-APA standard was added to a supernatant from the culture broth of *E. coli* LJ110 pC53BCAF **(c)**; LC-MS spectrum of 4-APA **(d)** and **(e)** 5 mM 4-APA standard. The HPLC system was equipped with a symmetry C18 silica column (Prontosil, 250 mm× 4 mm, CS Chromatography Service GmbH) and a UV detector operating at a wavelength of 210 nm. Retention time:

6.5 minutes represent 4-APA; absorption maximum at 210 nm; plotted as absorbance unit [mAU] versus time [min].]. Labeled peaks [1 and 2] are from the minimal medium components. Presumably peaks related to APAAL, APP, ADC or pABA were not detectable. 4-APA standard has a molar mass 151.16 g/mol (Appendix A3.).

No 4-APA formation could be detected in cultures of *E. coli* LJ110 harboring empty plasmid pJF119EH (Figure 3-14 (a)), while a new known peak (RT=6.5 min) was found in the supernatant of the *E. coli* LJ110 pC53BCAF (Figure 3-14 (b)). Additionally, a sharp peak [2] was observed in the HPLC chromatogram of empty plasmid (Figure 3-14 (a)), probably due to the accumulation of an intermediate metabolite from upstream pathway (Shikimate pathway), which is reduced in *E. coli* LJ110 carrying pC53BCAF (Figure 3-14 (b)).

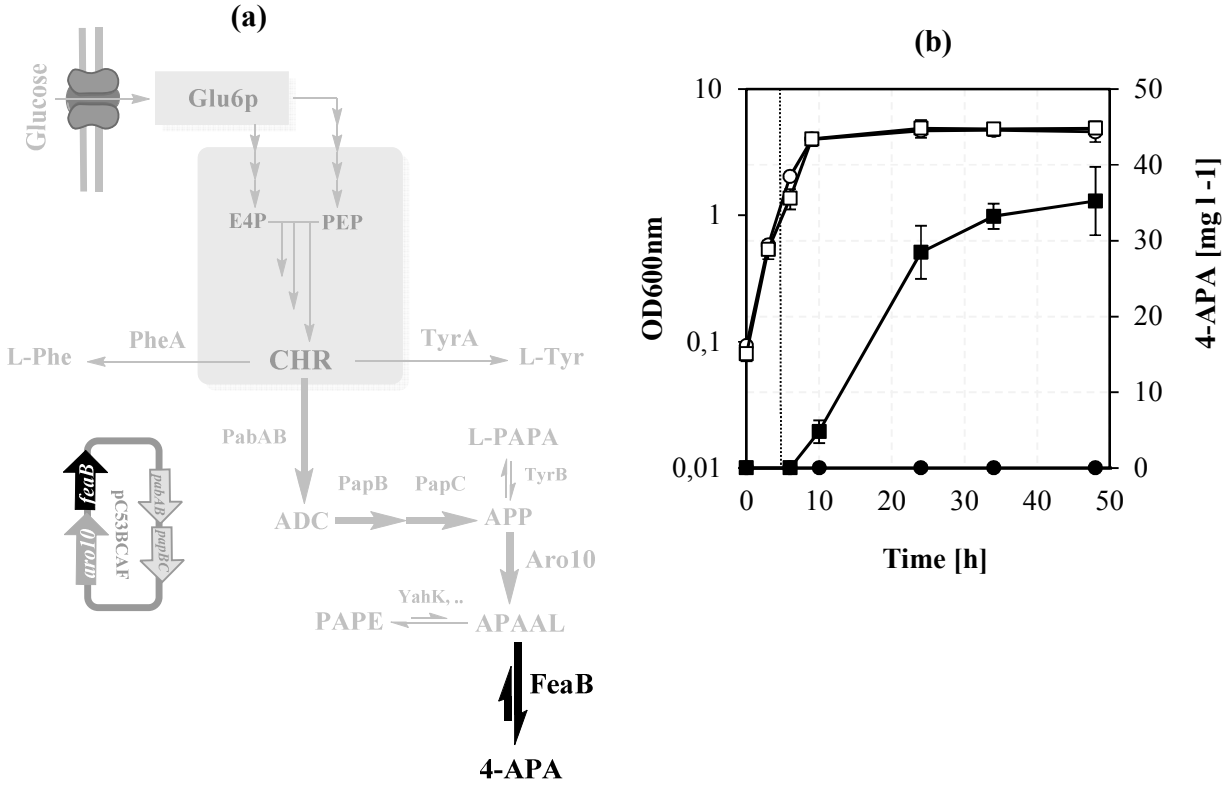

Figure 3-15 (a), Schematic represent de-novo 4-APA biosynthesis pathway from glucose in *E.coli* wild type harboring pC53BCAF. **(b),** Glucose batch cultivation of *E. coli* LJ110 /pC53BCAF and *E. coli* LJ110 /pJF119 (empty vector) in shake flasks. The initial glucose concentration was 4.5 g l^{-1}. After reaching OD600nm~ 0.6 (red dotted line), the culture was induced with 0.5 mM IPTG (final concentration). 4-APA concentration in *E. coli* LJ110 /pC53BCAF (■, filled squares); in *E. coli* LJ110/ pJF119 (●, filled circles) were determined by HPLC and OD600 is presented as empty squares (□) in *E.*

coli LJ110/pC53BCAF and empty circle (○) in *E. coli* LJ110 / pJF119. The data represent the mean and standard deviations (± SD) from measurements of three biological replicates.

As shown in (Figure 3-14 (b)), *E. coli* LJ110 carrying pC53BCAF produced a major product with a retention time 6.5 min at an absorption maximum 210 nm. The ESI mass spectrum of 4-APA displayed a dominant peak at 153 $[M+H^+]^+$ matches with m/z 152.1 ($[M+H^+]^+$) for 4-APA standard (Appendix-A3), there are also small peaks at 122 and 425 (Figure 3-14 (d)). A mixed spiking solution were prepared by mixing equal portions of 4-APA standard (Figure 3-14 (e)) and supernatant from *E. coli* LJ110 pC53BCAF (Figure 3-14 (b)). A sharper peak (Figure 3-14 (c)) with similar retention time to 4-APA was observed when spike test was performed. These data confirmed 4-APA is produced by recombinant *E.coli* and also showed in vivo functionality of the constructed pathway in the biosynthesis of 4-APA via plasmid based expression in *E. coli*. These results suggest that FeaB as an efficient phenyl acetaldehyde dehydrogenase in *E.coli* can catalyze the oxidation of APAAL to 4-APA (Figure 3-15 (a)). The titer of 4-APA produced by strain *E.coli* LJ110 pC53BCAF was enhanced to 36 mg l^{-1} after 48h cultivation (Figure 3-15 (b)). This indicates that introduction of an additional *feaB* led to a larger proportion of the carbon flux instead of being directed toward PAPE production, is directed toward the 4-APA. While overexpression of *feaB* can significantly increase 4-APA accumulation, there is still a minor amount of PAPE (7.5 ± 1.8 mg l^{-1}, data not shown) as byproduct, thus future improvements will be necessary (See section 3.1.4).

3.1.4 Metabolic engineering of *E. coli* for optimization of aromatic amines production

Different genetic approaches of pathway engineering were combined to improve production of aromatic amines in *E. coli* as described in the following. Both carbon sources (glucose and glycerol) are used in microbial biosynthesis of all three aromatic amines (data not shown), whereas better L-PAPA results are obtained with glycerol as carbon source, but for PAPE and 4-APA better results are observed on glucose (data not shown). Thus in all experiment, minimal medium supplemented with 5 g l^{-1} glycerol in case of PAPA and 4.5 g l^{-1} glucose in case of PAPE and 4-APA production.

3.1.4.1 Increasing aromatic amines production by elimination of competing pathways

To further increase flux (through shikimate pathway) towards aromatic amines, one possibility is the elimination of the competing pathways. Thus, genes involved in competing side reactions

need to be deleted to avoid the consumption or degradation of the desired intermediates (chorismate). For improved L-PAPA production a more advanced strain, *E. coli* FUS4 was used (Gottlieb et al. 2014). The *E. coli* FUS4 has an additional copy of *aroFBL* genes which is under the control of the P_{tac} promotor and has gene deletions of *pheA, tyrA* and *aroF*. *pheA* (encoding chorismate mutase / prephenate dehydrogenase, McCandliss et al. 1976) and *tyrA* (encoding chorismate mutase/prephenate dehydratase) were deleted to eliminate competing reaction for chorismate, which is the precursor of the aromatic amines pathway (Figure **3-16** (a)). Then, three plasmids pC53BC (see 3.1.2.2), pC53BCA (see 3.1.2.2) and pC53BCAF (3.1.3.2) that were previously used for production of L-PAPA, PAPE and 4-APA, respectively, were introduced into the strain *E. coli* FUS4. Batch cultivation for improvement of the production of all three aromatic amines with recombinant *E. coli* FUS4 was performed. After 48h cultivation in shake flasks containing minimal media, the production titer of all three aromatic amines was analyzed by HPLC. L-PAPA, PAPE and 4-APA titer showed an increasing titer (after IPTG induction) and then began to constant presumably due to a limitation factor in minimal medium. Using *E. coli* FUS4 as the host, a positive effect on production of all three aromatic amines (L-PAPA, PAPE and 4-APA) was observed.

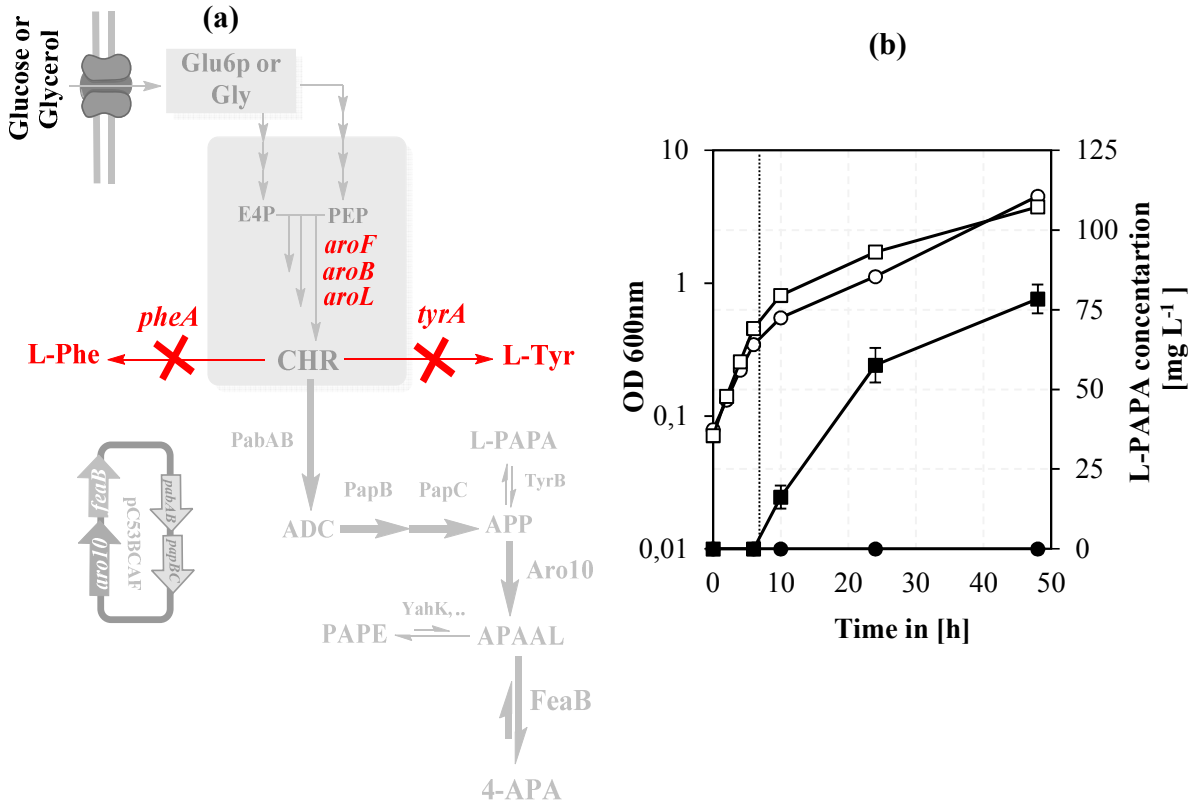

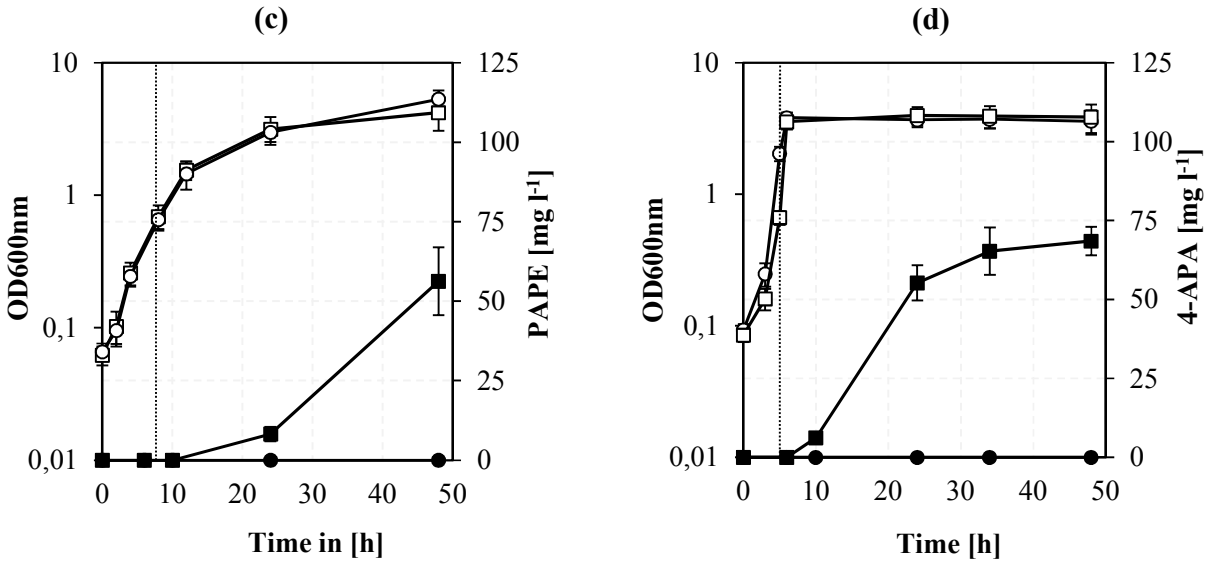

Figure 3-16 Batch cultivation of *E. coli* FUS4 with different plasmids in the shake flasks. *E. coli* FUS4 strain containing different recombinant plasmids were cultivated (48h) in shake flasks supplemented with 5 g l^{-1} glycerol in case of PAPA and 4.5 g l^{-1} glucose in case of PAPE and 4-APA production. After reaching OD_{600nm}~0.6 (red dotted line) the cultures were induced with 0.5 mM IPTG (final concentration) and further incubated at 30°C. **(a),** Schematic represents aromatic amines production in engineered *E.coli* FUS4; **(b),** Time course of L-PAPA (■) production using strain *E.coli* FUS4 pC53BC; **(c),** Time course of PAPE (■) production using strain *E. coli* FUS4 pC53BCA; **(d)**, Time course of 4-APA (■) production using strain *E. coli* FUS4 pC53BCAF. **Legends:** Filled square (■) represents aromatic amino production in full vector which is determined with HPLC, Filled circle (●) represents aromatic amino production in *E. coli* FUS4 pJF119EH (as control) and empty square (□) represents OD_{600nm} in full vector and empty circle (○) represents OD_{600nm} in *E .coli* FUS4 pJF119EH (as control). The data represent the mean and standard deviations (± SD) from measurements of three biological replicates.

Compared with the parental strain (Glycerol as C source), FUS4 showed much better results and L-PAPA titer reached 78.3 ± 5.2 mg l^{-1} with yield 0.015 g g^{-1} (L-PAPA/glycerol). Moreover, they exhibited an elevated product titer of 56.3 ± 10 mg l^{-1} PAPE (Glucose as C source) in FUS4/pC53BCA (Figure **3-16** (c)) and 68.2 ± 4.5 mg l^{-1} 4-APA (Glucose as C source) in FUS4/pC53BCAF (Figure **3-16** (d)) with only trace amount of L-PAPA accumulated (Table **3-2**). In contrast, no aromatic amines production was observed in *E. coli* FUS4 harboring empty plasmid pJF119EH Figure **3-16** (b, c and d)).

Table 3-2 Aromatic amine production in *E. coli* FUS4 (supplemented with 5 g l^{-1} glycerol in case of PAPA and 4.5 g l^{-1} glucose in case of PAPE and 4-APA) (n.d. stands for Not Detectable)

	titer (mg l^{-1})		
Plasmids	**PAPA**	**PAPE**	**4-APA**
pC53BC	78 ± 5.2	n.d.	n.d.
pC53BCA	5.6 ± 2.2	56 ± 10	n.d.
pC53BCAF	6.8 ± 3.2	n.d	68 ± 4.5

3.1.4.2 Increasing aromatic amines production by engineering of central metabolic pathway (additional chromosomal copies of *glpK* and *tktA*) and negative regulator (*tyrR*) elimination

The first committed step in shikimate pathway is catalyzed by the DAHP synthase (Pittard 1996; Sprenger 2007b; Gosset 2009). The greater activity of the DAHP synthase will result in higher E4P demands; therefore, it is necessary to increase the availability of E4P as main precursor of DAHP synthase (Bongaerts et al. 2001; Gottlieb et al. 2014). This can be achieved through overexpression of transketolase A (*tktA*) (Sprenger et al. 1995) and/or fructose-1,6-bisphosphatase (*glpX*) (Gottlieb et al. 2014), the enzymes are involved in central metabolism pathway. In order to increase the flux toward E4P one strategy is to amplify the gene for the major transketolase, *tktA* (Sprenger et al. 1995; Gottlieb et al. 2014) and *glpX* (Gottlieb et al. 2014). Thus, an additional copy of *glpX* and *tktA* genes under the control of a P*tac* promoter were chromosomally integrated into the *E. coli* FUS4, generating *E. coli* FUS4.7, as described before (Gottlieb et al. 2014). Also, the negative regulator (*tyrR*) which controls several genes in shikimate pathway (Wallace and Pittard 1969; Pittard et al. 2004) was deleted, resulting in strain FUS4.7R (Figure **3-17** (a)). Then *E. coli* FUS4.7R was transformed with plasmids pC53BC, pC53BCA and pC53BCAF yielding *E. coli* FUS4.7R/pC53BC, *E. coli* FUS4.7R/pC53BCA and *E. coli* FUS4.7R/pC53BCAF strains. Moreover, in order to evaluate the L-PAPA (Figure **3-17**-(a)), PAPE (Figure **3-17**- (b)) and 4-APA (Figure **3-17**- (c)) productivity of *E. coli* FUS4.7R, batch experiments were performed with 5 ± 0.21 g l^{-1} glycerol (for L-PAPA) or 4.5 ± 0.17 g l^{-1} glucose (for PAPE and 4-APA) as carbon source. Glycerol was preferred to glucose because it resulted in better result in case of PAPA production (data not shown). From the HPLC results, production of L-PAPA was enhanced to 304 ± 21 mg l^{-1} from 5 g l^{-1} glycerol with the yield of 0.06 g g^{-1} (Figure **3-17**-(b)) which was 3.8-fold higher than that of *E. coli* FUS4 strain (Figure **3-17** (b)). Production titer of PAPE and 4-APA in the culture supernatant were measured by HPLC. In the *E. coli* FUS4.7R strain, the production titer of PAPE and 4-APA was 117.3 ± 12 mg l^{-1} (Figure **3-17** (c)) and 138 ± 9.5 mg l^{-1} (Figure **3-17** (d)) which was 2 and 1.7-fold higher than that of *E. coli* FUS4 strain, respectively, (Figure **3-17** (c and d)). However these results indicate that an additional copy of *glpX* and *tktA* associated with knock out of negative regulator (*tyrR*) is effective for improvement of all three aromatic amino acid. It should also be noted that

no aromatic amines production was observed in *E. coli* FUS4.7R harboring empty plasmid pJF119EH (Figure **3-17** (b, c and d)).

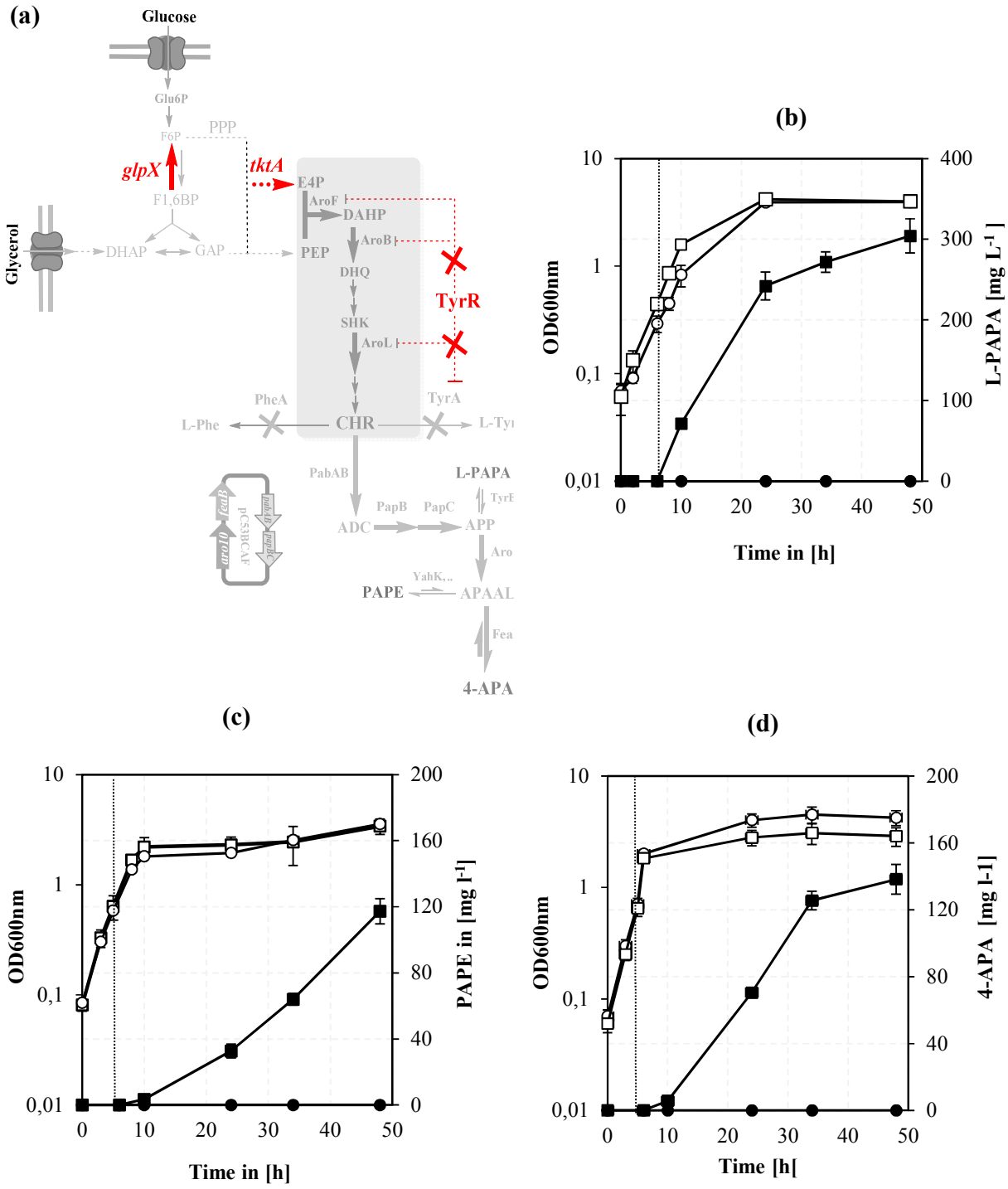

Figure 3-17 Batch cultivation of *E. coli* FUS4.7R with different plasmids in shake flasks. Cultivation was perfomed (48h) in shake flasks supplemented with 5 g l^{-1} glycerol in case of PAPA and 4.5 g l^{-1} glucose in

case of PAPE and 4-APA production. After reaching OD_{600nm}~0.6 (red dotted line) the cultures were induced with 0.5 mM IPTG (final concentration). **(a),** Schematic represent Aromatic amines production in *E. coli* FUS4.7R; **(b),** Time course of L-PAPA (■) production using strain *E. coli* FUS4.7R pC53BC; **(c)**, Time course of PAPE (■) production using strain *E. coli* FUS4.7R pC53BCA; **(d),** Time course of 4-APA (■) production using strain *E. coli* FUS4.7R pC53BCAF. Filled square (■) represents aromatic amino production in full vector which is determined with HPLC, Filled circle (●) represents aromatic amino production in *E. coli* FUS4.7F pJF119 (as control), empty square (□) represents OD600nm in full vector and empty circle (○) represents OD600nm in *E.coli* FUS4.7R pJF119 (as control). The data represent the mean and standard deviations (± SD) from measurements of three biological replicates.

3.1.4.3 Enhanced PAPE and 4-APA production by optimizing downstream pathway

One common strategy for enhancement of phenylpyruvate (PP) production and subsequently decarboxylation is reduction of the unwanted products (Sun et al. 2011; Li et al. 2016). Thus, aromatic amino acid aminotransferase encoded by *tyrB* and aspartate aminotransferase encoded by *aspC* (Fotheringham et al. 1986), which are involved in the reversible conversion of APP to L-PAPA (Figure **3-18** (a)), were deleted in L-Phe overproducing strain FUS4 (Table **2-2**) generating FUS4BC strain. A deletion of the genes encoding the main aminotransferases for L-Phe synthesis, *tyrB* and *aspC*, could lead to an increased APA supply for PAPE and 4-APA. Also, in order to eliminate the negative effect of *tyrR* on expression level of some involved genes in shikimate pathway (Wallace and Pittard 1969; Pittard et al. 2004) and consequently enhancement of flux toward APA and PAPE/4-APA, gene *tyrR* was deleted in *tyrB* and *aspC* double mutants strain (FUS4BC), creating strain FUSBCR (Figure **3-18** (a)). In order to accomplish the deletion, the *E. coli* strains FUS4 Δ *tyrB aspC*::cat and FUS4 Δ*tyrB aspC tyrR*::cat were constructed according to the method of Datsenko and Wanner (2000). Deletion of *aspC* and *tyrB* results in an *E. coli* strain that is auxotrophic for L-aspartic acid. While mineral salt medium normally contains 0.04 mg l^{-1} of the amino acid (L-Phe and L-Tyr) needed to overcome the autotrophy, complementation of L-aspartic acid autotrophy requires in the order of 3 g l^{-1} (Sun et al. 2011; Li et al. 2016). The novel strain *E. coli* FUSBCR, comprising (i) the heterologous plasmid, (ii) lacking tyrosine repressor and (iii) eliminated competitive routes for the precursors APP, were tested for PAPE and 4-APA production. Batch cultivation was performed in shake flasks for 48 h with 4.5± 0.24 g l^{-1} glucose as carbon source and the production titer of PAPE and 4-APA were measured by HPLC (Figure **3-18** (b-d)). As a negative control, the culture supernatant of *E. coli* FUS4BC/pJF119EH (Figure **3-18** (b and c)) and FUS4BCR/pJF119EH (Figure **3-18** (c and d)) were tested, no production of PAPE or 4-APA

was observed. Results showed that the deletion of *tyrB* and *aspC* increased PAPE and 4-APA production in FUSBC strain up to 108 ± 7.5 mg l^{-1} (Figure **3-18** (b)) and 224.6 ± 14.2 mg l^{-1} (Figure **3-18** (d)), respectively. This is almost compatible to PAPE and 4-APA amount produced by strain *E. coli* FU4.7R (Figure **3-17** (c and d)). In the second strategy, *tyrR* was chromosomally deleted from *E. coli* FUSBC, yielding FUS4BCR strain. *E. coli* strain FUS4BCR, was transformed with recombinant plasmids, showing a notable enhancement in PAPE and 4-APA production compared to other described strains. As mentioned above, the best strain FUSBCR produced 138 ± 14 mg l^{-1} of PAPE (Figure **3-18** (c)) and 264 ± 12 mg l^{-1} of 4-APP (Figure **3-18**, (e)) in shake flasks (Table **3-3**). It should also be noted that growth patterns of all cells were similar (Figure **3-18** (b-e)). Compared to strain FUS4 and FUS4.7R, *E. coli* strain FUSBCR containing recombinant plasmids produced far better titer of PAPE and 4-APA, although L-PAPA accumulation was not alleviated (Table **3-3**).

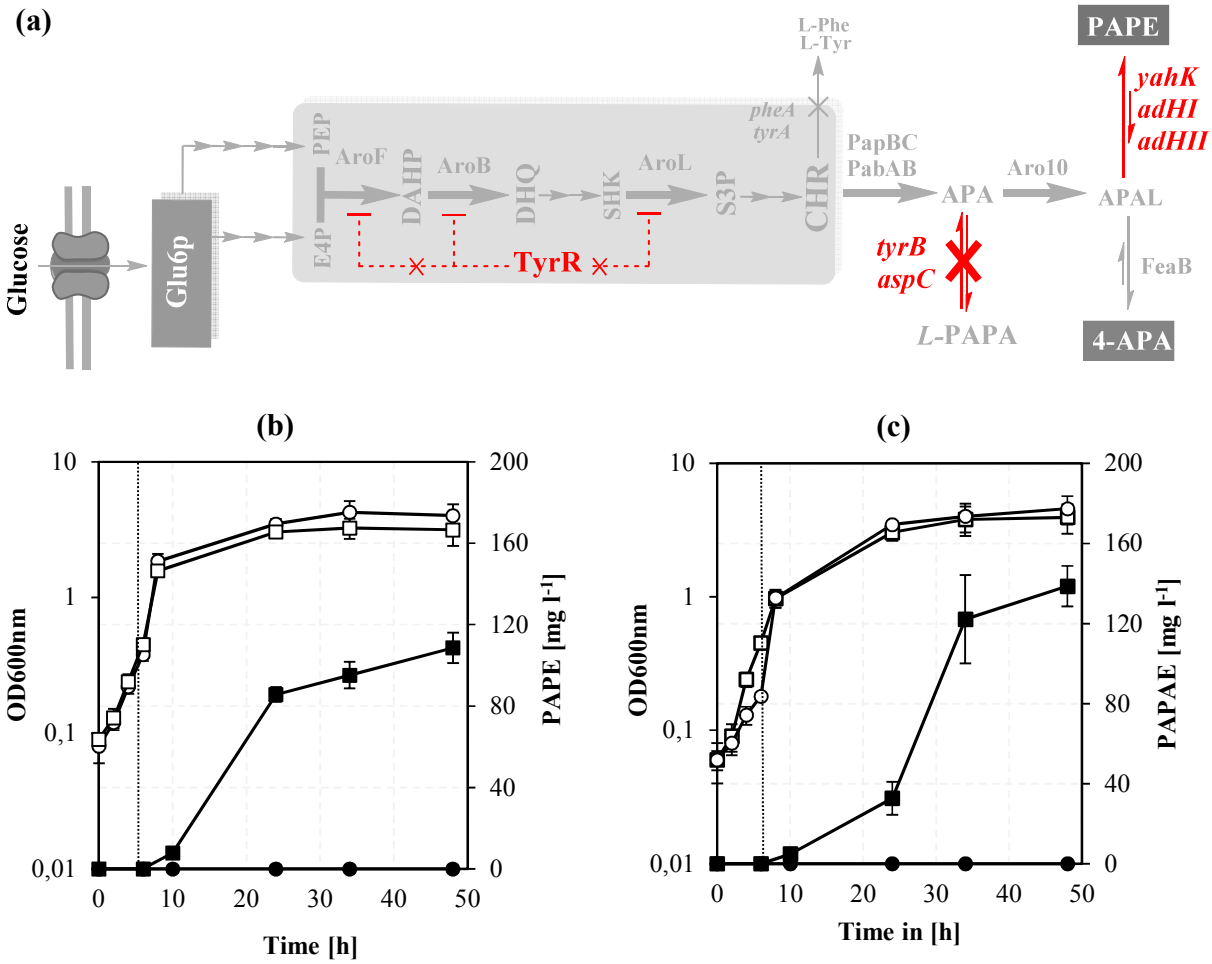

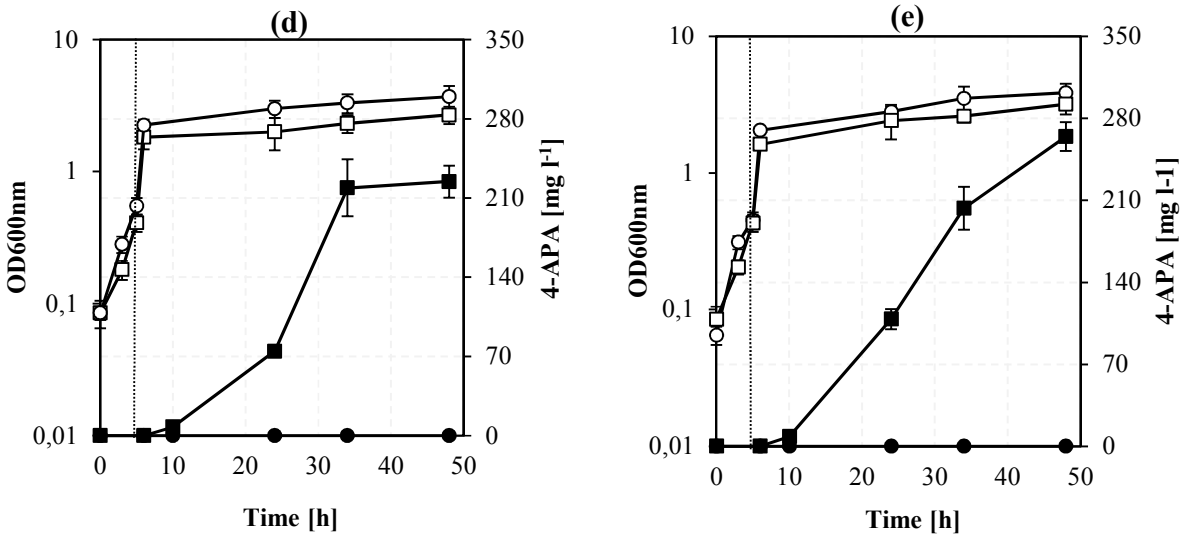

Figure 3-18 Glucose batch cultivation of *E. coli* FUS4BC and FUS4BCR strains with different plasmids in shake flasks. After reaching OD_{600nm}~0.6 the cultures were induced with 0.5 mM IPTG (final concentration).**(a),** Schematic represent Aromatic amines production in *E. coli* FUS4BC and FUS4BCR; **(b),** Time course of PAPE (■) production using strain *E. coli* FUS4BC pC53BCA; **(c),** Time course of PAPE (■) production using strain *E. coli* FUS4BCR pC53BCA; **(d),** Time course of 4-APA (■) production using strain *E. coli* FUS4BC pC53BCAF and **(e),** Time course of 4-APA (■) production using strain *E. coli* FUS4BCR pC53BCAF. Filled square (■) represents aromatic amino production in full vector which is determined with HPLC, Filled circle (●) represents aromatic amino production in *E. coli* FUS4BC/R pJF119 (as control), empty square (□) represents OD600nm in full vector and empty circle (○) represents OD600nm in *E. coli* FUS4BC/R pJF119 (as control). The data represent the mean and standard deviations (± SD) from measurements of three biological replicates.

Table 3-3 Aromatic amines production in *E.coli* FUS4BC and FUSBCR from glucose

	titer (mg l^{-1})		
Strain	L-**PAPA**	**PAPE**	**4-APA**
FUS4BC/pC53BCA	14.6 ± 3.2	108 ± 7.5	18.2 ± 9
FUS4BC**R**/pC53BCA	12.2 ± 4.6	138 ± 14	23 ± 7.5
FUS4BC/pC53BCAF	21.8 ± 4.5	n.d.[a]	224.6 ± 14.2
FUS4BC**R**/pC53BCAF	23.2 ± 8.6	n.d.	264 ± 12

[a] n.d. stands for Not Detectable.

Furthermore it can be suggested that APAAL (not detectable) may reduce to PAPE (Figure 3-11 (b)) by endogenous alcohol dehydrogenase or aldehyde reductases present in *E. coli*, encoded by 13 genes such as the *yqhD*, *yjgB* and *yahK* (Rodriguez et al. 2014; Koma et al. 2012). Hence in order to identify which reductases or alcohol dehydrogenase can facilitate more PAPE production in *E. coli*, two exogenous alcohol dehydrogenase genes *adHI* and *adHII* from *Saccharomyces cerevisiae* (de Smidt et al. 2008) and endogenous *yahK* gene, which has been

proposed for most efficient production of aromatic alcohols (Koma et al. 2012), were cloned into plasmid pC53BCA yielding three plasmids pC53BCAHII, pC53BCAHI and pC53BCAY (Table **3-4** and Table **2-3**). First, *E. coli* FUS4BCR as best candidate strain was transformed with plasmid pC53BCAHI, yielding strain *E. coli* FUS4BCR/ pC53BCAHI. In 48 h, this strain produced 34.3 ± 5.2 mg l^{-1} of PAPE with 26.2 ± 4.6 mg l^{-1} of L-PAPA as side product (Table **3-4**). Heterologous expression of pC53BCAHII plasmid into *E. coli* FUS4BCR produced 85.6 ± 5.2 mg l^{-1} of 4-APA and 37.1 ± 7.5 mg l^{-1} of L-PAPA as side product. It is noteworthy that PAPE was not detectable by HPLC analysis presumably due to either the AdHII protein was not present or AdHII enzyme prefers to catalyze the conversion of ethanol to acetaldehyde (Table **3-4**). Additional overexpression of endogenous *yahK* resulted in the pC53BCAY plasmid to facilitate PAPE biosynthetic routes. *E. coli* FUS4BCR with plasmid pC53BCAY produced 159.6 ± 14.2 mg l^{-1} of PAPE with negligible amount of L-PAPA (9.9 ± 3.5 mg l^{-1}) and 4-APA (11 ± 5 mg l^{-1}) as side product. Compared with other alcohol dehydrogenases (AdHI and AdHII), YahK showed slightly better performance in PAPE production (Table **3-4**).

Table 3-4 Effects of different alcohol dehydrogenase (*adHI*, *adHII*) and reductase (*yahK*) overexpression on PAPE production. The data were obtained after 48h batch cultivation in minimal media from 4.5 g l^{-1} glucose in *E. coli* FUSBCR pC53BCA harboring *adHI*, *adHII* or *YahK*.

	titer (mg l^{-1})		
Plasmids	**L-PAPA**	**PAPE**	**4-APA**
Empty plasmid (control)	n.d. [a]	n.d.	n.d.
pC53BCAY (*yahK*)	9.9 ± 3.5	159.6 ± 14.2	11 ± 5
pC53BCAHI (*adHI*)	26.2 ± 4.6	34.3 ± 5.2	15.3 ± 4.6
pC53BCAHII (*adHII*)	37.1 ± 7.5	n.d	85.6 ± 5.2

[a] n.d. stands for Not Detectable.

3.1.4.4 Plasmid-Borne Overexpression of Genes to Further Enhance PAPA, PAPE and 4-APA production

The effect of plasmid-borne overexpression of the genes *aroF* (DAHP synthase), *aroB* (dehydroquinate synthase) and *aroL* (shikimate kinase) was analyzed. This could overcome described bottlenecks and increase the flux through the shikimate pathway (Bongaerts et al. 2001; Sprenger 2007b; Gottlieb et al. 2014). Hence to improve the flux toward chorismate, as the main precursor for APP biosynthesis (Figure **3-20**), plasmid pJNT*aroFBL* was used. This plasmid was introduced into *E. coli* LJ110, FUS4, FUS4.7R and FUS4BCR. Furthermore, in

order to investigate how plasmid-encoded recombinant proteins were expressed in *E. coli* FUS4, 2D-SDS-PAGE was performed. To detection of individual protein spots, 2D-SDS gel from *E. coli* FUS4/pC53BC pJNTaroFBL (red spots) was compared with 2D-SDS gel from *E. coli* FUS4/pC53BC/pJNT (green spot). Differences in the protein composition of the two *E. coli* strain harboring different plasmid can be seen in Figure **3-19**. The plasmid-encoded proteins PabBC, PapB and PapC from both gels are detectable (labeled with black arrows). As labeled in Figure **3-19**, protein spots presumably related to AroF (38.8 kDa, pI~5.5), AroB (38.8 kDa, pI~6.01) and AroL (19.6 kDa, pI~4.6) proteins (labeled with blue arrows) from *E. coli* strain harboring pJNT*aroFBL* are recognizable (Figure **3-19**, red spots). Based on these results, it was assumed that plasmid-coded proteins are present in soluble form. Mass spectrometry analysis would be necessary to further prove that these soluble spots are related to the desired recombinant proteins.

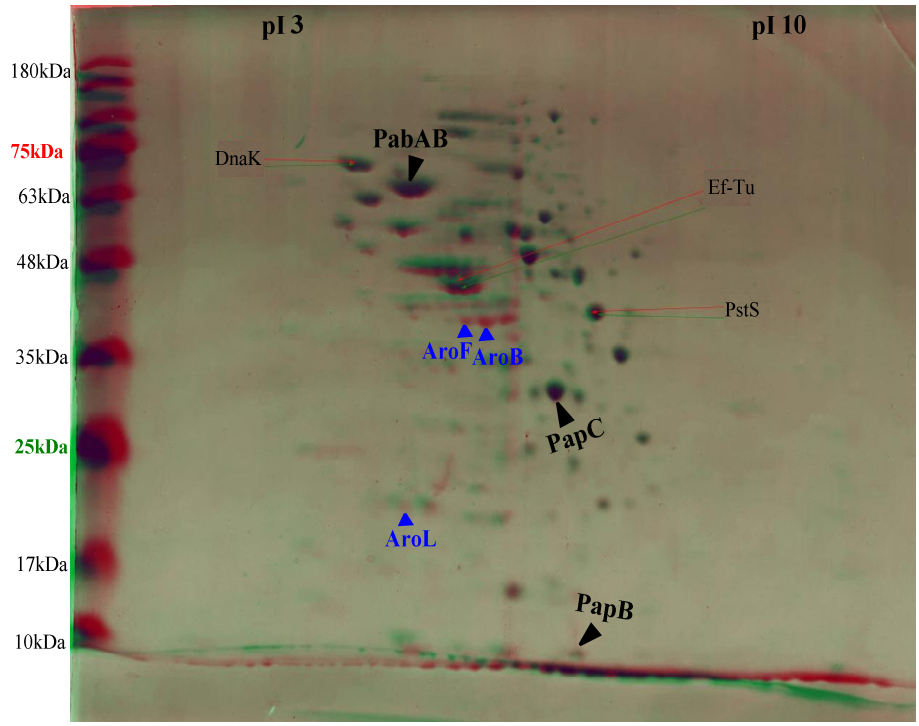

Figure 3-19 Comparison of 2D SDS gel electrophoresis of *E. coli* FUS4 /pC53BC pJNTaroFBL (48h, red spots) vs. FUS4 pC53BC pJNT (48h, green). For evaluation the software Delta2D Version 3.2 (Decodon GmbH) was used. Protein spots presumably related to PabBC, PapC and PapB are visible in both strains. Possible spots for protein expression from helper plasmid (pJNT*aroFBL*) including AroF (38.8kDa, 5.5), AroB (38.8kDa, 6.01) and AroL (19.6 kDa, 4.6) were identified by pI and size

comparison of the individual spots with the data EcoProDB Data bank. (http://eecoli.kaist.ac.kr/main.html).

In addition, shake flask experiments for 48h showed that additional expression of *aroFBL* (Rüffer et al. 2004) has a positive and noticeable effect on the L-PAPA production from 5 ± 0.31 g l^{-1} glycerol in the *E. coli* strain (Table **3-5**). The resulting strains *E. coli* LJ110/pC53BC/pJNT-aroFBL and *E. coli* FUS4/pC53BC/pJNT-*aroFBL* produced 86 mg l^{-1} and 203 mg l^{-1} L-PAPA (Table **3-5**) which are approximately 2-folds higher compared to the *E. coli* LJ110/pC53BC (Figure **3-6** (b)) and FUS4/pC53BC (Figure **3-16** (b)), respectively. Furthermore introduction of second plasmid (pJNT*aroFBL*) into strain *E. coli* FUS4.7R/pC53BC showed to be beneficial for the biosynthesis of L-PAPA as the titer was increased to 534.12 mg l^{-1} (Table **3-5**).

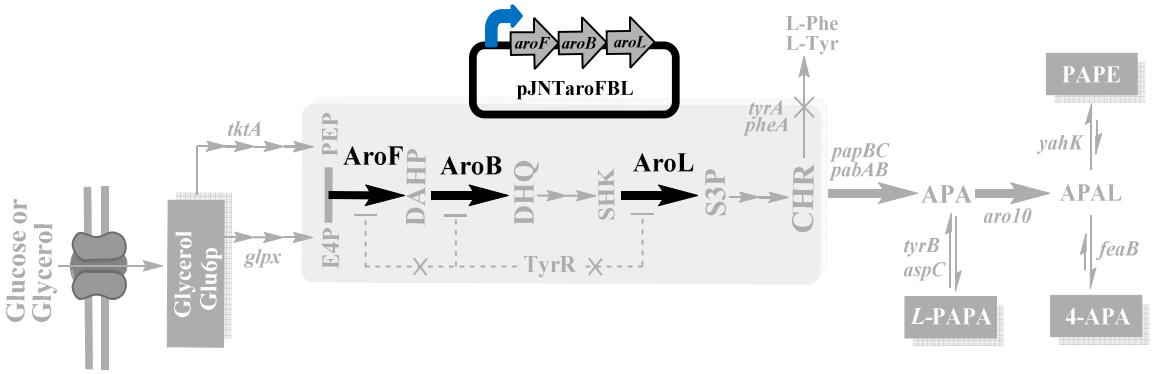

Figure 3-20 Scheme represent strategy to enhance the intracellular pool of chorismate using overexpression of plasmid pJNT*aroFBL*. This is a helper plasmid carrying genes responsible (*aroF*, *aroB* and *aroL*) for bottleneck steps in the shikimate pathway.

Table 3-5 Comparison of L-PAPA production after 48h shake flasks cultivation in minimal media with ~ 5 ± 0.23 g l^{-1} glycerol. Same plasmid combination of pC53BC and pJNT-*aroFBL* in different *E. coli* strains background. The cultivations were performed in triplicate and mean values are given.

		L-PAPA		
Plasmids	***E.coli* strains**	Final OD_{600nm}	Titer (mg l^{-1})	Yield L-PAPA/glycerol (g g^{-1})
pC53BC / pJNTaroFBL	*E. coli* W3110	4.75 ± 0.85	86.6 ± 3.7	0.02
	E. coli FUS4	3.75 ± 0.24	202.7 ± 4.5	0.04
	E. coli FUS4.7	3.65 ± 0.15	449.3 ± 29.4	0.09
	E. coli FUS4.7R	3.85 ± 0.13	534.1 ± 24.1	0.11

pJNT*aroFBL* plasmid was also introduced into five *E.coli* strains which are carrying genes required for synthesis of PAPE or 4-APA encoded on plasmid pC53BCAY and pC53BCAF,

respectively. Comparative batch cultivations of the different recombinant strains in shake flask for 48h with ~ 4.5 ± 0.16 g l^{-1} glucose showed a positive effect of the second plasmid pJNT*aroFBL* on the produced amount of PAPE and 4-APA (Table **3-6** and Table **3-7**). The result showed that 32.9 mg l^{-1} of PAPE (Table **3-6**) and 124 mg l^{-1} of 4-APA (Table **3-7**) was produced by the parental strain (LJ110), while 141.1 mg l^{-1}, 204.6 mg l^{-1} of PAPE (Table **3-6**) and 204.3 mg l^{-1}, 258.8 mg l^{-1} of 4-APA (Table **3-7**) were produced by the FUS4 and FUS4.7R strain, respectively. Results also showed that introduction of pJNT*aroFBL* plasmid in *E.coli* FUS4BC with both *tyrB* and *aspC* genes deleted enhanced PAPE and 4-APA production to 215.5 mg l^{-1} (Table **3-6**) and 272.5 mg l^{-1} (Table **3-7**), respectively.

Table 3-6 Comparison of PAPE production after 48h shake flasks cultivation in minimal media with ~ 4.5 ± 0.16 g l^{-1} glucose. Same plasmid combination of pC53BCAY and pJNT-*aroFBL* in different *E. coli* strains background. The cultivations were performed in triplicate and mean values are given.

		PAPE		
Plasmids	***E.coli* strains**	Final OD_{600nm}	Titer (mg l^{-1})	Yield PAPE/glucose (g g^{-1})
pC53BCAY/ pJNTaroFBL	*E. coli* W3110	3.65 ± 0.54	32.9 ± 4.6	0.01
	E. coli FUS4	3.25 ± 0.45	141.3 ± 15.2	0.03
	E. coli FUS4.7R	3.12 ± 0.65	204.6 ± 8.1	0.04
	E. coli FUS4BC	2.95 ± 0.54	215.5 ± 7.5	0.05
	E. coli FUS4BCR	3.1 ± 0.75	263.1 ± 25.2	0.06

As can be seen in Table **3-6** and Table **3-7** , highest PAPE and 4-APA titers were achieved with *E. coli* FUS4BCR pC53BCAY (Table **3-6**) and pC53BCAF (Table **3-7**) by combination with second plasmid pJNT*aroFBL.* These recombinant strains produces 263.1 mg l^{-1} of PAPE and 307.5 mg l^{-1} of 4-APA, which are 1.5-2 fold more than PAPE and 4-APA produced by *E. coli* harboring a single plasmid.

Table 3-7 Comparison of 4-APA production after 48h shake flasks cultivation in minimal media with ~ 4.5 ± 0.18 g l^{-1} glucose. Same plasmid combination of pC53BCAF and pJNT-*aroFBL* in different *E. coli* strains background. The cultivations were performed in triplicate and mean values are given.

		4-APA		
Plasmids	***E.coli* strains**	Final OD_{600nm}	Titer (mg l^{-1})	Yield 4-APA/glucose (g g^{-1})
pC53BCAF /pJNTaroFBL	*E. coli* LJ110	4.19 ± 0.65	124 ± 4.5	0.03
	E. coli FUS4	3.12 ± 0.55	204.3 ± 7.5	0.05
	E. coli FUS4.7R	3.08 ± 0.65	258.8 ± 8.9	0.06
	E. coli FUS4BC	2.98 ± 0.41	272.5 ± 14.2	0.06
	E. coli FUS4BCR	2.85 ± 0.75	307.5 ± 12.2	0.07

However, these findings further and importantly show that the overexpression of rate limiting enzymes AroFBL improved production of all three aromatic amines in all *E. coli* studied which are compatible with earlier studies that has demonstrated the positive effect of *aroFBL* overexpression on aromatic amino acid production (Rüffer et al. 2004; Gottlieb et al. 2014, Rodrigues et al. 2013).

3.1.4.5 Improving PAPE/4-APA production using overexpression of key enzymes in PAPE/4-APA pathway

One essential aspect of strain engineering is the appropriate balancing between recombinant pathway compartments (Pickens et al. 2011; Jones et al. 2015). It was observed (3.1.4.3) that overexpression of *yahK* gene encoding aldehyde reductase enzyme mediates the last enzymatic step in PAPE pathway resulted in a positive effect on PAPE titer (Table **3-6**). Thus an interesting strategy to improve the production of a molecule of interest (PAPE or 4-APA) is to modulate expression of genes which are involved in the last enzymatic step of its synthesis. It is necessary that the last step toward PAPE or 4-APA production (oxidation or reduction of APAAL, respectively) catalysis with great efficiency. Thus, an additional copy of *yahK* and *feaB* genes from *E. coli* was cloned into pJNT*aroFBL* plasmid (yielding pJNT*aroFBL-yahK* and pJNT*aroFBL-feaB* plasmids) to possibly accelerate the conversion of the last common precursor, APAAL to PAPE or 4-APA. Significantly, when these plasmids were introduced into *E. coli* FUS4BCR strain harboring pC53BCAY (Figure **3-21** (a)) or pC53BCAF (Figure **3-21** (b)). It was observed a 2-fold increase in PAPE content or a 1.5-fold increase in 4-APA production in comparison to highest PAPE or 4-APA titer produced earlier (Figure **3-21** (a and b)). Obviously, additional plasmid overexpression of *yahK* or *feaB* has been able to accelerate the effective conversion of precursor APAAL to PAPE or 4-APA. This strategy resulted in a titer of PAPE 526 ± 25 mg l^{-1} (Figure **3-21** (a)) or 458.6 ± 14.5 mg l^{-1} 4-APA (Figure **3-21** (b)) in batch cultivation in recombinant *E. coli* and was even higher than in a previous report (Masou et al. 2016). Compared to another studied strain, *E. coli* FUSBCR containing these two new plasmids (pJNT*aroFBL-yahK* or pJNT*aroFBL-feaB*) showed even no detectable amount of L-PAPA, which indicated that increasing *yahK* or *feaB* expression level indirectly reduced the accumulation of L-PAPA and, as a result, more carbon flux was directed towards targeted products (Table **3-5**).

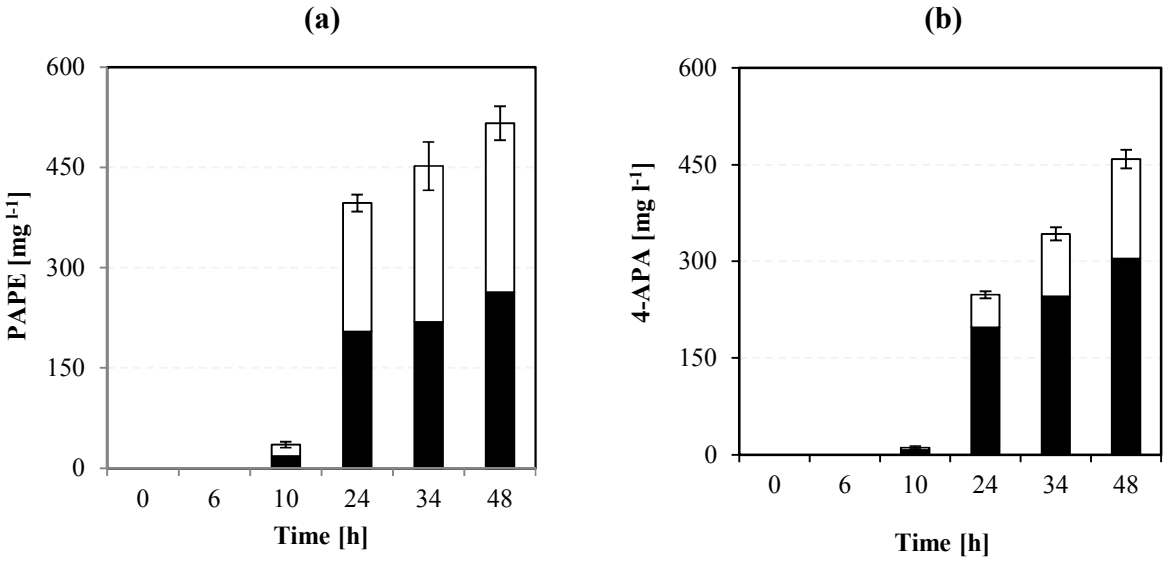

Figure 3-21 Impact of additional overexpression of *yahK* and *feaB* on PAPE **(a)** and 4-APA **(b)** production by recombinant *E. coli* FUS4BCR. The initial glucose concentration was 4.5± 0.34 g l^{-1}. After reaching OD_{600nm} ~0.6 (6h) the cultures were induced with 0.5 mM IPTG (final concentration). Black columns (■) represent PAPE/4-APA concentration in *E. coli* FUSBCR harboring pC53BCAY/pJNT*aroFBL* (Table 3-3) or pC53BCAF/pJNT*aroFBL* (Table 3-4) and, white columns (□) represent effect of additional overexpression of *yahK* or *feaB* on PAPE or 4-APA in *E.coli* FUSBCR harboring pC53BCAY/pJNT*aroFBL-yahK* **(a)** or *E. coli* FUSBCR harboring pC53BCAF/pJNT*aroFBL-fea* **(b),** respectively. Data are averages from three biological replicates. Error bars represent standard deviations from the means.

Table 3-8 The summarized results from Figure **3-21**.

	titer (mg l^{-1})		
Plasmids	**PAPA**	**PAPE**	**4-APA**
Empty plasmid (control)	n.d. [a]	n.d.	n.d.
pC53BCAY and pJNTaroFBL-***yahK***	n.d.	526 ± 25	n.d.
pC53BCAF and pJNTaroFBL-***feaB***	n.d.	n.d	458.6 ± 14.5

[a] n.d. stands for Not Detectable.

3.1.5 Fed batch cultivation of engineered *E.coli* for production of aromatic amines (L-PAPA, PAPE and 4-APA) in shake flasks

L-PAPA

In order to overcome problems caused by carbon source limitation during batch cultivation, fed-batch cultivation in shake flask was performed. *E. coli* FUS4.7R pC53BC pJNT*aroFBL* as best studied strain for production of L-PAPA (Table **3-5**) was transferred into a fed batch set-up.

It was reported that the optimum temperature for the Aro10 (Kneen et al. 2011) and AroF enzyme is 30°C. In addition, solubility of overexpressed Aro10 in *E.coli* was reduced by increasing temperature to 37°C (see section 3.1.2.2). Hence a two-step process was designed: an initial growth phase at 37 °C and a second production phase at 30 °C (red dotted line, Figure **3-22**). During the initial phase at 37 °C, no production of L-PAPA was observed, because there was no IPTG induction. After 24h (red dotted line), initial glycerol in batch phase was completely consumed (Figure **3-22**). Temperature was then shifted to 30 °C. During the fed-batch operation, 5 g l^{-1} glycerol was added about every 12 h intermittently when it became depleted, as determined by HPLC (Figure **3-22**). A total of 33.3 g l^{-1} glycerol was consumed in 134 h of cultivation and a titer of 5.47 g l^{-1} of L-PAPA (Figure **3-22**) was detected in the supernatant which corresponds to a yield of 16 % L-PAPA / glycerol (g g^{-1}). To my knowledge it is the highest described L-PAPA titer reached with *E. coli* (Masuo et al. 2016).

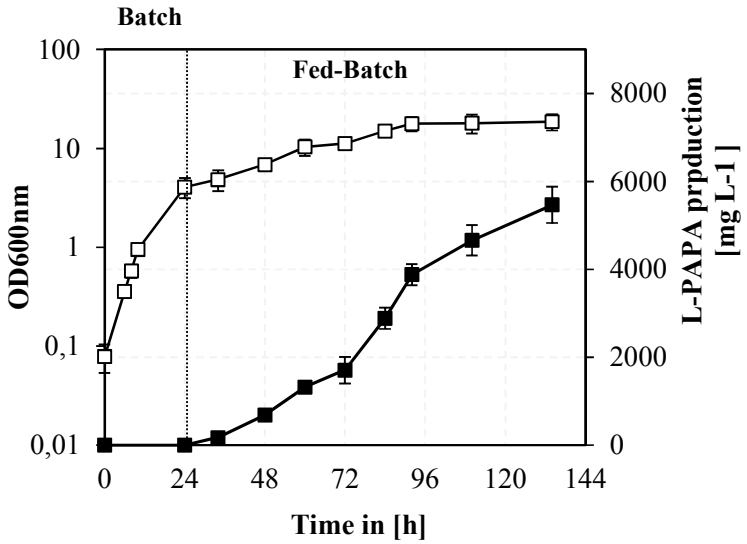

Figure 3-22 Glycerol fed-batch cultivation of *E. coli* FUS4.7R/pC53BC/pJNT*aroFBL* in shake flask. The initial glycerol concentration was 5 g l^{-1}. After 24h of cultivation (red dotted line) the cultures were induced with 0.5 mM IPTG (final concentration) and the shake flasks were transferred from 37°C to 30°C before giving pulses of ~ 5 g l^{-1} of glycerol every 12h. The respective symbols represent as follows: filled square (■), L-PAPA concentration and, empty Square (□), OD_{600nm}. Data are averages of results for three biological replicates. Error bars represent standard deviations from the means.

The analysis of the by-products formation at the end of cultivation represents the acetate and lactate concentration did not increase until after 60 hours (Figure **3-23**). It is also interesting that only acetate accumulated rapidly in the culture media while lactate remained consistently at a

low level (Figure 3-23). The highest acetate concentration was reached after 134 h, that is, 2.8 g l^{-1}. At this time, the final concentration of lactate remained below 0.3 g l^{-1} and the initial glycerol was completely exhausted. At the end of cultivation no accumulation of glycerol was observed (Figure **3-23**).

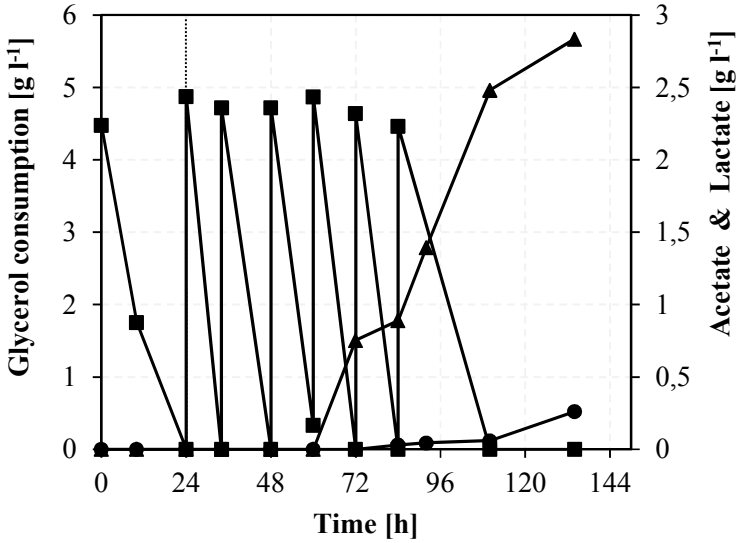

Figure 3-23 By-product formation during the glycerol fed batch cultivation of *E.coli* FUS4.7R /pC53BC/pJNT*aroFBL* in shake flasks (Figure **3-22**). After 24h of cultivation (red dotted line) the cultures were induced with 0.5 mM IPTG (final concentration) and the shaking flasks were transferred from 37°C to 30°C before giving pulses of ~ 5 g l^{-1} of glycerol every 12h. The respective symbols represent as follows: filled square (■), glycerol concentration; filled circle (●), lactate concentration and filled triangle (▲), acetate concentration.

PAPE and 4-APA

As high titer of PAPA or 4-APA was determined in batch cultivation with the strains *E. coli* FUSBCR (Figure **3-18**), the cultivation condition was shifted to fed-batch to increase the product titer. Thus, *E. coli* FUSBCR as best studied strain for production of PAPE or 4-APA was transformed with recombinant plasmids pC53BCAY/pJNT*aroFBL-yahK* or pC53BCAF/pJNT*aroFBL-feaB* and then cultivated under a fed batch strategy in shake flask. Similar to L-PAPA, fed batch process comprised two phases: an initial growth phase at 37 °C and a second production phase at 30 °C. Two carbon sources, glucose and glycerol, were used for PAPE or 4-APA production, unlike L-PAPA, with glucose as a carbon source better results (data not shown) was obtained. During the initial batch phase (24h), recombinant *E.coli* did not produce detectable PAPE or 4-APA (Figure **3-24** and Figure **3-25**). When glucose was

completely consumed (Figure **3-24** and Figure **3-25**), IPTG induction and the feed were started (red dotted line) and the process was continued. As time passed the concentration of PAPE (Figure **3-24**) and 4-APA (Figure **3-25**) began to increase in the medium. At this point (168h), PAPE and 4-APA amount began to become constant and then decreased after stop of glucose feeding, indicating inhibiting cultivation conditions or some unknown problems. After 168 h cultivation, 33 g l^{-1} glucose was consumed and a titer of 2.46 g l^{-1} PAPE with 0.08 g g^{-1} yield was achieved in *E.coli* FUSBCR/pC53BCAY/ pJNT-*aroFBL-yahK* (Figure **3-24**; (Table **3-9**)).

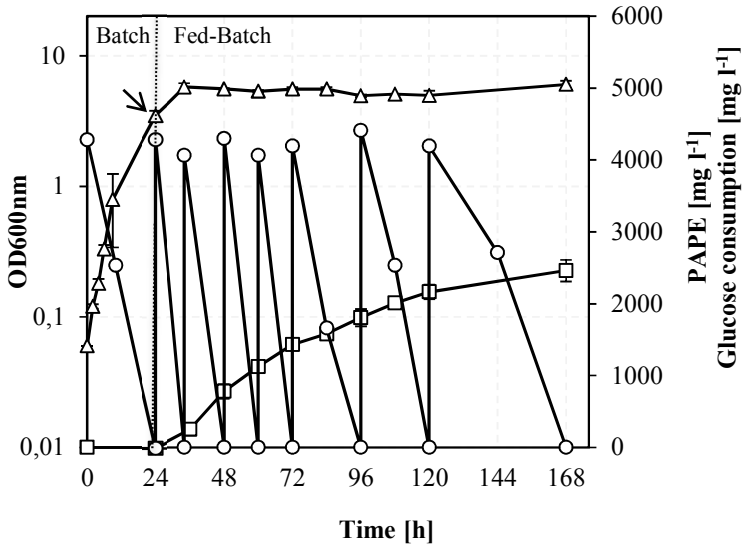

Figure 3-24 Fed-batch production of PAPE in *E. coli* FUS4BCR harboring pC53BCAY and pJNT*aroFBL-yahK* plasmids. The arrow indicates the time point of IPTG induction (after 24h), at which the experiment was switched from 37°C to 30°C before giving pulses of ~ 4.5 g l^{-1} of glucose every 12h. The red spotted line represent the beginning of the glucose feed phase. The respective symbols represent as follows: PAPE concentration (□); OD_{600nm} (Δ) and glucose consumption (○). Data are averages of results for three biological replicates. Error bars represent standard deviations from the means.

After 168 h of cultivation, 4-APA titer reached a maximum value of 3.42 g l^{-1} in *E. coli* FUSBCR/pC53BCAF/pJNT-*aroFBL-feaB* (Figure **3-25**). Overall 25 g l^{-1} glucose was consumed in the 4-APA fed batch cultivation and the final yield and volumetric productivity of 4-APA was 0.14 g g^{-1} and 0.02 g $l^{-1}h^{-1}$ (Table **3-9**). Here, unlike PAPE, the 4-APA titer was increased to 168 hours, but then it remained constant, so there was no reason for longer cultivation. However, although the reason was not clear, it may be because that one of the key nutrient elements in the Gerhardt minimal medium is depleted severely or activity of some recombinant enzymes

involved in 4-APA pathway is lost/decreased. Acetate/lactate accumulation may also be problem in an uncontrolled shake flask culture (Figure **3-25**).

Table 3-9 Fed-Batch production of PAPE and 4-APA from glucose by recombinant *E. coli* strains harboring different recombinant plasmids (after 168h)

Compound	*E. coli* strains	Titer (g l^{-1})	Yield (g product/ g glucose)	volumetric productivity (g l^{-1} h^{-1})
PAPE	FUS4BCR/pC53BCAY-pJNTaroFBL-yahK	2.5 ± 0.15	0.08	0.014
4-APA	FUS4BCR/pC53BCAF-pJNTaroFBL-feaB	3.4 ± 0.3	0.14	0.02

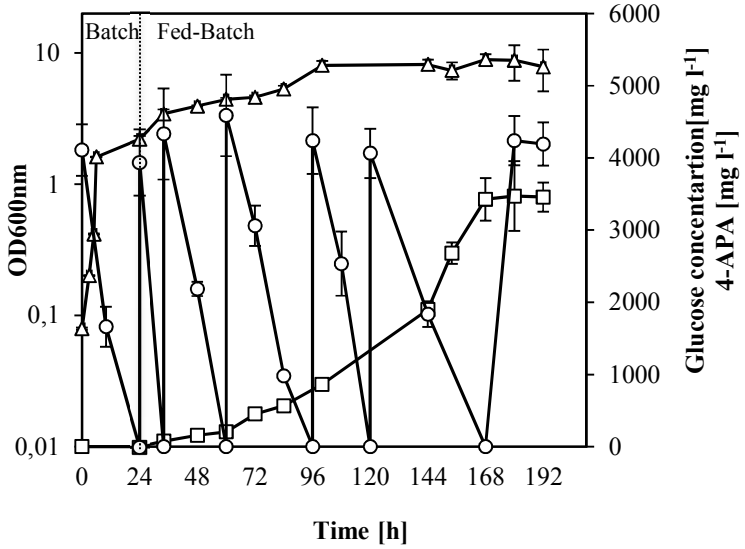

Figure 3-25 Fed-batch production of 4-APA in *E. coli* FUS4BCR harboring pC53BCAF and pJNT*aroFBL-feaB* plasmids. The arrow indicates the time point of IPTG induction (after 24h), at which the experiment was switched from 37°C to 30°C before giving pulses of ~ 4.5 g l^{-1} of glucose every 12h. The dashed line marks the beginning of the feed phase. The respective symbols represent as follows: PAPE concentration (□); OD_{600nm} (Δ) and glucose consumption (○). Data are averages of results for three biological replicates. Error bars represent standard deviations from the means.

In order to better understand the probable limitations during fed batch cultivation, by product formation (acetate and lactate) in culture medium was analyzed. As shown in Figure **3-26** acetate and lactate were accumulated in the culture during fed batch cultivation. Acetate concentration in the supernatant was increased from 72 h after of cultivation, reached rapidly a maximal concentration of 2.2 ± 0.11 g l^{-1} after 192 h. The highest concentration of lactate reached 0.99 ±

0.18 g l^{-1} in the fed-batch process of PAPE/4-APA, unlike L-PAPA, increased over the time. The behavior of acetate accumulation was similar to that observed in fed batch fermentation of L-PAPA (Figure 3-23). Although acetate/lactate accumulation may cause pH to fall and loss of carbon flux for cell growth, this, however, seems not to cause problems in 4-APA or PAPE production process. It could be summarized from these results that although the obtained yields of PAPE or 4-APA in this study are remarkably higher than the obtained yield in a previous report in *E.coli* (Masuo et al. 2016), additional efforts will be required to optimize fed batch process with controlled condition (feeding, PH and pO2 level) to reach further enhancement in PAPE or 4-APA titer.

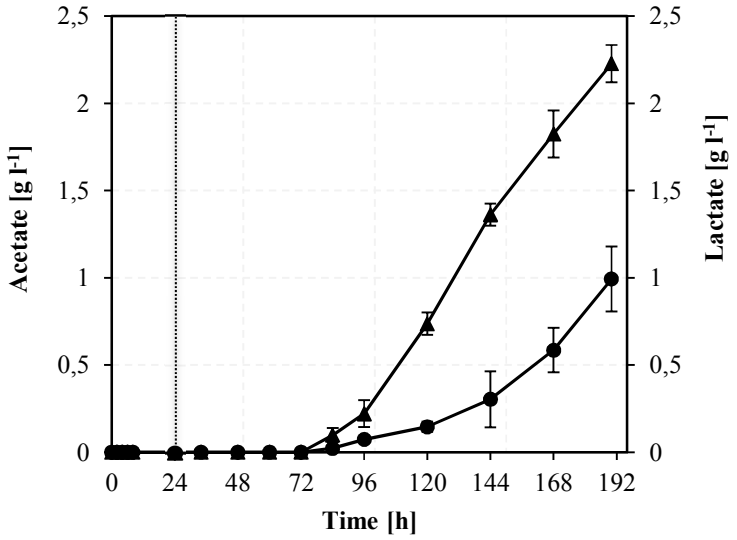

Figure 3-26 By-product formation during the glucose fed batch cultivation of *E.coli* FUS4BCR for PAPE or 4-APA production in shake flasks. After 24h of cultivation (red dotted line) the cultures were induced with 0.5 mM IPTG (final concentration) and the shaking flasks were transferred from 37°C to 30°C before giving pulses of ~ 5 g l^{-1} of glucose every 12h. The respective symbols represent as follows: filled circle (●), lactate concentration and filled triangle (▲), acetate concentration. Data are averages of results for three biological replicates. Error bars represent standard deviations from the means.

3.1.6 Fed-Batch fermentation of *E.coli* for production aromatic amines (L-PAPA, PAPE and 4-APA) in fermenter

L-PAPA

Earlier, the highest L-PAPA production was obtained in shake flask (Figure **3-22**) when glycerol was used as carbon source, thus, glycerol was preferred over glucose in the fed-batch process in a fermenter. In order to obtain a higher L-PAPA production, glycerol-limited fed-batch fermentation of *E. coli* FUS4.7R strain simultaneously harboring pC53BC and pJNT-

aroFBL was performed in a benchtop bioreactor system (0.5 l working volume) with pH controlled at 7.0. After glycerol consumption in the batch phase (red dotted line, Figure **3-27**) the culture was induced with IPTG and additional L-phenylalanine, L-tyrosine, glycerol and ammonia feeding were started. After 82 hours, a total L-PAPA concentration of 6.3 g l^{-1} (Figure **3-27**) was produced by final glycerol consumption of approx. 49.5 g l^{-1}. This equals to a yield of 0.13 L-PAPA / glycerol (g g^{-1}) and a space-time-yield of L-PAPA formation over the whole process of 0.04 g l^{-1} h^{-1}. The final glycerol concentration of the fed-batch culture was below the detection limit (Figure **3-27**).

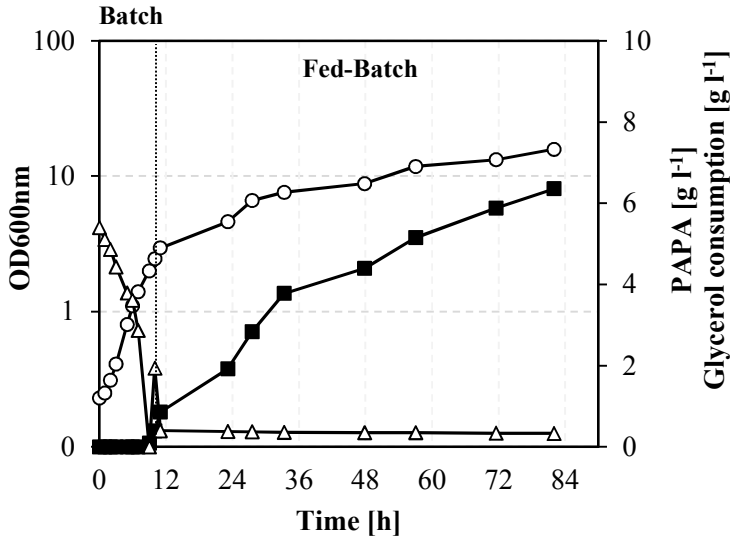

Figure 3-27 Fed-batch fermentation of *E. coli* FUS4.7R pC53BC /pJNT-*aroFBL* for production of L-PAPA. The glycerol feed started after 10h (red dotted line) and the fed was adjusted to maintain a concentration of 0.4-1.0 g l^{-1}. pH was controlled at 7 by the automatic addition of Ammonia 10%. At the time of inoculum, the pO2 detected by the oxygen sensor was 100% of the air saturation, at 400 rpm with an aeration rate of 0.1 - 1.0 L min^{-1}, when reaching 30 % the stirring rate was adjusted. Cell growth (OD 600, ○), glycerol consumption (g l^{-1}, Δ) and the L-PAPA concentration (g l^{-1}, ■) were determined during the cultivation. For more details see material and methods section 2.6.4.1. The result of one fermentation is presented with mean values and deviations of three technical replicates.

In order to allow the biomass formation, often encountered in industrial large-scale processes, minimal medium modification (50 % more) and periodical feeding of L-Phe and L-Tyr were investigated in a larger scale fermenter (30 l reactor) with *E. coli* FUS4.7R pC53BC/pJNT-*aroFBL* (Figure **3-28**). The feeding was started after consumption of the initial added glycerol (red dotted line, Figure **3-28**). The fed-batch phase is divided into three modes (mode1-3, Figure **3-28**) with constant feed rates. After 11.4 h (CDW=3.63 g l^{-1}), IPTG (0.5mM, final conc.) was added and glycerol feeding at a rate of 0.6 g l^{-1} (mode 1) was started. L-Phe and L-Tyr was

also added in a pulse 0.06 mg l^{-1} based on the actual volume of fermenter. Subsequently, glycerol feeding rate increased to 0.8 g l^{-1} (mode 2) when cultures reached CDW=10.44 g l^{-1} (after 34h) and then its reached 1 g l^{-1} (after 56h, mode 3). Then glycerol feeding rate was maintained constant until end of the cultivation. Additionally, L-Phe and L-Tyr were added in a periodical pulse (mode1, 2 and 3, see section 2.6.4.1) to allow further biomass formation. A typical process is depicted in Figure **3-28**.

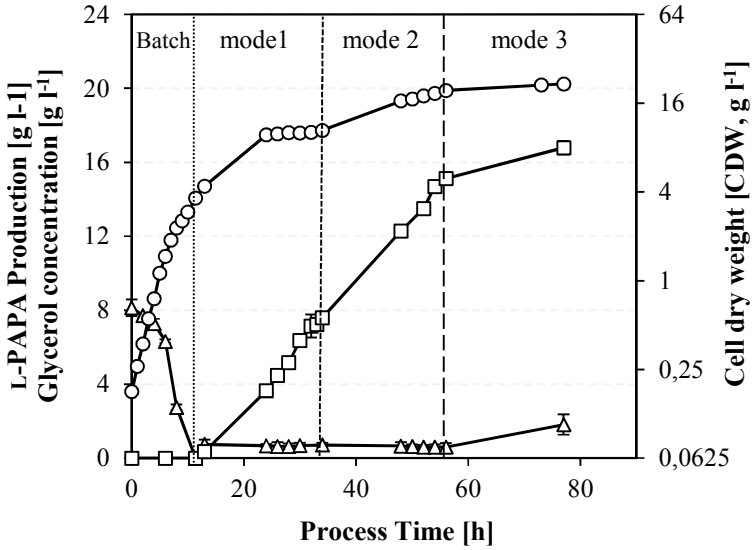

Figure 3-28 Fed-batch fermentation of *E. coli* FUS4.7R pC53BC/pJNT-*aroFBL* for production of L-PAPA in a 30 L stirred-tank reactor. The glycerol feed started after 11.4h (red spotted line, first pulse of L-Phe and L-Tyr) and the fed was adjusted to maintain a concentration of 0.6-1.0 g l^{-1}. Second pulse of L-Phe and L-Tyr (black dotted line) and third pulse of L-Phe and L-Tyr (black dash line) were fed to allow biomass formation. pH was controlled at 7 by the automatic addition of Ammonia 15%. At the time of inoculum, the pO2 detected by the oxygen sensor was ~ 100% of the air saturation, at 350 rpm with an aeration rate of 4 l min-1, when reaching 30 % the stirring rate was adjusted. Biomass (CDW, ○), glycerol concentration (g l^{-1}, Δ, represent actual glycerol concentration in the culture) and the L-PAPA concentration (g l^{-1}, □) were determined during the cultivation. The result of one fermentation is presented. For more details see material and methods section 2.6.4.1.

In fed-batch fermentation, initial 8.1± 0.45 g l^{-1} glycerol in less than 12 h was consumed and biomass formation exponentially increased to the CDW of 3.63 g l^{-1} in 12 h (Batch mode). Afterwards, the cell biomass increased by adding short pulses of L-Phe and L-Tyr to CDW~10.44 g l^{-1} (Fed-Batch mode 1) and then CDW~19.49 g l^{-1} (Fed-Batch mode 2) respectively. Biomass formation began to slow down thereafter (Fed-Batch mode 3, Figure **3-28**). The L-PAPA titer increased in parallel with biomass formation and the final titer reached 16.78± 0.36 g l^{-1} after 77h. A total of 131.7 g l^{-1} glycerol was consumed yielding a final cell dry weight

concentration of 21.6 g l^{-1} after 77h (Figure **3-28**). This equals a yield of 0.13 L-PAPA / glycerol (g g^{-1}) and a space-time-yield of L-PAPA formation over the whole process of 0.22 g l^{-1} h^{-1}. Total amount of L-PAPA produced during the 77h of fermentation was 205 g with a final volume of 12.25 l. Subsequently, L-PAPA was extracted from 2.25 l fermentation broth, concentrated and purified (see section 2.8 and 3.1.7).

PAPE and 4-APA

In a previous section (3.1.5), the high PAPE and 4-APA titer was achieved in shake flask (Figure 3-24 and 3-25) when glucose used as carbon source (data for glycerol was not shown), thus, glucose was preferred to glycerol in this experiment. In order to reach higher titer of PAPE and 4-APA in *E. coli* FUSBCR, a fed batch process in a benchtop bioreactor system (0.5l, working volume) similar to L-PAPA fermentation condition (section 3.1.5) was performed. During the initial batch phase in *E. coli* FUS4BCR pC53BCAY/pJNT*aroFBL-yahK* (Figure **3-29** (a)) and *E. coli* FUS4BCR pC53BCAF/PJNT*aroFBL-feaB* (Figure **3-29** (b)) while the initial glucose (5 g l^{-1}) began to decrease and was completely consumed after 10h in both of them, the feed-phase was initiated (red dotted line). After glucose consumption in the batch phase the culture was induced with IPTG and additional L-phenylalanine, L-tyrosine, glucose and ammonia feeding were started. Based on the glucose consumption from preceding shake flask cultivations, the feeding rate was adjusted to a constant rate of 0.4 – 0.8 g l^{-1}. After induction (10h), the PAPE or 4-APA began to accumulate at a much lower rate compared to prior shake flask cultivations, within 96 h, surprisingly the PAPE titer reached a final level of almost 215 mg l^{-1} (Figure **3-29** (a)). It is noteworthy that similar result was also observed for 4-APA with a final titer 422 mg l^{-1} (Figure **3-29** (c)) by consuming 30 g l^{-1} glucose. It should be also noted that when the experiment was repeated with similar conditions, the similar results for PAPE and 4-APA were obtained. During Fed-batch process, the dissolved oxygen was kept nearly constant 30% air saturation, temperature at 30 ◦ C and pH was set at 7 by 10 % ammonia solution, which indicates no technical problem during fed batch process. The concentration of oxygen initially was ~100 % and then rapidly depleted and stabilized to 30 %. After a while, glucose began to accumulate slowly and steadily as indicated by an increase in the dissolved-oxygen (pO2) concentration in the culture (Figure **3-29** (b and d)). This might turn glucose further into by-product (acetate and lactate) which can then be released into the culture. Nevertheless, the by-products, 1.56 g l^{-1} acetate and 0.7 g l^{-1} lactate were produced in quantities smaller than shake flasks (Figure **3-26**).

The limiting factor/s in the above fermentation process was unclear, presumably due to non-optimized conditions in fermenter (PAPE/4-APA sensitivity to high oxygen content).

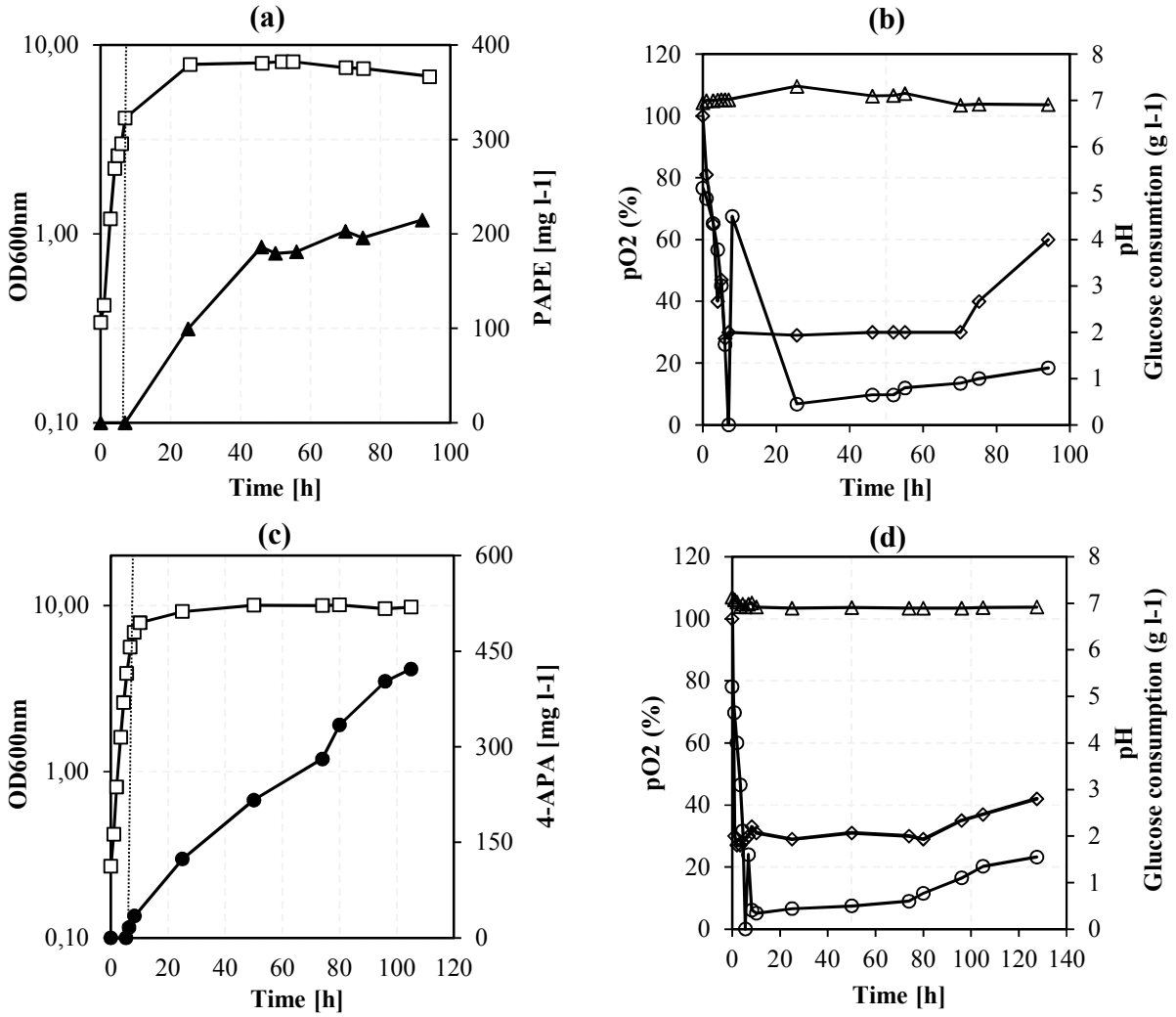

Figure 3-29 Glucose fed-batch cultivation of *E. coli* FUS4BCR/pC53BCAY/pJNT*aroFBL-yahK* for PAPE **(a)** and *E. coli* FUS4BCR /pC53BCAF/pJNT*aroFBL-feaB* for 4-APA **(b)** in bench top fermenter. After initially glucose was consumed (5 g l^{-1}), the cultures were induced with 0.5 mM IPTG (final concentration) and temperature was shifted from 37°C to 30°C (optimal temperature for Aro10 is 30°C) followed by glucose feeding (0.4-0.8 g l^{-1}). The respective symbols represent as follows: PAPE concentration (▲, mg l^{-1}), 4-APA concentration (●, mg l^{-1}), OD 600nm (□), pH (Δ), glucose consumption (○, g l^{-1}) and pO2 (◊, %). The result of one fermentation is presented with mean values and deviations of three technical replicates.

3.1.7 Isolation of L-PAPA from culture broth (Downstream processing)

Considering that so far no efficient and easy way to purify L-PAPA from culture broth has been reported, different organic solvents (Acetone, tetrahydrofuran, ethyl acetate, diethyl ether and

methyl tert-butyl ether (MTBE)) were investigated to see whether those can help with extraction of aromatic amines (L-PAPA) from fermentation culture broth. The most efficient solvents for extracting aromatic amines compounds (L-PAPA) were acetone (Konishi et al, 2016 US patent) and tetrahydrofuran. The product isolation of L-PAPA from fermentation culture broth was carried out according to the procedure described in Section 2.8.3. For the isolation of L-PAPA, the strain *E.coli* FUS4.7R/ pC53BC/pJNT*aroFBL* in a 30 L fermenter which has been described in section 2.6.4.1 was cultivated. The obtained fermentation culture from the previous 30 L fed batch fermentation experiment (section 3.1.6) was used. The first step was centrifugation followed by filtration step (pass through 0.2 µm filter). The 2.25 l of obtained supernatant was acidified (pH~1) by hydrogen chloride (37%) and then used for next extraction steps by acetone or tetrahydrofuran as described in Section 2.8.1. In the subsequent isolation of L-PAPA from the fermentation culture broth with a volume of 2.25 l, a total of 26 g of L-PAPA was isolated.

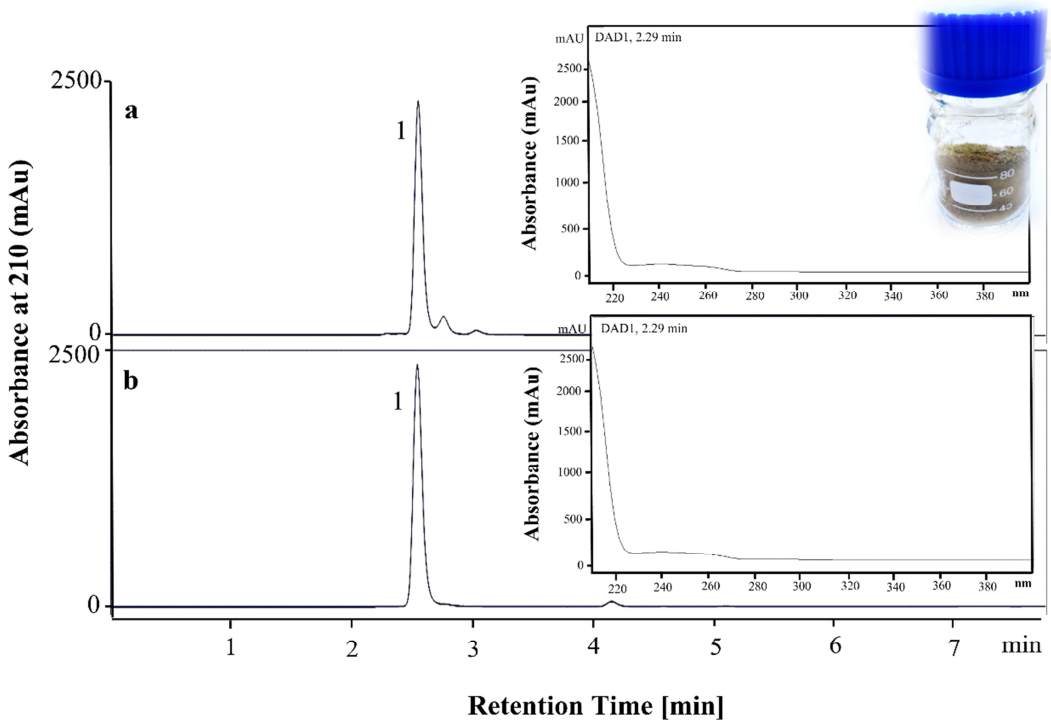

Figure 3-30 Reversed phase HPLC chromatograms obtained from sample extracted by acetone **(a)** and L-PAPA commercial standard **(b).** Extracted L-PAPA on gram-scale shown in a glass bottle **(c).** Peak identified as 1: L-PAPA. Absorption maximum at 210 nm; plotted as absorbance unit [mAU] versus time [min]. The HPLC system was equipped with a symmetry C18 silica column (Prontosil, 250 mm× 4 mm, CS chromatography service GmbH) and a UV detector operating at a wavelength of 210 nm. Retention time: 2.24 minutes represent L-PAPA; absorption maximum at 210 nm; plotted as absorbance unit [mAU] versus time [min].

Described methods resulted in a purity of ≥ 75 % L-PAPA (based on HPLC) isolated yield up to 69% (Konishi et al, 2016). As expected, L-PAPA extracted by acetone (Figure **3-30** (a)) showed same retention behavior as the commercial standard (Figure **3-30** (b)) in the HPLC analysis. It should also be noted that along with the dominant L-PAPA, some unknown impurities were also observed (Figure **3-30** (a)). The concentrated end product obtained after freeze-drying was a dark brown powder (Figure **3-30** (c)). Furthermore to obtain far better pure L-PAPA on a gram-scale, scale-up of the column chromatography process by FPLC (silica gel, Methanol) was performed according to the procedure described in Section 2.8.4. With a large Luna column (Phenomenex, C18 (2), 250 mm × 21.20 mm 5 micron), 1.65 g L-PAPA was obtained from fermentation broth (containing 2.3 g l^{-1} L-PAPA). Upon column chromatography, L-PAPA with high purity (≥ 93%) was separated rather well from the other reactants (Figure **3-31** (a)). The resulting yield of L-PAPA was 71.7 %. Freeze-drying of the selected eluents was performed to yield an end product of L-PAPA. HPLC analysis confirmed the presence of L-PAPA together with a little unknown impurities (Figure **3-31** (a), labeled with arrows). The concentrated end product is a yellow brown powder (Figure **3-31** (c)).

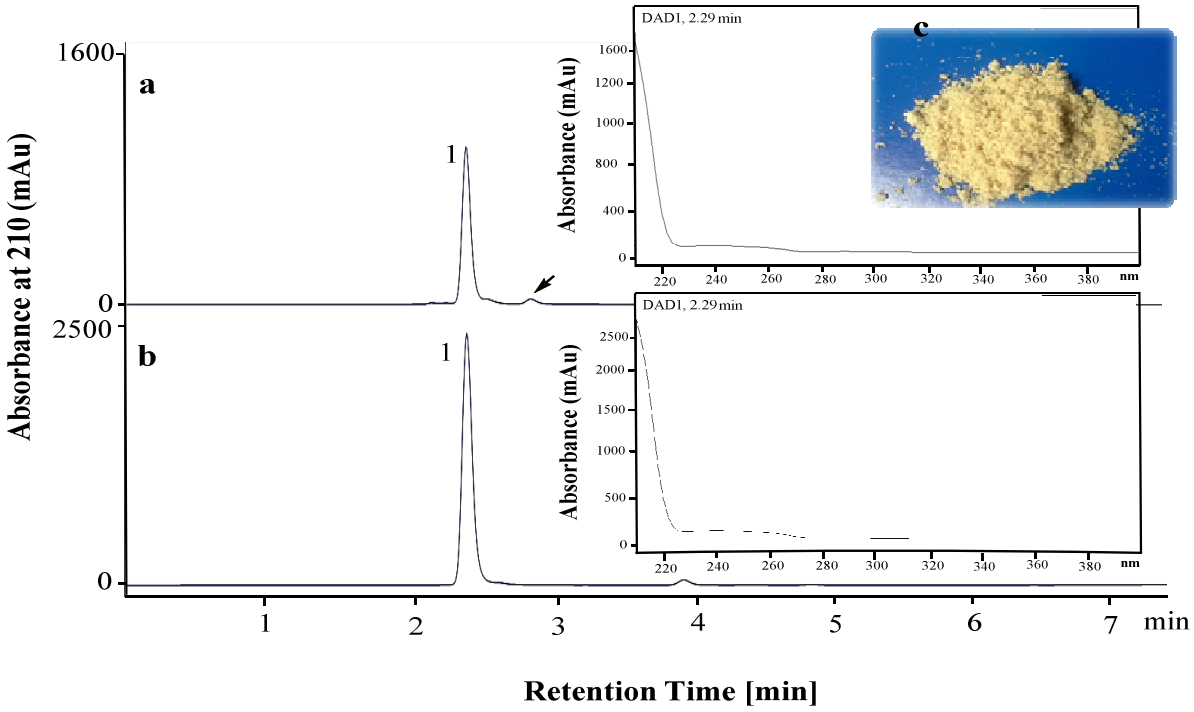

Figure 3-31 Separated of L-PAPA based on column chromatography process by FPLC. HPLC chromatogram of desire eluent FPLC fraction **(a)** compare to pure L-PAPA standard **(b)**. Final extracted product L-PAPA, yellow brown powder (c). Conditions: Flow rate = 1ml min^{-1}, 210nm, symmetry C18 column (Prontosil 250 mm× 4 mm, chromatography service GmbH, Germany).

3.2 Part II: Biosynthesis of aromatic alcohols and amino acids

The second part of this work was focused on the production of 2-PE, tyrosol, L-Phe and L-Tyr based on expression plasmids in the *E. coli* strains. This part begins with evaluating the proposed biotransformation pathway for production of 2-PE from L-Phe and tyrosol from L-Tyr. Then, a microbial platform for 2-PE and tyrosol production from cost-effective substrate (glucose) was designed that mimicked the yeast Ehrlich pathway in *E. coli*. The different metabolic engineering strategies including deletion of competing pathway and negative regulator, overexpression of rate limited enzyme in shikimate pathway were applied to improve the flux toward 2-PE or tyrosol production. In addition, different cultivation parameters were tested in order to improve glucose yield and titer by the recombinant strain *E. coli*. For instance, in the presence of high concentrations of aromatic alcohols (2-PE or tyrosol), the growth of the *E.coli* was limited, thus inhibited growth could limit *E. coli* productivity. To address this limitation, ISPR technique (two-phase strategy) was applied. A two-phase fed batch process in a lab-scale bioreactor to obtain high titer of 2-PE or tyrosol was investigated. Finally, a simple and easy modified method for extraction of 2-PE or tyrosol with good isolated yield and purity was established.

3.2.1 Metabolic engineering of *E. coli* for biosynthesis of L-phenylalanine and 2-phenylethanol (2-PE)

3.2.1.1 Biotransformation of L-phenylalanine to 2-phenylethanol

In order to evaluate and verify a proposed 2-PE biosynthesis pathway in *E. coli* (Figure **3-32**(a)), biotransformation of L-Phe to 2-PE was carried out according to the procedure described in section 2.6.3.1 using resting cells of *E. coli* LJ110 supplemented by ~1675 ± 215 mg l^{-1} L-Phe (10 mM) as substrate. As shown in Figure **3-32** (b), the initial L-Phe concentration did not noticeably change in *E. coli* LJ110 strain harboring empty vector (pJF119EH), consequently no detectable amount of 2-PE was formed after 8h. In contrast, biotransformation of L-Phe with *E. coli* LJ110 harboring pJFA10 (*aro10* gene) yielded 2-PE as new compound with total conversion yield 72 % g g^{-1} (98% mol mol^{-1}, including also endogenous L-phenylalanine). 1675 ± 215 mg l^{-1} starter L-Phe gradually decreased and 2-PE production simultaneously began to increase significantly and eventually was completely converted to 1217 ± 110 mg l^{-1} 2-PE

after 8h in *E. coli* LJ110/pJFA10. These results demonstrate appropriate activity of enzymes involved in the biosynthesis of 2-PE in *E. coli*. In addition, 132 ± 31 mg l^{-1} phenylacetic acid as a side product was detected after 8h in *E. coli* LJ110 pJFA10. Therefore, this enzyme (Aro10) can be used further for *de-novo* production of 2-PE in *E. coli*.

(a)

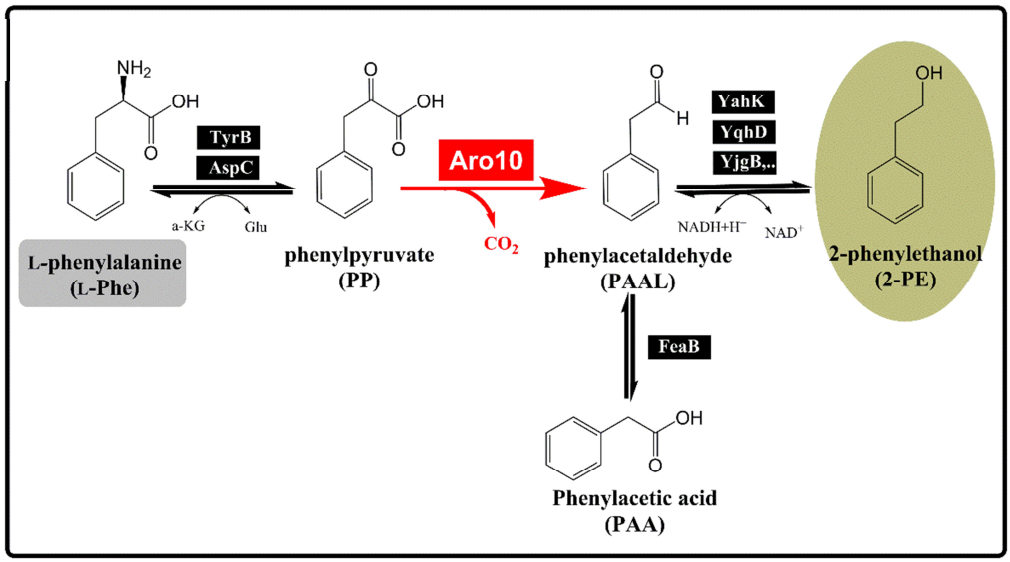

(b)

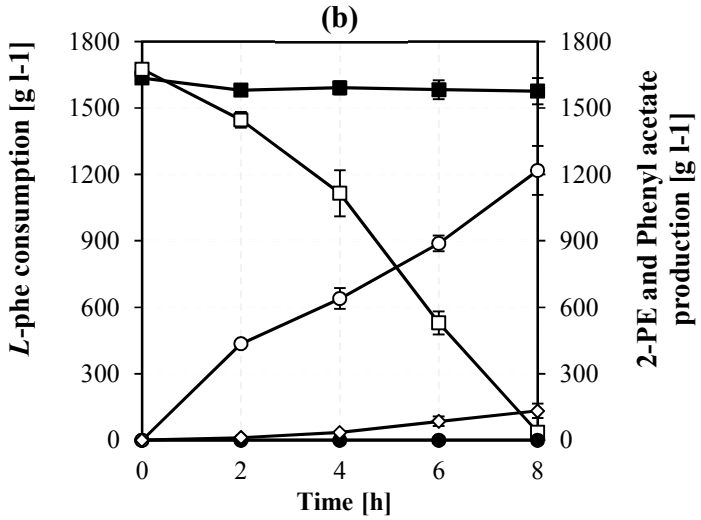

	Products			
	2-PE		**Phenylacetic acid**	
	mg l^{-1}	yield (% g g^{-1})	mg l^{-1}	yield (% g g^{-1})
pJF119EH	n.d.	-	n.d. [a]	-
pJFA10	1217 ± 110	72	132 ± 31	7.8

[n.d.] stands for Not Detectable and [-], stands for not calculable.

Figure 3-32 Scheme of biotransformation of L-Phe to 2-PE in *E. coli*. **(a)** Biotransformation pathway of L-Phe as substrate to 2-PE in *E. coli* LJ110 harboring pJFA10 plasmid (*aro10*). **(b)** Biological conversion L-Phe (10 ± 0.16 mM) by resting cell *E. coli* LJ110 pJF119EH (as control) and pJFA10 over the course of 8 h (b). *E. coli* cells were initially grown at 37°C until reach OD600nm 0.6. Afterwards, 0.5mM IPTG (final conc.) was added and incubated at 30°C for 4-6h (OD600nm ~5). The collected cells were resuspended in the 10 ml potassium buffer (pH~ 7) and followed by incubation in 30°C-110 rpm with start OD600nm ~18. Concentrations of L-Tyr and tyrosol were analyzed by HPLC. Filled square (■), L-Phe concentration in *E. coli* LJ110/pJF119 (empty plasmid as control); Empty Square (□), L-Phe concentration in *E. coli* LJ110/pJFA10; Filled circle (●), 2-PE production in *E. coli* LJ110/pJF119 (empty plasmid as control), Empty circle (○), 2-PE production and (◊),Phenylacetic acid production in *E. coli* LJ110/pJFA10. Triplicate assays were performed and the error bars indicated standard deviations. [n.d.] stands for Not Detectable and [-], stands for not calculable.

3.2.1.2 Construction of a de-novo 2-PE biosynthesis pathway in *E. coli*

In order to construct a de-novo pathway for 2-PE production in *E. coli*, a heterologous enzyme with ketoacid decarboxylase activity from yeast (Aro10, Kneen et al. 2011) is required for conversion of phenylpyruvate (PP) to phenylacetaldehyhe (PAAL), PAAL is then converted to 2-PE by endogenous reductase in *E.coli* (Koma et al. 2012, Kang et al. 2014). First overexpression of *aro10* gene from *Saccharomyces cerevisiae* was tested for de-novo biosynthesis of 2-PE directly from glucose in *E. coli* wild type. *E. coli* LJ110/pJFA10 was grown in the shake flasks containing minimal medium supplemented with 4.5 ± 0.12 g l^{-1} glucose for 48h. As expected, no 2-PE was detected in *E. coli* LJ110 harboring the control vector pJF119EH (Figure 3-33 (a)). A major 2-PE peak was detected in extracts of *E. coli* LJ110/pJFA10 culture (Figure 3-33 (b), labeled with (1) that eluted at the same retention time of 2-PE standard (Figure 3-33 (c)) and exhibited identical mass fragmentation pattern $[M+H]^+$ matching to 2-PE (Figure 3-33 (d)). Also, 11 ±1.5 mg l^{-1} 2-PE in *E. coli* LJ110/pJFA10 was accumulated (Figure 3-34 (b)), presumably "demonstrating that Aro10 is capable in conversion of PP to PAAL", which is then reduced to 2-PE by some kinds of endogenous reductase or alcohol dehydrogenase in *E. coli* host strain (YahK, YqhD, YjgB and more than 10 others. Figure 3-34 (a)).

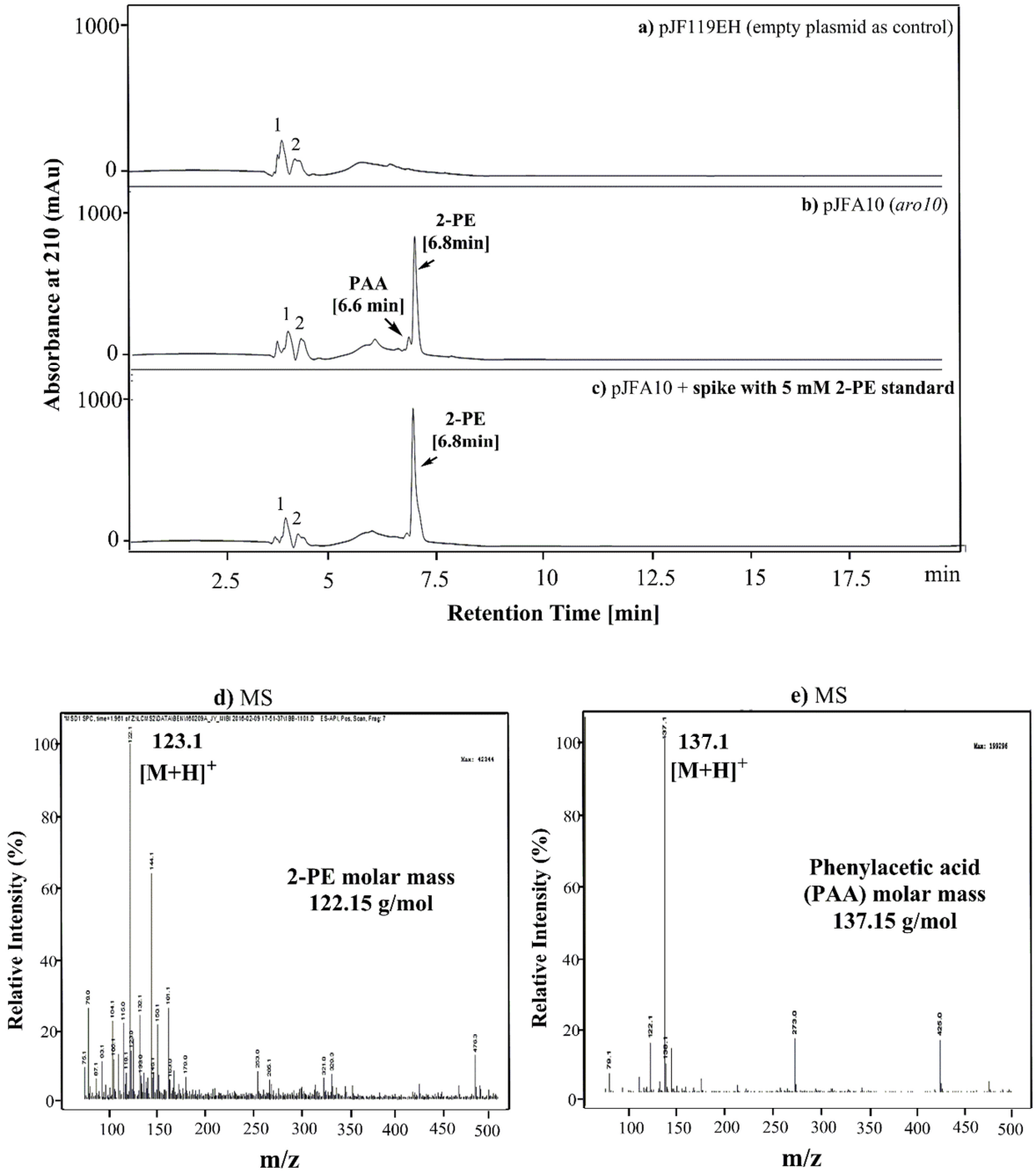

Figure 3-33 HPLC profile and mass ion chromatogram of 2-PE produced by engineered *E. coli*. The chromatograms derived from a supernatant of culture broth (after 48h) of *E. coli* LJ110 harboring empty plasmid pJF119 as control **(a)** or pJFA10 **(b)**. Spike test (**c**), 5 mM 2-PE standard was added to a supernatant from the culture broth of *E. coli* LJ110 pJFA10. The peak at 6.8 min [1] represent 2-PE which not present in supernatant from *E. coli* LJ110 harboring empty plasmid as control (a). In addition the peak at 6.69 min [2] represent phenylacetic acid as by product in *E. coli* LJ110 harboring pJFA10. **(d),** mass ion chromatogram of ([1]) 2-Phenylethanol (m/z 123.1 $[M + H]^+$) and **(e)**; ([2]) phenyl acetic acid (m/z 137.1 $[M + H]^+$) produced by *E.coli* LJ110 harboring pJFA10. Chemical structure of 2-PE and phenylacetic acid present on ESI-mass spectra. The HPLC system was equipped with a symmetry C18 silica column (Lichrospher 100 RP, 250 mm× 4 mm, chromatography service GmbH) and a UV detector

operating at a wavelength of 210 nm. The column was eluted with a gradient method at a flow rate of 0.4 ml min^{-1}. Labeled peaks [1 and 2] are from media.

In addition, phenylacetic acid (PAA, Figure 3-33 (b and e), labeled with 2) as by product was detected in trace amounts (approx. 4 mg l^{-1}), indicating probably that the activity of endogenous dehydrogenase (encoded by *feaB*) on phenyl acetic acid. The obtained results indicate that recombinant genes are functionally expressed in *E. coli* wild type, and the engineered strain can be used as a basic strain for further enhancement of the production of 2-PE from glucose as the sole carbon source. The proposed biosynthetic pathway for 2-PE production from glucose is schematically shown in Figure 3-34 (a).

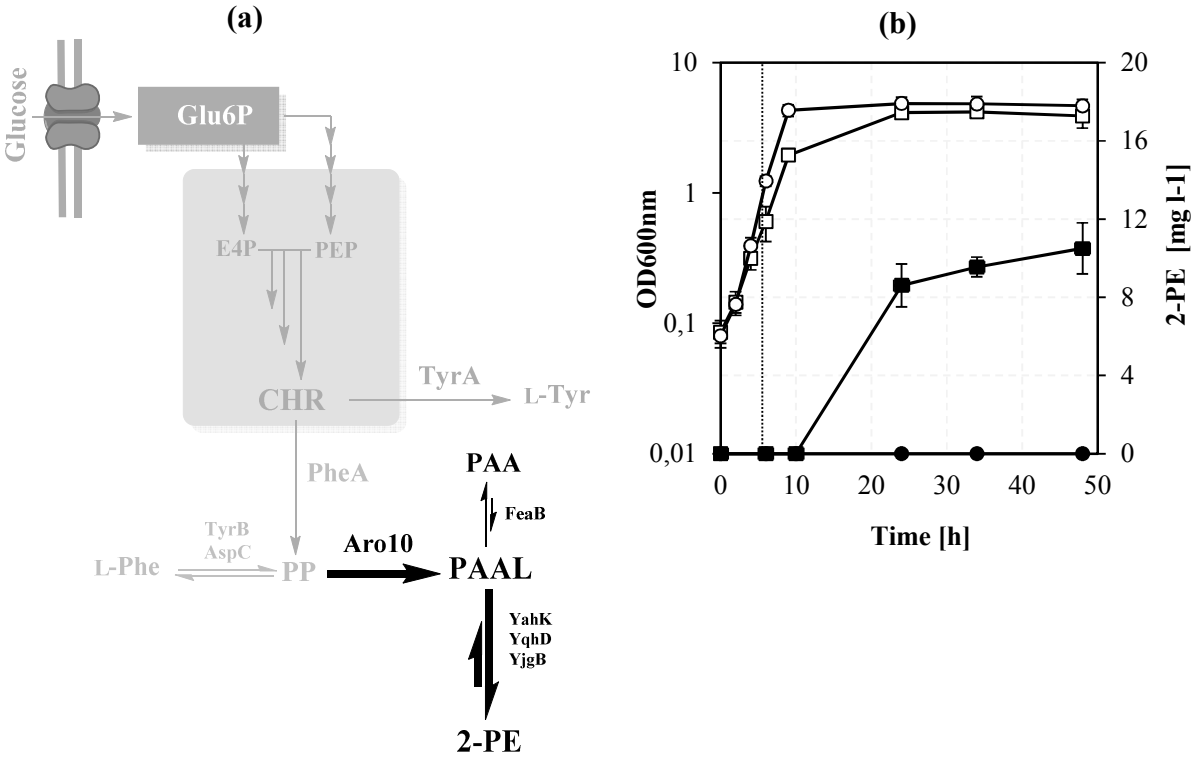

Figure 3-34 Proposed biosynthesis pathway for 2-PE production from glucose in *E.coli* wild type **(a).** Glucose batch cultivation of *E. coli* LJ110 /pJF119 (empty vector) and *E. coli* LJ110 /pJFA10 in shake flasks **(b).** The initial glucose concentration was 4.5 g l^{-1}. After reaching OD_{600nm}~ 0.6 (red dotted line) the cultures were induced with 0.5 mM IPTG (final concentration). The concentrations of 2-PE in *E. coli* LJ110/pJFA10 (■, filled squares); in *E. coli* LJ110 / pJF119 (●, filled circles) were determined by HPLC and OD_{600nm} is presented as empty squares (□) in *E.coli* LJ110 /pJFA10 and empty circle (○) in *E. coli* LJ110/pJF119. Data are averages of results from three biological replicates. Error bars represent standard deviations from the means.

3.2.2 Metabolic engineering of *E. coli* for biosynthesis of L-tyrosine and 2-(4-hydroxyphenyl) ethanol (tyrosol)

3.2.2.1 Whole cell biotransformation of L-tyrosine to tyrosol

For the synthesis of tyrosol in *E. coli*, a short bioconversion pathway from L-tyrosine to tyrosol using phenylpyruvate decarboxylase was constructed (Figure **3-35** (a)). Aro10, as described previously, is a thiamine-dependent decarboxylase enzyme that converts hydroxyphenylpyruvate (4-HPP) into 4-hydroxyphenylacetaldehyde (4-HPAAL, Chung et al. 2017; Xue et al. 2017). In recombinant *E. coli*, 4-HPAL is then converted to 2-(4-hydroxyphenyl) ethanol (tyrosol) by several endogenous aldehyde reductase or alcohol dehydrogenase (YahK, Yghd,YigB and more than 10 others) (Koma et al. 2012; Kunjapur et al. 2014; Rodriguez and Atsumi 2014). Hence, it was investigated whether tyrosol can be produced from tyrosine by expressing Aro10 gene from plasmid pJFA10 in *E. coli* LJ110. Biotransformation of L-Tyr to tyrosol was carried out in shake flasks at L-Tyr concentration of 9.75 mM with resting cell of *E. coli* LJ110 pJFA10 after Aro10 was induced by 0.5mM IPTG (See 2.6.3.1). This reaction was monitored by HPLC and LC-MS. As shown in Figure **3-35** (b), L-tyrosine was not converted to tyrosol in *E. coli* LJ110/pJF119 (as control). In contrast, 1772 ± 70 mg l^{-1} initial L-tyrosine gradually decreased during the biotransformation and in parallel tyrosol increased consistently in *E. coli* LJ110/pJFA10 (Figure **3-35** (b)). The highest tyrosol was obtained after 8 h and the concentration of tyrosol reached 1232 ± 85 mg l^{-1}, corresponding to a molar yield of 70 % g g^{-1} (91.2% mol mol^{-1}, including also endogenous L-tyrosine). In addition, 83.7 ± 36.2 mg l^{-1} 4-hydroxyphenyl acetic acid (4-HPAA) via the oxidation of 4-HPAAL probably by FeaB after 8h in *E.coli* LJ110/pJFA10 (Figure **3-35** (b)) was observed.

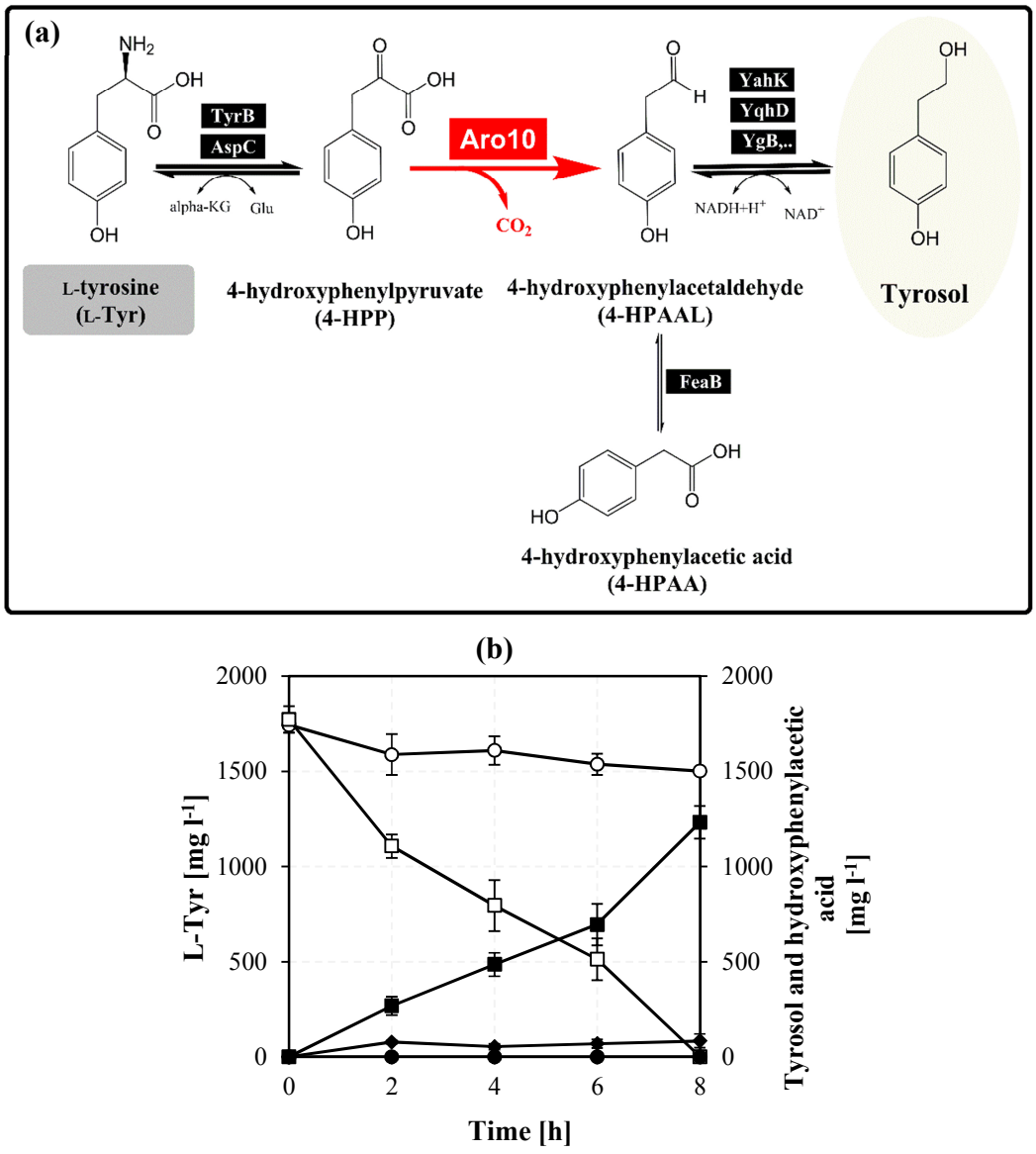

	Products			
	Tyrosol		**4-HPAA**	
	mg l^{-1}	yield (% g g^{-1})	mg l^{-1}	yield (% g g^{-1})
pJF119EH	n.d.	-	n.d.	-
pJFA10	1232 ± 85	70	83.7 ± 36.2	5

[n.d.] stands for Not Detectable and [-], stands for not calculable.

Figure 3-35 Biotransformation of L-Tyr to tyrosol. **(a)** Biotransformation pathway of L-Tyr to tyrosol in *E.coli* LJ110 harboring pJFA10 plasmid (aro10). **(b)** Biological conversion 1.7 g l-1 (9.75mM) exogenous L-Tyr by resting cell *E. coli* LJ110 pJF119EH (as control) and pJFA10 over the course of 8 h. *E. coli* cells were initially grown at 37°C until reach OD600nm 0.6. Afterwards, 0.5mM IPTG (final conc.) was added

and incubated at 30°C for 4-6h (OD600nm ~5-6). The collected cells were resuspended in the 10 ml potassium buffer (pH~ 7) and followed by incubation in 30°C-110 rpm with start OD600nm ~18.Symbols represent: ○, L-Tyr in *E. coli* LJ110/pJF119 (empty plasmid as control); □, L-Tyr in *E. coli* LJ110/pJFA10; ●, tyrosol in *E. coli* LJ110/pJF119 ; ■, tyrosol and ♦, 4-hydroxy phenylacetic acid in *E. coli* LJ110/pJFA10. Data are averages of results from three biological replicates. Error bars represent standard deviations from the means.

3.2.2.2 Construction of a de-novo tyrosol biosynthesis pathway in *E. coli*

For the synthesis of tyrosol in *E. coli,* a *de-novo* the biosynthesis pathway from glucose (Figure **3-37** (a)) was constructed. *E. coli* wild type requires a heterologous Ketoacid decarboxylase enzyme (encoded by *aro10*) in addition to the endogenous reductase, which produces tyrosol from glucose. The phenylpyruvate decarboxylase (Aro10) catalyzes the conversion of 4-HPP to 4-HPAAL (Chung et al. 2017), and endogenous reductase (YahK, Yghd, YigB and more than 10 others) performs the one-step reduction of the aldehyde intermediate 4-HPAAL to tyrosol (Figure **3-37** (a)). In addition, to optimize the flux toward 4-HPP production $TyrA^{fbr}$ (chorismate mutase/prephenate dehydrogenase feedback resistance version obtained from Dr. Natalie Trachtman) as key enzyme in L-Tyr pathway (in *E. coli*) was overexpressed with Aro10 (Figure **3-37** (a)). Therefore, simultaneous expression of *tyrA* and *aro10* under P*tac* promoters was constructed to examine tyrosine and tyrosol production in *E. coli* wild type. The already constructed plasmids pJFT and pJFTA10 that harbor $TyrA^{fbr}$ and Aro10 along with $TyrA^{fbr}$ respectively, was used and then introduced into *E. coli* wild-type LJ110. Hence, shake-flask cultures of recombinant strains were carried out in the presence of 4.5 ± 0.17 g l^{-1} glucose. After IPTG induction of recombinant proteins (OD600nm 0.6), the supernatant of culture broth was analyzed by HPLC and LC-MS, and tyrosine and tyrosol contents were identified on the basis of the retention time with standard and the LC–MS analysis (Figure 3-36). Figure 3-36 (a), shows the HPLC monitoring of the peaks at *E. coli* LJ110/pJF119EH as control, *E. coli* LJ110/pJFT (b) and *E. coli* LJ110/ pJFTA10 (c). While tyrosol peaks (RT~4.48 min, labeled with 2) was not detected over the time in *E. coli* LJ110/pJF119EH as control (Figure 3-36 (a); it began to appear as major product with a titer 36.8 ± 4.5 mg l^{-1} in *E. coli* LJ110/ pJFTA10 (Figure 3-37 (c)). In addition, although L-Tyr (Figure 3-36 (b), labeled with 1) was detected with a titer 108 ± 6.5 mg l^{-1} in *E. coli* LJ110/pJFT (Figure 3-37 (b)), it began to disappear after induction in *E. coli* LJ110/pJFTA10 (Figure 3-36 (c)). The identity of reaction product was determined to be tyrosol (122.1 $[M\text{-}H_2O+H]^+$, Figure 3-36 (e)) and tyrosine (182.1 $[M+H]^+$ Figure 3-36 (f)) using

electron spray ionization (LC-MS analysis). Reaction intermediates such as 4-HPAAL could not be simultaneously visualized presumably due to instability.

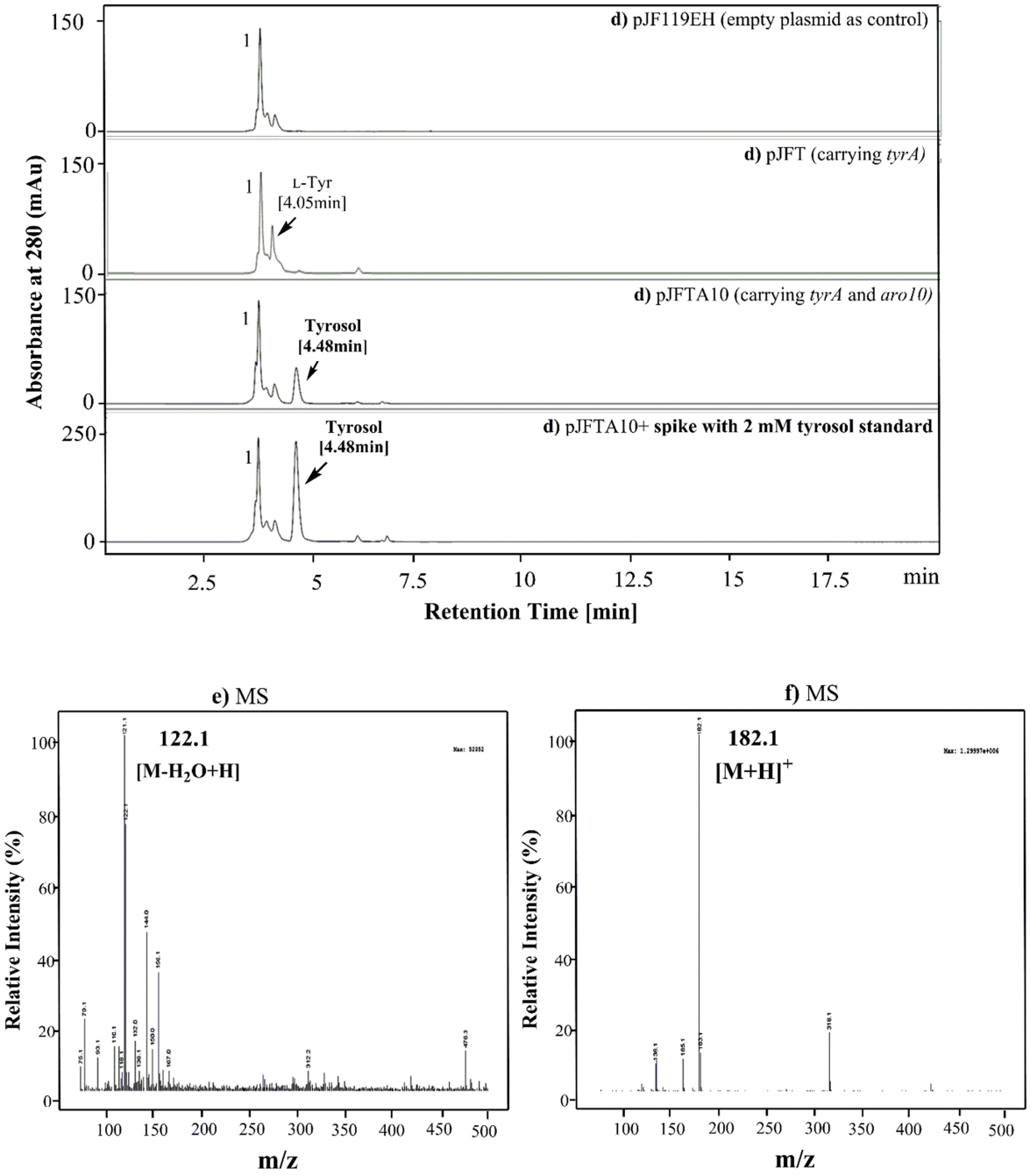

Figure 3-36 Reversed phase HPLC analysis and LC-MS analysis of L-tyrosine and tyrosol biosynthesis in *E. coli*. The chromatograms display **(a)** an extract (after 48h) from the culture broth of *E. coli* LJ110 pJF119EH (control); **(b)** an extract (after 48h) from the culture broth of *E. coli* LJ110 pJFT; **(c)** an extract from the culture broth of *E. coli* LJ110 pJFTA10; **(d)** an extract (after 48h) from the culture broth of *E.*

coli LJ110 pJFTA10 which was spiked with 2 mM tyrosol standard; **(e)** LC-MS spectrum of tyrosol derivate from culture broth of *E. coli* LJ110 pJFTA10 and **(f)** LC-MS spectrum of L-tyrosine derivate from culture broth of *E. coli* LJ110 pJFT. The HPLC system was equipped with a symmetry C18 silica column (Lichrospher 100 RP, 250 mm× 4 mm, chromatography service GmbH) and a UV detector operating at a wavelength of 280 nm. The column was eluted with a gradient method at a flow rate of 0.4 ml min^{-1}. The retention times of L-tyrosine and tyrosol were 4.05 min and 4.48 min, respectively (b and c). Quantitative data were obtained by comparing the peak areas of the query compounds with those of standards of known concentration. Tyrosol has a molar mass 138.16 g/mol. Tyrosine has a molar mass 181.19 g/mol.

Unlike biotransformation, no evidence of 4-hydroxyphenylacetic acid production was found following biosynthesis. As shown in Figure **3-37** (c), *E. coli* LJ110 pJFTA10 reached growth plateau phase at 10-12 h when glucose was almost consumed, while tyrosol was still accumulating.

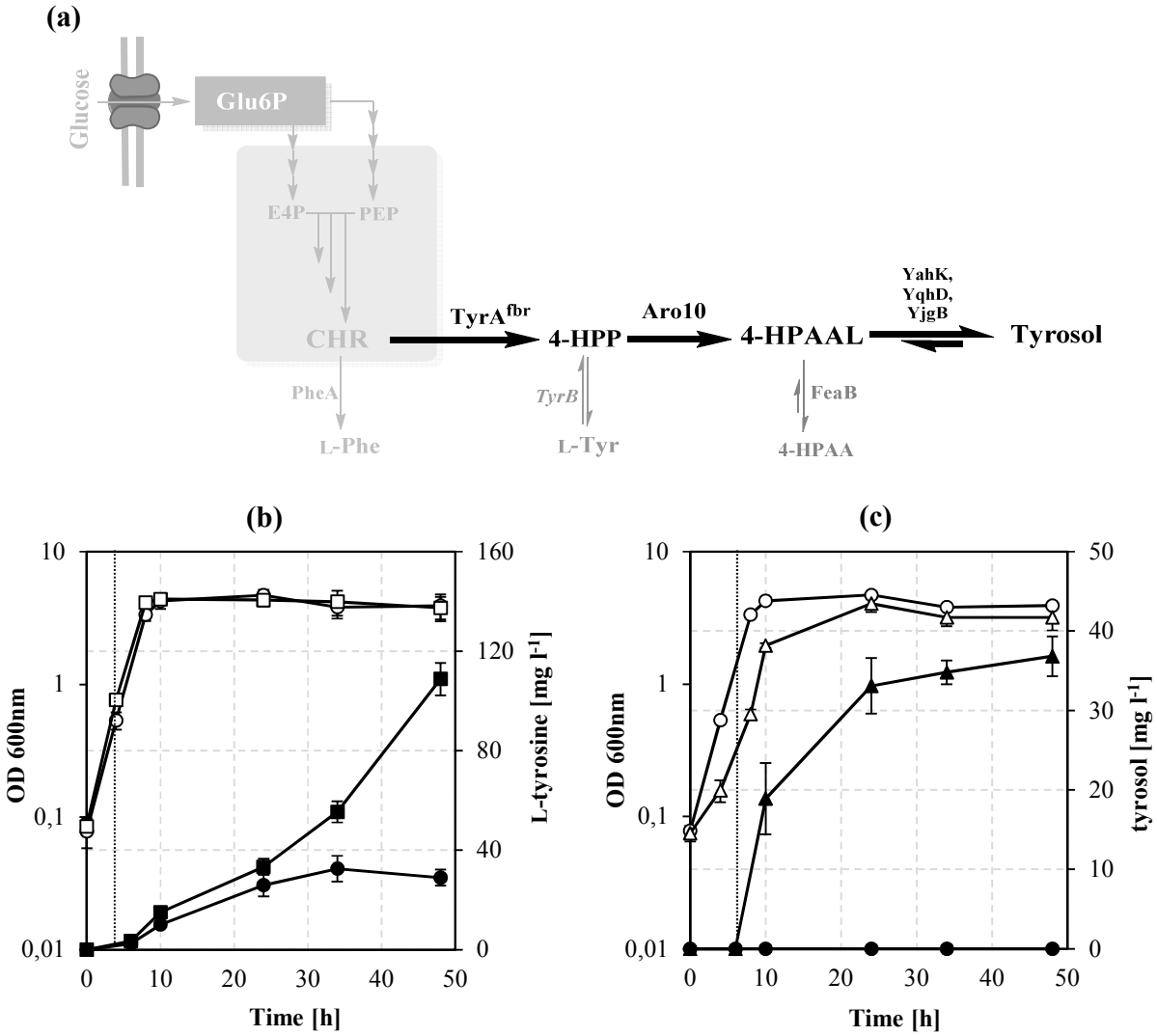

Figure 3-37 Glucose batch cultivation of *E. coli* for production of tyrosol. **(a)** Schematic diagram shown a tyrosol biosynthesis pathway in *E.coli* by expanding shikimate pathway; **(b)** L-tyrosine production in *E.coli* LJ110 harboring pJF119EH (●, as control) and pJFT plasmid (■); (c) tyrosol production in *E. coli* LJ110 harboring pJF119EH (●, as control) and pJFTA10 plasmid (▲). OD600nm is presented as empty circle (○) in *E. coli* LJ110/ pJF119 (as control), empty square (□) in pJFT plasmid and empty triangle (Δ) in pJFTA10 plasmid. The initial glucose concentration was 4.5 g l^{-1}. After reaching OD600nm~0.6-0.8 (red spotted line) the cultures were induced with 0.5 mM IPTG (final concentration). Data are averages of results from three biological replicates. Error bars represent standard deviations from the means.

3.2.3 Synthesis of hydroxytyrosol from L-DOPA in *E. coli*

Whole cell Biotransformation of L-DOPA to hydroxytyrosol

An attempt was made to construct a short pathway to test whether that *E.coli* harboring Aro10 can also accept and convert L-DOPA as substrate to hydroxytyrosol. The first step in the proposed hydroxytyrosol pathway (Figure 3-39 (a)) after L-DOPA deamination is the decarboxylation of 3,4-dihydroxy phenylpyruvate (3,4-DHPP) to 3,4-dihydroxy phenyl acetaldehyde (3,4-DHPAAL), which are shown also in a recent publication (Li et al. 2018 ; Chung et al. 2017). For this conversion it was assumed that thiamine-dependent decarboxylase enzyme (Aro10) with broad substrate activity can catalyze the decarboxylation of 3,4-DHPP to 3,4-DHPAAL (Figure 3-39 (a)). Then to achieve conversion of 3,4-DHPAAL to hydroxytyrosol, an endogenous alcohol dehydrogenase or reductase (YahK, Yghd,..) is needed. For this purpose, *E. coli* LJ110 was transformed with pJFA10 plasmid and then *E. coli* resting cells (See 2.6.3.1) were incubated in buffer supplemented with L-DOPA as substrate (12.8 mM), hydroxytyrosol production was monitored by HPLC and LC-MS. As shown in Figure 3-39 (a), the initial concentration of L-DOPA (RT~3.86 labeled with 1) did not change much over the time and there was no detectable hydroxytyrosol production in *E.coli* LJ110/pJF119EH (as control). Under this experimental condition, initial L-DOPA was consumed and hydroxytyrosol was detected by HPLC (Figure 3-38 (d)) and LC-MS analysis (Figure 3-38 (e)) in *E. coli* LJ110 pJFA10. LC–Mass spectrometry (LC-MS) analysis of the culture extracts exhibited identical mass fragmentation pattern $[M-H]^-$ and $[2M-H]^-$ matching to hydroxytyrosol (Figure 3-38 (e)).

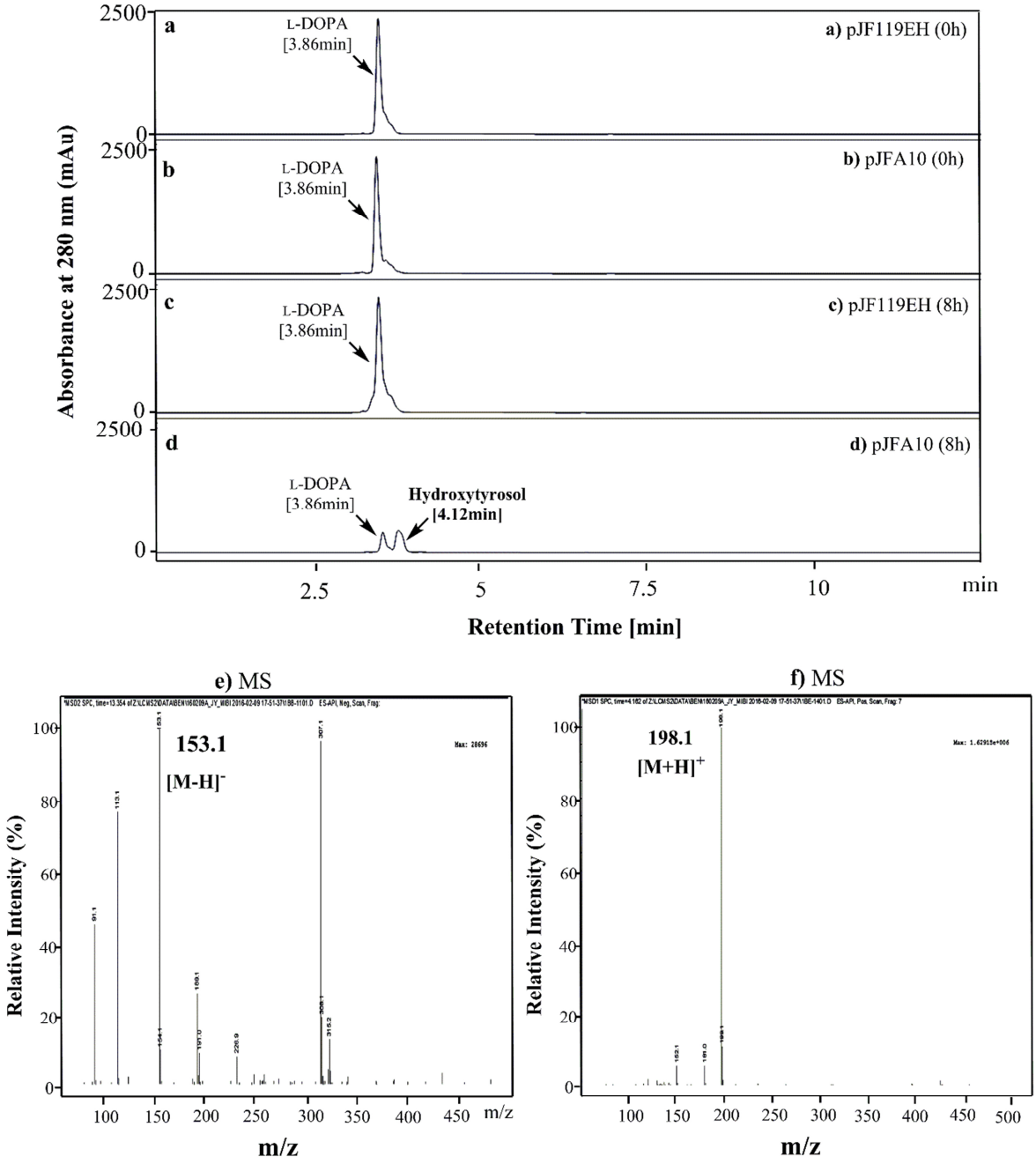

Figure 3-38 Reversed phase HPLC and LC-MS analysis of L-DOPA and hydroxytyrosol. The chromatograms represents: extract from the culture broth of *E. coli* LJ110 pJF119 (control) at time 0h **(a)** and 8h **(c)**; extract from the culture broth of *E. coli* LJ110 pJFA10 at time 0 h **(b)** and 8h **(d)**; LC-MS spectrum of hydroxytyrosol **(e)** and L-DOPA **(f)** derivate from culture broth of *E. coli* LJ110 pJFA10. The HPLC system was equipped with a symmetry C18 silica column (Lichrospher 100 RP, 250 mm× 4 mm, chromatography service GmbH) and a UV detector operating at a wavelength of 280 nm. The column was eluted with a gradient method at a flow rate of 0.4 ml min^{-1}. The retention times of L-DOPA and Hydroxytyrosol were 3.86 min and 4.12 min, respectively (1 and 2). Quantitative data were obtained by comparing the peak areas of the query compounds with those of standards of known concentration.

As shown in Figure 3-39 (b), 2.9 ± 0.19 g l^{-1} (12.8 mM) initial L-DOPA was consumed slowly (first 8 hours) and hydroxytyrosol production simultaneously began to increase constantly. While 74% of starter L-DOPA (2.2 g l^{-1}) was consumed, only 51% (approx. 1.1 ± 0.065 g l^{-1}) was converted to hydroxytyrosol (after 24) with a yield 39 % g g^{-1} (64 % mol mol^{-1}). These results strongly suggested the activities of Aro10 on 3,4-DHPP and endogenous reductases (YahK, Yghd,YigB and more than 10 others) on 3,4-DHPAAL in *E.coli,* which are compatible with recent studies (Chung et al. 2017; Li et al. 2018).

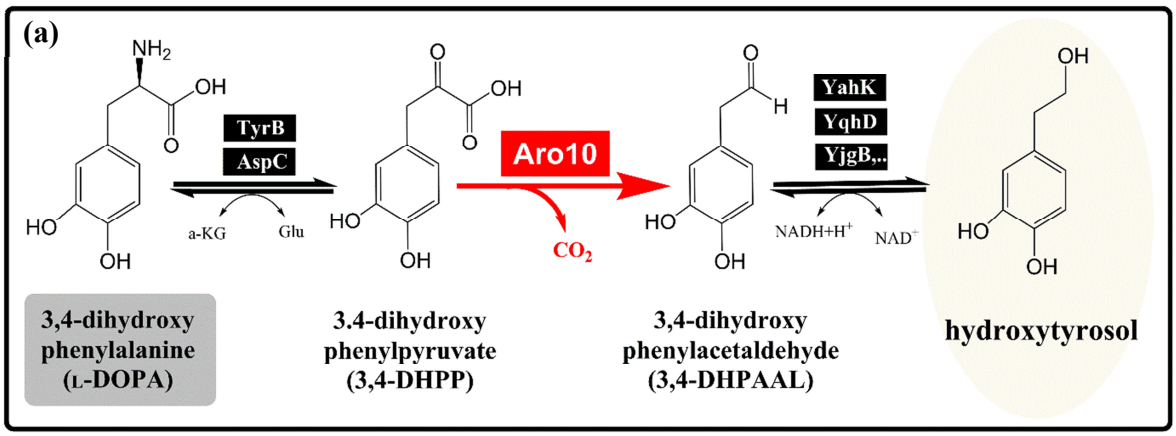

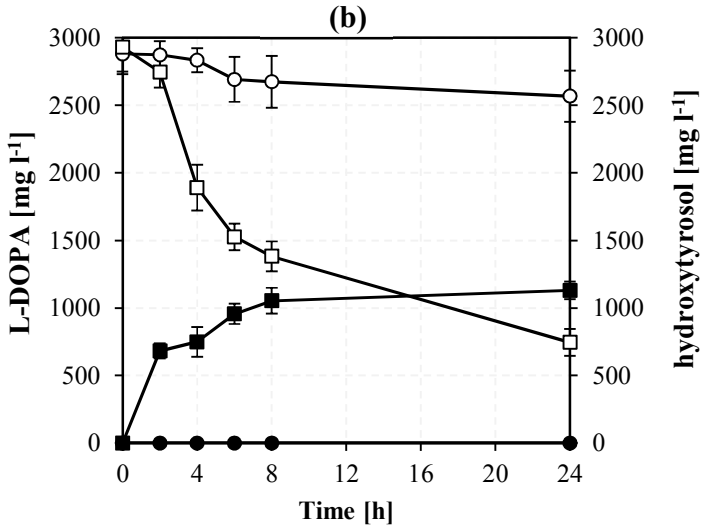

	hydroxytyrosol	
	mg l^{-1}	yield (% g g^{-1})
pJF119EH	n.d.	-
pJFA10	1129 ± 65	39

Figure 3-39 Biotransformation of L-DOPA to hydroxytyrosol in *E. coli*. **(a)** Schematic represents biotransformation of L-DOPA to Hydroxytyrosol in *E.coli* LJ110 harboring pJFA10 plasmid (*aro10*). **(b)** Biological conversion L-DOPA as substrate (2.9 g l^{-1}) by resting cell of *E. coli* LJ110 pJF119EH (as control) and pJFA10 over the course of 24h . *E. coli* cells were initially grown at 37°C until reach OD600nm 0.6. Afterwards, 0.5mM IPTG (final conc.) was added and incubated at 30°C for 4-6h (OD600nm ~5-6). The collected cells were resuspended in the 10 ml potassium buffer (pH~ 7) and followed by incubation in 30°C-110 rpm with start OD600nm ~16-18. Concentrations of L-DOPA and hydroxytyrosol were analyzed by HPLC. Symbols represent: ○, L-DOPA consumption in *E. coli* LJ110/pJF119 (as control); □, L-DOPA consumption in *E. coli* LJ110/pJFA10; ●, hydroxytyrosol production in *E. coli* LJ110/pJF119 and ■, hydroxytyrosol production in *E. coli* LJ110/pJFA10. Triplicate assays were performed and the error bars indicated standard deviations. [n.d.] stands for Not Detectable and [-], stands for not calculable.

Noteworthy here is that although Aro10 can accept 3,4-DHPP as substrate, the conversion rate (0.04 g h^{-1}) and obtained yield (39 % g g^{-1}) are less impressive in comparison with bioconversion of 2-phenylethanol (0.15 g h^{-1} and 72% g g^{-1}) and tyrosol (0.15 g h^{-1} and 70% g g^{-1}). It has generally been described that either oxidation by endogenous dehydrogenase to 3,4-DHPAA or oxidation to o-quinone and further to melanin (Ali et al. 2007) are presumable problems in the hydroxytyrosol production from L-DOPA.

3.2.4 Metabolic engineering of *E. coli* for optimization of aromatic alcohol production (2-PE/tyrosol)

3.2.4.1 Increasing carbon flux toward 2-PE/tyrosol pathway by removing bottlenecks

Subsequent enhancement of 2-PE and tyrosol production was achieved by increasing the activity of some main rate-limiting steps in the shikimate pathway (Báez-Viveros et al. 2007; Sprenger 2007; Chávez-Béjar et al. 2013) which is already described in section 3.1.4.4. Accordingly, in order to enhance the flux toward 2-PE pathway, the relevant genes of four rate limiting steps including (Figure **3-40**), condensation of DAHP from PEP/E4P by DAHP synthase (encoded by *aroF*), conversion of DAHP into DHQ by DHQ synthase (encoded by *aroB*), phosphorylation of shikimate to shikimate 3-phosphate by shikimate kinase I (encoded by *aroL*) and *pheA* encoding bifunctional chorismate mutase/prephenate dehydratase (feedback resistant form) for conversion of chorimate via prephenate to phenylpyruvate were cloned on pJNT plasmid and the resulting plasmid pFABL was introduced into *E.coli* LJ110. Production of 2-PE or tyrosol from 4.5 ± 0.25 g l^{-1} glucose was initiated with the addition of IPTG at an OD_{600nm} of ~0.6 (6-8 hours after inoculation). Overexpression of pFABL in the wild type *E. coli* LJ110

yielded 142 ± 11.5 mg l^{-1} L-Phe and 28.9 ± 5.4 mg l^{-1} L-Tyr after 48h in the supernatant (Table **3-10**). No 2-PE was detected when single plasmid pFABL was used. In contrast, *E. coli* LJ110 harboring two plasmids pFABL and pJFA10 showed an increased level of 2-PE to 71 ± 5.6 mg l^{-1} and a decreased level of L-Phe (25.4 ± 9.4 mg l^{-1}) compared to *E. coli* LJ110 carrying single plasmid pFABL. These results show that employing the four rate limiting enzymes is feasible for L-Phe and consequently 2-PE production in *E. coli* wild-type. It should be also noted that L-Phe was not accumulated and continuously converted to 2-PE in *E. coli* LJ110 harboring pFABL/pJFA10. To produce L-Tyr and tyrosol more efficiently, plasmid pJNT*aroFBL* was introduced into *E. coli* harboring pJFT or pJFTA10. As shown in Table **3-10**, the wild type *E. coli* harboring pJFT/pJNT*aroFBL* was successfully produced 148.7 ± 9.4 mg l^{-1} L-Tyr along with 18.2 ± 2.9 mg l^{-1} L-Phe over 48h from 4.5 g l^{-1} glucose. In addition, accumulation of 2-PE or tyrosol was not observed in this strain. To produce tyrosol, *E. coli* LJ110 harboring both pJFTA10 and pJNT*aroFBL* were cultured in minimal medium in shakes flasks. This resulted in the production of 128.6 ± 16.9 mg l^{-1} tyrosol within 48 h (Table **3-10**) whereas L-Tyr, L-Phe and 2-PE was not observed during most of the production period. Taken together, by using helper plasmids pFABL or pJNT*aroFBL* encoding the rate limiting enzymes (AroF, AroB and AroL), a positive effect on production of 2-PE/tyrosol was observed.

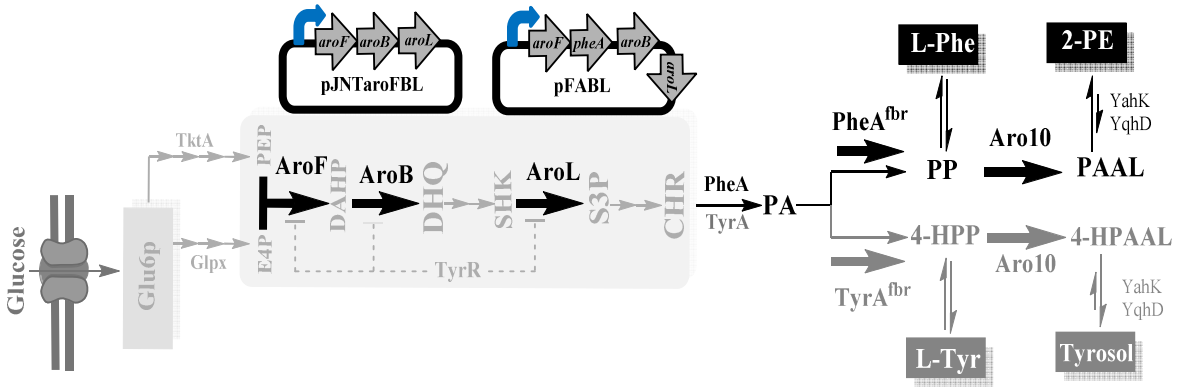

Figure 3-40 Biosynthesis of L-Phe and 2-PE, L-Tyr and tyrosol from glucose in the *E. coli* wild type. Increasing flux toward 2-PE/tyrosol pathway by plasmid overexpression (pFABL or pJNT*aroFBL*) of rate limiting enzymes

Table 3-10 Comparison of 2-PE, tyrosol, L-Phe and L-Tyr production in *E.coli* wild type. *E. coli* wild-type strain containing plasmids pFABL (for L-Phe), pFABL/pJFA10 (for 2-PE), pJFT/pJNT*aroFBL* (for L-Tyr) and pJFTA10/pJNT*aroFBL* (for tyrosol*)* were cultivated in shake flasks with 4.5 g l^{-1} glucose for 48h. After reaching OD600nm~ 0.6, IPTG induction was performed. The final products L-Phe, 2-PE, L-Tyr and tyrosol were analyzed by HPLC. The cultivations were performed in triplicate and mean values are given.

E. coli LJ110	**titer (mg l^{-1})**			
Plasmids	**L-Phe**	**2-PE**	**L-Tyr**	**tyrosol**
pFABL	**142 ± 11.5**	n.d. [a]	28.9 ± 5.4	n.d.
pFABL and pJFA10	25.4 ± 9.4	**71 ± 5.6**	n.d.	n.d.
pJFT and pJNT*aroFBL*	18.2 ± 2.9	n.d.	**148.7 ± 9.4**	n.d.
pJFTA10 and pJNT*aroFBL*	n.d.	n.d.	n.d.	**128.6 ± 16.9**

[a] n.d. stands for Not Detectable.

3.2.4.2 Improving production of 2-PE/tyrosol by combined deletion of competing pathway and negative regulator (*tyrR*)

For further enhancing the carbon flux toward 2-PE production and tyrosol, a more advanced strain FUS4 (Gottlieb et al. 2014) with double auxotrophy (auxotrophic for L-Phe and L-Tyr) was used. This strain lack genes *pheA* and *tyrA*, as these gene products directly compete for the same substrate chorismate. The L-Phe and 2-PE titer was enhanced to 433 ± 34.2 mg l^{-1} (Figure **3-41**(a)) and 247 ± 22.2 mg l^{-1} (Figure **3-41** (b)) after 48 h when the recombinant plasmids pFABL and both pJFA10/pFABL were introduced into *E. coli* FUS4 yielding *E. coli* FUS4 pFABL (Figure **3-41** (a)) and *E. coli* FUS4 pJFA10/pFABL (Figure **3-41** (b)), respectively. This was 3-times higher than the production (142 mg l^{-1} L-Phe and 69 mg l^{-1} 2-PE) from the wild type LJ110 (Table **3-10**). As predicted, the strain expressing pFABL accumulated L-Phe but not 2-PE, whereas the FUS4 pJFA10/pFABL strain significantly accumulated 2-PE, demonstrating sufficient expression of phenylpyruvate decarboxylase (Aro10) involved in 2-PE pathway. In addition, for further improvement of L-Tyr and tyrosol production in *E. coli*, the relevant recombinant plasmids pJFT/pJNT*aroFBL* (for L-Tyr, Figure **3-41** (c)) and pJFTA10 /pJNT*aroFBL* (for tyrosol, Figure **3-41** (d)) were introduced into strain FUS4. Compared to *E.coli* wild-type (Table **3-10**), strain FUS4 was produced 2.5 and 3-times more tyrosine and tyrosol, reaching 396 ± 45.6 mg l^{-1} (Figure **3-41** (d)) and 377 ± 15.1 mg l^{-1} (Figure **3-41** (d)) at 48 hours, respectively. It should also be noted that no 4-HPAAL or 4-HPAA accumulation was observed at any time for tyrosol producer recombinant *E.coli* strain (pJFTA10 /pJNT*aroFBL,* Figure **3-41** (d)), again confirming that sufficient expression of endogenous reductase genes

(*yahK, yghD, yigB* and more than 10 others; (Rodriguez and Atsumi 2014)) involved in tyrosol pathway.

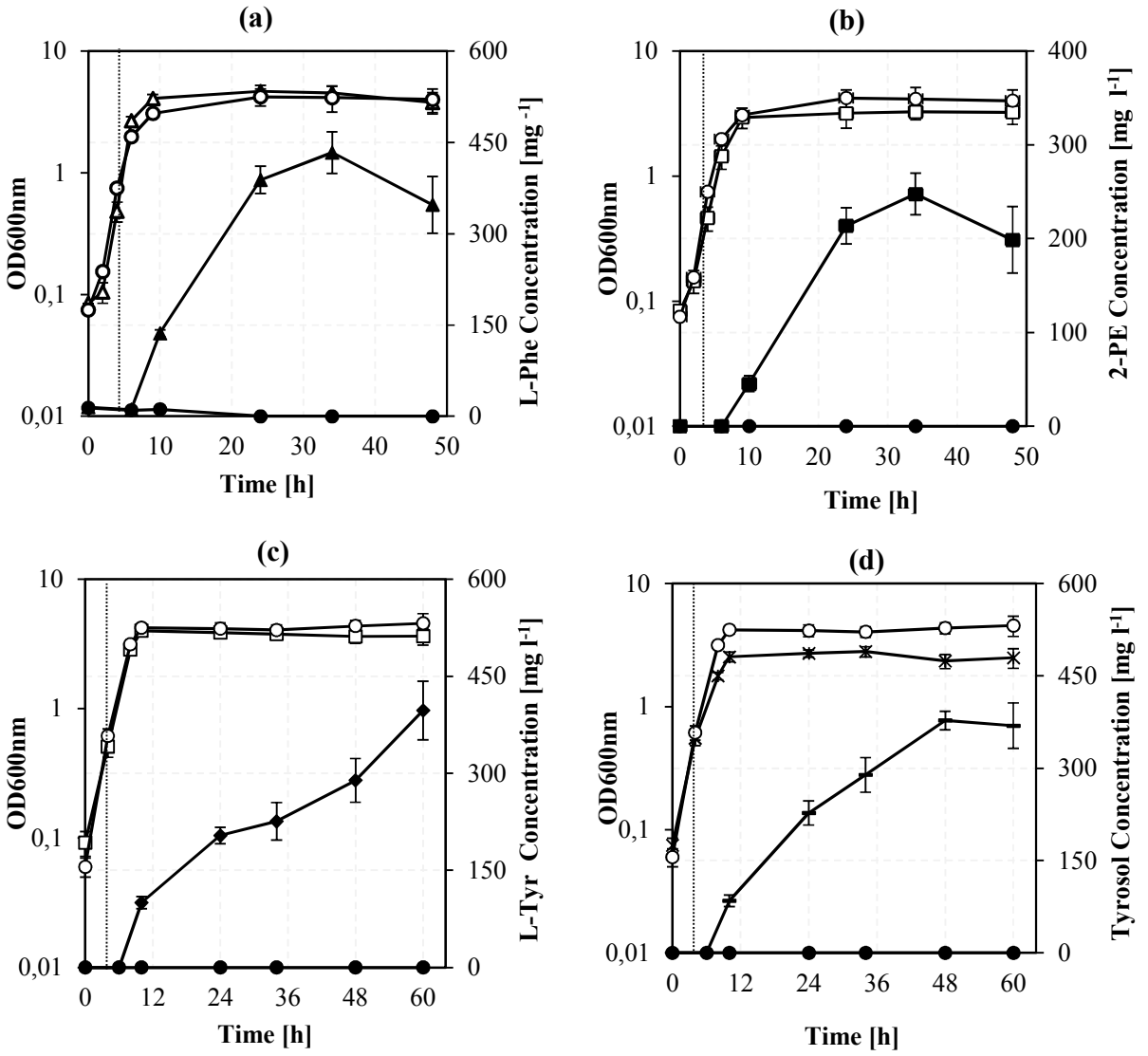

Figure 3-41 Biosynthesis of L-Phe, 2-PE, L-Tyr and tyrosol from glucose in the *E. coli* FUS4. *E. coli* strain containing different recombinant plasmids pFABL (**a**, L-Phe), pFABL/pJFA10 (**b**, 2-PE), pJFT/pJNT*aroFBL* (**c**, L-Tyr) and pJFTA10/pJNT*aroFBL* (**d,** tyrosol*)* were cultivated in shake flasks with 4.5 ± 0.18 g l^{-1} glucose for 60h. All cultivations were performed under aerobic condition (150 rpm) at 37 °C and then shifted to 30 °C after induction. Empty circle (○) represents OD_{600nm} and filled circle (●) represents final products in *E.coli* FUS4 pJF119/pJNT (as control). The final products L-Phe, 2-PE, L-Tyr and tyrosol were analyzed by HPLC. Data shown are means ± standard deviations, calculated from triplicate individual experiments.

One common strategy for enhancement of PP/4-HPP production and subsequently conversation to 2-PE/tyrosol, is reduction of the unwanted byproducts (Sun et al. 2011; Li et al. 2016). Thus, aromatic amino acid aminotransferase encoded by *tyrB* and aspartate aminotransferase encoded by *aspC* were deleted in FUS4 strain to generate FUS4BC strain. Furthermore, in order to eliminate the negative effect of TyrR regulator on expression level of some involved genes in shikimate pathway, gene *tyrR* was deleted in FUS4BC, yielding *E.coli* FUSBCR (described in section 3.1.4.4). The results showed that production of 2-PE was reduced to 90.6 ± 5.6 mg l^{-1} (Figure **3-42** (a)) and 162.2 ± 13.5 mg l^{-1} (Figure **3-42** (b)), likewise the tyrosol production was 253 ± 12.2 mg l^{-1} (Figure **3-42** (c)) and 288.5 ± 15.2 mg l^{-1} (Figure **3-42** (d)) in FUSBC and FUSBCR strain, respectively. Compared to strain FUS4, *E. coli* strain FUSBC and FUSBCR containing recombinant plasmids were produced lower amounts of 2-PE or tyrosol. Moreover, although FUSBC and FUSBCR strains are still efficient for 2-PE/tyrosol production compared to wild type LJ110 (Table **3-10**) even under batch conditions, other genetic improvements might be more suitable for 2-PE/tyrosol production. In both *E.coli* strains FUSBC and FUSBCR, reduced 2-PE/tyrosol production was met with corresponding decreases in both L-Phe/ L-Tyr (data not shown) and growth rate. This result suggested that deletion of two aromatic aminotransferase (*tyrB* and *aspC*) did not help to improve 2-PE/tyrosol production in *E. coli.*

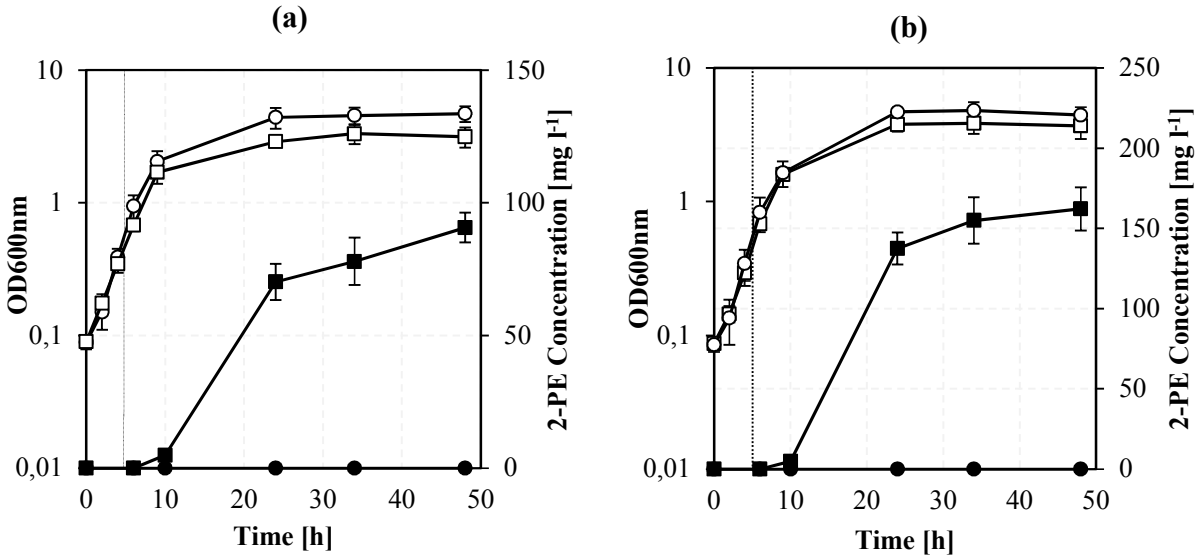

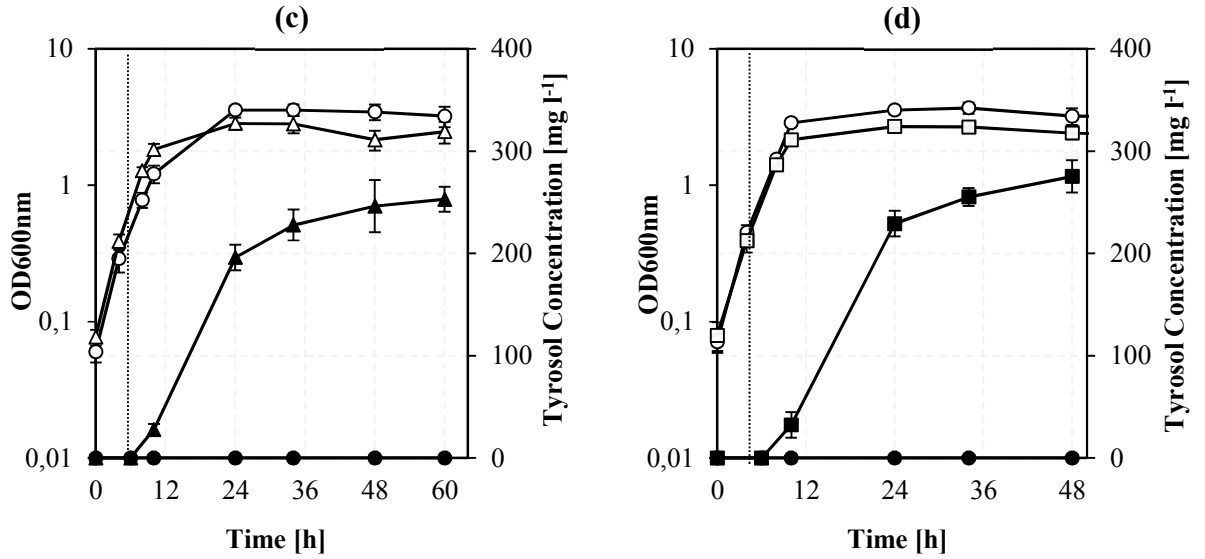

Figure 3-42 Biosynthesis of 2-PE (a and b) and tyrosol (c and d) from glucose in the *E. coli* FUS4BC (a and c) and FUSBCR (b and d). **(a)** Production of 2-PE (■) by *E.coli* FUS4BC pFABL/pJFA10; **(b)** production of 2-PE (■) by *E. coli* FUS4BCR pFABL/pJFA10; **(c)** production of tyrosol (▲) by *E.coli* FUS4BC pJFTA10 /pJNT*aroFBL*; **(d)** production of tyrosol (▲) by *E.coli* FUS4BCR pJFTA10 /pJNT*aroFBL*. Empty circle (○) represents OD_{600nm} and filled circle (●) represents 2-PE/Tyrosol production in *E.coli* FUS4BC or FUSBCR harboring pJF119/pJNT522 (as control). strains containing recombinant plasmids were cultivated in shake flasks with 4.5 ± 0.18 g l^{-1} glucose for 60h and after reaching OD600nm~0.6 the cultures were induced with 0.5 mM IPTG (final concentration). All cultivations were performed under aerobic condition (150 rpm) at 37 °C and then shifted to 30 °C after induction. The final products 2-PE and tyrosol were analyzed by HPLC. Data shown are means ± standard deviations, calculated from triplicate individual experiments.

3.2.4.3 Increasing flux toward 2-PE/tyrosol pathway with an additional chromosomal gene copies of *glpX* and *tktA* in *E.coli* FUS4.7R

To enhance the precursor supply of erythrose-4-phosphate (E4P) for the shikimate pathway the strain *E. coli* FUS4.7R which is already described in section 3.1.4.2 was used. The strain FUS4.7R has an additional copy of *glpX* (fructose-1, 6-bisphosphatase) and *tktA* (transketolase A) (Gottlieb et al. 2014) and *tyrR* (transcriptional regulatory protein TyrR) deletion. To evaluate the 2-PE/tyrosol productivity, *E. coli* FUS4.7R was transformed with plasmids expressing the required genes for biosynthesis of L-Phe or L-Tyr and 2-PE or tyrosol and then batch experiments were performed with 4.5 ± 0.25 g l^{-1} glucose as carbon source in shake flask (Figure **3-43** (a-d)). These modifications (chromosome overexpression of *tktA* and *glpX* / *tyrR* deletion) led to L-Phe and L-Tyr accumulation by 1.5- and 2.2-times more than FUS4 (Figure **3-41** (a and c)), reaching 616 ± 41.2 mg l^{-1} (Figure **3-43** (a)) and 721 ± 48.2 mg l^{-1} (Figure **3-43** (c)) at 48h, respectively.

Likewise, 2-PE and tyrosol production were also increased to 368 ± 25.2 mg l^{-1} (Figure **3-43** (b)) and 437 ± 33.2 mg l^{-1} (Figure **3-43** (d)) on glucose, respectively. Compared to the FUS4 strain (Figure **3-41** (b and d)) cultivated under the same conditions, this is an increase of 49.3% and 20.1 % in 2-PE and tyrosol, respectively.

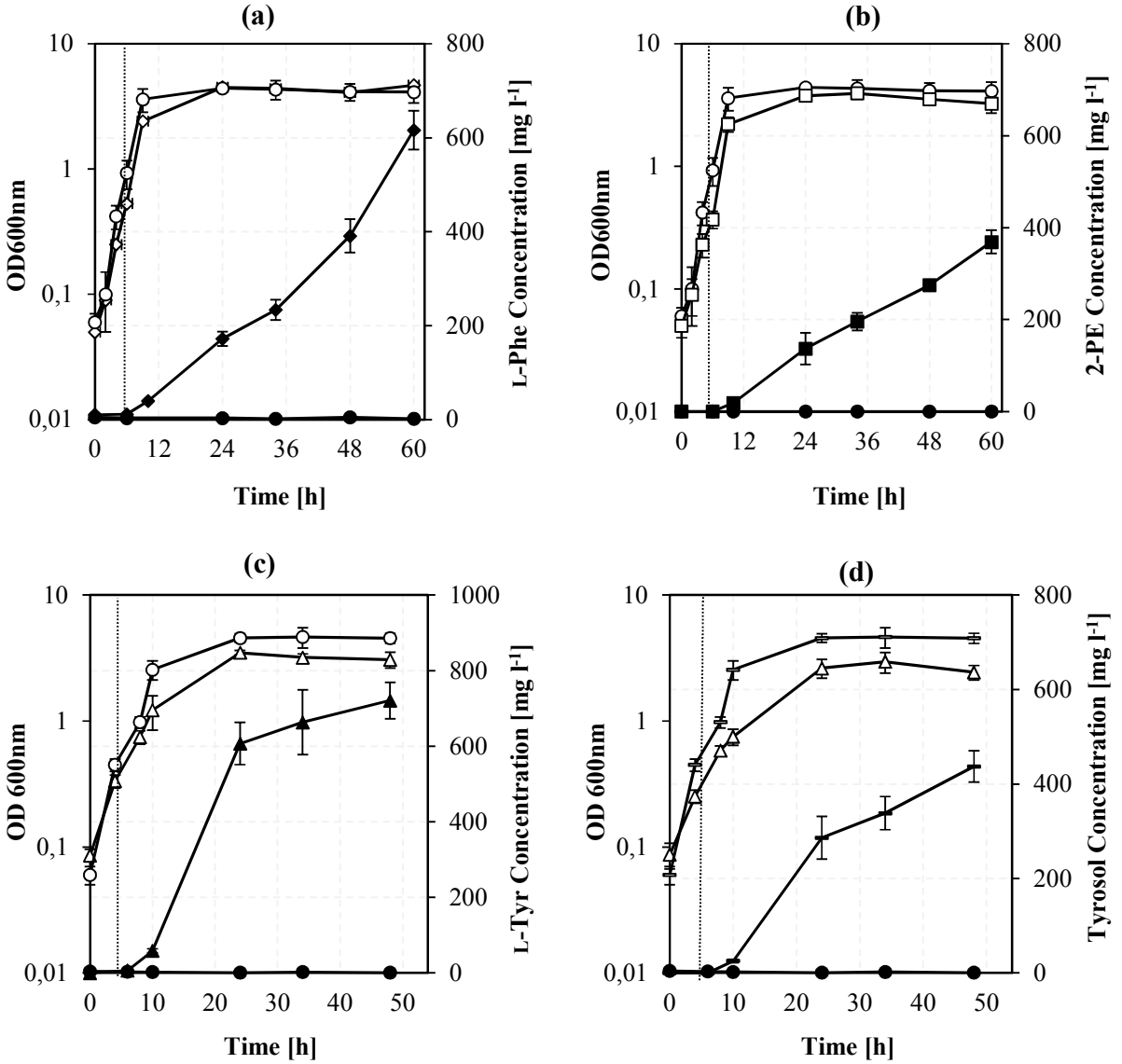

Figure 3-43 Batch cultivations of *E. coli* FUS4.7R for production 2-PE and tyrosol with putatively increased flux through the E4P. Batch cultivation was conducted in minimal medium with 4.5 ± 0.25 g l^{-1} glucose. All cultivations were performed under aerobic condition (150 rpm) at 37 °C and then shifted to 30 °C after induction. Cell growth (empty symbols), L-Phe (♦), 2-PE (■), L-Tyr (▲) and tyrosol (-) concentrations are shown in the diagrams (a-c). **(a)** FUS4.7R/pFABL, **(b)** FUS4.7R/pFABL-pJFA10, **(c)** FUS4.7R/pJFT-pJNT*aroFBL* and **(d)** FUS4.7R/pJFTA10 -pJNT*aroFBL*. Empty circle (○) represents OD_{600nm} and filled circle (●) represents final products in *E. coli* FUS4.7R harboring pJF119/pJNT522 (as

control). The final products L-Phe, 2-PE, L-Tyr and tyrosol were analyzed by HPLC. Data shown are means ± standard deviations, calculated from triplicate individual experiments.

It is worth mentioning that the additional chromosomal expression of *tktA* and *glpX* genes together with the deletion of negative regulator (*tyrR*) may potentially increase carbon flux to production of 2-PE/tyrosol. The fed batch cultivation might also result in 2-PE/tyrosol production in the g/l range. Therefore, the *E. coli* FUS4.7R pFABL (Figure **3-43** (a)) and *E. coli* FUS4.7R pJFA10/pFABL (Figure **3-43** (b)), which produced L-Phe and 2-PE most efficiently on a favorable carbon source, respectively, were considered for fed batch cultivation (see section 3.2.5). In addition, *E. coli* FUS4.7R pJFT/pJNT*aroFBL* (Figure **3-43** (c)) and *E. coli* FUS4.7R pJFTA10/pJNT*aroFBL* (Figure **3-43** (d)) which produced L-Tyr and tyrosol most efficiently on glucose, respectively, were selected for fed batch cultivation (see section 3.2.5).

3.2.5 Glucose-limited fed-batch cultivation of engineered *E.coli* FUS4.7R for production of 2-PE and tyrosol

In order to overcome the carbon limitation which is considered as the major limitation of batch cultivation, hence, fed-batch cultivation was performed as alternative cultivation process. *E. coli* FUS4.7R was used as the best titer 2-PE/tyrosol in batch cultivation (Figure 3-42 (b and d)) was obtained. The fed batch medium contained initially 4.5 g l^{-1} glucose, 0.04 mg l^{-1} L-Phe and L-Tyr. Cell growth, L-Phe, L-Tyr, 2-PE, tyrosol as well as glucose concentrations were measured periodically (Figuure 3-44). Glucose was added to the medium every 12h during the cultivation to maintain cell growth and target production. After 96 h of cultivation, 25.5 g l^{-1} glucose was consumed and a titer of 4.97 ± 0.38 g l^{-1} L-Phe (Figure 3-44 (a)) and 1.75 ± 0.12 g l^{-1} 2-PE (Figuure 3-44 (b)) was reached with *E. coli* FUS4.7R/pFABL and *E. coli* FUS4.7R pFABL/pJFA10, respectively. In addition, to investigate whether fed batch cultivation would have a beneficial effect on L-Tyr and tyrosol production, a similar fed batch strategy was applied by FUS4.7R as best candidate strain. The fed batch results using strain FUS4.7R pJFTA10 /pJNT*aroFBL* (for tyrosol) showed an increase in tyrosol production to 1.68 ± 0.19 g l^{-1} (Figure 3-44 (d)). The *E. coli* FUS4.7R harboring pJFT and pJNT*aroFBL* strain (for L-Tyr) was then cultured in minimal medium in shake flask, showed a maximal concentration of 4.7 ± 0.11 g l^{-1} (Figuure 3-44 (c)) on glucose as carbon source. Overall, 34.4 g l^{-1} glucose for L-Ty and 25.7 g l^{-1} glucose for tyrosol production were consumed in the fed batch cultivation and the final yield and

volumetric productivity 0.13 g g^{-1} and 0.032 g l^{-1} h^{-1} for L-Tyr and 0.065 g g^{-1} and 0.014 g l^{-1} h^{-1} for tyrosol were obtained. Although the obtained titer of 2-PE/tyrosol (1.75 ± 0.12 g l^{-1} 2-PE and 1.68 ± 0.19 g l^{-1} tyrosol) in this study are relatively higher than the obtained yield in the previous reports in *E.coli* (Koma et al. 2012; Kang et al. 2014), further optimizations including fed-batch cultivation methods combine with ISPR (*in-situ* product removal) techniques (Etschmann et al. 2002; Etschmann and Schrader 2006) would be an alternative method to consider for further enhancement of 2-PE/tyrosol titer (see section 3.2.6).

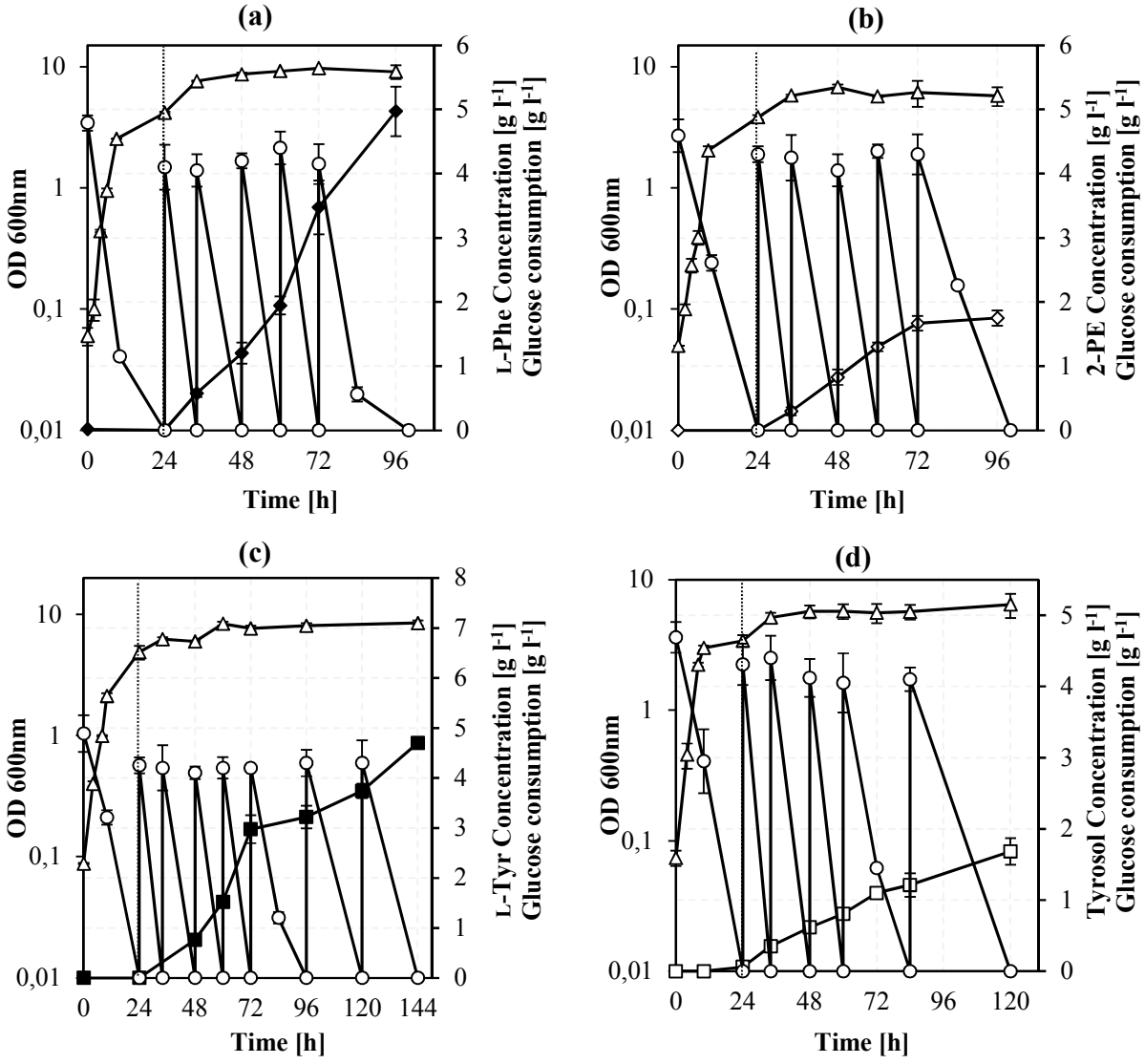

Figure 3-44 Time course analyses of glucose fed-batch production L-Phe **(a)**, 2-PE **(b)**, L-Tyr **(c)** and tyrosol **(d)** by the constructed *E. coli* FUS4.7R strain. Glucose fed batch cultivation was carried out on a rotary shaker with 150 rpm at 37°C with 4.5 g l^{-1} glucose as carbon source. After 24h of cultivation the

cultures were induced with 0.5 mM IPTG (spotted dotted line) and the shaking flasks were transferred from 37°C to 30°C before giving pulses of ~ 4.5 g l^{-1} of glucose every 12h. The respective symbols represent as follows: ♦, L-Phe production in *E. coli* FUS4.7R pFABL; ◊, 2-PE production in *E. coli* FUS4.7R pJFA10/pFABL; ■, L-Tyr production in *E. coli* FUS4.7R pJFT/pJNTaroFBL; □, tyrosol production in *E. coli* FUS4.7R pJFTA10 /pJNT*aroFBL*; Δ, OD600nm and ○, glucose consumption. Data shown are means ± standard deviations, calculated from triplicate individual experiments.

3.2.6 Two-phase fed batch cultivation of *E. coli FUS4.7R* for 2PE/tyrosol enhancement

It has been demonstrated that the most important factors limiting the 2-PE/tyrosol production is high product toxicity (Etschmann and Schrader 2006; Kang et al. 2014). Thus, 2-PE/tyrosol toxicity was investigated in *E. coli* wild type LJ110 in minimal medium with different exogenous concentration of 2-PE or tyrosol. Cells exposed to 5 mM 2-PE or tyrosol (equivalent to 0.61 g l^{-1} 2-PE or to 0.7 g l^{-1} tyrosol), no cell growth inhibition was observed. Cells were still able to grow in the presence of 10 mM 2-PE or tyrosol (equivalent to 1.21 g l^{-1} 2-PE or 1.38 g l^{-1} tyrosol), even though the growth rate was relatively affected by this concentration. However, 15 mM 2-PE (Figure **3-45** (a)) or tyrosol (Figure **3-45** (b)) remarkably inhibited cell growth compared to control. Eventually was completely inhibited when concentration of 2-PE or tyrosol increased to 20 mM (2.4 g l^{-1} 2-PE (Figure **3-45** (a)) and 2.7 g l^{-1} tyrosol (Figure **3-45** (b)), which is compatible with the observations of other studies (Kang et al. 2014; Li et al. 2018). These results suggest that *E. coli* wild type LJ110 can tolerate at least 10-15 mM 2-PE or tyrosol. Thus, 1.75 g l^{-1} 2-PE or 1.68 g l^{-1} tyrosol is in the toxicity range that possibly limits the 2-PE/tyrosol production in fed batch cultures (Figure **3-44** (b and d)), which would be overcome by employing ISPR techniques (Figure **3-45** (c)).

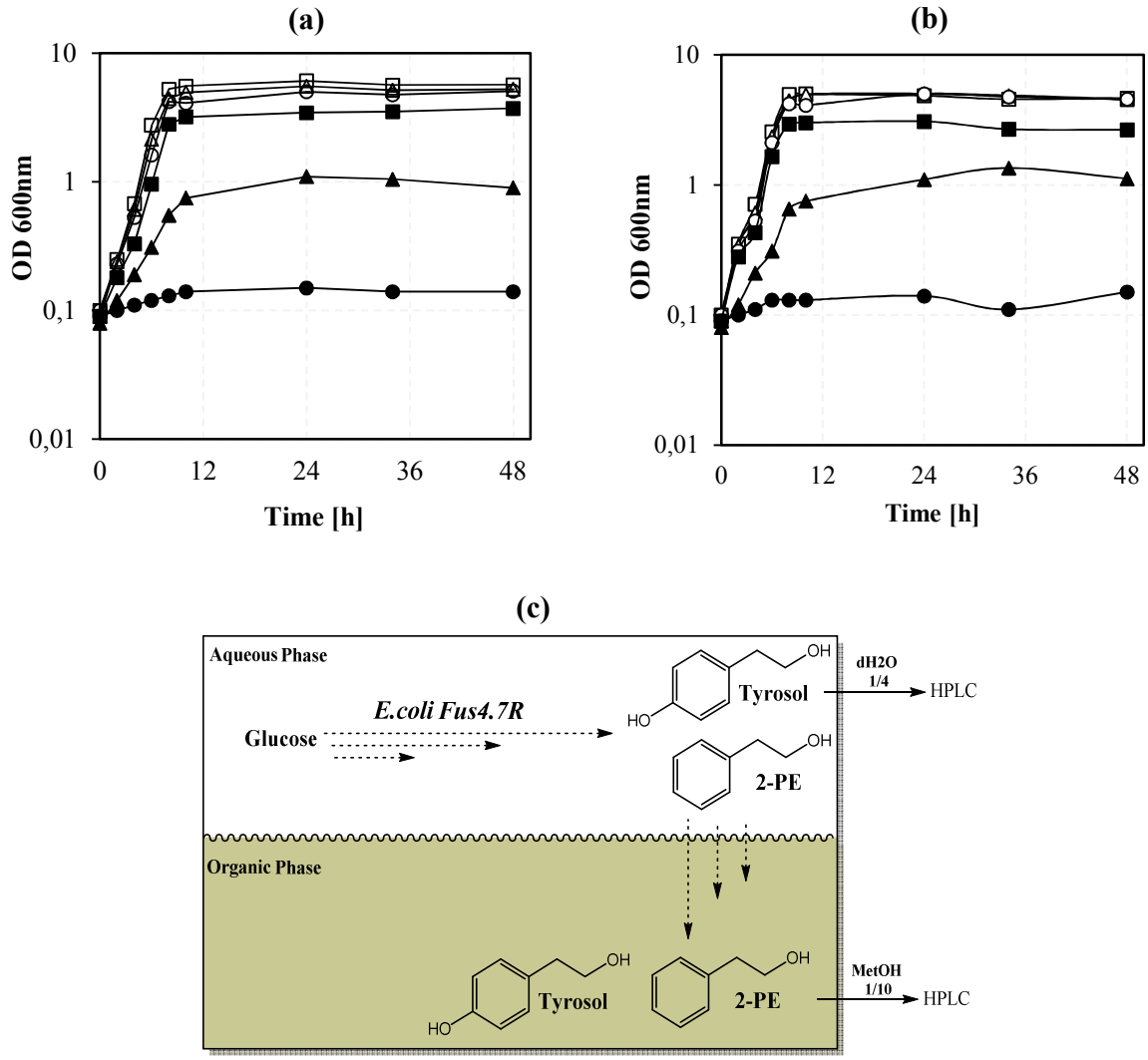

Figure 3-45 Toxicity effects of 2-PE **(a)** and tyrosol **(b)** on the growth of *E. coli* LJ110 (as genetic background) as measured by OD_{600nm}. **(c)** Schematic represents mechanism of two phase extraction of 2-PE and tyrosol from *E.coli* culture broth. The growth of the bacterial culture was determined by measuring the OD_{600nm} at 2, 4, 6, 8, 10, 24, 34 and 48h after inoculation. The concentrations of 2-PE/tyrosol were added to the medium as follows: 0 mM (control, □); 2.5 mM (Δ); 5 mM (○); 10 mM (■); 15 mM (▲) and 20 mM (●).The cultivations were performed duplicate and the mean values are given.

The ISPR (*in-situ* product removal) technique was applied to relieve the problem of 2-PE/tyrosol toxicity. The most commonly used technique among ISPR techniques for 2-PE/tyrosol production is two-phase extraction (Hua and Xu 2011; Li et al. 2018). Hence, three organic solvents including dodecane (data not shown), polypropylene glycol 1200 (PPG1200) (Etschmann and Schrader 2006) and tributyrin (Kim et al. 2014b) as in situ extractants were tested for their extractive capacities (Etschmann and Schrader 2006; Kim et al. 2014a; Kim et al.

2014b; Miao et al. 2015). It should also be noted that organic solvents with log P values lower than 4 were considered extremely toxic due to high degree of accumulation of the solvent in the membrane (Sardessa and Bhosle 2002; Zhang et al. 2015). Thus, only organic solvents with log P values higher than 4 should be considered. Hence, to achieve higher 2-PE/tyrosol production, two-phase fed batch cultivation of *E. coli* FUS4.7R pJFA10/pFABL (for 2-PE, Table **3-11**) and *E. coli* FUS4.7R pJFTA10/pJNT*aroFBL* (for tyrosol, Table **3-12**) strains were performed with different concentration of organic solvents on glucose as carbon source in the shake flasks. After 146h of cultivation, total 26.2 g l^{-1} glucose for 2-PE and 25.6 g l^{-1} glucose for tyrosol was consumed and 2-PE or tyrosol with good yield and productivity was accumulated. Results from two-phase extraction experiments indicated that PPG 1200 and tributyrin have the highest extractive capacity (most of target product was extracted in organic phase, Table **3-11** and Table **3-12**), also no negative effect on cell growth was observed, suggesting that these solvents are not toxic to the *E. coli* cell and are more efficient for obtaining higher 2-PE/tyrosol production in the fed batch cultures. Furthermore, different concentrations of tributyrin and PPG 1200 (10, 30, 40 and 50%, Table **3-11** and Table **3-12**) were tested in order to find the best concentration of the solvents for enhanced production of 2-PE/tyrosol. As shown in Table **3-11**, 10% tributyrin raised the 2-PE concentration in the organic phase to 5.5 g l^{-1}, whereas 2-PE final titer (~1.3 g l^{-1}) was still less than 2-PE titer in the single phase (Figure **3-44** (b)). The best effect of the tributyrin for 2-PE extraction on the concentration of 30% was obtained where 2-PE concentration in the organic phase reached 4.2 g l^{-1} and 2-PE titer in both phase nearly reached 2.1 g l^{-1} (Table **3-11**). Also, by utilization of 40 or 50% tributyrin, the 2-PE concentration in the both aqueous and organic phase as well as 2-PE titer sharply decreased (Table **3-11**). In contrast, the best positive effect of the tributyrin on tyrosol accumulation was obtained at 50 % tributyrin with final titer reached 2.5 g l^{-1} (Table **3-12**), which is 1.5-times more than tyrosol produced in the single phase (Figure **3-44** (d)). As shown in Table **3-12**, 10% and 40% tributyrin also increased the tyrosol accumulation to 2 and 2.3 g l^{-1}, respectively. In addition, 2-PE and tyrosol concentration in the organic phase reached its highest concentration of approx. 5.9 g l^{-1} (Table **3-11**) and 3.89 g l^{-1} (Table **3-12**) in 10% PPG 1200, respectively, but final 2-PE (1.1 g l^{-1}) and tyrosol (2.1 g l^{-1}) titer was still low due to the low volume of the organic phase.

Table 3-11 Single and two phase fed-batch cultivation of *E.coli* FUS4.7R harboring pJFA10 and pFABL plasmids in different concentration of organic solvents for enhance production of 2-PE.

	organic solvents	Organic phase concentration (%)	2-PE in organic phase (g l^{-1})[a]	2-PE in aqueous phase (g l^{-1})[a]	Titer (g $^{l-1}$)	Yield (g g^{-1} glucose)
Single phase (fed- batch)	-	0	0	1.75	1.75	0.07
Two phase (fed- batch)	tributyrin	10	5.49 ± 0.15	0.69 ± 0.04	1.30	0.05
		30	4.21 ± 0.21	0.265 ± 0.05	2.01	0.08
		40	0.81 ± 0.13	0.01 ± 0.00	0.55	0.02
		50	0.79 ± 0.08	0.10 ± 0.02	0.80	0.03
	PPG 1200	10	5.89± 0.17	0.46 ± 0.06	1.11	0.04
		30	5.44± 0.10	0.24 ± 0.03	2.57	0.1
		40	3.49± 0.21	0.10 ± 0.01	2.42	0.09
		50	2.39± 0.11	0.07 ± 0.01	2.46	0.09

[a,] phase between aqueous culture media, and organic phase was separated by centrifugation and the 2-PE concentrations was determined in each phase separately. 2-PE content in aqueous phase was analyzed directly by HPLC, organic phase was further diluted with MetOH (1:10) and then analyzed by HPLC. Data shown are means ± standard deviations, calculated from triplicate individual experiments.

Table 3-12 Single and two phase fed-batch cultivation of *E.coli* FUS4.7R harboring pJFA10T and pJNT*aroFBL* plasmids in different concentration of organic solvents for enhance production of tyrosol.

	Organic solvents	Organic phase Concentration (%)	tyrosol in organic phase (g l^{-1})[a]	tyrosol in aqueous phase (g l^{-1})[a]	Titer (g l^{-1})	Yield (g g $^{-1}$ glucose)
Single phase (fed- batch)	-	0	0	1.68	1.68	0.07
Two phase (fed- batch)	tributyrin	30	1.13 ± 0.07	1.51 ± 0.03	2	0.08
		40	1.14 ± 0.04	1.58 ± 0.09	2.34	0.10
		50	0.97 ± 0.06	1.57 ± 0.12	2.54	0.10
	PPG 1200	10	3.89 ± 0.17	1.68 ± 0.04	2.1	0.08
		30	3.81 ± 0.26	1.35 ± 0.01	3	0.12
		40	2.93 ± 0.15	0.57 ± 0.05	2.52	0.10
		50	1.96 ± 0.19	0.49 ± 0.07	2.44	0.10

[a,] phase between aqueous culture media, and organic phase was separated by centrifugation and the tyrosol concentrations was determined in each phase separately. 2-PE content in aqueous phase was analyzed directly by HPLC, organic phase was further diluted with MetOH (1:10) and then analyzed by HPLC. The data are averages of triplicate cultures. Data shown are means ± standard deviations, calculated from triplicate individual experiments.

By increasing the concentration of PPG 1200 to 30%, total 2-PE and tyrosol concentration reached 2.57 g l^{-1} **(**Table **3-11)** and 3 g l^{-1} (Table **3-12**) in both phase, respectively. These results indicated that 30 % PPG 1200 has the highest extractive capacity for improving production of 2-PE (Table **3-11**) as well as tyrosol (Table **3-12**), resulting in 47 and 78 % improvement of total 2-

PE and tyrosol production, with the ratio of 2-PE and tyrosol titer in the organic phase to aqueous phase of 22:1 and 2.8:1, respectively.

3.2.7 2-PE /tyrosol production in a laboratory scale bioreactor

From the above results, PPG 1200 (30%) was chosen for two phase fed-batch fermentation due to its high extraction capacity for 2-PE/tyrosol production in *E.coli* (Table **3-11** and Table **3-12**). Therefore, based on two phase cultivation carried out in shaking flask, higher 2-PE/tyrosol production was performed in a benchtop bioreactor system (0.5 l, working volume) with pH controlled at 7.0 according to the procedure described in section 2.6.4.3. *E. coli* FUS4.7R pJFA10/pFABL (for 2-PE) and *E. coli* FUS4.7R pJFTA10/pJNT*aroFBL* (for tyrosol) strain cultivated in a two-phase fed batch fermentation process in a 0.5 L fermenter containing 175 ml of minimal medium. Cell growth, pH, glucose and 2-PE/tyrosol concentrations were measured periodically (within 96 h cultivation). After initial glucose (~ 5 g l^{-1}) consumption in the batch phase (red dotted line) the culture was induced with IPTG (0.5mM, final conc.) and additional L-Phe, L-Tyr, glucose and ammonia feeding were started (See section 2.6.4.3). As shown in Figure **3-46** (a), *E. coli* FUS4.7R pJFA10/pFABL (for 2-PE) consumed the initial 5.1 g l^{-1} glucose in less than 10 h and OD_{600nm} exponentially reached 4.1 within 9.9h (red dotted line) and began to slow down thereafter. Subsequently, when 75 ml (30%) of PPG 1200 were added to the fermenter, 2-PE began to accumulate in organic phase and reached 6.1 g l^{-1} at the end fermentation process. On the other hand, the 2-PE concentration in the culture broth was maintained below 0.5 g l^{-1} throughout the fed-batch fermentation, suggesting that extraction of 2-PE by PPG 1200 was very effective (below toxicity level of 2-PE, Figure **3-46** (a)). After 96 h, a total of 41.4 g glucose was consumed and the final titer, yield and productivity of 2-PE were 3.1 g l^{-1}, 0.07 g g^{-1} glucose, and 0.03 g l^{-1} h^{-1}, respectively (Figure **3-46** (a)). Similarity in tyrosol production, initial glucose 4.9 g l^{-1} consumed in less than 10 h (red dotted line) and OD_{600nm} exponentially increased to 5.2 within 9.9h and then, unlike 2-PE, cell growth began to increase up to OD_{600nm} ~19. Subsequently, when the volume of fermentation culture was increased with 75ml (30%) of PPG 1200, the tyrosol concentration in the organic phase began to accumulate 5.6 g l^{-1}, while the tyrosol concentration in the culture broth was maintained below toxicity level around 1.2 g l^{-1} (Figure **3-46** (b)). A total of 43.5 g glucose was consumed in 96 h and the final titer, yield and volumetric productivity of tyrosol were 3.6 g l^{-1}, 0.08 g g^{-1} glucose, and 0.04 g l^{-1}

h^{-1}, respectively (Figure **3-46** (b). However, compared with shake flask under the same two-phase culture conditions, fermentation results showed an increase in 2-PE/tyrosol production but further optimization would be necessary.

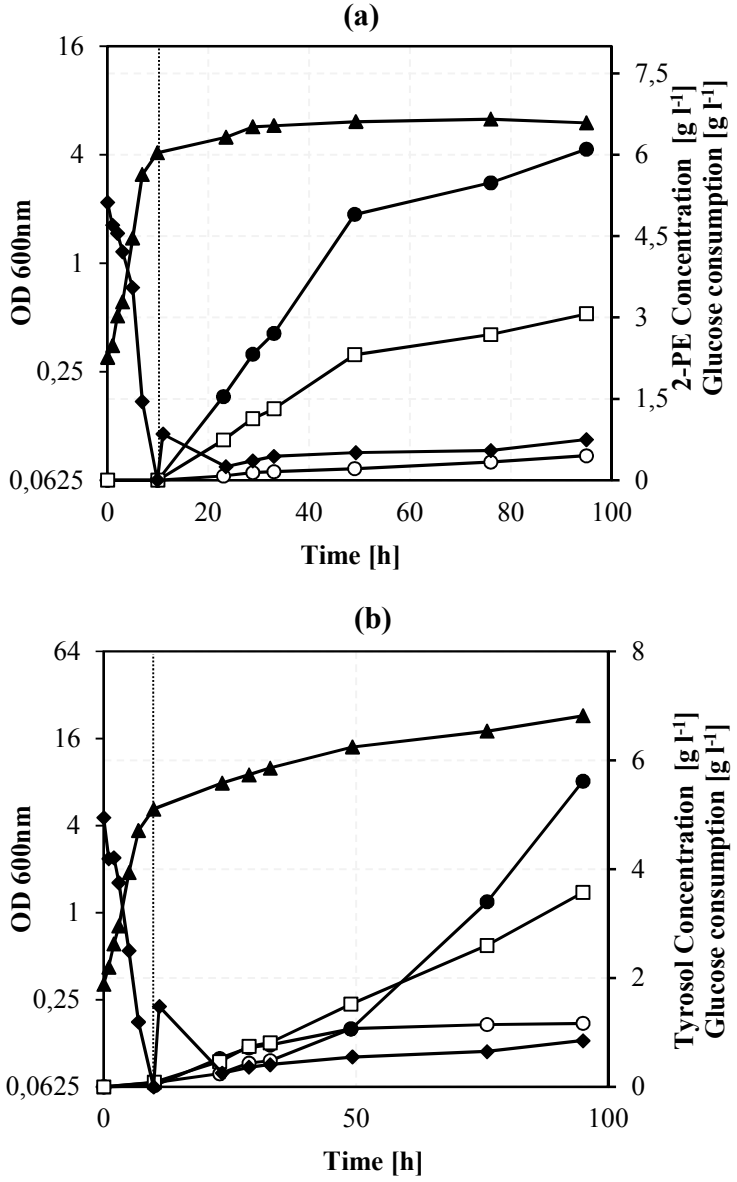

Figure 3-46 Two phase fed batch fermentation of *E. coli* for 2-PE **(a)** and tyrosol **(b)** production. *E.coli* FUS4.7R pJFA10/pFABL (**a,** 2-PE) and *E.coli* FUS4.7R pJFTA10/pJNT*aroFBL* (**b,** tyrosol) were grown in a batch culture in the bioreactor for 9.9 h at 37 °C, and then shifted to 30 °C followed by addition 30% PPG 1200 (75ml) as organic solvent. The glucose feed started after 9.9 h (red dotted line, first pulse of L-Phe and L-Tyr, IPTG induction) and the fed was adjusted to maintain a concentration of 0.4-1.0 g l^{-1}. Symbols represents as following: OD600nm (▲), glucose consumption (g l^{-1}, ♦), 2-PE or tyrosol in aqueous phase (g l^{-1}, ○), 2-PE or tyrosol in organic phase (g l^{-1}, ●) and 2-PE or tyrosol in total (g l^{-1}, □). The result of one fermentation is presented.

3.2.8 Isolation of 2-PE/tyrosol from culture broth (Downstream processing)

In order to isolate 2-PE and tyrosol from fermentation culture broth, a liquid–liquid extraction method with ethyl acetate (Chreptowicz et al. 2016) according to the procedure described in section 2.8.2 was applied. It has previously been reported that ethyl acetate has good property to separate 2-PE from culture broth, which showed that 2-PE can be obtained in the organic phase (Chreptowicz et al. 2016). However, because of the similar properties of 2-PE and tyrosol, similar method was used to extract tyrosol from culture broth. For this purpose, culture broths containing 2-PE or tyrosol were separated following to the procedure described in Section 2.8.2. As shown in Figure 3-47 (a) and Figure 3-48 (a), efficient amount of 2-PE or tyrosol can be extracted after the third extraction stages with ethyl acetate, respectively. After distillation the HPLC chromatographic analysis confirmed the presence of 2-PE (Figure 3-47 (a)) or tyrosol (Figure 3-48 (a)) together with some impurities (labeled with black arrow) in extraction liquid, which could possibly be the other intermediate compounds in biosynthetic pathway.

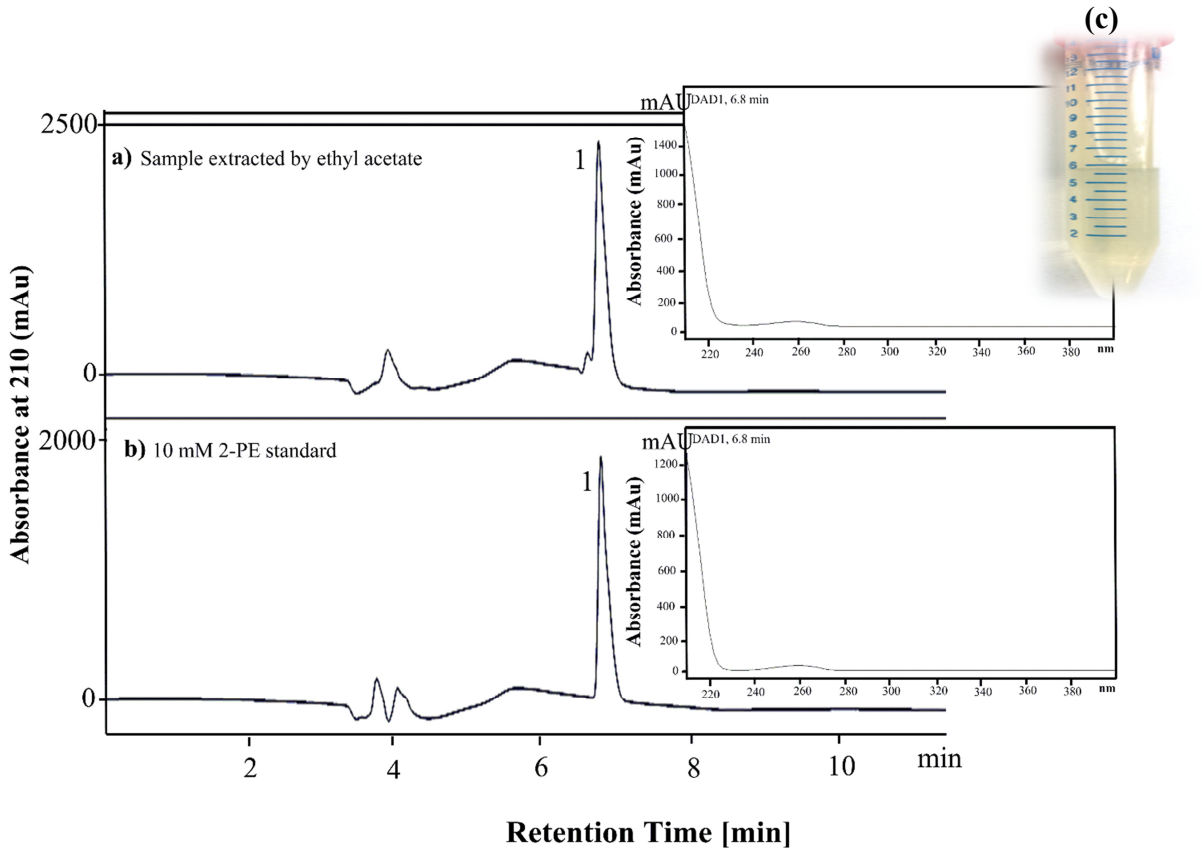

Figure 3-47 Reversed phase HPLC chromatograms obtained from sample extracted by ethyl acetate **(a)** and 10mM 2-PE commercial standard **(b). (c)** Condensed 2-PE from extraction by ethyl acetate. Peak identified as 1: 2-PE. Absorption maximum at 210 nm; plotted as absorbance unit [mAU] versus time [min]. The HPLC system was equipped with a symmetry C18 silica column (Lichrospher 100 RP, 250 mm× 4 mm, chromatography service GmbH) and a UV detector operating at a wavelength of 210 nm. The column was eluted with a gradient method at a flow rate of 0.4 ml min^{-1}.

This resulted in efficiency and purity of 69.6% and ≥ 81 % for 2-PE and 50.3% and ≥71% for tyrosol (base on HPLC), respectively. As expected, extracted 2-PE (Figure 3-47 (a)) and tyrosol (Figure 3-48 (a)) showed same retention behavior as the commercially standard (Figure 3-47 (b) for 2-PE and Figure 3-48 (b) for tyrosol) in the HPLC analysis. 2-PE end product extracted is a light yellow liquid with a pleasant odor (Figure 3-47 (c)) and tyrosol end product is a liquid with ocher color (Figure 3-48 (c)).

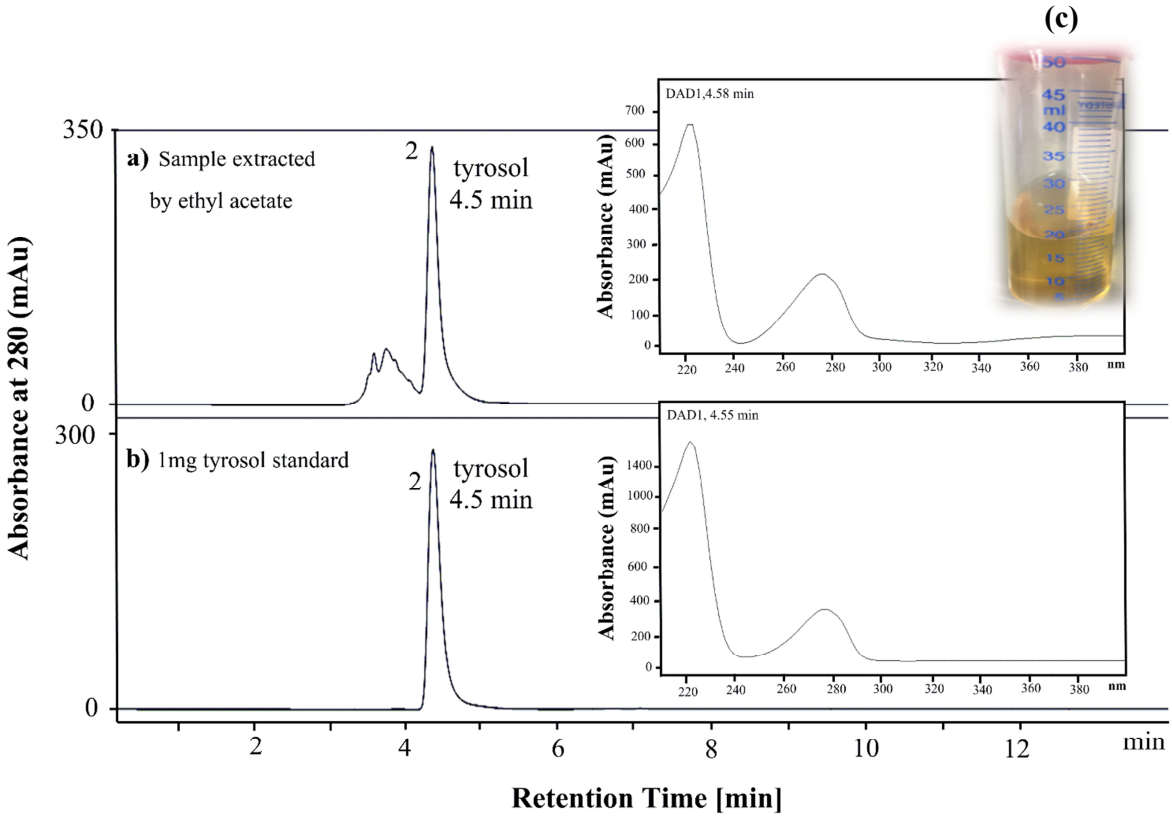

Figure 3-48 Reversed phase HPLC chromatograms obtained from sample extracted by ethyl acetate **(a)** and 1mg tyrosol commercial standard **(b). (c)** Condensed tyrosol from extraction by ethyl acetate. Peak identified as 2: tyrosol. Absorption maximum at 280 nm; plotted as absorbance unit [mAU] versus time [min]. The HPLC system was equipped with a symmetry C18 silica column (Lichrospher 100 RP, 250 mm× 4 mm, chromatography service GmbH) and a UV detector operating at a wavelength of 280 nm. The column was eluted with a gradient method at a flow rate of 0.4 ml min^{-1}.

4. Discussion

4.1 Part I: Biosynthesis of Aromatic Amines (AAs)

In the first part of this thesis, microbial production of three valuable AAs by metabolic grafting" of *Escherichia coli* was investigated. Currently, most of these plastic monomers (AAs) are commercially produced from petroleum-derived benzene via *para*-nitrobenzene or *para*-nitrotoluene (Mattocks and Hartung 1946; Schul'tsev 2011; Jobdevairakkam and Velladurai 2013). Since the chemical synthesis process is not an environmentally friendly process, thus microbial biosynthesis of these monomers from renewable resources can be an alternative to chemical synthesis (Fujita et al. 2013; Kawaguchi et al. 2017). This microbial production approach has created a 'green process' not only for L-PAPA, as the most important AA monomer, but also for other aromatic amines (AAs) e.g., PAPE and 4-APA as bio-monomers for bioplastic production (Tsuge et al. 2016; Kawasaki et al. 2018). The microbial production of these valuable AAs has been particularly poorly studied, especially regarding to the production of small amounts of these compounds. Most of the research carried out so far has investigated microbial production of these compounds from glucose as carbon source (Mehl et al. 2003; Masuo et al. 2016; Tateyama et al. 2016). In this work, for the first time, it was shown that L-PAPA can be efficiently produced from glycerol by *E. coli* with a combination of genetic engineering and cultivation condition. In another effort, for the first time, a scalable approach was established for high-titer production of PAPE and 4-APA from cost-effective substrate (glucose). Also, various metabolic grafting approaches were employed to improve the existing process for the production of AAs with recombinant *E.coli*. Further attempts were also made for scaling-up from laboratory to pilot scale. In addition, a valuable method with new extractants has been designed to separate L-PAPA with good isolated yield and purity (Konishi et al. 2016). These findings provide new information and are superior compared to previous studies. Previous studies (Mehl et al. 2003; Masuo et al. 2016; Tateyama et al. 2016) have especially focused on genetic engineering, such as codon optimization, different copy number of plasmid, etc., but have not provided detailed information about recombinant protein expression, enzyme activity, possible bottlenecks, product susceptibility and product purification and identification

(Table **4-1**). In the present study, all these aspects as well as large-scale production and downstream processing were addressed and investigated.

4.1.1 Construction of platform strain for biosynthesis of L-PAPA

In order to enable efficient production of aromatic amines (AA) from simple carbon sources, an *E.coli* platform strain was established. A "platform strain" is a production chassis that well-modified and improved by applying metabolic engineering strategies (genetic engineering, modeling and characterizing flux) to produce large amounts of target compounds from cost effective substrate for research or industrial uses (Woodruff et al. 2013; Matsumoto and Tanaka 2017). In the present study, a three-step artificial L-PAPA pathway (Figure **1-8**) was constructed based on some parts of chloramphenicol biosynthesis pathway in *Streptomyces venezuelae* (Brown et al. 1996; Chang et al. 2001; He et al. 2001). In the mid-1980's, before discovering chloramphenicol biosynthesis pathway in *Streptomyces sp.* (Brown et al. 1996; Blanc et al. 1997). Teng et al. (1985) suggested that L-PAPA is delivered from chorismic via ADC and then directed towards the biosynthesis of pABA. The first step in L-PAPA biosynthesis (Figure **1-5**) is conversion of chorismic acid and glutamine (or NH_4) into ADC and glutamate (or NH_3) (Teng et al. 1985). It has been previously reported that the conversion of chorismic acid to ADC is catalyzed by PabA and PabB which reside in the *E. coli* chromosome (Kaplan and Nichols 1983; Goncharoff and Nichols 1984; Nichols et al. 1989; Green and Nichols 1991; Viswanathan et al. 1995). A single enzyme PapA from *Streptomyces venezuelae* with amino acid sequence homology to both PabA and PabB was also identified (Brown et al. 1996; Chang et al. 2001; He et al. 2001; Stolz et al. 2007). It was reported that DNA sequence of PapA from *Streptomyces venezuelae* has many rare codons (over 100 rare amino acid codons) and is GC-rich (73% GC) (Wright and Bibb 1992; Brown et al. 1996). Therefore, expression of *papA* gene may result in protein expression limitations when expressed in *E.coli*. Based on a previous observation (Kozak 2006), $PapB_{S.ven}$ is not well suited for the microbial conversion of chorismic acid into ADC in *E.coli*. It was shown that *pabAB* gene from folate biosynthetic pathway in *Corynebacterium glutamicum*, containing 24 rare codons in total (Stolz et al. 2007; Kubota et al. 2016), was far better suited for expression in *E. coli* (Kozak 2006). Since the two recombinant enzymes $PabA/PabB_{E.coli}$ and $PapA_{S.ven}$ failed to efficiently convert chorismic acid into ADC, therefore, $PabAB_{C.gl}$ on a described vector pC53 (Kozak 2006) was chosen in this study. The genes *pabAB* and codon optimized genes of *papB* and *papC* from *Streptomyces venezuelae* were combined in

an artificial plasmid-based operon (pC53BC). In vitro analysis by HPLC and LC-MS showed formation of PAPA by heterologous expression of these three genes in *E.coli* LJ110 pC53BC (Figure **3-5**, b, c and d). The last step apparently is catalyzed by endogenous aminotransferase (Figure **3-5** (a)); this led to formation of 43± 2 mg l^{-1} L-PAPA in the recombinant *E.coli* (Figure **3-5** (b)). Also, no accumulation of the APP intermediate was observed (Figure **3-5**, b), presumably due to the instability of APP, which was shown for ADC and ADP as well (Teng et al. 1985; Wubbolts et al. 2005). Production of L-PAPA from recombinant *E.coli* and the lack of accumulation of the APP intermediate suggest that the APP intermediate is presumably transaminated by the aminotransferases, indicating proper function of the endogenous aminotransferases. In *E. coli* several aminotransferases are described (*aspC, tyrB, ilvE, avtA*) that catalyze the terminal steps in amino acid biosynthesis (Fotheringham et al. 1986; Inoue et al. 1988; Pittard 1996). Two main aminotransferases *aspC* (aspartate aminotransferase) and *tyrB* (aromatic amino acid aminotransferase) probably are involved in the last step of the biosynthesis of L-PAPA (Mehl et al. 2003; Masuo et al. 2016; Tateyama et al. 2016). Furthermore, analysis of recombinant proteins in *E.coli* by 2D-SDS-PAGE gels was performed. Considering the predicted isoelectric point (pI) and molecular size (MW) of recombinant proteins, number of spots, each one correspond to soluble form of $PabAB_{C.gl}$, PapB and PapC (Figure **3-3**) were observed. To prove that these soluble spots are related to the desired recombinant proteins, mass analysis is necessary to be conducted. Considering that the expression of recombinant proteins in *E. coli* often results in insoluble and/or misfolded proteins and forming inclusion bodies (Sørensen and Mortensen 2005), but contrary to it, herein, target recombinant proteins are found in the cytoplasm in the soluble forms (as demonstrated in Figure **3-3** and Figure **3-19**). As illustrated in Figure **3-5** (b), *E. coli* LJ110 harboring the pC53BC produced presumably L-PAPA (L-isomer), this was verified by mass spectrometry and employing the commercially available PAPA as the standard compound (Figure **3-5** d and e, Appendix A1.). This should be taken into consideration that amino phenylalanine (PAPA) can occur in L- and D-forms, a further advanced confirmation by NMR spectroscopy is required to determine the accuracy of the produced PAPA isomers (L or D-isomer). PAPA accumulation in supernatant suggests that endogenous exporters and/or passive diffusion are sufficient enough to allow the exit of PAPA out of the cell. Recently, a genetically modified *E. coli* has been reported for production of PAPA from glucose. In this study, the gene cluster *papABC* from *Pseudomonas fluorescens* was used, minimal media was

also supplemented with tryptone (5 g l^{-1}) and yeast extract (2.5 g l^{-1}) (Masuo et al. 2016). A similar strategy was also implemented by Tateyama and coworker for production of L-PAPA from glucose (Tateyama et al. 2016). Also, contrary to the previous report (Masuo et al. 2016; Tateyama et al. 2016), which are used a complex medium with uncertain amount of carbon source (Table **4-1**), in this study a defined minimal minimal medium with a certain amount of carbon source was applied (Mohammadi et al. 2018). Apart from glucose, which is most widely used in the microbial production of fine chemicals in *E.coli* (Koma et al. 2012; Kim et al. 2014b, Masuo et al. 2016; Tateyama et al. 2016; Li et al. 2018), also, glycerol has become a favorable carbon source for the production of most valuable fine chemicals (da Silva et al. 2009; Almeida et al. 2012; Khanna et al. 2012; Meiswinkel et al. 2013; Gottlieb et al. 2014; Weiner et al. 2014; Sprenger 2017). In several studies, glycerol as cost-effective carbon source (Lin et al. 1976; Sprenger 2017) was applied for microbial production of bulk chemicals or fine chemicals (da Silva et al. 2009) such as lactic acid (Mazumdar et al. 2013), succinic acid (Blankschien et al. 2010), propionic acid (Barbirato et al. 1997), citric acid (Papanikolaou et al. 2002), salicylic acid (Lin et al. 2014), L-phenylalanine (Khamduang et al. 2009; Thongchuang et al. 2012; Weiner et al. 2014; Gottlieb et al. 2014) and others (Silva et al. 2009; Martínez-Gómez et al. 2012). Considering that better results were obtained when glycerol was used as an alternative carbon source and even glycerol has not been explored for production of aromatic amines. Using glycerol instead of glucose resulted in higher L-PAPA formation in *E.coli*, probably due to the increased availability of PEP (as precursor of shikimate pathway), unlike the glucose which requires phosphoenolpyruvate (PEP) for its uptake into *E.coli* (PTS dependent glucose uptake) (Andersen and von Meyenburg 1980; Yazdani and Gonzalez 2007; Gonzalez et al. 2008; Ahn et al. 2008; Gottlieb et al. 2014). (C6). Apart of low conversion rate of glycerol (C3 less energy than glucose (C6)), *E. coli* grows more slowly on glycerol during the lag phase (Figure **3-16**). However, glycerol was preferred as carbon source, and a different approach for the biosynthesis of L-PAPA from glycerol by utilizing genes *pabAB* from *C. glutamicum* and *papBC* from *S. venezuelae* was applied. One metabolic engineering strategy to improve efficient conversion of glycerol toward target product is modifications of genes are involved in central metabolism pathway such as overexpression *ppsA* encoding PEP synthetase, *glpX* encoding fructose 1,6-bisphosphatase, *tktA* encoding transketolase A or inactivation of the endogenous genes encoding

pyruvate kinase (*pykF* and *pykA*) (Lütke-Eversloh and Stephanopoulos 2007; Gottlieb et al. 2014; Weiner et al. 2014; Lin et al. 2014; Noda et al. 2016; Liu et al. 2018).

4.1.2 Expanding the L-PAPA pathway toward biosynthesis of PAPE and 4-APA

Following the production of L-PAPA in *E.coli*, production of other aromatic amines such as PAPE and 4-APA was investigated (Figure 3-8 (a) and Figure 3-13 (a)). A prerequisite for the artificial PAPE/4-APA pathway is the heterologous overexpression of a gene encoding a decarboxylase which is capable of converting *p*-amino-phenylpyruvate (APP) into *p*-amino-phenylacetaldehyde (APAAL) (Masuo et al. 2016). Among many ketoacid decarboxylases, which have been found and studied in different species of bacteria, fungi and yeast (Yep et al. 2009; Kuberl et al. 2011; Chandra et al. 2001; Siegert et al. 2005), *aro10* gene, encoding the ThDP-ketoacid decarboxylase existing in *Saccharomyces cerevisiae*, was employed, since it was reported as a catalyst that can accept a wide variety of substrates such as phenylpyruvate (PP), 4-hydroxyphenylpyruvate (4HPP) and *p*-amino-phenylpyruvate (APP) (Kneen et al. 2011; Masuo et al. 2016). Aro10 is belonging to a group of Thiamin diphosphate-dependent enzymes "mainly pyruvate decarboxylase, transketolase, benzoylformate decarboxylase" whose main function is the non-oxidative decarboxylation of 2-keto acids (Sprenger and Pohl 1999). These enzymes utilize Mg^{2+} and thiamin diphosphate (ThDP) as cofactor (Yep et al. 2006). It should also be noted that thiamine diphosphate (ThDP)-dependent enzymes are involved in many different pathways and perform a diverse range of reactions including cleavage and C–C bond formation and transferase reactions (Pohl et al. 2002; Pohl et al. 2004). They are finding increasing acceptance as catalyst due to regio- and enantioselective reactions in chemo enzymatic syntheses (Sprenger and Pohl 1999).

Aro10, as one of the well-studied ThDP-ketoacid decarboxylase, is easily expressed in *E.coli* (Vuralhan et al. 2003 and 2005; Kneen et al. 2011). It has been successfully used in the microbial production of several fine chemicals such as PAPE, 4-APA (Masuo et al. 2016), 1-propanol, 1-butanol (Atsumi et al. 2008b), 2-phenylethanol (Atsumi et al. 2008b; Kang et al. 2014), salidroside (Bai et al. 2014; Liu et al. 2018), tyrosol (Satoh et al. 2012b; Bai et al. 2014; Liu et al. 2018) and hydroxytyrosol (Li et al. 2018) in *E.coli*. ThDP-ketoacid decarboxylase encoded by *aro10* overexpressed in *E. coli* showed to be mostly soluble (Figure **3-9**) and active on phenylpyruvate (PP) as substrate (Table **3-1**). The Aro10 cell-free extract specific activity

obtained in this study, 107 ± 9 nmol min^{-1} mg^{-1} (Table **3-1**), is comparable to previously reports for specific activity of *aro10* using phenylpyruvate as substrate, 220 nmol min^{-1} mg^{-1} (Vuralhan et al. 2003) and 270 nmol min^{-1} mg^{-1} (Vuralhan et al. 2005). Compared to other keto acid decarboxylase such as BFDC1, KivD, ZmPDC, KdcA and PpdA (Polovnikova et al. 2003; de la Plaza et al. 2004; Siegert et al. 2005; Yep et al. 2006; Yep et al. 2008; Kuberl et al. 2011; Masuo et al. 2015), the obtained Aro10 specific activity is relatively low. Results obtained from previous study have revealed that purified Aro10 exhibited better specific activity with K_m, K_{cat} and catalytic efficiency of 0.1 mM, 20 S^{-1} and 200 $mM^{-1}S^{-1}$ for phenylpyruvate compared to results obtained in this study, respectively (Kneen et al. 2011). It has also been shown that Aro10 can utilize a wide range of 2-ketoacid substrates particularly aromatic keto acids such as 4-hydroxyphenylpyruvate (Tyr, K_m~0.09 and K_{cat}~11) and indole-3-pyruvic acid (Trp, K_m~0.03 and K_{cat}~ 5.4) with significant efficiency and to some extent can accept aliphatic ketoacids such as 4-methylthio-2-ketobutanoic acid (Met), 4-Methyl-2-ketopentanoic acid (Leu) as well as 3-Methyl-2-ketopentanoic acid (Ile) (Kneen et al. 2011). As described previously, *aro10* gene product was not able to efficiently utilize pyruvate as substrate (K_m~ 9.7 (mM), K_{cat}~ 0.34 (S^{-1}) and K_m/K_{cat}~ 0.035 ($mM^{-1.}$ S^{-1})) (Vuralhan et al. 2005; Kneen et al. 2011). The obtained results show that Aro10 was in a soluble form (Figure **3-9**) in *E.coli* and Aro10 gene product is a functional active phenylpyruvate decarboxylase (Table **3-1**), which is in accordance with previous reports (Vuralhan et al. 2003; Vuralhan et al. 2005; Kneen et al. 2011). The gene *aro10* alone or combined with *feaB* was overexpressed on an expression plasmid (pJFA10 or pJFA10F), and the whole cell biotransformation reported here verified the decarboxylation of APP (transamination from L-PAPA as substrate) to APAAL by *aro10* which is then either reduced to PAPE (Figure 3-8 (a)) by endogenous alcohol dehydrogenase/reductase (Rodriguez et al. 2014; Atsumi et al. 2010; Liu et al. 2015) or oxidized to 4-APA (Figure 3-13 (a)) by a phenyl acetaldehyde dehydrogenase (FeaB) (Hanlon et al. 1997). The highest PAPE and 4-APA content obtained in *E.coli* wild type strain LJ110, was 698 ± 34 mg l^{-1} PAPE with 89% C mol mol^{-1} yield (Figure 3-8, b) and 899 ± 32 mg l^{-1} 4-APA with 96 % C mol mol^{-1} yield (Figure 3-8, b), comparable with a previous report in *E. coli* using whole cell biotransformation (Masuo et al. 2016). These results and others showed that Aro10 can accept APP as substrate and convert it to amino-phenyl acetaldehyde (APAAL) which can be subsequently either reduced to PAPE or oxidized to 4-APA (Masuo et al. 2016). In this approach, PAPE and 4-APA production was

associated with 4-APA and PAPE as side-product by endogenous aldehyde reductase or aldehyde dehydrogenase in *E.coli*, respectively, whereas no intermediates such as APP or APAAL were detected.

Table 4-1 Comparison strategies used in this study (Mohammadi et al. 2018 and 2019) to Takaya's group (Masou et al. 2016; Tateyama et al. 2016)

	Takaya's group	**This study**
***E.coli* strain**	*E.coli NST37* (*DE3*) Auxotrophic for L-Phe, L-Tyr and L-Trp	different strains: *E.coli* FUS4, FUS4.7R and FUSBCR: Auxotrophic for L-Phe and L-Tyr
Gene expression	expression plasmid (LacI/PT7)	expression plasmid (LacI/Ptac)
PAPA genes	artificially synthesized: codon optimized *papA, papB* and *papC* from *P. fluorescens*	PCR synthesized: *pabAB* from *C. glutamicum,* codon optimized *papB* and *papC* from *S. venezuelae*
PAPE or 4-APA genes	PCR synthesized: *aro10 (S. cerevisiae)* *pparo10 (p. pastoris)* *ppdA (A.oryzae)* and three DHase genes: *aldH 2 (S. cerevisiae)* *aldH 3 (S. cerevisiae)* *padA (E.coli)*	PCR synthesized: *aro10 (S. cerevisiae)* and three DHase genes: *adHI (S. cerevisiae)* *adHII (S. cerevisiae)* *feaB* and *yahK (E.coli)*
Shikimate pathway engineering	Overexpression of AroG4^{fbr}	overexpression of *aroF, aroB and aroL*
Central metabolism pathways engineering	Overexpression of *pps* and *tktA*	overexpression of *glpX and tktA*
Culture media	M9 medium, supplemented by tryptone, yeast and ammonium sulfate	minimal medium (Gerhardt)
Product analysis	detection of final products based on HPLC No information about by product, possible bottlenecks and product susceptibility	detection of final products based on HPLC and LC-MS By product analysis, susceptibility of target product against *E.coli*
Downstream processing	No-data	L-PAPA with yield ~70% and purity > 93%
Protein expression	No-data	protein expression based on 2D-SDS PAGE, enzyme specific activity (crude extract)
L-PAPA final titer in fermenter	~4.4 g l^{-1} L-PAPA (yield 17% g g^{-1} glucose) by Fed-batch cultivation	16.7 g l^{-1} L-PAPA (yield 13 % g g^{-1} glycerol) by Fed-batch cultivation- 205 g L-PAPA in total
PAPE final titer	~0.24 g l^{-1} PAPE (yield 1.2 % g g^{-1} glucose) by Fed-batch cultivation	2.5 ± 0.15 g l^{-1} 4-APA (yield 8 % g g^{-1} glucose) by Fed-batch cultivation
4-APA final titer	~0.19 g l^{-1} 4-APA (yield 0.9 % g g^{-1} glucose) by Fed-batch cultivation	3.4 ± 0.3 g l^{-1} 4-APA (yield 14 % g g^{-1} glucose) by Fed-batch cultivation

In order to establish a de-no pathway for PAPE/4-APA production, flux from intermediate APP needs to be directed towards APAAL and then PAPE or 4-APA (Figure 3-11 (a) and Figure **3-15** (a)). Expanding L-PAPA pathway by the addition of *aro10* alone or *aro10* and *feaB* on plasmid in combination with the heterologous L-PAPA genes (*pabAB, papB* and *papC*) in *E. coli* wild type was investigated and resulted in fermentative production of PAPE (Figure 3-11, b) and 4-APA (Figure **3-15**, b) in shake flasks, indicating successful production of PAPE and 4-APA from renewable resources by multi-step pathway grafting. Additionally, PAPE and 4-APA were accumulated in the culture medium suggesting that these components sufficiently exit out of the cell by endogenous exporters and/or diffusion in *E.coli*. Another approach has been recently reported for the biosynthesis of PAPE and 4-APA by expression of a phenylpyruvate decarboxylase (Aro10) and different alcohol or aldehyde dehydrogenase from *S. cerevisiae* in an *E. coli* strain optimized for the production of the L-PAPA (Table **4-1**). The final PAPE and 4-APA titer of about 0.24 g l^{-1} and 0.19 g l^{-1} were obtained with the genetically modified *E. coli* strain, respectively (Table **4-2**) (Masuo et al. 2016). Results from this study and a previous study (Masuo et al. 2016) showed that Aro10 can accept APP as substrate and convert it into *para*-amino-phenyl acetaldehyde (APAAL) which can be subsequently either reduced to PAPE by endogenous aldehyde reductases or oxidized to 4-APA by aldehyde dehydrogenases (Koma et al. 2012; Pug et al. 2015; Liu et al. 2015).

4.1.3 Improvement of AAs production

In order to improve the AAs production titer in the established biosynthetic pathway further strain modification and process optimization can be effective. In previous investigations (Backman et al. 1990; Rüffer et al. 2004; Olson et al. 2007; Patnaik et al. 2008; Santos et al. 2012; Liu et al. 2014; Weiner et al. 2014; Gottlieb et al. 2014), increasing the intercellular formation of chorismic acid in *E. coli* was achieved by a double deletion of *pheA* and/or *tyrA* to prevent the carbon flux toward L-Tyr and L-Phe biosynthesis. In order to systematically improve the biosynthetic capacity of cells producing chorismate, the strain *E. coli* FUS4 (Gottlieb et al. 2014) based on *E. coli* LJ110 (Table **2-2**) was employed. This strain improvement enhanced L-PAPA, PAPE as well as 4-APA production to 78 ± 5 mg l^{-1}, 56 ± 10 mg l^{-1} and 68 ± 4 mg l^{-1}, respectively, after incubation in shake flask for 48 h, which is two-fold higher than the wild type strain LJ110 (Table **4-2**).

Present study and previous studies (Rüffer et al. 2004; Zhao et al. 2011; Koma et al. 2012; Yao et al. 2013; Huang et al. 2013; Gottlieb et al. 2014; Weiner et al. 2014; Liu et al. 2014; Pugh et al. 2014; Lin et al. 2014; Li et al. 2018) showed that blocking the competing pathways (lacking *pheA/tyrA*) can efficiently increase the flux into the target downstream pathway expanded from chorismic acid. Takaya's group and coworkers in another approach (Masuo et al. 2016; Tateyama et al. 2016) employed an *E.coli* strain deficient in *pheA/tyrA* genes to prevent the conversion of chorismic acid into L-Phe/L-Tyr in order to increase the carbon flux towards L-PAPA production pathway. Studies that focus on overproduction of aromatic amino acid and valuable compounds in *E. coli* can guide further metabolic engineering (Berry 1996; Bongaerts et al. 2001; Sprenger 2007b; Pittard and Yang 2008; Gosset 2009; Rodriguez et al. 2014; Liu et al. 2015).

As example, in order to improve the carbon flux towards the shikimate pathway, a higher precursor supply is needed to form the initial intermediate DAHP from erythrose 4-phosphate (E4P) and PEP (Patnaik et al. 1995; Bongaerts et al. 2001; Sprenger 2007b; Gosset 2009; Rodriguez et al. 2014). Several studies investigated the modifications of the central metabolic pathway to increase the E4P and PEP supply by overexpression of transketolase (encoded by *tktA*) (Draths et al. 1992; Balderas-Hernandez et al. 2005; Lutke-Eversloh and Stephanopoulos 2007; Juminaga et al. 2012; Wang et al. 2013; Rodriguez et al. 2013; Cui et al. 2014; Gottlieb et al. 2014; Vargas-Tah et al. 2015; Masuo et al. 2016), PEP synthase (encoded by *ppsA*) (Lutke-Eversloh and Stephanopoulos 2005; Chandran et al. 2003; Juminaga et al. 2012; Huang et al. 2013; Cui et al. 2014; Masuo et al. 2016) carbon storage regulator (Csr) (Gudapaty et al. 2001) and fructose 1,6-bisphosphatase (encoded by *glpX*) (Donahue et al. 2000; Gottlieb et al. 2014). It has been indicated that overexpression of *ppsA* and *tktA* in *E. coli* increases production of L-PAPA (Masuo et al. 2016), shikimic acid (Cui et al. 2014), L-Tyr (Juminaga et al. 2012), L-Trp (Wang et al. 2013), anthranilic acid (Balderas-Hernandez et al. 2009), salvianic acid (Yao et al. 2013; Zhou et al. 2017), caffeic acid (Huang et al. 2013), muconic acid and its precursor salicylic acid (Lin et al. 2014), cinnamic and *para*-hydroxycinnamic (Vargas-Tah et al. 2015) and avenanthramides (Eudes et al. 2013). Gottlieb and coworkers have shown a significant increase in L-Phe productivity (0.37 g l^{-1} h^{-1}) with combination of an extra copies of *glpX* and *tktA* in *E.coli* FUS4.7 (Gottlieb et al. 2014; Weiner et al. 2014). These studies demonstrate that overexpression of some candidate genes in the central metabolism pathway has a positive impact on yield and productivity of many aromatic compounds. Further modifications were followed by

sequential inactivation of the pathway-specific transcription regulator *tyrR* gene (as transcription repressor) in *E. coli*. The transcriptional regulon of TyrR is well characterized in *E. coli* (Pittard et al. 2004). It has been shown in previous studies that inactivation of *tyrR* results in enhanced expression of several genes relevant to aromatic biosynthesis, including *aroG, tyrB, tyrP, aroP, tyrA* and *aroL* (Pittard 1996; Bongaerts et al. 2001; Pittard et al. 2004; Salgado et al. 2006). Many previous reports also showed that elimination of *tyrR* gene can increase the final titer of product, including L-Phe (Doroshenko et al. 2015), L-Tyr (Lutke-Eversloh and Stephanopoulos 2007; Munoz et al. 2011; Santos et al. 2012), cinnamaldehyde (Bang et al. 2016), 4-hydroxymandelic acid (Li et al. 2016), salidroside (Bai et al. 2014; Liu et al. 2018), caffeic acid, 4-coumaric acid, ferulic acid (Kang et al. 2012) and salvianic acid (Yao et al. 2013; Zhou et al. 2017). A beneficial effect on AAs titer and yield (Table **4-2**) was found by employing a more advanced strain *E. coli* FUS4.7R (Gottlieb et al. 2014). The engineered strains showed an increase in L-PAPA, PAPE as well as 4-APA production, enhancing L-PAPA titers to ~304 ± 21 mg l^{-1}, which is four-fold titer compared to *E. coli* FUS4 (Table **4-2**). Moreover, PAPE or 4-APA was produced two-fold higher in comparison with FUS4 (Table **4-2**). These results agreed well on previous studies that revealed the positive effect of *tyrR* deletion leads to increase transcriptional expression and increased specific activities of the TyrR regulon (Lutke-Eversloh and Stephanopoulos 2005; Munoz et al. 2011; Santos et al. 2012; Yao et al. 2013; Bang et al. 2016; Li et al. 2016). It should be noted that in PAPE or 4-APA production process, a slight amount of L-PAPA (10-15 % of total titer) was detected as byproduct. Therefore, through suppressing competing pathway, PAPE and 4-APA titer can be probably improved. The terminal step in in amino acid biosynthesis catalyze by different kind of aminotransferase (*aspC, tyrB, ilvE, avtA*) (Pittard 1996; Fotheringham et al. 1986; Inoue et al. 1988). Two main aminotransferases encoded by *aspC* and *tyrB* are involved in the last step of the biosynthesis of aromatic amino acids (Pittard 1996; Fotheringham et al. 1986). In order to prevent the competing pathway (conversion of APP into L-PAPA) and consequently to improve the PAPE/4-APA productivity, *E. coli* FUS4BCR deficient in *aspC* and *tyrB* as well as *tyrR* (transcriptional repressor) genes was employed. Based on the results presented in Table **4-2**, deletion of *aspC* and *tyrB*, creating an L-aspartic acid auxotroph (Sun et al. 2011; Liu et al. 2014; Li et al. 2016), can led to decrease in the byproduct L-PAPA amount and direct more flux to PAPE/4-APA production. A slight increase in PAPE and 4-APA titter was observed in the strain FUS4BCR

compared to FUS4 and FUS4.7R (Table **4-2**). This approach has been previously investigated in *E. coli* through the blocking L-Phe or L-Tyr biosynthesis to enhance the precursor supply of aromatic ketoacids (Liu et al. 2014 and 2015), such as phenylpyruvate (PP)/4-hydroxyphenylpyruvate (4-HPP) for the biosynthesis of S- or R-mandelic acid (Sun et al. 2011), L/D-phenylglycine (Müller et al. 2006; Liu et al. 2014), benzyl alcohol (Pugh et al. 2015), 4-hydroxymandelic acid (Li et al. 2016) and salvianic acid (Yao et al. 2013).

Also, a detectable amount of L-PAPA was formed in the *aspC/tyrB* double mutants, presumably due to the presence of other aminotransferases such as IlvE in *E. coli* that can produce L-PAPA from APP (Inoue et al. 1988). To prevent this from happening, *ilvE* gene knockout may be a possible solution, but since this gene plays a key role in the synthesis of several branched amino acids such as leucine, isoleucine and valine, the deletion of *ilvE* can result in a multi-auxotrophic strain for a wide range of amino acids (Liu et al. 2014). Furthermore, it has been previously indicated that the double mutant (*aspC/tyrB*) and the triple mutant (*aspC/tyrB/ilvE*) showed similar effect on L-Phe production in *E.coli* (Liu et al. 2014); therefore, no deletion of *ilvE* is necessary.

The second reaction in PAPE biosynthesis pathway, namely reduction of APAAL to PAPE, is accomplished by endogenous aldehyde reductases in *E. coli* encoded by 13 genes such as the *yqhD*, *yjgB*, and *yahK* (Koma et al. 2012; Rodriguez et al. 2014). Moreover, the engineered *E.coli* FUS4BCR pCA53BCA strains produced approximately 23 ± 7.5 mg l^{-1} 4-Amino phenyl acetate (4-APA) as a byproduct (Table **3-3**), indicating the presence of endogenous dehydrogenase gene (*feaB*) in the genome of *E. coli* which enables the potential conversion of APAAL to 4-APA, limiting the PAPE production (Masuo et al. 2016). Therefore, to avoid the unwanted 4-APA accumulation, three alcohol dehydrogenase genes *yahK* from *E.coli*, *adHI* and *adhII* from *S.cerevisiae* were overexpressed in order to accelerate the PAPE formation (Dickinson et al. 2003; Koma et al. 2012 ; Kim et al. 2014 a and b). Introducing *adHII* into strain *E. coli* FUSBCR pCA53BCA suppressed PAPE production, probably due to either AdHII enzyme preference for conversion of ethanol to acetaldehyde (Thomson et al. 2005; de Smidt et al. 2008 and Kang et al. 2014) or lacking the AdHII enzyme, which can be an explanation for abolishing PAPE formation (Table **3-4**). Recently it was shown that overexpression of *adhI* in *E.coli* can reduce alcohol production presumably due to destruction of cellular redox balance (Liu et al. 2018). Also, introducing *adHI* lowered the level of PAPE accumulation (34.3 ± 5 mg

l^{-1} , Table **3-4**) compared to *E. coli* FUSBCR pC53BCA (Table **3-3**). It has been reported that AdHI enzyme can also function in the oxidation of all primary alcohols under the high alcohol concentration conditions in yeast (Schöpp and Aurich 1976; de Smidt et al. 2008). Introducing an additional copy of aldehyde reductase gene (Atsumi et al. 2010; Koma et al. 2012; Rodriguez and Atsumi 2014b), *yahK* in pC53BCA plasmid showed a positive effect on PAPE production in *E. coli* FUSBCR (Table **3-4**). This enzyme is also able to act as an alcohol dehydrogenase, increasing 2-PE and tyrosol production in recombinant *E. coli* (Koma et al. 2012). Interestingly, although the results showed that overexpression of *yahK* resulted in slight increase of PAPE production up to 159 ± 6 mg l^{-1}, PAPA and 4-APA were still produced as byproduct (Table **3-4**). This means that the obstacle has not been removed and probably the *yahK* gene's expression was not sufficient, also a significant amount of flux from APAAL was oxidized through the endogenous activity of FeaB into 4-APA. It has been also reported that endogenous oxidation of *para*-amino phenyl acetaldehyde (APAAL) limits PAPE production in *E.coli* (Masuo et al. 2016). To overcome this, one possible solution is to integrate an additional copy of *yahK* into host-chromosome (Datsenko and Warnner 2000; Albermann et al. 2010; Gottlieb et al. 2014; Jiang et al. 2015) or alternatively, the biosynthesis pathway of 4-APA can be blocked via chromosomal deletion of phenyl acetaldehyde dehydrogenase (*feaB* or *padA*) from *E.coli* (Satoh et al. 2012a; Bai et al. 2014; Machas et al. 2017).

A further increase in carbon flux through the shikimate pathway is an essential strategy to ensure a sufficient supply of chorismic acid for the biosynthesis of AAs. This can be achieved by deregulation of expression of *aroF* (DAHP synthase) and relieving limiting enzymatic reactions of DHQ synthase (encoded by *aroB*) and shikimate kinase I (encoded by *aroL)* (Báez-Viveros et al. 2007; Sprenger 2007b). Likewise, *aroB* and *aroL* are the rate-limiting enzymes in the common aromatic amino acid pathway in *E. coli* (Dell and Frost 1993; Oldiges et al. 2004). Therefore, pJNT*aroFBL* was used harboring second copies of genes *aroF, aroB* and *aroL* under the control of P_{tac} promoter (Mohammadi et al. 2018). Indeed, the expression of plasmid-encoded second copies of *aroF, aroB* and *aroL* genes (pJNT*aroFBL*) combined in engineered *E.coli* FUS4.7R (in case of L-PAPA) and FUSBCR (in case of PAPE or 4-APA) strains, resulted in increased carbon flow toward production of AAs. As shown in Table 4-1, co-expression of second plasmid (pJNT*aroFBL*) led to 1.5~2-fold increase of all three AAs (L-PAPA, PAPE and 4-APA) titer in all strains (Table **4-2**) during batch condition. This finding demonstrates that

additional copies of *aroF, aroB* and *aroL* can overcome existing limiting enzymatic reactions in shikimate pathway, enhancing the final AAs production. Likewise, the yield was increased by ~ 44 % for L-PAPA/glycerol (g g^{-1}), 14 % for PAPE / glucose (g g^{-1}) and 68% for 4-APA / glucose (g g^{-1}). These results agreed well with previous reports, showing that overexpression of *aroF*, *aroB* and *aroL* can enhance the flux from DAHP to chorismic acid for production of aromatic amino acids (Rodrigues et al. 2013; Weiner et al. 2014; Gottlieb et al. 2014) or other chorismic acid derivatives such as avenanthramide (Eudes et al. 2013), phenol (Kim et al. 2014b), 2-phenylethanol (Kang et al. 2014), salvianic acid (Yao et al. 2013), muconic acid and its precursors salicylic acid (Lin et al. 2014) and violacein (Rodrigues et al. 2013). Although the results showed a remarkable enhancement in L-PAPA production up to 534 ± 24 mg l^{-1}, the production of PAPE and 4-APA derived from APP (intermediate in PAPA pathway) was still low compared to L-PAPA enhancement (Table **3-4**).

Also, a small amount of PAPE or 4-APA was observed as a byproduct during the production of 4-APA or PAPE (Table **3-4**), respectively, presumably due to the weak expression of the plasmid-encoded copies of *yahK* and *feaB*. To circumvent this obstacle, the last step of PAPE and-APA pathway must be catalyzed with great efficiency and constantly toward PAPE or 4-APA production. In light of the previous reports (Koma et al. 2012; Masou et al. 2016), the appropriate balance between reduced (PAPE) and oxidized (4-APA) forms can be obtained by additional expression of *yahK* and *feaB* in combination with PAPE/4-APA genes. Therefore, an extra copy of *yahK* or *feaB* genes was inserted into pJNT*aroFBL* vector carrying *aroFBL* genes under the control of a P*tac* inducible promoter. The extra copies of *yahK* and *feaB* remarkably improved the final titer of PAPE and 4-APA up to two-fold higher than previous results (Table **3-8**; Figure **3-21**), demonstrating the effectiveness of the applied strategy in the regulation of oxidation/reduction reactions. These observations indicate that extra copies of *yahK* and *feaB* have the best possible effect on the cost-effective production process, resulted in a significant increase in PAPE (by 90%) and 4-APA (by 50%) yield (g g^{-1}) from glucose. Aside from the different strategies applied so far, this strategy seemed to be very effective in the production of PAPE and 4-APA, since unwanted side-reactions (oxidation or reduction of APAAL) can be avoided without inactivation of dehydrogenase (*feaB*) or oxidoreductase (*yahK*, *yqhD*, *yjgB* and the other 10 genes) (Rodriguez and Atsumi 2014b; Machas et al. 2017). Moreover, no detectable

amount of L-PAPA was observed any longer as an unwanted product during batch fermentation of PAPE or 4-APA (Table **3-8**). Overexpression of last enzyme of the PAPE/4-APA pathway resulted in more flux directed from APP towards the end metabolite of PAPE/4-APA pathway, preventing the accumulation of L-PAPA during batch fermentation of PAPE/4-APA. According to the obtained results, *E.coli* FUS4.7R/ pC53BC pJNT*aroFBL* as the best overproducer of L-PAPA, *E.coli* FUS4BCR/ pC53BCAY pJNT*aroFBL-yahK* as the best overproducer of PAPE and *E.coli* FUS4BCR /pC53BCAF pJNT*aroFBL-feaB* as the best 4-APA overproducer strain for fed-batch cultivation were employed.

It should be noted that the strategies for AAs production used in this work differ not only in the type of candidate genes on expression plasmids, but also in the type of carbon sources (Mohammadi et al. 2018 and 2019; Table 4-1). In contrast to Takaya and coworker, who designed an artificial L-PAPA pathway from glucose (Masuo et al. 2016; Tateyama et al. 2016), in this study a de-novo synthetic pathway for the formation of L-PAPA from both carbon source glucose/glycerol was constructed. This was achieved by recombinant expression of the genes *pabAB* from *C. glutamicum* and *papB/papC* from *S. venezuelae*, under *Ptac* promoters, whereas in the previous works an artificial gene operon of *papABC* from *Pseudomonas fluorescens* (Masuo et al. 2016; Tateyama et al. 2016) or *pabABC* from *S. venezuelae* (Mehl et al. 2003) was recombinantly expressed in *E. coli* for synthesis of L-PAPA (Table 4-2). Considering that better results (L-PAPA titer and yield) were obtained when glycerol used as carbon source, hence glycerol was applied for fed batch cultivation in the shake flask and fermenter. In addition, in the present study it was demonstrated that PAPE and 4-APA can be produced with better titer and yield by recombinant *E. coli* from glucose compare to previous study (Masuo et al. 2016). Although PAPE and 4-APA, like L-PAPA, are valuable aromatic amine compounds, their microbial production are still poorly understood (Masuo et al. 2016). To best of my knowledge, only one study has explored microbial biosynthesis of PAPE and 4-APA via overexpression of different phenylpyruvate decarboxylase and alcohol dehydrogenase on expression plasmid with T7 promoter (Masou et al. 2016). However, their strategy was not successful, and very small amount of PAPE (0.24 g l^{-1}) and 4-APA (0.19 g l^{-1}) from 20 g l^{-1} glucose was produced after long-term fermentation on minimal medium supplemented by tryptone and yeast. In this study, a better titer and yield of PAPA and PAPE/4-APA were achieved using a different strategy from

glucose or glycerol compared to previous studies (Mehl et al. 2003; Masou et al. 2016; Tateyama et al. 2016), as shown in Table 4-2.

Table 4-2 Comparison of Batch production of L-PAPA, PAPE, and 4-APA after 48 h by *E. coli* strains harboring different recombinant plasmids.

	L-PAPA		**PAPE**		**4-APA**	
	Titer (mg l^{-1})	Yield (%, g g^{-1} glycerol)	Titer (mg l^{-1})	Yield (%, g g^{-1} glucose)	Titer (mg l^{-1})	Yield (%, g g^{-1} glucose)
***E.coli* LJ110**	43 ± 1.8	0.8	12 ± 1.5	0.3	36 ± 5	0.8
***E.coli* FUS4**	78 ± 5.2	1.5	56 ± 10	1.2	68 ± 4.5	1.4
***E.coli* FUS4.7R**	304 ± 21	6	117 ± 12	2.6	138 ± 9.5	3
***E.coli* FUS4BCR**	23 ± 8.6	0.5	138 ± 14	3	264 ± 12	5.8
aroFBL (FUS4.7R or FUS4BCR)	534 ± 24	10	263 ± 15	5.8	307 ±12	6.8
aroFBL-yahK (FUS4BCR)	ND	-	526 ± 25	11	ND	-
aroFBL-feaB (FUS4BCR)	ND	-	ND	-	458 ±14.5	10

4.1.4 Fed batch fermentation of AAs

Maintaining the production process for a longer time is also an important factor in optimization of the production of L-PAPA, PAPE and 4-APA. Therefore, to keep sufficient supply of carbon sources for biosynthesis of AAs, the cultivation condition of engineered *E. coli* FUS4.7R and *E.coli* FUSBCR was switched to fed-batch cultivation. This strategy improves final titers up to 5.5 ± 0.4 g l^{-1} L-PAPA and yield of 0.16 L-PAPA / glycerol (g g^{-1}) after 134 hours (Table 4-3). In addition, titer of 2.5 ± 0.15 g l^{-1} PAPE and 3.4 ± 0.3 g l^{-1} 4-APA (Table 4-3) were obtained with a yield of 0.08 PAPE/glucose (g g^{-1}) and 0.14 4-APA/glucose (g g^{-1}). Also, concentrations of organic acids were observed by analysis acetate and lactate accumulation during fed batch cultivation. Whereas, less than 0.3 ± 0.05 g l^{-1} lactate was formed as by-product, acetate with a maximum concentration of 2.8 ± 0.2 g l^{-1} was accumulated by the fed batch fermentation in the shake flask (Figure **3-23**).

Table 4-3 Comparison of Fed-Batch production of L-PAPA, PAPE or 4-APA by recombinant *E. coli* strains harboring different recombinant plasmids.

Compound	**Fed-batch culture**	***E.coli* strains**	**Titer (g l^{-1})**	**Isolated amount (g)**
L-PAPA (Glycerol as C source)	Shake flask Fermenter (0.75 l volume) Fermenter (30 l volume)	FUS4.7R/ pC53BC-pJNTaroFBL	5.5 ± 0.4 6.4 16.8	- - 26 (≥ 93 purity)
PAPE (Glucose as C source)	Shake flask Fermenter (0.75 l volume)	FUS4BCR/ pC53BCAY-pJNT*aroFBL-yahK*	2.5 ± 0.15 0.21	- -
4-APA (Glucose as C source)	Shake flask Fermenter (0.75 l volume)	FUS4BCR/ pC53BCAF-pJNT*aroFBL-feaB*	3.4 ± 0.3 0.42	- -

The initial concentration of acetate was undetectable but it began to accumulate after 60 hours, causing acetate overflow and changes in pH. Acetate accumulation can led to loss of carbon flux for *E.coli* cell growth and loss of aromatic amines production. In practice, acetate accumulation in *E. coli* can be caused by several combined factors effect (Vicente et al. 2016), however, the most likely ones are high carbon source concentration (result in unbalanced carbon-flux between carbon uptake and conversion into biomass) in the medium and oxygen consumption rate (how quickly oxygen is supplied to the culture) (Varma and Palsson 1994; Eiteman and Altman 2006; De Mey et al. 2007). Different strategies have been developed to reduce acetate formation in *E.coli* (Dedhia et al. 1994; Aristidos et al. 1994 and 1995; Contiero et al. 2000; Shiloacha and Fass 2005). An optimized growth condition (feeding, oxygen supply, and pH) is a possible solution to avoid accumulation of acetate. However, as the cultivation in shake flask is not optimal in term of oxygen supply and pH stability, it is necessary to perform the cultivation in optimized condition, in which the cultivation condition can be controlled. In order to circumvent the batch limitations, fed batch cultivation of engineered *E. coli* FUS4.7R and *E.coli* FUSBCR was performed in benchtop bioreactor system. Results showed that glycerol fed-batch cultivation improved the final titer of L-PAPA to 6.4 g l^{-1} on benchtop bioreactor (Table 4-3) with 0.13 L-PAPA / glycerol (g g^{-1}) yield, 22% greater than L-PAPA obtained in glycerol batch culture in shake flask (Table 4-3).

In the fed batch fermentation, the well-designed medium and feeding strategies are the most important parameters that should be carefully considered for large scale fermentations (Shiloach

and Fass 2005). Since the engineered *E. coli* strain used in this study was an auxotrophic strain (Gottlieb et al. 2014), thus cell growth velocity and biomass production can be controlled with a limitation factor (L-Tyr/L-Phe), providing the best conditions for process handling and cultivation of bacterial strain producing L-PAPA. To avoid this limitation, L-Phe/L-Tyr feeding strategy was designed to allow achieving high biomass production in a controlled cell growth process, as described in section 2.6.4.1. This approach led to formation 16.7 g l^{-1} L-PAPA with yield 13% g g^{-1}, which was 2.5-fold higher compared to obtained titer in 0.25 l benchtop bioreactor (Table 4-3; Figure **3-27**). The increased cell biomass (CDW~21.6 g l^{-1}) by fed-batch culture contributed to the improved production of L-PAPA. The obtained titer for L-PAPA in this study was four-fold (Masou et al. 2016) and eight-fold (Tateyama et al. 2016) greater than titer achieved with engineered *E. coli* strain in the previous studies (Table 4-1). Whereas, in the previous studies (Masou et al. 2016; Tateyama et al. 2016) higher initial glucose concentration and higher feeding rate was applied, the feeding strategy with low glycerol pumping rate (constant feeding rate: 0.4-1.0 g l^{-1}) in this study found to reduce further obstacles, such as acetate accumulation and foam formation. It is known that high-cell-density culture has several disadvantages, including limited access to dissolved oxygen, heat generation and high levels of carbon dioxide which reduce cell growth and stimulate acetate accumulation (Lee 1996; Makrides 1996; Shiloach and Fass 2005). Through the feeding strategy in this study acetate accumulation was avoided and remained below the threshold value (2 g l^{-1}) which is not inhibitory to the cell growth (Riesenberg 1991).

L-PAPA formation in the fermenter did not continue after 96 hours which can be described by several reasons (Figure **3-27** and Figure **3-22**). One possible reason is inability of the enzymes which are involved in L-PAPA pathway (PabAB and PapB/PapC) or shikimate pathway after long fermentation. Other important possibility is that recombinant plasmid may loss after long fermentation (due to growth rate reduction), leading domination of non-productive plasmid-free *E.coli* cells in the total cell population, and may reduce the overall level of L-PAPA formation (Park et al. 1990; Cheng et al. 1977; Caunt et al. 1988; Baheri et al. 2001). One possible approach to dealing with the genetic instability (plasmid loss) is chromosome integration of recombinant genes (Datsenko and Warnner 2000; Albermann et al. 2010; Gottlieb et al. 2014; Baumgärtner et al. 2013 and 2014; Jiang et al. 2015). L-PAPA inhibitory effect against *E.coli* growth may be another reason for L-PAPA stagnation (Figure **3-2**). In the fed batch fermentation,

L-PAPA was obtained at a concentration of 6.4 g l^{-1}, however, reached a higher rate than toxicity limit of L-PAPA (6 g l^{-1}) against *E.coli* (Figure **3-2**). Also, low intracellular glutamine concentration might interrupt the conversion of chorismic acid to ADC by the enzyme $PabAB_{C.gl.}$ (Kozak 2006), preventing L-PAPA formation through conversion of ADC to APP after longer fermentation. Adding ammonium ions during the fermentation process can be a solution. Therefore, ammonia solution was added during the fermentation process to control the pH and to maintain nitrogen sources.

In the case of PAPE and 4-APA bioreactor cultivation (Figure **3-29** (a and c)) using similar L-PAPA fermentation protocol, the results showed that, however, the growth conditions in the bioreactor was not effective, so that at the end of process the obtained productivity was lower than shake flask (Table 4-3). One possible explanation could be decomposition of final products to oxidized form (R-OH to R-CO2H) or eliminated form (H2N-Ph-CH=CH2) (Figure 4-1) (Dr. Thomas Rawner, European Technical Service, Sigma-Aldrich Company Ltd (personal communication)). The decomposition of final products can be resulted from high oxygen pressure (set to above 30% in the fermentation process), indicating sensitivity of PAPE/4-APA to oxygen and decompose in the presence of excess oxygen to other compounds such as 4-vinylaniline (4-aminostyrene, Figure 4-1) (Schul'tsev 2011). These results suggested that non-optimized oxygen supply and oxygen transfer rate may lead to lower PAPE/4-APA production compared to shake flask. One way to produce PAPE/4-APA in the optimized fermentation process is to return the oxidized form (4-APA) to the reduced form (PAPE) by applying reducing agents such as ascorbic acid, β-cyclodextrin, potassium sulfite, potassium sorbate, dithiothreitol and etc. (Espín et al. 2001; Byun et al. 2010; Byun and Whiteside 2012; Souza Cuz et al. 2012; Li et al. 2018), or even to reduce the concentration of dissolved oxygen and oxygen transfer rate. The concentration of dissolved oxygen is known as a crucial factor on enzymes activity such as dehydrogenase and oxidases in many fermentation processes (Unden and Bongaerts 1997), leading to production of metabolites such as organic acids (Hua and Shimizu 1999), amino acids (Xu et al. 2009), vitamin B12 (Wang et al. 2010) and polysaccharides production (Tang and Zhong 2003; Huang et al. 2006). However, over-supply of oxygen may also reduce productivity due to the loss of substrate through direct oxidation, adding extra costs on the production process (Wang et al. 2010). On the other hand, the concentration of dissolved oxygen in the bioreactor is strongly dependent on the aeration rate and agitation speed (Chisti and Jauregui-Haza 2002), so

that, reducing oxygen transfer rate (Wang et al. 2010) possibly reduces the supply of dissolved oxygen to fermentation and consequently decomposition of PAPE or 4-APA in the fermentation can be avoided. Another one alternative approach is immobilization of whole cells using oxygen-scavenger film such as hydroxyethyl cellulose (HEC) and polyvinyl alcohol (PVOH) to reduce oxygen content (Altiere et al. 2004). Among them, ascorbic acid was applied as the most well-known reducing agent to decrease product polymerization in microbial culture media (Espín et al. 2001; Li et al. 2018).

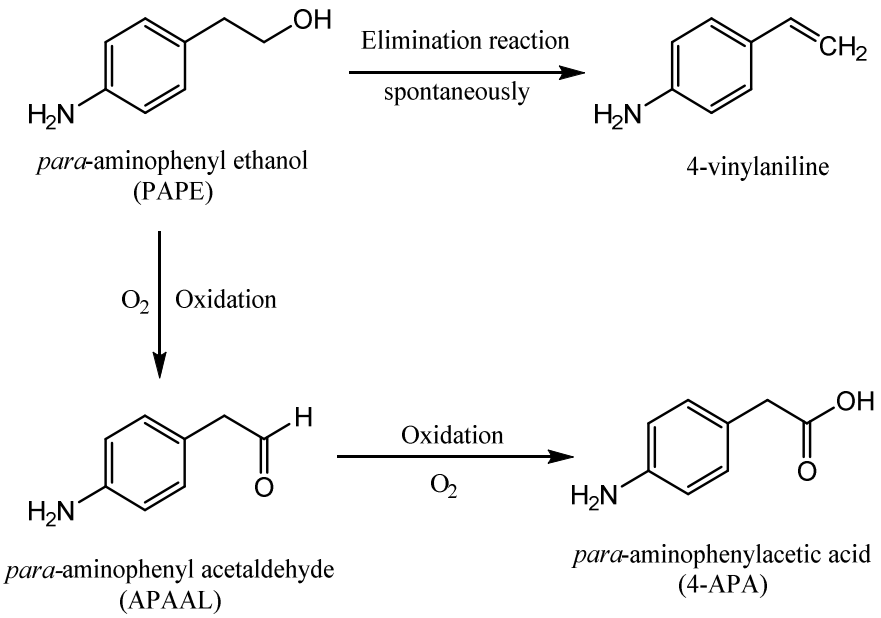

Figure 4-1 possible decomposition of PAPE in the fed batch cultivation in a fermenter (Schul'tsev 2011; Dr. Thomas Rawner, European Technical Service, Sigma-Aldrich Company Ltd (personal communication)).

The method of choice for purification of L-PAPA is FLPC analysis based on column chromatography and extraction with organic solvents (Konishi et al. 2016). The HPLC-based analysis of the separated products (Figure **3-30** and Figure **3-31**) showed L-PAPA with yield ~70% and purity > 93% from fermentation broth. This provides also a valuable guideline for the purification of other important aromatic amines (PAPE, 4-APA). Obviously, other analytical methods with higher accuracy should be employed to obtain a higher purity of L-PAPA.

4.2 Part II: Biosynthesis of aromatic alcohols and amino acids

In the second part of this study, the possibility of using *E. coli* as a cell factory system for production of higher valuable aromatic alcohols was investigated. Aromatic alcohols play an important role in the fine-chemical and pharmaceutical industry, as well as fragrance and cosmetic production (Hua and Xu 2011; Liu et al. 2015). Many of these compounds have limited natural resources or cannot easily be synthesized chemically, but some microorganisms such as yeast are capable to produce them from an aromatic compound through Ehrlich pathway (Etschmann et al. 2002; Suastegui and Shao 2016). Recent examples have impressively demonstrated the power of systems metabolic engineering for microbial overproduction of aromatic amino acids and aromatic alcohols (Atsumi et al. 2008b; Koma et al. 2012; Kang et al. 2014; Bai et al. 2015; Suastegui and Shao 2016; Li et al. 2018; Guo et al. 2018 (Table **4-4**)). Artificial biosynthesis pathways, mimicking the Ehrlich pathway in yeast, were designed to simulate the de-novo production of 2-PE/tyrosol from glucose in *E.coli* (Etschmann et al. 2002).

4.2.1 Construction of a platform strain for biosynthesis of aromatic alcohols

In this study, construction of a recombinant 2-PE and tyrosol overproducing *E. coli* strain by introduction of the yeast phenylpyruvate decarboxylase (*aro10*) was investigated. To achieve this goal, different strategies were employed and their potential in biotransformation (Figure **3-32** and Figure **3-35**) and biosynthesis (Figure **3-34** and Figure **3-37**) of 2-PE and tyrosol in *E.coli* were studied. Several studies have elucidated de novo biosynthesis of 2-PE (Liu et al. 2015) and tyrosol in many fungi (Liu et al. 2014; Masuo et al. 2015), yeast species (Etschmann and Schrader 2005 and 2006; Kim et al. 2014 a and c; Yin et al. 2015) and *E.coli* strain (Atsumi et al. 2008b; Koma et al. 2012; Satoh et al. 2012 a and b; Kang et al. 2014; Bai et al. 2014; Machas et al. 2017; Li et al. 2018; Liu et al. 2018; Guo et al. 2018 (Table **4-4**)). A summary of recombinant production of 2-PE, tyrosol and hydroxytyrosl in engineered *E.coli* was shown in Table **4-4**. Also, many types of yeast, as most prominent natural 2-PE/tyrosol-synthesizing microorganisms, produce 2-PE and tyrosol naturally through Ehrlich pathway (Etschmann et al. 2002; Hu and Xu 2011; Kim et al. 2014c).

As shown in bioconversion pathway of L-Phe to 2-PE (Figure **3-32**) and L-Tyr to tyrosol (Figure **3-35**), in the initial stage L-Phe/L-Tyr is converted to PP/HPP by aminotransferase (*tyrB, aspC*, *ilvE*), followed by decarboxylation (phenylpyruvate decarboxylase, *aro10*) to PAAL/4-

HPAAL, and finally spontaneously reduced to 2-PE/tyrosol by endogenous reductase in *E.coli* (Atsumi et al. 2010; Koma et al. 2012; Rodriguez et al. 2014b; Liu et al. 2015). The bioconversion results indicated that L-Phe or L-Tyr as initial substrates, were completely converted to 2-PE with yield 98 % mol mol^{-1} and tyrosol with yield 92.1 % mol mol^{-1}, respectively, in less than 8 hours, demonstrating proper activity of Aro10 as an overexpressed exogenous enzyme as well as endogenous enzymes involved in pathway such as aminotransferase (*tyrB, aspC*) and aldehyde reductase (*yahK, yqhD, yqhB*) in *E. coli*. Tyrosol production in *E. coli* resting cells was reported (Table **4-4**) by overexpression of either phenylpyruvate decarboxylase (Aro10) (Satoh et al. 2012b; Li et al. 2018) or Aro10 and an aromatic amino acid aminotransferase (ARO8) (Xue et al. 2017). Since, the proposed bioconversion pathways showed better performance compared to previous studies (Table **4-4**), therefore, biosynthesis of 2-PE/tyrosol with resting *E.coli* cells based on a two-step process can be a very interesting and promising target for future process engineering research.

In addition, L-DOPA as another attractive substrate was tested; whole cell biotransformation results revealed that the hydroxytyrosol was formed with yield 64% mol mol^{-1} (Figure **3-39**). It has generally been described that the aldehyde oxidation by endogenous dehydrogenase (*feaB*) or easy access out of L-DOPA by oxidization to o-quinone and further to melanin (Ali et al. 2007) are probably problems in the hydroxytyrosol production from L-DOPA. These results indicated that although the Aro10 can accept 3,4-dihydroxyphenylpyruvate (3,4-DHPP) as substrate, the conversion rate (0.34 mol h^{-1}) and molar yield (64%) are less impressive in comparison with bioconversion 2-phenylethanol (1.25 mol h^{-1}, 99 % mol mol^{-1}) and tyrosol (1.1 mol h^{-1}, 92.1 % mol mol^{-1}). It was previously reported (Table **4-4**) that hydroxytyrosol can be synthesized from a relative expensive precursor tyrosol via whole cell bioconversion (Liebgott et al. 2009; Li et al. 2018), here however for the first time a short bioconversion pathway for production of hydroxytyrosol from L-DOPA as substrate via whole cell bioconversion was established. In order to establish a *de-novo* pathway to achieve hydroxytyrosol production from simple carbon sources such as glucose and glycerol further pathway engineering is required.

Table 4-4 Recombinant production of 2-PE, tyrosol and hydroxytyrosol in previous studies (in recombinant *E. coli*)

Organisms	Recombinant genes	Culture conditions (carbon source)	Main compound produced (titer, and/or yield)	References
E.coli	2-keto acids decarboxylase (*aro10*) from *S. cerevisiae, Kivd* from *Lactococcus lactis* and alcohol dehydrogenase 2 (*adh2*) from *S. cerevisiae*	Minimal medium + supplemented with 0.5% yeast extract + 0.2M glucose	0.46 mM **2-PE**	Atsumi et al., 2008.
E.coli (L-Phe overproducer*)*	*ipdC* (phenylpyruvate decarboxylase gene) from *Azospirillum brasilense* and *yahK* (aldehyde reductase gene) from *E.coli*	Minimal medium + 51.7 mM glucose	941mg l^{-1} **2-PE**, (yield~ 0.10 g g^{-1})	Koma et al. 2012.
E. coli (L-Phe overproducer*)*	*adh1* (alcohol dehydrogenase) from *S.cerevisiae* and *kdc* (phenylpyruvate decarboxylase) from *Pichia pastoris*	Minimal medium + 20 g glucose	285 mg/L **2-PE**	Kang et al. 2014.
E.coli (L-Tyr overproducer-*feaB*-knockout mutant*)*	*ipdC* (phenylpyruvate decarboxylase gene) from *Azospirillum brasilense* and *yahK* (aldehyde reductase gene) from *E.coli*	Minimal medium + 51.7 mM glucose	1.1 g l^{-1} **tyrosol**, (yield~ 0.11 g g^{-1})	Koma et al. 2012
E. coli BW25113 (*feaB*-knockout mutant)	tyrosine hydroxylase (TH) from mouse , L-DOPA decarboxylase (DDC) from pig, tyramine oxidase (TYO) from *Micrococcus luteus* and dihydropteridine reductase (DHPR) from human	M9 medium + 0.1% glucose + 1 mM tyrosine	0.08 mM **hydroxytyrosol**	Satoh et al. 2012a.
E. coli BW25113 (*feaB*-knockout mutant)	codon optimized tyramine oxidase (TYO) gene from *Micrococcus luteus* and tyrosine decarboxylase (TDC) gene from *Papaver somniferum*	M9 medium + 1% glucose (w/v)+ supplemented with 0.025% (w/v) of yeast extract	0.5 mM **tyrosol**	Satoh et al. 2012b.
E. coli (L-Tyr overproducer and *feaB*-knockout mutant)	pyruvate decarboxylase (*aro10*) from *S. cerevisiae*	M9 medium + 2% glucose (w/v)+ supplemented with 0.025% (w/v) of yeast extract	926.9 mg l^{-1} **tyrosol**	Bai et al. 2014.
E. coli (*feaB*-knockout mutant)	pyruvate decarboxylase (*aro10*) from *S. cerevisiae* and aromatic hydroxylase encoded by the *hpaBC* gene from *E.coli*	Modified M9 medium + supplemented with 10 g/L glycerol, 2.5 g/L glucose and 2 g L-1 yeast	620 ± 23 mg l^{-1} **tyrosol** 647 ± 35 mg l^{-1} **hydroxytyrosol**	Li et al. 2018.
E.coli (L-Tyr overproducer-*feaB*-knockout mutant*)*	codon optimized decarboxylase genes *kdc4* from *Pichia pastoris* and alcohol dehydrogenase *adh1* of *S. cerevisiae*	M9 medium + supplemented with glucose/xylose	1.46 g l^{-1} **tyrosol**	Liu et al. 2018

Beside production of 2-PE and tyrosol via whole cell biotransformation, a *de-novo* biosynthesis platform for production of 2-PE/tyrosol in *E.coli* from inexpensive carbon source, glucose, was successfully established (Figure **3-34**(a) and Figure **3-37** (a)). For this purpose, PP/4HPP from L-Phe and L-Tyr biosynthesis pathway was expanded toward 2-PE/tyrosol by plasmid expressing the ThDP-ketoacid decarboxylase (Aro10), as already explained in Section 4.1.2. Therefore, two plasmids were tested in the context of 2-PE/tyrosol production from glucose in *E. coli* wild type. The expression of the ThDP-dependent Aro10 combination with endogenous reductase or dehydrogenase favored 2-PE (Figure **3-34**(a)) and tyrosol (Figure **3-37** (a)) production, demonstrating properly coupling of L-Phe/L-Tyr produced through shikimate pathway in *E. coli* wild type with the recombinant pathway. Based on these results, it seems that 2-PE and tyrosol can be produced through expanded shikimate pathway and then transported via a passive diffusion or flux pump, resulting in accumulation of 11± 1.5 mg l^{-1} 2-PE and 37± 2.5 mg l^{-1} tyrosol (Table **4-5**) in culture broth. However, it is important to note that *E.coli* wild type did not have the ability to synthesize the detectable amount of 2-PE (Figure **3-34**(a)) and tyrosol (Figure **3-37** (a)) even when supplemented with L-Phe and L-Tyr.

This study and other studies showed that the Ehrlich pathway is not active in *E.coli* wild type due to the lack of or low activity of phenylpyruvate decarboxylase (Satoh et al. 2012b; Bai et al. 2014; Kang et al. 2014; Xue et al. 2017), however, our results showed that a recombinant *E. coli* containing phenylpyruvate decarboxylase (Aro10 enzyme) was able to produce 2-PE or tyrosol efficiently. The strategy described for 2-PE and tyrosol production was previously described in several previous studies (Table 4-4). Here, unlike other previous studies, product confirmation by LC-MS analysis and downstream processing was performed. Additionally, this described strategy gives advantage (only one heterologous gene is required) to possibly channels different native amino acid intermediates (indole-3-pyruvic acid, α-ketoisocaproic acid, α-ketoisovaleric acid, α-keto-β-methylvaleric) to the 2-keto acid degradation pathway for different alcohols (tryptophol, isoamyl alcohol; isobutanol; active amyl alcohol) production in *E.coli* (Hazelwood et al. 2008; Atsumi et al. 2008b). Furthermore, the recombinant *E. coli* strain overproducing L-Phe/ L-Tyr has been previously constructed (Ikeda 2006; Juminaga et al. 2012; Santos et al. 2012; Gottlieb et al. 2014; Weiner et al. 2014), therefore to improve 2-PE/tyrosol production further, this can be the most straightforward way to modify an L-Phe/L-Tyr overproducing strain with applying the above strategy for 2-PE/tyrosol overproduction (Suastegui and Shao 2016).

4.2.2 Improvement of Aromatic alcohols production

As known, for the efficient production of 2-PE/tyrosol sufficient supply of precursors is required (Kang et al. 2014; Chreptowicz et al. 2016). PP/4-HPP is the direct and upstream precursor of 2-PE/tyrosol production (Liu et al. 2015). Therefore, strategies that increase carbon flow from upstream towards PP/4-HPP can be very effective. Accordingly, introducing three genes in *E. coli* wild type strain enhanced L-Phe/L-Tyr and 2-PE/tyrosol production more significantly, indicating that introduction of three rate limiting enzymes involved in shikimate pathway (AroF, AroB and AroL on pJNTaroFBL vector) has a positive effect on the productivity of 2-PE as well as tyrosol (Figure **3-40**). The titer of 2-PE and tyrosol in this strain are found to be elevated to 65 ± 5.5 mg l^{-1} and 128 ± 17 mg l^{-1}, respectively (Table **4-5**). These results showed a five-fold increase for 2-PE titer and four-fold increase for tyrosol titer compared to wildtype LJ110 (Table **4-5**). Meanwhile, in addition to serving as a precursor to L-Phe/ L-Tyr, chorismic acid is also the key branch point metabolite in synthesis of other aromatic compounds (Ikeda 2006; Sprenger 2007b). Moreover, the enzymes involved in the biosynthesis of L-Phe (PheA) and L-Tyr (TyrA) in *E.coli* were found to be strictly controlled by feedback inhibition of L-Phe and L-Tyr (Ikeda 2006; Yakandawala et al. 2008; Sun et al. 2011), respectively, limiting the supply of sufficient amounts of L-Phe/L-Tyr for enhanced production of 2-PE/tyrosol in *E. coli*. While, *pheA* and *tyrA* deletion lead to L-phe and L-tyr auxotrophic (supplementation to the cultures), but these may improve production levels by auxotrophic *E.coli* strain. Therefore, engineered FUS4 strain (Rüffer et al. 2004; Gottlieb et al. 2014) has been used for 2-PE/tyrosol overproduction. Meanwhile, it was described that the overexpression of L-Phe feedback resistant version of PheA ($PheA^{fbr}$) and TyrA ($TyrA^{fbr}$) can increase the production of L-Phe (Ikeda 2006; Sprenger 2007b; Sun et al. 2011; Liu et al. 2014; Weiner et al. 2014; Gottlieb et al. 2014) and L-Tyr (Juminaga et al. 2012; Santos et al. 2012; Bai et al. 2014), respectively. Therefore, *pheA* (encoding $PheA^{fbr}$-feedback resistance) gene was cloned on to pJNTaroFBL vector and overexpressed to increase the production of L-Phe and consequently 2-PE production. In case of L-Tyr overproduction, *tyrA* (encoding $TyrA^{fbr}$-feedback resistance) was cloned on to pJFA10 vector and subsequently overexpressed to direct more flux from chorismic acid towards 4-HPP and consequently tyrosol. As seen in Figure **3-40**, by combining the deletion of the native genes *tyrA/pheA* and overexpression of *pheA* ($PheA^{fbr}$-feedback resistance) and *tyrA* ($TyrA^{fbr}$-feedback resistance), the recombinant FUS4 strain was able to improve L-Phe/L-Tyr titer and yield by two- and three-folds

compared to the wild type strain (Table **4-5**). Accordingly, producing more L-Phe/L-Tyr with FUS4 as host, both 2-PE and tyrosol titers was greatly increased almost 2.5 fold compared to wild type strain LJ110, reaching the final titer of 247 ± 22 mg l^{-1} ^{1} (0.05 g/g) and 377 ± 37 mg l^{-1} (0.08 g/g), respectively (Table **4-5**). These results provided support for further improvement of the 2-PE/tyrosol production through development of cost-efficient microbial platforms to produce this important monomer at high levels from renewable resources. It should be also noted that 2-PE or tyrosol was determined as major end-product, L-Phe, L-Tyr, or even phenyl acetate/4-hydroxy phenyl acetate were observed as byproduct (Figure **3-33** and
Figure **3-36**).

These results demonstrate that it is necessary to minimize the L-Phe/L-Tyr production in order to drive flux through PP/4-HPP towards the 2-PE/tyrosol pathway. At this point, further strain improvements were necessary to increase PE/tyrosol titers. Due to the endogenous L-Phe/L-Tyr pathway present in *E.coli*, PP/4-HPP is subsequently converted to L-Phe or L-Tyr by means of endogenous aminotransferase (Fotheringham et al. 1986; Pittard 1996). Therefore to avoid the limitation caused by PP/4-HPP (PP), also to redirect these intermediate to the 2-PE/tyrosol pathways as well as to partially eliminate pathway bottlenecks, inactivation of two aminotransferase *tyrB* and *aspC* involved in the competitive pathway (Li et al. 2016; Sun et al. 2011) as well as *tyrR* (Bai et al. 2014), were investigated (Pittard et al. 2004). However, the attempts made for enhancement of production of 2-PE by deletion of *tyrB*, *aspC* and *tyrR* were not successful and 2-PE/tyrosol production remarkably reduced in aminotransferase deficient strain, which is not compatible with 2-PE/tyrosol production in FUS4 strain (Table **4-5**). Although many previous studies revealed positive impact of the deletion *tyrB*, *aspC* (Sun et al. 2011; Li et al. 2016) and *tyrR* (Berry 1996; Koma et al. 2012; Yao et al. 2013; Bang et al. 2016; Li et al. 2016) on the enhanced production of some aromatic compounds, but it seems that deletion of *tyrB*, *aspC* and *tyrR* not only has failed to improve the production of 2-PE/tyrosol, but also has adverse effects on the 2-PE/tyrosol productivity, due to some unexpected phenomenon such as accumulation of PAAL/4-HPAAL, which are toxic and inhibited cell growth (Kang et al. 2014). The other possibility is that *tyrB/aspC* might be partially contributed to the formation of 2-PE/tyrosol, since, strain FUS4BC differs from FUS4 strain only in terms of the inactivation of *tyrB/aspC*, as was previously reported that *tyrB* deletion has a negative impact on salvianic acid production in *E.coli* (Yao et al. 2013).

As a result, although flux through the L-Phe/L-Tyr pathway was improved in FUS4, indicating that the activity of last step, reduction PAAL/4-HPAAL to 2-PE/tyrosol is not sufficient enough to draw flux from PAAL/4-HPAAL. The low reduction activity showed that PAAL/4-HPAAL accumulated within the cell and subsequently imposed further feedback regulation upon cell growth. Furthermore, since, reduction activity is low, it most likely cannot compete with the oxidation reaction, and thus it is assumed that significant part of the carbon flow (15-20% of total) is converted to unwanted Phenyl acetate/4-Hydroxy phenyl acetate (data not shown) by the activity of the endogenous *E. coli* phenyl acetaldehyde dehydrogenase (FeaB), and then may be accumulated as a byproduct. The accumulation of Phenyl acetate/4-hydroxyphenylacetate in the culture of *E. coli* FUS4, a strain K-12 derivative, is likely to be due to presence of FeaB (Koma et al. 2012; Satoh et al. 2012 a and b; Bai et al. 2014; Machas et al. 2017; Liu et al. 2018) as well as the absence of the genes responsible for the Phenyl acetate/4-hydroxy phenyl acetate degradation pathway which is found in the *E. coli* B, C, and W strains (Diaz et al. 2001). The deletion of the *feaB* might significantly decrease the amount of the byproduct phenyl acetate/4-hydroxy phenyl acetate base on this hypothesis. It has been reported that 4-hydroxyphenylacetaet accumulation can be avoided by *feaB* deletion (Satoh et al. 2012b; Xue et al. 2017; Liu et al. 2018). In another study, *feaB* deletion was proven to be a promising strategy for enhanced tyrosol (Li et al. 2018; Liu et al. 2018) and hydroxytyrosol production in *E. coli* (Li et al. 2018). Liu et al. (2018) showed that deletions of *feaB* can completely inhibit 4-hydroxyphenylacetate accumulation. In contrast, it was shown that disruption of *feaB* can remarkably reduce but cannot completely eliminate 4-hydroxyphenyl acetate accumulation, demonstrating this fact that there are other aldehyde dehydrogenases that can oxidize 4-hydroxyphenyl acetate (Li et al. 2018). In addition, unexpected oxidation of tyrosol may also occur through the aromatic hydroxylase encoded by the *hpaBC* genes, especially when using *E. coli* B, C, or W (Diaz et al. 2001). In this study *E. coli* K-12 derivatives were employed which have neither *hpaB*C gene nor its homologs (Cooper and Skinner 1980; Burlingame and Chapman 1983; Prieto et al. 1996); however, deletion of *hpaBC* gene may need to be considered when using *E. coli* B, C, or W strains for heterologous production of tyrosol (Satoh et al. 2012b). Another easy-to-use solution is applying reducing agents, such as ascorbic acid (Espín et al. 2001). In one study, ascorbic acid was used as a reducing agent to prevent over oxidation of hydroxytyrosol. Adding ascorbic acid improved the tyrosol and hydroxytyrosol titer by 17% (Li et al. 2018).

In order to make better *E. coli* strain for 2-PE/tyrosol production considering enhance the production of the shikimate pathway precursor, erythrose-4-phosphate via overexpression of the transketolase *tktA* and fructose 1,6-bisphosphate *glpX* (Gottlieb et al. 2014) combined with *tyrR* inactivation resulted in significant impact on improving L-Phe, L-Tyr as well as 2-PE and tyrosol titers ~ 616 ± 41 mg l^{-1}, 721 ± 48 mg l^{-1}, 369 ± 25 mg l^{-1} and 437 ± 33 mg l^{-1} (Table **4-5**), a 46, 82, 49 and 16% increase in compared to FUS4 strain, respectively. Previous studies have also revealed that strains with an additional *tktA* (Chandran et al. 2003; Kraemer et al. 2003; Gottlieb et al. 2014) and *glpX* (Gottlieb et al. 2014; Weiner et al. 2014) are more efficient for production of aromatic compounds. As a result, it is interesting to note that the 2-PE and tyrosol titer obtained with FUS4.7R strain in batch culture were more than 5 and 3-folds in compared to wild type strain, respectively (Table **4-5**), These results are comparable with highest obtained titer of 2-PE and tyrosol (Table **4-5**) by batch culture of recombinant *E. coli* system (Kang et al. 2014; Li et al. 2018; Liu et al. 2018). In this study attempts were made to increase the 2-PE/tyrosol production by stepwise pathway engineering in *E. coli*. This can be used as a suitable guideline for the production of other aromatic alcohol such as hydroxytrylosol. Also, other studies have used a minimal medium which was supplemented either with yeast/tryptone extract or L-Phe/L-Tyr as substrate to improve 2-PE/tyrosol production in *E.coli* (Table **4-5**)), unlike them here, a *de-novo* pathway from glucose and minimal medium was established. In this work it was shown that *E. coli* native aminotransferase (*tyrB, aspC, ilvE*) and dehydrogenases or reductase are sufficient to carry out the transamination and reduction in recombinant 2-PE/tyrosol pathway. Also, the *in-vivo* activity of Aro10 to the L-DOPA as substrate was described, which has not been reported in any previous studies. Nevertheless, Aro10 is known to exhibit broad substrate specificity (Vuralhan et al. 2003 and 2005; Kneen et al. 2011), especially on α-ketoacids such as PP and 4-HPP, as described in this study. However, apart from the recent attention on aromatic alcohols in the industry (Etschmann et al. 2002; Atsumi et al. 2008b and 2010; Hu and Xu 2011), to best of my knowledge, only a few studies (Table **4-5**) have been explored microbial biosynthesis of 2-PE (Atsumi et al. 2008b; Koma et al. 2012; Kang et al. 2014) and tyrosol (Satoh et al. 2012 a and b; Koma et al. 2012; Bai et al. 2014; Xue et al. 2017; Li et al. 2018; Liu et al. 2018) via overexpression of different phenylpyruvate decarboxylases and alcohol dehydrogenases on expression plasmid in recombinant *E.coli*. In this study, unlike them, both 2-PE and tyrosol were produced by expanded shikimate pathway from glucose in better titer and

yield using a single step decarboxylase reaction catalyzed by Aro10, as explained in section 2.2.1.

Table 4-5 Comparison of 2-PE and tyrosol production after 48 h by different *E. coli* host strains harboring recombinant plasmids

	2-PE		tyrosol	
	Titer (mg l^{-1})	Yield (%, g g^{-1} glucose)	Titer (mg l^{-1})	Yield (%, g g^{-1} glucose)
E.coli LJ110	11 ±1.5	0.2	37 ± 2.5	0.8
aroFBL	65 ± 5.5	1.5	128 ± 17	2.8
E.coli FUS4	247 ± 22	5.5	377 ± 37	8.3
E.coli FUS4BCR	162 ± 13	3.6	275 ± 12.2	6.1
E.coli FUS4.7R	369 ± 25	8.2	437 ± 33	10

As a conclusion, the biosynthetic production of 2-PE/tyrosol from glucose by *E. coli* was successfully demonstrated through pathway grafting. Although reductase activity as limited last step as well as excess oxidation, limits the overall productivity and remain a challenge, therefore continual improvements on enhancing reductase activity as well as deletion of *feaB* (phenyl acetaldehyde dehydrogenase) might lead to greater yields and a more sustainable approach for 2-PE/tyrosol biosynthesis (Machas et al. 2017).

4.2.3 Single phase and two phase fed batch cultivation of aromatic alcohols

To overcome limited access of sufficient amount of carbon source, fed batch cultivation was conducted. Results showed (Figure **3-44**) that fed-batch cultivation of FUS4.7R, as the best strain in the batch cultivation improved the final titer of L-Phe to 4.97 ± 0.38 g l^{-1} and L-Tyr to 4.7 ± 0.11 g l^{-1} on glucose, from which approximately one third is directed toward the production of 2-PE (1.75 ± 0.12 g l^{-1}) and tyrosol (1.68 ± 0.19 g l^{-1}) (Table **4-6**). These values are almost five and four-folds higher than 2-PE and tyrosol obtained in glucose batch culture (Table **4-6**), respectively. Koma and coworker (Table **4-6**) reported the highest amount of 2-PE (0.94 g l^{-1}) in recombinant *E. coli* from glucose without supplementing with expensive precursors (Koma et al. 2012). Recently Liu et al. (2018) through a synthetic *E. coli*- *E. coli* coculture enhanced the biosynthesis of tyrosol to 1.46 g l^{-1} in 36 h (Table **4-6**). If this results is compared to the best 2-

PE (Koma et al. 2012) and tyrosol (Liu et al. 2018) production published so far in recombinant *E.coli* (Table 4-3), these results (Table **4-6**) presented in this study are superior to the results of all previous studies (Atsumi et al. 2008b; Koma et al. 2012; Satoh et al. 2012b; Kang et al. 2014; Bai et al. 2014; Xue et al. 2017; Li et al. 2018; Liu et al. 2018). On the other hand, the toxicity of most aromatic alcohols against non-native hosts such as *E. coli* and other Gram-negative bacteria has been previously reported (Ramos et al. 2002; Fraud et al. 2003; Atsumi et al. 2008b; Li et al. 2018). Although a causal relationship was not fully proven, close exposure to the related aromatic alcohols, 2-phenylethanol, for example, has been shown that RNA and protein syntheses were immediately decreased and DNA synthesis was inhibited at lethal concentrations (75 mM 2-PE) (Lucchini et al. 1993). Mechanism of bactericidal action of 2-phenylethanol has been previously reported that it can be penetrate into the cell through the lipid bilayer of the membrane or through transmembrane channels, and then in the next step probably turns into phenyl acetaldehyde due to the activity of alcohol dehydrogenase which can demonstrate undesirable effects of 2-PE (Lang and Rye 1972; Ingram and Buttke 1985; Lucchini et al. 1993; Pugh et al. 2015). Moreover, according to 2-PE and tyrosol cell toxicity results (Figure **3-45**), the final titer of 2-PE (1.75 ± 0.12 g l^{-1}, Figure **3-44** (b)) and tyrosol (1.68 ± 0.19 g l^{-1}, Figure **3-44** (d)) in the present study were above the level causing cell growth inhibition, which was reported as about 1 g l^{-1} for *E.coli* (Kang et al. 2014), 2-3 g l^{-1} for *Neurospora crassa* (Lester 1965) and 2.5 g l^{-1} for *S. cerevisiae* (Stark et al. 2003).

One of the most frequently applied concepts to relieve limitations arising from product toxicity is in situ product removal (two phase system) (Etschmann et al. 2002; Rüffer et al. 2004; Schügerl and Hubbuch 2005; Atsumi et al. 2008a; Hu and Xu 2011; Chreptowicz et al. 2016; Chreptowicz et al. 2018). The aqueous phase containing the whole-cell and the second phase (organic solvent, solid resin, gas) is selected based on the specific properties of the product and the tolerance on the whole-cell. Two factors are determining the proper choice of the organic solvent for microorganisms: (i) organic solvent not be toxic to the microorganisms, and (ii) the preference of the product to reside in the organic phase must be much higher as in the aqueous phase (Perez 2001; Schügerl and Hubbuch 2005). Previously, tributyrin has been used as an extractant for phenol production by recombinant *E. coli*, leading to a 2-fold increase in phenol titer (Kim et al. 2014; Miao et al. 2015). In another study, 1-dodecanol was found to be a promising solvent for hydroxytyrosol production in a two phase system, improved final titer in

recombinant *E. coli* by 75% (Li et al. 2018). Besides, a varying of organic solvents such as kerosene /cation- selective carrier D2EHPA (Rüffer et al. 2004), oleic acid (Stark et al. 2002; Wang et al. 2008; Lu and Zhang 2008), PPG1500 (Wang et al. 2008), PPG 1200 (Etschmann and Schrader 2006), oleyl alcohol (Etschmann and Schrader 2003), octanol (Wireckx et al. 2005; Miao et al. 2015) and dodecane (Miao et al. 2015) were used as an extractant for in situ extractive fed-batch fermentation of *E. coli*, *S. cerevisiae*, *P. putida* and *K. marxianus*. Recently it has been also shown that rapeseed oil can be used as an extractant to increases the yield of 2-phenylethanol production in a biphasic system in yeast (Chreptowicz and Mierzejewska 2018). Therefore, to avoid 2-PE/tyrosol toxicity and consequently to increase microbial production of 2-PE/tyrosol, different extractants were investigated and PPG 1200 (Etschmann and Schrader 2006) with highest extractive capability (Table **3-11** and Table **3-12**) was selected as an extractant for the two-phase fed-batch cultivation of FUS4.7R strain. PPG 1200 as an extractant has unique properties including, high extractive capacity, low price and safety (non-flammable and non-toxic to human) for in situ extraction of 2-PE (Etschmann and Schrader 2006; Kim et al. 2014 a and c). Moreover, in the previous studies it is suggested that extraction of 2-PE by PPG 1200 is very effective during the cultivation of *Saccharomyces cerevisiae* (Etschmann and Schrader 2006; Kim et al. 2014a). To understand the extraction potential capacities of PPG 1200, different concentration of PPG 1200 for enhanced production of 2-PE (Table **3-11**) and tyrosol (Table **3-12**) were investigated. These results clearly showed that using 30 % PPG1200 effectively increases the production of 2-PE as well as tyrosol titer to 2.5 ± 0.07 g l^{-1} and 3 ± 0.06 g l^{-1}, respectively (Table **3-11** and Table **3-12**). However, production of 2-PE/tyrosol is reduced by reducing PPG 1200 concentration in the culture; the highest concentration of 2-PE (5.9 ± 0.36 g l^{-1}) and tyrosol (3.9 ± 0.29 g l^{-1}) were obtained in organic phase when 10% PPG1200 was applied. As expected, current achievable 2-PE titers in aqueous phase remained well below the apparent toxicity threshold and accumulated in organic phase during fed batch cultivation (Table **3-11** and Table **3-12**). In the case of tyrosol, product toxicity remains the greatest hindrance in achieving a high titer production. Tyrosol titer in aqueous phase was 1.35± 0.16 g l^{-1}, which is approximately 50% of the maximum estimated toxicity limit (2.75 g l^{-1}) that can completely inhibit growth of *E.coli* (Figure **3-45** (b)).

Table 4-6 Comparison of Fed-Batch production of 2-PE, tyrosol, L-Phe and L-Tyr from glucose by recombinant *E. coli* strains harboring different recombinant plasmids

Compound	Fed-batch culture	*E.coli* strains	Titer (g l^{-1})	Purity (%)	Yield (%)
2-PE	Single phase in shake flask	FUS4.37R/	1.75 ± 0.12	-	-
	Two phase (30% PPG) in shake flask	pJFA10-	2.55± 0.07	-	-
	Two phase (30% PPG) in Fermenter	pFABL	3.1	≥ 81	69
Tyrosol	Single phase in shake flask	FUS4.37R/	1.68 ± 0.19	-	-
	Two phase (30% PPG) in shake flask	pJFTA-	3 ± 0.06	-	-
	Two phase (30% PPG) in Fermenter	pJNT*aroFBL*	3.57	≥ 71	50
L-Phe	Single phase in shake flask	FUS4.37R/ pFABL	4.97 ± 0.38	-	-
L-Tyr	Single phase in shake flask	FUS4.37R/ pJFT- pJNT*aroFBL*	4.7 ± 0.11	-	-

In comparison, 2-PE/tyrosol production in FUS4.7R strain in the two-phase fed batch culture seems to be an efficient system for converting L-Phe/ L-Tyr to 2-PE/tyrosol and showed a modest 1.5-fold improvement in 2-PE/tyrosol production in comparison with the single-phase shake flask culture (Table **4-6**). This represents an improvement in 2-PE and tyrosol production and is the highest titer of 2-PE and tyrosol that has ever been achieved in *E. coli* (Table 4-4) (Atsumi et al. 2008b; Satoh et al. 2012b; Koma et al. 2012; Bai et al. 2014; Kang et al. 2014; Xue et al. 2017; Li et al. 2018). The maximum 2-PE yield is 0.1 g g^{-1} glucose (19.8% C mol.mol^{-1} glucose) and tyrosol is 0.12 g g^{-1} glucose (20.3% C mol.mol^{-1} glucose), which is comparable to results obtained in previous studies in *E.coli* (Table 4-4) (Atsumi et al. 2008b; Koma et al. 2012; Bai et al. 2014; Kang et al. 2014; Satoh et al. 2012b; Xue et al. 2017; Li et al. 2018; Liu et al. 2018) or even 2-PE/tyrosol production results in *Saccharomyces cerevisiae* (Etschmann and Schrader 2003; Wang et al. 2008; Kim et al. 2014 a and c).

As previously mentioned, non-optimized conditions in the shake flask is one of the biggest concerns in the production process. Strategies to address this concern will ultimately be required as process optimization to further improve 2-PE/tyrosol production. To optimize culture condition in shake flask several strategies can be applied (Vasala et al. 2006). For example, an online system can be applied to enable the remote-monitoring and control some parameters such as pH, O_2 and feeds in shake flask (Vasala et al. 2006; Scheidle et al. 2007). In addition, small changes such as shake flask design and plug material can be improved the oxygen transfer rate

(Mrotzek et al. 2001; Maier and Büchs 2001). Controlling of oxygen consumption rate in shake flask is a simple strategy that can be occurred by cultivation in lower temperature and limitation of carbon source feeding (Yamanè and Shimizu 1984, p 147). As an alternative strategy, an enzyme or polymer-controlled glucose auto-delivery system with an optimized medium in shake flasks may allow reducing carbon overflow and acetate accumulation (avoiding pH drop) (Jeude et al. 2006; Panula-Perälä et al. 2008; Krause et al. 2010). One attractive approach to this end is fed batch process in a benchtop bioreactor. A two-step fed-batch fermentation, which can overcome limitations of conventional fed-batch cultivation in the shake flasks for recombinant *E. coli* FUS4.7R was attempted to enhance the 2-PE/tyrosol productivity (Figure **3-46**). Therefore, the cultivation was shifted to the two-phase fed batch mode after complete exhaustion of glucose, indicated by a sudden increase in the PO_2. Like the previous fed-batch cultivation (Figure **3-27**), the linear gradient feeding method was then employed to control the glucose concentration in the fed-batch fermentation. In addition, the organic solvent (30% PPG 1200) was added to the fed batch process when recombinant *E.coli* had sufficiently grown, thereby possible side effects on the early growth of the *E.coli* were also prevented (Li et al. 2018). In the two-phase process, the highest aqueous 2-PE and tyrosol concentration was 0.45 and 1.2 g l^{-1} after approximately 95 hours, respectively (Figure **3-46**). In contrast, in the organic phase, the highest amount of 2-PE and tyrosol, 6.1 and 5.6 g l^{-1} was found, at a phase ratio of 1 (aqueous): 13.5 (organic) (v/v) and 1: 4.5 (v/v), respectively. These results suggested that 2-PE production rate is less than the 2-PE accumulation rate, which results in a higher accumulation of 2-PE in organic phase than aqueous phase. Furthermore, it seems that production of tyrosol in this process is apparently faster than extraction to organic phase throughout the process, demonstrating the high concentration of tyrosol in the aqueous phase (low ratio 1:4.5). However, in both case of 2-PE and tyrosol, the final concentration in the aqueous phase is still lower than concentration that causes toxicity (Figure **3-46**). In the present work, the best results were obtained in the bioreactor with glucose as carbon source (Table **4-6**), resulting in a final 2-PE and tyrosol concentration of 3.1 g l^{-1} and 3.6 g l^{-1} with yields of 0.07 g g^{-1} of glucose (15 % C mol.mol^{-1}) and 0.08 g g^{-1} of glucose (14 % C mol.mol^{-1}), respectively. In spite of the fact that the overall production yield decreased somewhat compared to the shake flask (Table **3-11** and Table **3-12**), the process was faster than shake flask, also downstream processing of the 2-PE/tyrosol in two-phase process was facilitated, as described in the next paragraph. To the best

of my knowledge, the 2-PE/tyrosol overall yield obtained in this work was higher than those previously reported either using single phase (Satoh et al. 2012b; Koma et al. 2012; Kang et al. 2014; Bai et al. 2014; Xue et al. 2017) or a two phase fed batch process (Li et al. 2018) (Table 4-4). The organic phase contained some extracted minimal medium components and the majority of the product 2-PE/tyrosol. Purification steps are required to obtain the pure product. The boiling point of 2-PE and tyrosol is 225 °C and 158°C, respectively, while PPG1200 has a boiling point of 287.6 °C at atmospheric pressure. Therefore the product can be easily evaporated from the organic solvent, but nevertheless evaporation from the aqueous phase is slow and difficult (Hua and Xu 2011).

One of the problems in using of PPG 1200, despite of high partition coefficient in extracting 2-PE from the water phase, is that it forms emulsions with the water phase, causing further problems in the extraction process (Gao and Daugulis 2009). There are several alternative ways to recover the product from the organic phase or aqueous phase. Product recovery by liquid-liquid extraction (ethyl acetate) is a possibility (Allouche et al. 2004; Chreptowicz et al. 2016), although competition between 2-PE/tyrosol and extracted minimal medium components with similar chemical/physical properties for binding onto the organic phase may limit the efficiency of this method. In this research, the 2-PE/tyrosol into an ethyl acetate phase was extracted. If only one extraction step is applied, aqueous phase still contains a large amount of 2-PE/tyrosol. Additional extraction steps (3-5 steps) will obviously result in a higher recovery. Subsequent phase separation and solvent evaporation then resulted in 2-PE as well as tyrosol production with high yield efficiency (69.6% 2-PE and 50.3% tyrosol) and purity (~ > 81% 2-PE and > 71% tyrosol) in a biotechnological process utilizing *E.coli* (Figure 3-47 and Figure 3-48). In addition, the major point here is that the solvent used is non-toxic and suitable for the extraction of natural products, which may later be used as a food additive (Chreptowicz et al. 2016). Moreover, ethyl acetate is easily recyclable, which is economically interesting due to reducing waste and saving money. Although, this method is previously described as simple and rapid methods which can effectively extracted 2-PE from broth culture, it is the first report of a complete methodology for 2-PE as well as tyrosol production, from biosynthesis to purification of the final product. In conclusion, the purification methods described here are very general, and the other alternative methods e.g., biphasic Ionic Liquid (Sendovski et al. 2010) can be used to further improve downstream processing of 2-PE/tyrosol or any other aromatic alcohols.

5. Outlook

In this study several recombinant plasmids and *E. coli* strains were constructed and employed for the whole-cell synthesis of various aromatic amines and aromatic alcohols. The results presented here are promising for the development of production processes of other aromatic amines/aromatic alcohols from simple sugars by *E. coli*. Although, many attempts have been made to recombinantly produce various aromatic amines and aromatic alcohols by *E. coli*, different approaches were applied and the final titer, yield and productivity obtained was not as high as in this study (Mehl et al. 2003; Atsumi et al. 2008b; Koma et al. 2012; Satoh et al. 2012b; Kang et al. 2014; Bai et al. 2014; Masuo et al. 2016; Tateyama et al. 2016; Xue et al. 2017; Machas et al. 2017; Li et al. 2018; Liu et al. 2018).

In order to make the described whole-cell synthesis of the aromatic amines or aromatic alcohols even more efficient with higher yields and the lowest possible cost, further suggestions can be considered. One approach is to optimize the fermentation process such as medium composition (modified for N source, in case of aromatic amine production), oxygen supply (too much supplemental oxygen apparently cause decomposition of PAPE and 4-APA) and glucose/glycerol and L-Phe/L-Tyr feeding (exponential feeding). The bioreactor system used in this study was a closed system; it would be interesting to apply fed-batch cultivation in a bioreactor system through which the final product can be continuously harvested (in case of 4-APA and PAPE that are sensitive to the excess of oxygen, also for 2-PE/tyrosol that are toxic for *E.coli*) while feeding simultaneously. Another possibility is employing complete integration of the heterologous pathways into the chromosome to decrease the cell growth burden on the host that results from overexpression of heterologous genes and the elimination of using antibiotics, possibly allowing increase of growth and production rates (Albermann et al. 2010; Baumgärtner et al. 2013). Analysis of the codon usage of heterologous genes (*aro10*, *pabAB*) followed by replacement of rare codons can also be effective for the improvement of production. The enhanced flux through the shikimate pathway by overexpression of *aroFBL* showed a beneficial effect in this study. Other studies demonstrated that the overexpression of the other shikimate pathway genes (*aroA,C, D* and *E*) led to the improved formation of L-Tyr (Juminaga et al. 2012), salvianic acid A (Zhou et al. 2017) and avenanthramide D (Eudes et al. 2013) which are derived

from chorismic acid. This positive effect can be also observed for the target products in this study. Another strategy is *feaB* inactivation (Satoh et al. 2012b; Bai et al. 2014; Xue et al. 2017; Machas et al. 2017; Liu et al. 2018) to suppress phenylacetic acid (PAA)/4-hydroxyphenyl acetic acid (4-HPAA) competing pathway. It is therefore of interest to investigate *feaB* mutation, resulting in a further improved process. An alternative to the *E. coli* strains, gram-positive microorganisms such as *Bacillus*, *Corynebacterium, Clostridium* or yeasts (with higher resistance to aromatic alcohols) can be used (Hara et al. 2014; Li and Borodina 2014; Choi et al. 2014). Over the years, several microbial platform strains have significantly improved, allowing the production fine chemicals and higher alcohols such as isobutanol and 2-methyl-1-propanol in *Bacillus subtilis* (Li et al. 2011 and 2012), 1-butanol in *clostridia* (Lee et al. 2008), several amino acids and valuable chemicals (Becker et al. 2011; Schneider et al. 2011; Shi et al. 2013; Park et al. 2014; Baritugo et al. 2018) and C4-C5 higher alcohols in *Corynebacterium glutamicum* (Blombach et al. 2011; Su et al. 2014 and 2016).

These works constitute a 'proof of concept' that it is possible to create a platform producers, which comprise a high-flux shikimate pathway and aromatic amines or aromatic alcohols pathway as powerful starting points to derive other high-value aromatic amines or alcohols. Prominent candidates are described in the following (Figure **5-1**): One possibility is conversion of *para*-aminophenylpyruvate (APP), as main intermediate in L-PAPA pathway, to *para*-aminophenyllactic acid (PAPL) through the expression of lactate dehydrogenase (LDH) (Koma et al. 2012; Yao et al. 2013). Additionally, through expression of phenylammonia lyase (PAL), L-PAPA can be converted to 4-aminocinnamic acid (4-ACA) (Suvannasara et al. 2014) and subsequently reduced to 4-aminohydrocinnamic acid (4-AHCA) by enoate reductase (*ca2ENR*) from *Clostridium acetobutylicum* (Kawasaki et al. 2018). Another possibility would be L-amino acid decarboxylation of L-PAPA to *para*-aminophenyl ethylamine (PAPEA) by heterologous expression of aromatic amino acid decarboxylases AADC from *Solanum lycopersicum* or *Aspergillus oryzae* (Tieman et al. 2006; Masuo et al. 2016). Heterologous expression of heme oxygenase (ObiL) and ThdP-decarboxylase (ObiG) from *Pseudomonas fluorescens*, possibly allow oxidation of L-PAPA to *para*-nitrophenylalanine (PNPA) and then decarboxylation of PNPA to *para*-nitrophenylacetaldehyde (PNPAL) (Schaffer et al. 2017). Furthermore, it might be possible that pyridoxal-5′-phosphate (PLP)-dependent l-threonine aldolase (ObiH) convert

produced PNPAL from the previous step into the β-hydroxy-*para*-nitrohomophenylalanine (β-OH-PNHP) by adding the serine group, a part of obaflurin biosynthesis pathway in *Pseudomonas fluorescens* (Schaffer et al. 2017).

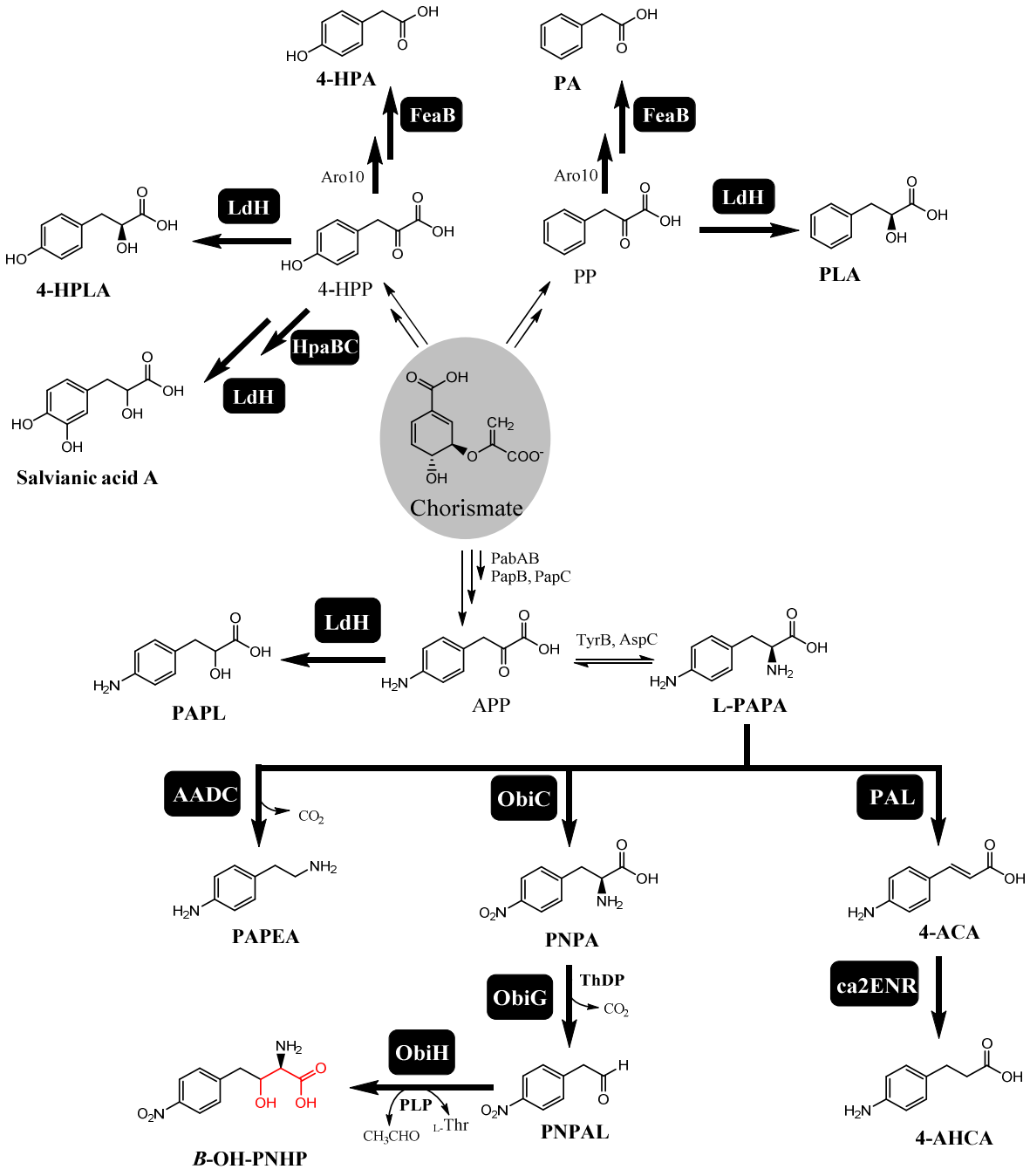

Figure 5-1 Possible perspectives in this study. The information given in this figure is taken from previous works (Koma et al. 2012; Masuo et al. 2016; Schaffer et al. 2017; Zhou et al. 2017; Kawasaki et al. 2018).

On the other side, other aromatic alcohols can also be produced through the Ehrlich pathway, which has been successfully established in *E.coli*. For instance (Figure **5-1**), it is possible to produce two analogs of pheyllactic acid and 4-hydroxy phenyllactic acid from PP and 4-HPP, respectively, through the expression of lactate dehydrogenase (LDH) (Koma et al. 2012). Also, 4-HPP can be converted to Salvianic acid A (SAA) via two enzymes 4-hydroxyphenylacetate 3-hydroxylase (encoded by *hpaBC*) and lactate dehydrogenase (*ldh*) (Zhou et al. 2017). Additionally, produced tyrosol can either be converted to hydroxytyrosol by HpaBC (Li et al. 2018) or salidroside by glucosyltransferase from *Rhodiola sachalinensis* (Bai et al. 2014). Production of phenyl acetic acid and 4-hydroxyl phenyl acetic acid as other valuable aromatic alcohols will be possible by expression of the phenyl acetaldehyde dehydrogenase (*feaB*) from *E. coli* (Koma et al. 2012). Besides classic metabolic engineering, metabolic flux analysis (13CFlux) would be an attractive approach to understand how aromatic amine/aromatic alcohols influence carbon balances of central metabolism pathway or shikimate pathway (possibly find the bottlenecks and improve final product) and get more information about the regulatory points in *E.coli* (Lee et al. 2011; Buchholz et al. 2014; Antoniewicz 2015; Wada et al. 2017; Okahashi et al. 2017). However, as explained in this thesis, the effective combination of microbial and process-engineering principles offer bioprocesses at high productivity. This study demonstrates that it is possible to manipulate precursor levels through metabolic grafting, providing ways to further improve final titer of target products.

6. Appendix

DNA sequences

Sequence of phenylpyruvate decarboxylase (*aro10*), *Saccharomyces cerevisiae S288c*

NCBI Gene ID: 851987

5´**ATG**GCACCTGTTACAATTGAAAAGTTCGTAAATCAAGAAGAACGACACCTTGTTTCCAACCGATCAGCAACAAT
TCCGTTTGGTGAATACATATTTAAAAGATTGTTGTCCATCGATACGAAATCAGTTTTCGGTGTTCCTGGTGACTTCA
ACTTATCTCTATTAGAATATCTCTATTCACCTAGTGTTGAATCAGCTGGCCTAAGATGGGTCGGCACGTGTAATGAA
CTGAACGCCGCTTATGCGGCCGACGGATATTCCCGTTACTCTAATAAGATTGGCTGTTTAATAACCACGTATGGCG
TTGGTGAATTAAGCGCCTTGAACGGTATAGCCGGTTCGTTCGCTGAAAATGTCAAAGTTTTGCACATTGTTGGTGT
GGCCAAGTCCATAGATTCGCGTTCAAGTAACTTTAGTGATCGGAACCTACATCATTTGGTCCCACAGCTACATGAT
TCAAATTTTAAAGGGCCAAATCATAAAGTATATCATGATATGGTAAAAGATAGAGTCGCTTGCTCGGTAGCCTACT
TGGAGGATATTGAAACTGCATGTGACCAAGTCGATAATGTTATCCGCGATATTTACAAGTATTCTAAACCTGGTTA
TATTTTTGTTCCTGCAGATTTTGCGGATATGTCTGTTACATGTGATAATTTGGTTAATGTTCCACGTATATCTCAACA
AGATTGTATAGTATACCCTTCTGAAAACCAATTGTCTGACATAATCAACAAGATTACTAGTTGGATATATTCCAGT
AAAACACCTGCGATCCTTGGAGACGTACTGACTGATAGGTATGGTGTGAGTAACTTTTTGAACAAGCTTATCTGCA
AAACTGGGATTTGGAATTTTTCCACTGTTATGGGAAAATCTGTAATTGATGAGTCAAACCCAACTTATATGGGTCA
ATATAATGGTAAAGAAGGTTTAAAACAAGTCTATGAACATTTTGAACTGTGCGACTTGGTCTTGCATTTTGGAGTC
GACATCAATGAAATTAATAATGGGCATTATACTTTTACTTATAAACCAAATGCTAAAATCATTCAATTTCATCCGA
ATTATATTCGCCTTGTGGACACTAGGCAGGGCAATGAGCAAATGTTCAAAGGAATCAATTTTGCCCCTATTTTAAA
AGAACTATACAAGCGCATTGACGTTTCTAAACTTTCTTTGCAATATGATTCAAATGTAACTCAATATACGAACGAA
ACAATGCGGTTAGAAGATCCTACCAATGGACAATCAAGCATTATTACACAAGTTCACTTACAAAAGACGATGCCT
AAATTTTTGAACCCTGGTGATGTTGTCGTTTGTGAAACAGGCTCTTTTCAATTCTCTGTTCGTGATTTCGCGTTTCCT
TCGCAATTAAAATATATATCGCAAGGATTTTTCCTTTCCATTGGCATGGCCCTTCCTGCCGCCCTAGGTGTTGGAAT
TGCCATGCAAGACCACTCAAACGCTCACATCAATGGTGGCAACGTAAAAGAGGACTATAAGCCAAGATTAATTTT
GTTTGAAGGTGACGGTGCAGCACAGATGACAATCCAAGAACTGAGCACCATTCTGAAGTGCAATATTCCACTAGA
AGTTATCATTTGGAACAATAACGGCTACACTATTGAAAGAGCCATCATGGGCCCTACCAGGTCGTATAACGACGTT
ATGTCTTGGAAATGGACCAAACTATTTGAAGCATTCGGAGACTTCGACGGAAAGTATACTAATAGCACTCTCATTC
AATGTCCCTCTAAATTAGCACTGAAATTGGAGGAGCTTAAGAATTCAAACAAAAGAAGCGGGATAGAACTTTTAG
AAGTCAAATTAGGCGAATTGGATTTCCCCGAACAGCTAAAGTGCATGGTTGAAGCAGCGGCACTTAAAAGAAATA
AAAAATAG 3´

Alcohol dehydrogenase (*adHI*), *Saccharomyces cerevisiae S288c*

NCBI Gene ID: 854068

5'**ATG** TCTATCCCAGAAACTCAAAAAGGTGTTATCTTCTACGAATCCCACGGTAAGTTGGAATACAAAGATA
TTCCAGTTCCAAAGCCAAAGGCCAACGAATTGTTGATCAACGTTAAATACTCTGGTGTCTGTCACACTGA
CTTGCACGCTTGGCACGGTGACTGGCCATTGCCAGTTAAGCTACCATTAGTCGGTGGTCACGAAGGTGCC
GGTGTCGTTGTCGGCATGGGTGAAAACGTTAAGGGCTGGAAGATCGGTGACTACGCCGGTATCAAATGGT
TGAACGGTTCTTGTATGGCCTGTGAATACTGTGAATTGGGTAACGAATCCAACTGTCCTCACGCTGACTT
GTCTGGTTACACCCACGACGGTTCTTTCCAACAATACGCTACCGCTGACGCTGTTCAAGCCGCTCACATT
CCTCAAGGTACCGACTTGGCCCAAGTCGCCCCCATCTTGTGTGCTGGTATCACCGTCTACAAGGCTTTGA
AGTCTGCTAACTTGATGGCCGGTCACTGGGTTGCTATCTCCGGTGCTGCTGGTGGTCTAGGTTCTTTGGC
TGTTCAATACGCCAAGGCTATGGGTTACAGAGTCTTGGGTATTGACGGTGGTGAAGGTAAGGAAGAATTA
TTCAGATCCATCGGTGGTGAAGTCTTCATTGACTTCACTAAGGAAAAGGACATTGTCGGTGCTGTTCTAA
AGGCCACTGACGGTGGTGCTCACGGTGTCATCAACGTTTCCGTTTCCGAAGCCGCTATTGAAGCTTCTAC
CAGATACGTTAGAGCTAACGGTACCACCGTTTTGGTCGGTATGCCAGCTGGTGCCAAGTGTTGTTCTGAT
GTCTTCAACCAAGTCGTCAAGTCCATCTCTATTGTTGGTTCTTACGTCGGTAACAGAGCTGACACCAGAG
AAGCTTTGGACTTCTTCGCCAGAGGTTTGGTCAAGTCTCCAATCAAGGTTGTCGGCTTGTCTACCTTGCC
AGAAATTTACGAAAAGATGGAAAAGGGTCAAATCGTTGGTAGATACGTTGTTGACACTTCTAAATAA 3'

Alcohol dehydrogenase (*adHII*), *Saccharomyces cerevisiae S288c*

NCBI Gene ID: 855349

5´ATGTCTATTCCAGAAACTCAAAAAGCCATTATCTTCTACGAATCCAACGGCAAGTTGGAGCATAAGGATATCCCA
GTTCCAAAGCCAAAGCCCAACGAATTGTTAATCAACGTCAAGTACTCTGGTGTCTGCCACACCGATTTGCACGCTT
GGCATGGTGACTGGCCATTGCCAACTAAGTTACCATTAGTTGGTGGTCACGAAGGTGCCGGTGTCGTTGTCGGCAT
GGGTGAAAACGTTAAGGGCTGGAAGATCGGTGACTACGCCGGTATCAAATGGTTGAACGGTTCTTGTATGGCCTGT
GAATACTGTGAATTGGGTAACGAATCCAACTGTCCTCACGCTGACTTGTCAGGTTACACCCACGACGGTTCTTTCC
AAGAATACGCTACCGCTGACGCTGTTCAAGCCGCTCACATTCCTCAAGGTACTGACTTGGCTGAAGTCGCGCCAAT
CTTGTGTGCTGGTATCACCGTATACAAGGCTTTGAAGTCTGCCAACTTGAGAGCAGGCCACTGGGCGGCCATTTCT
GGTGCTGCTGGTGGTCTAGGTTCTTTGGCTGTTCAATATGCTAAGGCGATGGGTTACAGAGTCTTAGGTATTGATG
GTGGTCCAGGAAAGGAAGAATTGTTTACCTCGCTCGGTGGTGAAGTATTCATCGACTTCACCAAAGAGAAGGACA
TTGTTAGCGCAGTCGTTAAGGCTACCAACGGCGGTGCCCACGGTATCATCAATGTTTCCGTTTCCGAAGCCGCTAT
CGAAGCTTCTACCAGATACTGTAGGGCGAACGGTACTGTTGTCTTGGTTGGTTTGCCAGCCGGTGCAAAGTGCTCC
TCTGATGTCTTCAACCACGTTGTCAAGTCTATCTCCATTGTCGGCTCTTACGTGGGGAACAGAGCTGATACCAGAG
AAGCCTTAGATTTCTTTGCCAGAGGTCTAGTCAAGTCTCCAATAAAGGTAGTTGGCTTATCCAGTTTACCAGAAATT
TACGAAAAGATGGAGAAGGGCCAAATTGCTGGTAGATACGTTGTTGACACTTCTAAA TAA 3´

Phenylacetaldehyde dehydrogenase (*feaB*), *Escherichia coli str. K-12 substr. MG1655*

NCBI Gene ID: 945933

5' **ATG**ACAGAGCCGCATGTAGCAGTATTAAGCCAGGTCCAACAGTTTCTCGATCGTCAACACGGTCTTTATA
TTGATGGTCGTCCTGGCCCCGCACAAAGTGAAAAACGGTTGGCGATCTTTGATCCGGCCACCGGGCAAGA
AATTGCGTCTACTGCTGATGCCAACGAAGCGGATGTAGATAACGCAGTCATGTCTGCCTGGCGGGCCTTT
GTCTCGCGTCGCTGGGCCGGGCGATTACCCGCAGAGCGTGAACGTATTCTGCTACGTTTTGCTGATCTGG
TGGAGCAGCACAGTGAGGAGCTGGCGCAACTGGAAACCCTGGAGCAAGGCAAGTCAATTGCCATTTCCCG
TGCTTTTGAAGTGGGCTGTACGCTGAACTGGATGCGTTATACCGCCGGGTTAACGACCAAAATCGCGGGT
AAAACGCTGGACTTGTCGATTCCCTTACCCCAGGGGGCGCGTTATCAGGCCTGGACGCGTAAAGAGCCGG
TTGGCGTAGTGGCGGGAATTGTGCCATGGAACTTTCCGTTGATGATTGGTATGTGGAAGGTGATGCCAGC
ACTGGCAGCAGGCTGTTCAATCGTGATTAAGCCTTCGGAAACCACGCCACTGACGATGTTGCGCGTGGCG
GAACTGGCCAGCGAGGCTGGTATCCCTGATGGCGTTTTTAATGTCGTCACCGGGTCAGGTGCTGTATGCG
GCGCGGCCCTGACGTCACATCCTCATGTTGCGAAAATCAGTTTTACCGGTTCAACCGCGACGGGAAAAGG
TATTGCCAGAACTGCTGCTGATCACTTAACGCGTGTAACGCTGGAACTGGGCGGTAAAAACCCGGCAATT
GTATTAAAAGATGCTGATCCGCAATGGGTTATTGAAGGCTTGATGACCGGAAGCTTCCTGAATCAAGGGC
AAGTATGCGCCGCCAGTTCGCGAATTTATATTGAAGCGCCGTTGTTTGACACGCTGGTTAGTGGATTTGA
GCAGGCGGTAAAATCGTTGCAAGTGGGACCGGGGATGTCACCTGTTGCACAGATTAACCCTTTGGTTTCT
CGTGCGCACTGCGACAAAGTGTGTTCATTCCTCGACGATGCGCAGGCACAGCAAGCAGAGCTGATTCGCG
GGTCGAATGGACCAGCCGGAGAGGGGTATTATGTTGCGCCAACGCTGGTGGTAAATCCCGATGCTAAATT
GCGCTTAACTCGTGAAGAGGTGTTTGGTCCGGTGGTAAACCTGGTGCGAGTAGCGGATGGAGAAGAGGCG
TTACAACTGGCAAACGACACGGAATATGGCTTAACTGCCAGTGTCTGGACGCAAAATCTCTCCCAGGCTC
TGGAATATAGCGATCGCTTACAGGCAGGGACGGTGTGGGTAAACAGCCATACCTTAATTGACGCTAACTT
ACCGTTTGGTGGGATGAAGCAGTCAGGAACGGGCCGTGATTTTGGCCCCGACTGGCTGGACGGTTGGTGT
GAAACTAAGTCGGTGTGTGTACGGTATTAA 3'

Aldehyde dehydrogenase (*yahK*), *Escherichia coli str. K-12 substr. MG1655*

NCBI Gene ID: 944975

5'**ATG**AAGATCAAAGCTGTTGGTGCATATTCCGCTAAACAACCACTTGAACCGATGGATATCACCCGGCGTG
AACCGGGACCGAATGATGTCAAAATCGAAATCGCTTACTGTGGCGTTTGCCATTCCGATCTCCACCAGGT
CCGTTCCGAGTGGGCGGGGACGGTTTACCCCTGCGTGCCGGGTCATGAAATTGTGGGGCGTGTGGTAGCC
GTTGGTGATCAGGTAGAAAAATATGCGCCGGGCGATCTGGTCGGTGTCGGCTGCATTGTCGACAGTTGTA
AACATTGCGAAGAGTGTGAAGACGGGTTGGAAAACTACTGTGATCACATGACCGGCACCTATAACTCGCC
GACGCCGGACGAACCGGGCCATACTCTGGGCGGCTACTCACAACAGATCGTCGTTCATGAGCGATATGTT
CTGCGTATTCGTCACCCGCAAGAGCAGCTGGCGGCGGTGGCTCCTTTGTTGTGTGCAGGGATCACCACGT
ATTCGCCGCTACGTCACTGGCAGGCCGGGCCGGGTAAAAAAGTGGGCGTGGTCGGCATCGGCGGTCTGGG
ACATATGGGGATTAAGCTGGCCCACGCGATGGGGGCACATGTGGTGGCATTTACCACTTCTGAGGCAAAA
CGCGAAGCGGCAAAAGCCCTGGGGGCCGATGAAGTTGTTAACTCACGCAATGCCGATGAGATGGCGGCTC
ATCTGAAGAGTTTCGATTTCATTTTGAATACAGTAGCTGCGCCACATAATCTCGACGATTTTACCACCTT
GCTGAAGCGTGATGGCACCATGACGCTGGTTGGTGCGCCTGCGACACCGCATAAATCGCCGGAAGTTTTC
AACCTGATCATGAAACGCCGTGCGATAGCCGGTTCTATGATTGGCGGCATTCCAGAAACTCAGGAGATGC

TCGATTTTTGCGCCGAACATGGCATCGTGGCTGATATAGAGATGATTCGGGCCGATCAAATTAATGAAGC
CTATGAGCGAATGCTGCGCGGTGATGTGAAATATCGTTTTGTTATCGATAATCGCACACTAACAGACTGA 3'

LC-MS Analysis

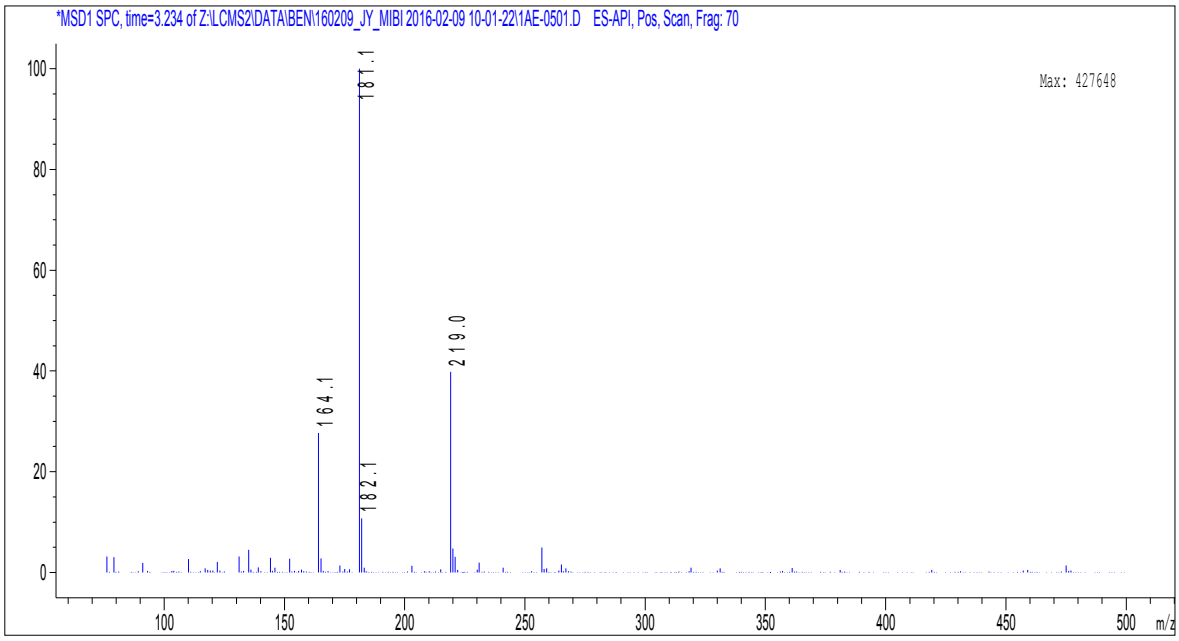

Appendix-A1 ESI mass spectrum of PAPA standard. Recorded by Agilent 6130 mass spectrometer, TOF-Q system in the positive field of view. The strongest signal corresponds to the mass of the H^+ adduct to PAPA (m / z = 181.1).

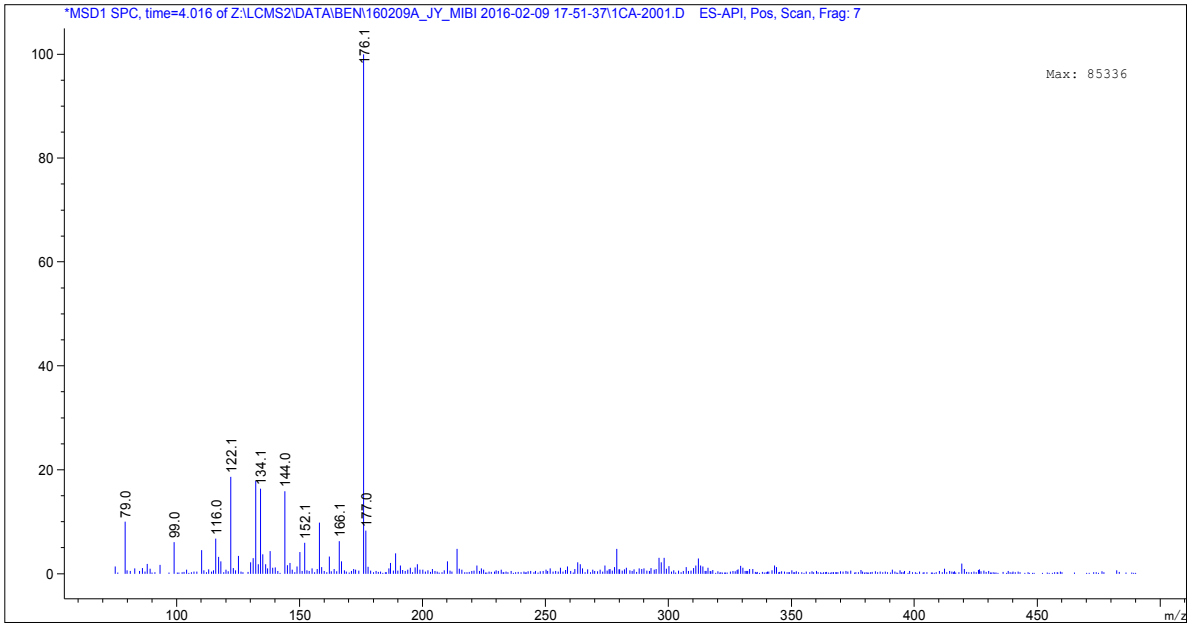

Appendix-A2. ESI mass spectrum of PAPE standard. Recorded by Agilent 6130 mass spectrometer, TOF-Q system in the positive field of view. The strongest signal corresponds to the mass of the K^+ adduct to PAPE (m / z = 176.1).

Appendix-A3. ESI mass spectrum of 4-APA standard. Recorded by Agilent 6130 mass spectrometer, TOF-Q system in the positive field of view. The strongest signal corresponds to the mass of the H^+ adduct to 4-APA (m / z = 153).

7. References

Achmon Y, Fishman A (2015) The antioxidant hydroxytyrosol: biotechnological production challenges and opportunities. *Appl Microbiol Biotechnol* 99:1119–1130 .

Ahn JO, Lee HW, Saha R, Park MS, Jung J-K, Lee D-Y (2008) Exploring the effects of carbon sources on the metabolic capacity for shikimic acid production in *Escherichia coli* using in silico metabolic predictions. *J Microbiol Biotechnol* 18:1773–84

Ajikumar PK, Xiao W-H, Tyo KEJ, Wang Y, Simeon F, Leonard E, Mucha O, Phon TH, Pfeifer B, Stephanopoulos G (2010) Isoprenoid pathway optimization for Taxol precursor overproduction in *Escherichia coli*. *Science* 330:70–4 .

Albermann C, Ghanegaonkar S, Lemuth K, Vallon T, Reuss M, Armbruster W, Sprenger GA (2008) Biosynthesis of the Vitamin E Compound δ-Tocotrienol in Recombinant *Escherichia coli* Cells. *ChemBioChem* 9:2524–2533 .

Albermann C, Trachtmann N, Sprenger GA (2010) A simple and reliable method to conduct and monitor expression cassette integration into the *Escherichia coli* chromosome. *Biotechnol* J 5:32–38.

Allouche N, Damak M, Ellouz R, Sayadi S (2004) Use of Whole Cells of Pseudomonas aeruginosa for Synthesis of the Antioxidant Hydroxytyrosol via Conversion of Tyrosol. *Appl Environ Microbiol* 70:2105–2109 .

Ali S, Shultz JL, and Ikram-ul-Haq (2007) High performance microbiological transformation of L-tyrosine to L-dopa by *Yarrowia lipolytica NRRL*-143. *BMC Biotechnol*. 7(1): 50.

Almeida JRM, Fávaro LCL, Quirino BF (2012) Biodiesel biorefinery: opportunities and challenges for microbial production of fuels and chemicals from glycerol waste. *Biotechnol Biofuels* 5:48 .

Altieri C, Sinigaglia M, Corbo M, Buonocore G, Falcone P, Del Nobile M (2004) Use of entrapped microorganisms as biological oxygen scavengers in food packaging applications. *LWT - Food Sci Technol* 37:9–15 .

Andersen KB, von Meyenburg K (1980) Are growth rates of *Escherichia coli* in batch cultures limited by respiration? *J Bacteriol* 144:114–23

Andrianantoandro E, Basu S, Karig DK, Weiss R (2006) Synthetic biology: new engineering rules for an emerging discipline. *Mol Syst Biol* 2:2006.0028 .

Anter J, Tasset I, Demyda-Peyrás S, Ranchal I, Moreno-Millán M, Romero-Jimenez M, Muntané J, Luque de Castro MD, Muñoz-Serrano A, Alonso-Moraga Á (2014) Evaluation of potential antigenotoxic, cytotoxic and proapoptotic effects of the olive oil by-product “alperujo”, hydroxytyrosol, tyrosol and verbascoside. *Mutat Res Toxicol Environ Mutagen* 772:25–33 .

Antoni D, Zverlov V V., Schwarz WH (2007) Biofuels from microbes. *Appl Microbiol Biotechnol* 77:23–35 .

Antoniewicz MR (2015) Methods and advances in metabolic flux analysis: a mini-review. *J Ind Microbiol Biotechnol* 42:317–325 .

Aristidou AA, San K-Y, Bennett GN (1995) Metabolic engineering of *Escherichia coli* to enhance recombinant protein production through acetate reduction. *Biotechnol Prog* 11:475–478 .

Aristidou AA, San K-Y, Bennett GN (1994) Modification of central metabolic pathway in *Escherichia coli* to reduce acetate accumulation by heterologous expression of thebacillus subtilis acetolactate synthase gene. *Biotechnol Bioeng* 44:944–951 .

Arora PK (2015) Bacterial degradation of monocyclic aromatic amines. *Front Microbiol* 6:820 .

Atsumi S, Cann AF, Connor MR, Shen CR, Smith KM, Brynildsen MP, Chou KJY, Hanai T, Liao JC (2008) Metabolic engineering of *Escherichia coli* for 1-butanol production. *Metab Eng* 10:305–311 .

Atsumi S, Hanai T, Liao JC (2008) Non-fermentative pathways for synthesis of branched-chain higher alcohols as biofuels. *Nature* 451:86–89 .

Atsumi S, Wu T-Y, Eckl E-M, Hawkins SD, Buelter T, Liao JC (2010) Engineering the isobutanol biosynthetic pathway in *Escherichia coli* by comparison of three aldehyde reductase/alcohol dehydrogenase genes. *Appl Microbiol Biotechnol* 85:651–657 .

Backman K, O'Connor MJ, Maruya A, Rudd E, McKay D, Balakrishnan R, Radjai M, DiPasquantonio V, Shoda D, Hatch R (1990) Genetic engineering of metabolic pathways applied to the production of phenylalanine. *Ann N Y Acad Sci* 589:16–24

Báez-Viveros JL, Flores N, Juárez K, Castillo-España P, Bolivar F, Gosset G (2007) Metabolic transcription analysis of engineered *Escherichia coli* strains that overproduce L-phenylalanine. *Microb Cell Fact* 6:30 .

Baheri H, Hill G, Roesler W (2001) Modelling plasmid instability in batch and continuous fermentors. *Biochem Eng J* 8:45–50 . doi:

Bai Y, Bi H, Zhuang Y, Liu C, Cai T, Liu X, Zhang X, Liu T, Ma Y (2014) Production of salidroside in metabolically engineered Escherichia coli. *Sci Rep* 4:6640 .

Bailey JE (1991) Toward a science of metabolic engineering. *Science* 252:1668–75

Balderas-Hernandez VE, Sabido-Ramos A, Silva P, Cabrera-Valladares N, Hernandez-Chavez G, Baez-Viveros JL, Martinez A, Bolivar F, Gosset G (2009) Metabolic engineering for improving anthranilate synthesis from glucose in Escherichia coli. *Microb Cell Fact* 8:19 .

Bang HB, Lee YH, Kim SC, Sung CK, Jeong KJ (2016) Metabolic engineering of *Escherichia coli* for the production of cinnamaldehyde. *Microb Cell Fact* 15:16 .

Barbirato F, Chedaille D, Bories A (1997) Propionic acid fermentation from glycerol: comparison with conventional substrates. *Appl Microbiol Biotechnol* 47:441–446 .

Baritugo K-A, Kim HT, David Y, Choi J, Hong SH, Jeong KJ, Choi JH, Joo JC, Park SJ (2018) Metabolic engineering of *Corynebacterium glutamicum* for fermentative production of chemicals in biorefinery. *Appl Microbiol Biotechnol* 102:3915–3937 .

Barker JL, Frost JW (2001) Microbial synthesis of p-hydroxybenzoic acid from glucose. *Biotechnol Bioeng* 76:376–90

Baumgärtner F (2016) Biotechnologische Darstellung und strukturelle Charakterisierung fucosylierter Oligosaccharide. Univ Stuttgart, PhD Thesis.

Baumgärtner F, Conrad J, Sprenger GA, Albermann C (2014) Synthesis of the human milk oligosaccharide lacto-N-tetraose in metabolically engineered, plasmid-free E. coli. *Chembiochem* 15:1896–1900 .

Baumgärtner F, Seitz L, Sprenger GA, Albermann C (2013) Construction of *Escherichia coli* strains with chromosomally integrated expression cassettes for the synthesis of 2'-fucosyllactose. *Microb Cell Fact* 12:1–13 .

Becker J, Zelder O, Häfner S, Schröder H, Wittmann C (2011) From zero to hero—Design-based systems metabolic engineering of Corynebacterium glutamicum for l-lysine production. *Metab Eng* 13:159–168 .

Bedair AH, Ali FM, El-Agrody AM, Eid FA, El-Nassag MAA, El-Sherbeny G (2006) Preparation of 4-aminophenylacetic acid derivatives with promising antimicrobial activity. *Acta Pharm* 56:273–84

Benner SA, Sismour AM (2005) Synthetic biology. *Nat Rev Genet* 6:533–543 .

Bergel F, Stock JA (1954) Cyto-active amino-acid and peptide derivatives. Part I. Substituted phenylalanines. *J Chem Soc* 0:2409 .

Berry A (1996) Improving production of aromatic compounds in *Escherichia coli* by metabolic engineering. *Trends Biotechnol* 14:250–256 .

Birch ANE, Fellows LE, Evans S V., Doherty K (1986) Para-aminophenylalanine in vigna: Possible taxonomic and ecological significance as a seed defence against bruchids. *Phytochemistry* 25:2745–2749 .

Biotechnology Market Size, Share, Industry Analysis Report 2014-2025. https://www.grandviewresearch.com/industry-analysis/biotechnology-market

Bjellqvist B, Ek K, Giorgio Righetti P, Gianazza E, Görg A, Westermeier R, Postel W (1982) Isoelectric focusing in immobilized pH gradients: Principle, methodology and some applications. *J Biochem Biophys Methods* 6:317–339 .

Blanc V, Gil P, Bamas-Jacques N, Lorenzon S, Zagorec M, Schleuniger J, Bisch D, Blanche F, Debussche L, Crouzet J, Thibaut D (1997) Identification and analysis of genes from Streptomyces pristinaespiralis encoding enzymes involved in the biosynthesis of the 4-dimethylamino-l-phenylalanine precursor of pristinamycin I. *Mol Microbiol* 23:191–202 .

Blankschien MD, Clomburg JM, Gonzalez R (2010) Metabolic engineering of *Escherichia coli* for the production of succinate from glycerol. *Metab Eng* 12:409–419 .

Blattner FR, Plunkett G, Bloch CA, Perna NT, Burland V, Riley M, Collado-Vides J, Glasner JD, Rode CK, Mayhew GF, Gregor J, Davis NW, Kirkpatrick HA, Goeden MA, Rose DJ, Mau B, Shao Y (1997) The complete genome sequence of *Escherichia coli* K-12. *Science* 277:1453–62 .

Bloch SE (2014) Plant phenylpropanoid biosynthesis in Escherichia coli: engineering novel pathways and tools. Univ Minnesota PhD Diss 147. Retrieved from the University of Minnesota Digital Conservancy, http://hdl.handle.net/11299/168157.

Bloch SE, Schmidt-Dannert C (2014) Construction of a Chimeric Biosynthetic Pathway for the De Novo Biosynthesis of Rosmarinic Acid in *Escherichia coli*. *ChemBioChem* 15:2393–2401 .

Blombach B, Riester T, Wieschalka S, Ziert C, Youn J-W, Wendisch VF, Eikmanns BJ (2011) *Corynebacterium glutamicum* tailored for efficient isobutanol production. Appl Environ Microbiol 77:3300–10 .

Bodanszky M, Ondetti Ma (1963) Structures of the vernamycin b group of antibiotics. *Antimicrob Agents Chemother* 161:360–5

Bongaerts J, Krämer M, Müller U, Raeven L, Wubbolts M (2001) Metabolic Engineering for Microbial Production of Aromatic Amino Acids and Derived Compounds. *Metab Eng* 3:289–300 .

Bongaerts J, Esser S, Lorbach V, Al-Momani L, Müller MA, Franke D, Grondal C, Kurutsch A, Bujnicki R, Takors R, Raeven L, Wubbolts M, Bovenberg R, Nieger M, Schürmann M, Trachtmann N, Kozak S, Sprenger GA, Müller MA (2011) Diversity-Oriented Production of Metabolites Derived from Chorismate and Their Use in Organic Synthesis. *Angew Chemie Int Ed* 50:7781–7786 .

Borchard U (1998) Indexed in Chemical Abstracts EMBASE/Excerpta Medica J ournal of Clinical and Basic Cardiology www.kup.at/jcbc Pharmacological properties of beta-adrenoceptor blocking drugs. *J Clin Bas Cardiol* 1:5–9

Bouallagui Z, Sayadi S (2006) Production of High Hydroxytyrosol Yields via Tyrosol Conversion by Pseudomonas aeruginosa Immobilized Resting Cells. *J Agric Food Chem* 54:9906–11.

Bozell JJ, Petersen GR (2010) Technology development for the production of biobased products from biorefinery carbohydrates—the US Department of Energy's "Top 10" revisited. *Green Chem* 12:539.

Bradford MM (1976) A rapid and sensitive method for the quantitation of microgram quantities of protein utilizing the principle of protein-dye binding. *Anal Biochem*. 72(1–2): 248–254.

Bren A, Park JO, Towbin BD, Dekel E, Rabinowitz JD, Alon U (2016) Glucose becomes one of the worst carbon sources for E.coli on poor nitrogen sources due to suboptimal levels of cAMP. *Sci Rep* 6:24834 .

Brooks SJ, Doyle EM, O 'connor KE (2006) Tyrosol to hydroxytyrosol biotransformation by immobilised cell extracts of Pseudomonas putida F6. *Enzyme Microb Technol* 39:191–196 .

Brown MP, Aidoo KA, Vining LC (1996) A role for pabAB, a p-aminobenzoate synthase gene of Streptomyces venezuelae ISP5230, in chloramphenicol biosynthesis. *Microbiology* 142:1345–1355 .

Bruschi F, Dundar M, Gahan P, Gartland K, Szente M, Viola-Magni M, Akbarova Y (2011) Biotechnology worldwide and the 'European Biotechnology Thematic Network' Association (EBTNA). *Curr Opin Biotechnol* 22:S7–S14 .

Buchholz J, Graf M, Blombach B, Takors R (2014) Improving the carbon balance of fermentations by total carbon analyses. *Biochem Eng J* 90:162–169 .

Buijs NA, Siewers V, Nielsen J (2013) Advanced biofuel production by the yeast *Saccharomyces cerevisiae*. *Curr Opin Chem Biol* 17:480–488 .

Burgard A, Burk MJ, Osterhout R, Van Dien S, Yim H (2016) Development of a commercial scale process for production of 1,4-butanediol from sugar. *Curr Opin Biotechnol* 42:118–125 .

Burlingame R and Chapman P (1983) Catabolism of phenylpropionic acid and its 3-hydroxy derivative by *Escherichia coli*. *Journal of bacteriology*. 1983 vol: 155 (1) pp: 113-21

Byun Y, Kim YT, Whiteside S (2010) Characterization of an antioxidant polylactic acid (PLA) film prepared with α-tocopherol, BHT and polyethylene glycol using film cast extruder. *J Food Eng* 100:239–244 .

Byun Y, Whiteside S (2012) Ascorbyl palmitate-β-cyclodextrin inclusion complex as an oxygen scavenging microparticle. *Carbohydr Polym* 87:2114–2119 .

Camakaris J and Pittard J (1974) Purification and Properties of 3-Deoxy-D-arabinoheptulosonic acid-7-Phosphate Synthetase (trp) from Escherichia coli. *J Bacteriol* 120:590–597.

Caruso D, Berra B, Giavarini F, Cortesi N, Fedeli E, Galli G (1999) Effect of virgin olive oil phenolic compounds on in vitro oxidation of human low density lipoproteins. *Nutr Metab Cardiovasc Dis* 9:102–7

Caunt P, Impoolsup A, Greenfield PF (1988) Stability of recombinant plasmids in yeast. *J Biotechnol* 8:173–192 .

Chandra Raj K, Ingram L, Maupin-Furlow J (2001) Pyruvate decarboxylase: a key enzyme for the oxidative metabolism of lactic acid by Acetobacter pasteurianus. *Arch Microbiol* 176:443–451 .

Chandran SS, Yi J, Draths KM, von Daeniken R, Weber W, Frost JW (2003) Phosphoenolpyruvate Availability and the Biosynthesis of Shikimic Acid. *Biotechnol Prog* 19:808–814 .

Chang Z, Sun Y, He J VL (2001) p-Aminobenzoic acid and chloramphenicol biosynthesis in Streptomyces venezuelae: gene sets for a key enzyme, 4-amino-4-deoxychorismate synthase. *Microbiology* 147:2113–2126 .

Chen L, Zeng AP (2017) Rational design and metabolic analysis of *Escherichia coli* for effective production of L-tryptophan at high concentration. *Appl Microbiol Biot*.101(2):559–568.

Cheng C, Huang YL, Yang S-T (1997) A novel feeding strategy for enhanced plasmid stability and protein production in recombinant yeast fedbatch fermentation. *Biotechnol Bioeng* 56:23–31 .

Cheng Q, Tao L (2012) Engineering *Escherichia coli* for Canthaxanthin and Astaxanthin Biosynthesis. In: Methods in molecular biology (Clifton, N.J.). pp 143–158

Chisti Y, Jauregui-Haza UJ (2002) Oxygen transfer and mixing in mechanically agitated airlift bioreactors. *Biochem Eng J* 10:143–153 .

Choi YJ, Lee J, Jang Y-S, Lee SY (2014) Metabolic engineering of microorganisms for the production of higher alcohols. *MBio* 5:e01524-14 .

Chreptowicz K, Wielechowska M, Główczyk-Zubek J, Rybak E, Mierzejewska J (2016) Production of natural 2-phenylethanol: From biotransformation to purified product. *Food Bioprod Process* 100:275–281 .

Chreptowicz K, Mierzejewska J (2018) Enhanced bioproduction of 2-phenylethanol in a biphasic system with rapeseed oil. *New Biotechnology,* 42:56–61 .

Chung D, Kim SY, Ahn J-H (2017) Production of three phenylethanoids, tyrosol, hydroxytyrosol, and salidroside, using plant genes expressing in *Escherichia coli*. *Sci Rep* 7:2578 .

Clomburg JM, Gonzalez R (2011) Metabolic engineering of *Escherichia coli* for the production of 1,2-propanediol from glycerol. *Biotechnol Bioeng* 108:867–879 .

Cocito C (1979) Antibiotics of the virginiamycin family, inhibitors which contain synergistic components. Microbiol Rev 43:145–92

Cole ST, Eiglmeier K, Ahmed S, Honore N, Elmes L, Anderson WF and Weiner JH (1988) Nucleotide sequence and gene-polypeptide relationships of the glpABC operon encoding the anaerobic sn-glycerol-3-phosphate dehydrogenase of *Escherichia coli K-12*. *J Bacteriol*, 170(6): 2448–2456.

Cohen SN, Chang AC, Hsu L (1972) Nonchromosomal antibiotic resistance in bacteria: genetic transformation of *Escherichia coli* by R-factor DNA. *Proc. Natl. Acad. Sci*. USA, 69: 2110-2114.

Contiero J, Beatty C, Kumari S, DeSanti CL, Strohl WR, Wolfe A (2000) Effects of mutations in acetate metabolism on high-cell-density growth of *Escherichia coli. J Ind Microbiol Biotechnol* 24:421–430.

Cooper R and Skinner M (1980) Catabolism of 3- and 4-hydroxyphenylacetate by the 3,4-dihydroxyphenylacetate pathway in *Escherichia coli*. *Journal of bacteriology*. 1980 vol: 143 (1) pp: 302-6.

Covas MI, Miró-Casas E, Fitó M, Farré-Albadalejo M, Gimeno E, Marrugat J, De La Torre R (2003) Bioavailability of tyrosol, an antioxidant phenolic compound present in wine and olive oil, in humans. *Drugs Exp Clin Res* 29:203–6.

Cui Y-Y, Ling C, Zhang Y-Y, Huang J, Liu J-Z (2014) Production of shikimic acid from *Escherichia coli* through chemically inducible chromosomal evolution and cofactor metabolic engineering. *Microb Cell Fact* 13:21 .

da Silva GP, Mack M, Contiero J (2009) Glycerol: A promising and abundant carbon source for industrial microbiology. *Biotechnol Adv* 27:30–39

Dardenne GA, Larsen PO, Wieczorkowska E (1975) Biosynthesis of p-aminophenylalanine: part of a general scheme for the biosynthesis of chorisimic acid derivatives. *Biochim Biophys Acta* 381:416–23

Datsenko KA, Wanner BL (2000) One-step inactivation of chromosomal genes in *Escherichia coli* K-12 using PCR products. *Proc Natl Acad Sci* 97:6640–6645 .

De Mey M, De Maeseneire S, Soetaert W, Vandamme E (2007) Minimizing acetate formation in *E. coli* fermentations. *J Ind Microbiol Biotechnol* 34:689–700 .

de Smidt O, du Preez JC, Albertyn J (2008) The alcohol dehydrogenases of *Saccharomyces cerevisiae* : a comprehensive review. *FEMS Yeast Res* 8:967–978 .

Dedhia NN, Hottiger T, Bailey JE (1994) Overproduction of glycogen in *Escherichia coli* blocked in the acetate pathway improves cell growth. *Biotechnol Bioeng* 44:132–139 .

Delaplaza M, Fernandezdepalencia P, Pelaez C, Requena T (2004) Biochemical and molecular characterization of alpha-ketoisovalerate decarboxylase, an enzyme involved in the formation of aldehydes from amino acids by. *FEMS Microbiol Lett* 238:367–374 .

Dell KA, Frost JW (1993) Identification and removal of impediments to biocatalytic synthesis of aromatics from D-glucose: rate-limiting enzymes in the common pathway of aromatic amino acid biosynthesis. *J Am Chem Soc* 115:11581–11589 .

di Benedetto R, Varì R, Scazzocchio B, Filesi C, Santangelo C, Giovannini C, Matarrese P, D'Archivio M, Masella R (2007) Tyrosol, the major extra virgin olive oil compound, restored intracellular antioxidant defences in spite of its weak antioxidative effectiveness. *Nutr Metab Cardiovasc Dis* 17:535–545 .

Diaz E, Ferrandez A, Prieto MA, Garcia JL (2001) Biodegradation of Aromatic Compounds by Escherichia coli. *Microbiol Mol Biol Rev* 65:523–569 .

Dickinson JR, Harrison SJ, Dickinson JA, Hewlins MJ (2000) An investigation of the metabolism of isoleucine to active Amyl alcohol in *Saccharomyces cerevisiae*. *J Biol Chem* 275:10937–42 .

Dickinson JR, Salgado LEJ, Hewlins MJE (2003) The catabolism of amino acids to long chain and complex alcohols in *Saccharomyces cerevisiae*. *J Biol Chem* 278:8028–34 .

Donahue JL, Bownas JL, Niehaus WG, Larson TJ (2000) Purification and characterization of glpX-encoded fructose 1, 6-bisphosphatase, a new enzyme of the glycerol 3-phosphate regulon of Escherichia coli. *J Bacteriol* 182:5624–7

Doroshenko VG, Livshits VA, Airich LG, Shmagina IS, Savrasova EA, Ovsienko M V., Mashko S V. (2015) Metabolic engineering of *Escherichia coli* for the production of phenylalanine and related compounds. *Appl Biochem Microbiol* 51:733–750 .

Dower WJ, Miller JF, Ragsdale CW (1988) High efficiency transformation of *E. coli* by high voltage electroporation. *Nucleic Acids Res*. 16:6127.

Draths KM, Pompliano DL, Conley DL, Frost JW, Berry A, Disbrow GL, Staversky RJ, Lievense JC (1992) Biocatalytic synthesis of aromatics from D-glucose: the role of transketolase. *J Am Chem Soc* 114:3956–3962 .

Edman JC, Goldstein AL, Erbe JG (1993) Para-aminobenzoate synthase gene of*Saccharomyces cerevisiae* encodes a bifunctional enzyme. *Yeast* 9:669–675 .

Ehrlich F (1907) Über die Bedingungen der Fuselölbildung und über ihren Zusammenhang mit dem Eiweißaufbau der Hefe. Berichte der Dtsch Chem Gesellschaft 40:1027–1047 .

Eiteman MA, Altman E (2006) Overcoming acetate in *Escherichia coli* recombinant protein fermentations. Trends Biotechnol 24:530–536 .

Engels B, Dahm P, Jennewein S (2008) Metabolic engineering of taxadiene biosynthesis in yeast as a first step towards Taxol (Paclitaxel) production. *Metab Eng* 10:201–206 .

Espín JC, Soler-Rivas C, Cantos E, Tomá S-Barberán FA, Wichers HJ (2001) Synthesis of the Antioxidant Hydroxytyrosol Using Tyrosinase as Biocatalyst. *J Agric Food Chem* 49:1187–1193 .

Etschmann MMW, Schrader J (2006) An aqueous–organic two-phase bioprocess for efficient production of the natural aroma chemicals 2-phenylethanol and 2-phenylethylacetate with yeast. Appl Microbiol Biotechnol 71:440–443 .

Etschmann MMW, Sell D, Schrader J (2005) Production of 2-phenylethanol and 2-phenylethylacetate fromL-phenylalanine by coupling whole-cell biocatalysis with organophilic pervaporation. *Biotechnol Bioeng* 92:624–634 .

Etschmann MMW, Sell D SJ (2003) Screening of yeasts for the production of the aroma compound 2-phenylethanol in a molasses-based medium. *Biotechnol Lett* 25:531–536 .

Etschmann MMW, Bluemke W, Sell D, Schrader J (2002) Biotechnological production of 2-phenylethanol. *Appl Microbiol Biotechnol* 59:1–8 .

Eudes A, Juminaga D, Baidoo EEK, Collins F, Keasling JD, Loqué D (2013) Production of hydroxycinnamoyl anthranilates from glucose in *Escherichia coli. Microb Cell Fact* 12:62 .

Fang M-Y, Zhang C, Yang S, Cui J-Y, Jiang P-X, Lou K, Wachi M, Xing X-H (2015) High crude violacein production from glucose by *Escherichia coli* engineered with interactive control of tryptophan pathway and violacein biosynthetic pathway. *Microb Cell Fact* 14:8 .

Fernández-Martínez LT, Borsetto C, Gomez-Escribano JP, Bibb MJ, Al-Bassam MM, Chandra G, Bibb MJ (2014) New Insights into Chloramphenicol Biosynthesis in *Streptomyces venezuelae* ATCC 10712. *Antimicrob Agents Chemother* 58:7441–7450 .

Ferrández A, Prieto MA, García JL, Díaz E (1997) Molecular characterization of PadA, a phenylacetaldehyde dehydrogenase from *Escherichia coli*. FEBS Lett 406:23–27 .

Ferrer-Miralles N, Domingo-Espín J, Corchero J, Vázquez E, Villaverde A (2009) Microbial factories for recombinant pharmaceuticals. *Microb Cell Fact* 8:17 .

Floss HG. (1996) Biosynthesis of Some Aromatic Antibiotics. In Biosynthesis Book, Springer Berlin Heidelberg, pp 236-261

Fortman JL, Chhabra S, Mukhopadhyay A, Chou H, Lee TS, Steen E, Keasling JD (2008) Biofuel alternatives to ethanol: pumping the microbial well. *Trends Biotechnol* 26:375–81 .

Fotheringham IG, Dacey SA, Taylor PP, Smith TJ, Hunter MG, Finlay ME, Primrose SB, Parker DM, Edwards RM (1986) The cloning and sequence analysis of the *aspC* and *tyrB* genes from *Escherichia coli* K12. Comparison of the primary structures of the aspartate aminotransferase and aromatic aminotransferase of *E. coli* with those of the pig aspartate aminotransferase isoenzymes. *Biochem J* 234:593–604

Fraud S, Rees EL, Mahenthiralingam E, Russell AD, Maillard J-Y (2003) Aromatic alcohols and their effect on Gram- negative bacteria, cocci and mycobacteria. *J Antimicrob Chemother* 51:1435–1436 .

Frost JW, Draths KM (1995) Biocatalytic Syntheses of Aromatics from D-Glucose: Renewable Microbial Sources of Aromatic Compounds. *Annu Rev Microbiol* 49:557–579 .

Fujita T, Duc Nguyen H, Ito T, Zhou S, Osada L, Tateyama S, Kaneko T, Takaya N (2013) Microbial monomers custom-synthesized to build true bio-derived aromatic polymers. *Appl Microbiol Biotechnol* 97:8887–8894

Fürste JP, Pansegrau W, Frank R, Blöcker H, Scholz P, Bagdasarian M, Lanka E (1986) Molecular cloning of the plasmid RP4 primase region in a multi-host-range tacP expression vector. *Gene* 48:119–131 .

Gao F, Daugulis AJ (2009) Bioproduction of the aroma compound 2-Phenylethanol in a solid-liquid two-phase partitioning bioreactor system by *Kluyveromyces marxianus*. *Biotechnol Bioeng* 104:332–339.

Gerhardt P, R. G. E. Murray WAW and NRK (1996) Methods for General and Molecular Bacteriology. Edited by P. Gerhardt, R. G. E. Murray, W. A. Wood and N. R. Krieg. 791 pages, numerous figures and tables. American Society for Microbiology, Washington, D.C. Food / Nahrung 40:103–103 .

Ghanegaonkar S, Conrad J, Beifuss U, Sprenger GA, Albermann C (2013) Towards the in vivo production of tocotrienol compounds: Engineering of a plasmid-free *Escherichia coli* strain for the heterologous synthesis of 2-methyl-6-geranylgeranyl-benzoquinol. *J Biotechnol* 164:238–247 .

Ghosh S, Kebaara BW, Atkin AL, Nickerson KW (2008) Regulation of aromatic alcohol production in *Candida albicans*. *Appl Environ Microbiol* 74:7211–8 .

Gibson F (1964) Chorismic acid: purification and some chemical and physical studies. *Biochem J* 90:256–61

Giovannini C, Straface E, Modesti D, Coni E, Cantafora A, De Vincenzi M, Malorni W, Masella R (1999) Tyrosol, the Major Olive Oil Biophenol, Protects Against Oxidized-LDL-Induced Injury in Caco-2 Cells. *J Nutr* 129:1269–1277 .

Goncharoff P, Nichols BP (1984) Nucleotide sequence of *Escherichia coli pabB* indicates a common evolutionary origin of p-aminobenzoate synthetase and anthranilate synthetase. *J Bacteriol* 159:57–62

González B, Vázquez J, Morcillo-Parra MÁ, Mas A, Torija MJ, Beltran G (2018) The production of aromatic alcohols in non-Saccharomyces wine yeast is modulated by nutrient availability. *Food Microbiol* 74:64–74 .

Gonzalez R, Murarka A, Dharmadi Y, Yazdani SS (2008) A new model for the anaerobic fermentation of glycerol in enteric bacteria: Trunk and auxiliary pathways in *Escherichia coli. Metab Eng* 10:234–245 .

Gosset G (2009) Production of aromatic compounds in bacteria. *Curr Opin Biotechnol* 20:651–658 .

Gottlieb K (2011) Nutzung von Glycerin und Rohglycerin als C-Quelle für die Produktion von L-Phenylalanin mit rekombinanten Escherichia coli-Stämmen. Univ Stuttgart, PhD Thesis.

Gottlieb K, Albermann C, Sprenger GA (2014) Improvement of L-phenylalanine production from glycerol by recombinant *Escherichia coli* strains: The role of extra copies of *glpK, glpX,* and *tktA* genes. *Microb Cell Fact* 13:96 .

Green JM, Nichols BP (1991) p-Aminobenzoate biosynthesis in *Escherichia coli*. Purification of aminodeoxychorismate lyase and cloning of pabC. *J Biol Chem* 266:12971–5.

Guo D, Zhang L, Kong S, Liu Z, Li X, and Pan H (2018) Metabolic Engineering of *Escherichia coli* for Production of 2-Phenylethanol and 2-Phenylethyl Acetate from Glucose. *J Agric Food Chem*. 66(23): 5886–5891.

Hanahan D (1983) Studies on transformation of *Escherichia coli* with plasmids. *J Mol Biol* 166:557–580 .

Hanlon SP, Hill TK, Flavell MA, Stringfellow JM, Cooper RA (1997) 2-Phenylethylamine catabolism by *Escherichia coli* K-12: gene organization and expression. *Microbiology* 143:513–518 .

Hara KY, Araki M, Okai N, Wakai S, Hasunuma T, Kondo A (2014) Development of bio-based fine chemical production through synthetic bioengineering. *Microb Cell Fact* 13:173 .

Haslam E (1974) The shikimate pathway: Metabolism and Metabolites. Halstead Press, Wiley: New York

Hayashi H, Inoue K, Nagata T, Kuramitsu S, Kagamiyama H (1993) *Escherichia coli* aromatic amino acid aminotransferase: Characterization and comparison with aspartate aminotransferase. *Biochemistry* 32:12229–12239 .

Hayashi K, Morooka N, Yamamoto Y, Fujita K, Isono K, Choi S, Ohtsubo E, Baba T, Wanner BL, Mori H, Horiuchi T (2006) Highly accurate genome sequences of *Escherichia coli* K-12 strains MG1655 and W3110. *Mol Syst Biol* 2:2006.0007 .

Hazelwood LA, Daran J-M, van Maris AJA, Pronk JT, Dickinson JR (2008) The Ehrlich pathway for fusel alcohol production: a century of research on *Saccharomyces cerevisiae* metabolism. *Appl Environ Microbiol* 74:2259–66 .

He J, Magarvey N, Piraee M, Vining LC (2001) The gene cluster for chloramphenicol biosynthesis in Streptomyces venezuelae ISP5230 includes novel shikimate pathway homologues and a monomodular non- ribosomal peptide synthetase gene. *Microbiology* 2331:2817–2829

Heatwole VM, Somerville RL (1991) The tryptophan-specific permease gene, mtr, is differentially regulated by the tryptophan and tyrosine repressors in *Escherichia coli K-12*. *J Bacteriol* 173:3601–4

Heller KB, Lin EC, Wilson TH (1980) Substrate specificity and transport properties of the glycerol facilitator of Escherichia coli. *J Bacteriol* 144:274–8

Herbert RB, Knaggs AR (1988) The biosynthesis of the antibiotic obafluorin from p-aminophenylalanine in Pseudomonas fluorescens. *Tetrahedron Lett* 29:6353–6356 .

Herrmann KM (1995) The shikimate pathway as an entry to aromatic secondary metabolism. *Plant Physiol* 107:7–12

Herrmann KM, Weaver LM (1999) The Shikimate Pathway. *Annu Rev Plant Physiol Plant Mol Biol* 50:473–503 .

Herrmann K, Entus R (2001) Shikimate Pathway: Aromatic Amino Acids and Beyond. Encycl LIFE Sci © 2001, John Wiley Sons, Ltd www.els.net

Hobom B (1980) Gene surgery: on the threshold of synthetic biology. *Med. Klin*. 75, 834–41.

Ho KK, Weiner H (2005) Isolation and Characterization of an Aldehyde Dehydrogenase Encoded by the aldB Gene of Escherichia coli. *J Bacteriol* 187:1067–1073 .

Hohmann S, Cederberg H (1990) Autoregulation may control the expression of yeast pyruvate decarboxylase structural genes PDC1 and PDC5. *Eur J Biochem* 188:615–621 .

Hohmann S, Meacock PA (1998) Thiamin metabolism and thiamin diphosphate-dependent enzymes in the yeast *Saccharomyces cerevisiae*: genetic regulation. *Protein Struct Mol Enzymol* 1385:201–219 .

Hua D, Ma C, Lin S, Song L, Deng Z, Maomy Z, Zhang Z, Yu B, Xu P (2007a) Biotransformation of isoeugenol to vanillin by a newly isolated Bacillus pumilus strain: Identification of major metabolites. *J Biotechnol* 130:463–470 .

Hua D, Ma C, Song L, Lin S, Zhang Z, Deng Z, Xu P (2007b) Enhanced vanillin production from ferulic acid using adsorbent resin. *Appl Microbiol Biotechnol* 74:783–790 .

Hua D, Lin S, Li Y, Chen H, Zhang Z, Du Y, Zhang X, Xu P (2010) Enhanced 2-phenylethanol production from L-phenylalanine via *in situ* product adsorption. *Biocatal Biotransformation* 28:259–266 .

Hua D, Xu P (2011) Recent advances in biotechnological production of 2-phenylethanol. *Biotechnol Adv* 29:654–660 .

Hua Q, Shimizu K (1999) Effect of dissolved oxygen concentration on the intracellular flux distribution for pyruvate fermentation. *J Biotechnol* 68:135–147 .

Huang C-J, Lin H, Yang X (2012) Industrial production of recombinant therapeutics in *Escherichia coli* and its recent advancements. *J Ind Microbiol Biotechnol* 39:383–399 .

Huang Q, Roessner CA, Croteau R, Scott AI (2001) Engineering *Escherichia coli* for the synthesis of taxadiene, a key intermediate in the biosynthesis of taxol. *Bioorg Med Chem* 9:2237–42

Huang Q, Lin Y, Yan Y (2013) Caffeic acid production enhancement by engineering a phenylalanine over-producing *Escherichia coli* strain. *Biotechnol Bioeng* 110:3188–3196 .

Huang W-C, Chen S-J, Chen T-L (2006) The role of dissolved oxygen and function of agitation in hyaluronic acid fermentation. *Biochem Eng* J 32:239–243 .

Human insulin receives FDA approval (1982). FDA, Drug Bull 12:18–9.

Ikeda M (2006) Towards bacterial strains overproducing l-tryptophan and other aromatics by metabolic engineering. *Appl Microbiol Biotechnol* 69:615–626 .

Ingram LO, Buttke TM (1985) Effects of Alcohols on Micro-Organisms. *Adv Microb Physiol* 25:253–300.

Inoue K, Kuramitsu S, Aki K, Watanabe Y, Takagi T, Nishigai M, Ikai A, Kagamiyama H (1988) Branched-chain amino acid aminotransferase of Escherichia coli: overproduction and properties. *J Biochem* 104:777–84

Ippolito RM. and Vigmond S. (1988) Process for preparing substituted phenol ethers via oxazolidine-structure intermediates, US patent US4760182A.

Ishige T, Honda K, Shimizu S (2005) Whole organism biocatalysis. *Curr Opin Chem Biol* 9:174–180 .

Jackson B, Brocker C, Thompson DC, Black W, Vasiliou K, Nebert DW, Vasiliou V (2011) Update on the aldehyde dehydrogenase gene (ALDH) superfamily. *Hum Genomics* 5:283–303 .

Jeude M, Dittrich B, Niederschulte H, Anderlei T, Knocke C, Klee D, Büchs J (2006) Fed-batch mode in shake flasks by slow-release technique. *Biotechnol Bioeng* 95:433–445 .

Jewison T, Knox C, Neveu V, Djoumbou Y, Guo AC, Lee J, Liu P, Mandal R, Krishnamurthy R, Sinelnikov I, Wilson M, Wishart DS (2012) YMDB: the Yeast Metabolome Database. *Nucleic Acids Res* 40:D815–D820 .

Jiang M, Zhang H (2016) Engineering the shikimate pathway for biosynthesis of molecules with pharmaceutical activities in *E. coli*. *Curr Opin Biotechnol* 42:1–6

Jiang Y, Chen B, Duan C, Sun B, Yang J, Yang S (2015) Multigene editing in the *Escherichia coli* genome via the CRISPR-Cas9 system. *Appl Environ Microbiol* 81:2506–14 .

Jin RZ, Lin ECC (1984) An Inducible Phosphoenolpyruvate: Dihydroxyacetone Phosphotransferase System in *Escherichia coli*. *Microbiology* 130:83–88 .

Jo J-E, Mohan Raj S, Rathnasingh C, Selvakumar E, Jung W-C, Park S (2008) Cloning, expression, and characterization of an aldehyde dehydrogenase from *Escherichia coli* K-12 that utilizes 3-Hydroxypropionaldehyde as a substrate. *Appl Microbiol Biotechnol* 81:51–60 .

Jobdevairakkam Christopher N and Hero Velladurai (2013) Process of making optically pure melphalan. US patent 8,575,385.

Jollivet N, Bézenger M-C, Vayssier Y, Belin J-M (1992) Production of volatile compounds in liquid cultures by six strains of coryneform bacteria. *Appl Microbiol Biotechnol* 36:790–794 .

Jones KL, Kim S-W, Keasling J. (2000) Low-Copy Plasmids can Perform as Well as or Better Than High-Copy Plasmids for Metabolic Engineering of Bacteria. *Metab Eng* 2:328–338 .

Jörnvall H, Persson B, Jeffery J (1987) Characteristics of alcohol/polyol dehydrogenases. The zinc-containing long-chain alcohol dehydrogenases. *Eur J Biochem* 167:195–201

Jozala AF, Geraldes DC, Tundisi LL, Feitosa V de A, Breyer CA, Cardoso SL, Mazzola PG, Oliveira-Nascimento L de, Rangel-Yagui C de O, Magalhães P de O, Oliveira MA de, Pessoa A (2016) Biopharmaceuticals from microorganisms: from production to purification. *Brazilian J Microbiol* 47:51–63

Juminaga D, Baidoo EEK, Redding-Johanson AM, Batth TS, Burd H, Mukhopadhyay A, Petzold CJ, Keasling JD (2012) Modular engineering of L-tyrosine production in *Escherichia coli*. *Appl Environ Microbiol* 78:89–98 .

Kalinowski J, Bathe B, Bartels D, Bischoff N, Bott M, Burkovski A, Dusch N, Eggeling L, Eikmanns BJ, Gaigalat L, Goesmann A, Hartmann M, Huthmacher K, Krämer R, Linke B, McHardy AC, Meyer F, Möckel B, Pfefferle W, Pühler A, Rey DA, Rückert C, Rupp O, Sahm H, Wendisch VF, Wiegräbe I, Tauch A (2003) The complete *Corynebacterium glutamicum* ATCC 13032 genome sequence and its impact on the production of L-aspartate-derived amino acids and vitamins. *J Biotechnol* 104:5–25

Kalscheuer R, Stölting T, Steinbüchel A (2006) Microdiesel: *Escherichia coli* engineered for fuel production. *Microbiology* 152:2529–2536 .

Kang S-Y, Choi O, Lee J, Hwang B, Uhm T-B, Hong Y-S (2012) Artificial biosynthesis of phenylpropanoic acids in a tyrosine overproducing *Escherichia coli* strain. *Microb Cell Fact* 11:153.

Kang Z, Zhang C, Du G, Chen J (2014) Metabolic engineering of *Escherichia coli* for production of 2-phenylethanol from renewable glucose. *Appl Biochem Biotechnol* 172:2012–2021 .

Kaplan JB, Nichols BP (1983) Nucleotide sequence of *Escherichia coli pabA* and its evolutionary relationship to *trp(G)D*. *J Mol Biol* 168:451–68.

Kaplan JB, Merkel WK, Nichols BP (1985) Evolution of glutamine amidotransferase genes. Nucleotide sequences of the pabA genes from *Salmonella typhimurium, Klebsiella aerogenes and Serratia marcescens*. *J Mol Biol* 183:327–40.

Karp PD, Riley M, Saier M, Paulsen IT, Collado-Vides J, Paley SM, Pellegrini-Toole A, Bonavides C, Gama-Castro S (2002) The EcoCyc Database. *Nucleic Acids Res* 30:56–58 .

Kawaguchi H, Ogino C, Kondo A (2017) Microbial conversion of biomass into bio-based polymers. *Bioresour Technol* 245:1664–1673 .

Kawasaki Y, Aniruddha N, Minakawa H, Masuo S, Kaneko T, Takaya N (2018) Novel polycondensed biopolyamide generated from biomass-derived 4-aminohydrocinnamic acid. *Appl Microbiol Biotechnol* 102:631–639 .

Keasling J (2006) The Promise of Synthetic Biology. Frontiers of Engineering: Reports on Leading-Edge Engineering from the 2005 Symposium. *The National Academies Press,* 35, 18–22.

Khamduang M, Packdibamrung K, Chutmanop J, Chisti Y, Srinophakun P (2009) Production of l-phenylalanine from glycerol by a recombinant Escherichia coli. *J Ind Microbiol Biotechnol* 36:1267–1274 .

Khanna S, Goyal A, Moholkar VS (2012) Microbial conversion of glycerol: present status and future prospects. *Crit Rev Biotechnol* 32:235–262 .

Khosla C, Keasling JD (2003) Timeline: Metabolic engineering for drug discovery and development. *Nat Rev Drug Discov* 2:1019–1025 .

Kim B, Cho BR, Hahn JS (2014a) Metabolic engineering of *Saccharomyces cerevisiae* for the production of 2-phenylethanol via Ehrlich pathway. *Biotechnol Bioeng* 111:115–124 .

Kim B, Park H, Na D, Lee SY (2014b) Metabolic engineering of *Escherichia coli* for the production of phenol from glucose. *Biotechnol J* 9:621–629 .

Kim BH, Gadd GM (2008) Bacterial physiology and metabolism, 3rd edn. Cambridge University Press, Cambridge University Press. page 60-81.

Kim T-Y, Lee S-W, Oh M-K (2014c) Biosynthesis of 2-phenylethanol from glucose with genetically engineered Kluyveromyces marxianus. *Enzyme Microb Technol* 61–62:44–47 .

Kirschner MW (2005) Commentary The Meaning of Systems Biology. *Cell* 121:503–504 .

Klose J (1975) Protein Mapping by Combined Isoelectric Focusing and Electrophoresis of Mouse Tissues - Novel Approach to Testing for Induced Point Mutations in Mammals. *Humangenetik* 26, 231-243.

Kneen MM, Stan R, Yep A, Tyler RP, Saehuan C, McLeish MJ (2011) Characterization of a thiamin diphosphate-dependent phenylpyruvate decarboxylase from S*accharomyces cerevisiae*. *FEBS J* 278:1842–1853 .

Koma D, Yamanaka H, Moriyoshi K, Ohmoto T, Sakai K (2012) Production of aromatic compounds by metabolically engineered *Escherichia coli* with an expanded shikimate pathway. *Appl Environ Microbiol* 78:6203–16 .

Koma D, Yamanaka H, Moriyoshi K, Sakai K, Masuda T, Sato Y, Toida K, Ohmoto T (2014) Production of *p* -Aminobenzoic acid by metabolically engineered *Escherichia coli*. *Biosci Biotechnol Biochem* 78:350–357 .

König S (1998) Subunit structure, function and organisation of pyruvate decarboxylases from various organisms. *Biochim Biophys Acta* 1385:271–86

Konishi K, Takaya N MS and ZS (2016) 4-amino cinnamic acid production method using enzyme. US Pat US20160362:

Kovacheva N, Rusanov K, Atanassov I (2010) Industrial Cultivation of Oil Bearing Rose and Rose Oil Production in Bulgaria During 21 ST Century, Directions and Challenges. *Biotechnol Biotechnol Equip* 24:1793–1798 .

Kozak S (2006) Mikrobielle Biosynthese von (3S,4R)-4-Amino-3-hydroxycyclohexa-1,5-diencarbonsäure mit rekombinanten Escherichia coliZellen: Molekulargenetische und biochemische Untersuchungen. Ph.D dissertation, University Stuttgart.

Krämer M, Bongaerts J, Bovenberg R, Kremer S, Müller U, Orf S, Wubbolts M, Raeven L (2003) Metabolic engineering for microbial production of shikimic acid. *Metab Eng* 5:277–283 .

Krause M, Ukkonen K, Haataja T, Ruottinen M, Glumoff T, Neubauer A, Neubauer P, Vasala A (2010) A novel fed-batch based cultivation method provides high cell-density and improves yield of soluble recombinant proteins in shaken cultures. *Microb Cell Fact* 9:11 .

Krings U, Berger RG (1998) Biotechnological production of flavours and fragrances. *Appl Microbiol Biotechnol* 49:1–8 .

Küberl A, Schneider J, Thallinger GG, Anderl I, Wibberg D, Hajek T, Jaenicke S, Brinkrolf K, Goesmann A, Szczepanowski R, Pühler A, Schwab H, Glieder A, Pichler H (2011) High-quality genome sequence of *Pichia pastoris* CBS7435. *J Biotechnol* 154:312–320 .

Kubota T, Watanabe A, Suda M, Kogure T, Hiraga K, Inui M (2016) Production of para -aminobenzoate by genetically engineered *Corynebacterium glutamicum* and non-biological formation of an N -glucosyl byproduct. *Metab Eng* 38:322–330 .

Kumar A, Tateyama S, Yasaki K, Ali MA, Takaya N, Singh R, Kaneko T (2016) (1)H NMR and FT-IR dataset based structural investigation of poly(amic acid)s and polyimides from 4,4'-diaminostilbene. *Data Br* 7:123–8 .

Kunjapur AM, Tarasova Y, Prather KLJ (2014) Synthesis and Accumulation of Aromatic Aldehydes in an Engineered Strain of *Escherichia coli*. *J Am Chem Soc* 136:11644–11654 .

Laemmli UK (1970) Cleavage of structural proteins during the assembly of the head of bacteriophage T4. *Nature*, vol: 227 (5259) pp: 680-685.

Lang M, Rye RM (1972) The uptake by *Escherichia coli* and growth inhibitory properties of benzyl alcohol and phenethyl alcohol. *J Pharm Pharmacol.* 24:219–226

Lee J-H, Wendisch VF (2017) Biotechnological production of aromatic compounds of the extended shikimate pathway from renewable biomass. *J Biotechnol* 257:211–221 .

Lee KH, Park JH, Kim TY, Kim KU, Lee SY (2007) Systems metabolic engineering of *Escherichia coli* for L-threonine production. *Mol Syst Biol.* 3(1):2025.

Lee SY (1996) High cell-density culture of *Escherichia coli*. *Trends Biotechnol* 14:98–105 .

Lee SY, Park JH, Jang SH, Nielsen LK, Kim J, Jung KS (2008) Fermentative butanol production by clostridia. *Biotechnol Bioeng* 101:209–228 .

Lee SY, Park JM, Kim TY (2011) Application of Metabolic Flux Analysis in Metabolic Engineering. *Methods Enzymol* 498:67–93 .

Lester G (1965) Inhibition of Growth, Synthesis, and Permeability in *Neurospora crassa* by Phenethyl Alcohol. *J Bacteriol* 90:29–37

Li K and Frost J (1998) Synthesis of Vanillin from Glucose. *J Am Chem Soc* 120:10545–10546 .

Li Li, Hiroshi Seino, Koichiro Yonetake A, Ueda M (1999) Synthesis and Characterization of Ordered Poly(amide−ester)s from Isophthaloyl Chloride and 4-(2-Aminoethyl)phenol. *Macromolecules* 32:3851–3858 .

Li F-F, Zhao Y, Li B-Z, Qiao J-J, Zhao G-R (2016) Engineering *Escherichia coli* for production of 4-hydroxymandelic acid using glucose–xylose mixture. *Microb Cell Fact* 15:90 .

Li M, Borodina I (2014) Application of synthetic biology for production of chemicals in yeast *Saccharomyces cerevisiae*. *FEMS Yeast Res* 15:n/a-n/a .

Li S, Jia X, Wen J (2012) Improved 2-methyl-1-propanol production in an engineered Bacillus subtilis by constructing inducible pathways. *Biotechnol Lett* 34:2253–2258 .

Li X, Chen Z, Wu Y, Yan Y, Sun X, Yuan Q (2018) Establishing an Artificial Pathway for Efficient Biosynthesis of Hydroxytyrosol. *ACS Synth Biol* 7:647–654 .

Li Y, Lin Z, Huang C, Zhang Y, Wang Z, Tang Y, Chen T, Zhao X (2015) Metabolic engineering of *Escherichia coli* using CRISPR–Cas9 meditated genome editing. *Metab Eng* 31:13–21 .

Liebgott P-P, Amouric A, Comte A, Tholozan J-L, Lorquin J (2009) Hydroxytyrosol from tyrosol using hydroxyphenylacetic acid-induced bacterial cultures and evidence of the role of 4-HPA 3-hydroxylase. *Res Microbiol* 160:757–766 .

Liese A, Villela Filho M (1999) Production of fine chemicals using biocatalysis. *Curr Opin Biotechnol* 10:595–603 .

Lin ECC (1976) Glycerol Dissimilation and its Regulation in Bacteria. *Annu Rev Microbiol* 30:535–578 .

Lin Y, Sun X, Yuan Q, Yan Y (2014) Extending shikimate pathway for the production of muconic acid and its precursor salicylic acid in *Escherichia coli*. *Metab Eng* 23:62–69 .

Lingens F (1968) The Biosynthesis of Aromatic Amino Acids and its Regulation. Angew Chemie Int Ed English 7:350–360 .

Liu SP, Zhang L, Mao J, Ding ZY, Shi GY (2015) Metabolic engineering of *Escherichia coli* for the production of phenylpyruvate derivatives. *Metab Eng* 32:55–65 .

Liu SP, Liu RX, Xiao MR, Zhang L, Ding ZY, Gu ZH, Shi GY (2014) A systems level engineered *E. coli* capable of efficiently producing L-phenylalanine. *Process Biochem* 49:751–757 .

Liu X, Li X-B, Jiang J, Liu Z-N, Qiao B, Li F-F, Cheng J-S, Sun X, Yuan Y-J, Qiao J, Zhao G-R (2018) Convergent engineering of syntrophic *Escherichia coli* coculture for efficient production of glycosides. *Metab Eng* 47:243–253 .

Lomascolo A, Lesage-Meessen L, Haon M, Navarro D, Antona C, Faulds C, Marcel A (2001) Evaluation of the potential of *Aspergillus niger* species for the bioconversion of L-phenylalanine into 2-phenylethanol. *World J Microbiol Biotechnol* 17:99–102

Lu J and Zhang W.G. (2008) Production of 2-phenylethylalcohol from L-phenylalanine by bioconversion in biphasic system. *Chem Ind Eng Prog* 27:417–420

Lucchini JJ, Bonnaveiro N, Cremieux A, Le Goffic F (1993) Mechanism of bactericidal action of phenethyl alcohol inEscherichia coli. *Curr Microbiol* 27:295–300 .

Lütke-Eversloh T, Stephanopoulos G (2005) Feedback inhibition of chorismate mutase/prephenate dehydrogenase (TyrA) of *Escherichia coli*: generation and characterization of tyrosine-insensitive mutants. *Appl Environ Microbiol* 71:7224–8 .

Macheroux P, Schmid J, Amrhein N, Schaller A (1999) A unique reaction in a common pathway: mechanism and function of chorismate synthase in the shikimate pathway. *Planta* 207:325–334 .

Machas MS, McKenna R, and Nielsen DR (2017) Expanding Upon Styrene Biosynthesis to Engineer a Novel Route to 2-Phenylethanol. *Biotechnol J.* 12(10): 1–10.

Madigan MT, Martinko JM, Stahl DA and Clark DP (2012) Brock biology of microorganisms, 13th edn. San Francisco: Benjamin Cummings, 2012.

Maekawa M, Kanno Z, Wada T, Hongo T, Doi H, Hanawa T, Ono T, Uo M (2015) Mechanical properties of orthodontic wires made of super engineering plastic. *Dent Mater* J 34:114–119 .

Maier U, Büchs J (2001) Characterisation of the gas–liquid mass transfer in shaking bioreactors. *Biochem Eng J* 7:99–106 .

Mainguet SE, Liao JC (2010) Bioengineering of microorganisms for C3 to C5 alcohols production. *Biotechnol J* 5:1297–1308 .

Makrides SC (1996) Strategies for achieving high-level expression of genes in *Escherichia coli*. *Microbiol Rev* 60:512–38

Mamedov MK (2006) Synthesis of Aromatic Alcohols and Their Alkanoic Acid Esters. *ISSN Russ J Appl Chem Orig Russ* 79:1070–4272 .

Martínez JA, Bolívar F, Escalante A (2015) Shikimic Acid Production in *Escherichia coli*: From Classical Metabolic Engineering Strategies to Omics Applied to Improve Its Production. *Front Bioeng Biotechnol* 3:145 .

Martínez-Gómez K, Flores N, Castañeda HM, Martínez-Batallar G, Hernández-Chávez G, Ramírez OT, Gosset G, Encarnación S, Bolivar F (2012) New insights into *Escherichia coli* metabolism: carbon scavenging, acetate metabolism and carbon recycling responses during growth on glycerol. *Microb Cell Fact* 11:46 .

Masker WE, and Eberle H (1972) Effect of phenethyl alcohol on deoxyribonucleic acid-membrane association in *Escherichia coli*. *J. Bacteriol*. 109, 1170–1174.

Mast YJ, Wohlleben W, Schinko E (2011) Identification and functional characterization of phenylglycine biosynthetic genes involved in pristinamycin biosynthesis in *Streptomyces pristinaespiralis*. *J Biotechnol* 155:63–67 .

Masuo S, Osada L, Zhou S, Fujita T, Takaya N (2015) Aspergillus oryzae pathways that convert phenylalanine into the flavor volatile 2-phenylethanol. *Fungal Genet Biol* 77:22–30 .

Masuo S, Zhou S, Kaneko T, Takaya N (2016) Bacterial fermentation platform for producing artificial aromatic amines. *Sci Rep* 6:25764 .

Matsumoto T, Tanaka T (2017) Engineering metabolic pathways in *Escherichia coli* for constructing a “microbial chassis” for biochemical production. *Bioresour Technol* 245:1362–1368 .

Mattocks AM, Hartung WH (1946) A synthesis of p-aminophenylalanine. *J Am Pharm Assoc Am Pharm Assoc* (Baltim) 35:18.

Mazumdar S, Blankschien MD, Clomburg JM, Gonzalez R (2013) Efficient synthesis of L-lactic acid from glycerol by metabolically engineered Escherichia coli. *Microb Cell Fact* 12:7 .

Meng C, Xu D, Son YJ, Kubota C (2012) Simulation-based economic feasibility analysis of grafting technology for propagation operation. Proceedings of the 2012 Industrial and Systems Engineering Research Conference. IIE Annual Conference. Norcross: Institute of Industrial Engineers.

McCandliss RJ, Poling MD and Herrmann KM (1978) 3-Deoxy-D-arabino-heptulosonate 7-phosphate synthase. Purification and molecular characterization of the phenylalanine-sensitive isoenzyme from Escherichia coli. *J Biol Chem* 253:4259 –4265

McKenna R, Nielsen DR (2011) Styrene biosynthesis from glucose by engineered *E. coli*. *Metab Eng* 13:544–554 .

Mehl RA, Anderson JC, Santoro SW, Wang L, Martin AB, King DS, Horn DM, Schultz PG (2003) Generation of a Bacterium with a 21 Amino Acid Genetic Code. *J Am Chem Soc* 125:935–939 .

Meng C, Xu D, Son YJ, Kubota C (2012) Simulation-based economic feasibility analysis of grafting technology for propagation operation. Proc 2012 Ind Syst Eng Res Conf IIE Annu Conf Norcross Inst Ind Eng.

Miao L, Li Q, Diao A, Zhang X, Ma Y (2015) Construction of a novel phenol synthetic pathway in *Escherichia coli* through 4-hydroxybenzoate decarboxylation. *Appl Microbiol Biotechnol* 99:5163–5173 .

Min K, Park K, Park D-H, Yoo YJ (2015) Overview on the biotechnological production of l-DOPA. *Appl Microbiol Biotechnol* 99:575–584 .

Mingeot-Leclercq MP, Glupczynski Y, Tulkens PM (1999) Aminoglycosides: activity and resistance. *Antimicrob Agents Chemother* 43:727–37

Miro-Casas E, Covas M-I, Farre M, Fito M, Ortuñ J, Weinbrenner T, Roset P, De La Torre R (2003) Hydroxytyrosol Disposition in Humans. *Clin Chem* 49:945–952.

Mohammadi Nargesi B, Sprenger GA, and Youn J-W (2019) Metabolic Engineering of *Escherichia coli* for para-Amino-Phenylethanol and para-Amino-Phenylacetic Acid Biosynthesis. *Front Bioeng Biotechnol.* 6: 201.

Mohammadi Nargesi B, Trachtmann N, Sprenger GA, and Youn J-W (2018) Production of p-amino-l-phenylalanine (L-PAPA) from glycerol by metabolic grafting of *Escherichia coli*. *Microb Cell Fact.* 17(1): 149.

Mrotzek C, Anderlei T, Henzler H-J, Büchs J (2001) Mass transfer resistance of sterile plugs in shaking bioreactors. *Biochem Eng* J 7:107–112 .

Müller U, van Assema F, Gunsior M, Orf S, Kremer S, Schipper D, Wagemans A, Townsend CA, Sonke T, Bovenberg R, Wubbolts M (2006) Metabolic engineering of the *E. coli* l-phenylalanine pathway for the production of d-phenylglycine (d-Phg). *Metab Eng* 8:196–208 .

Muñoz AJ, Hernández-Chávez G, de Anda R, Martínez A, Bolívar F, Gosset G (2011) Metabolic engineering of *Escherichia coli* for improving l-3,4-dihydroxyphenylalanine (l-DOPA) synthesis from glucose. *J Ind Microbiol Biotechnol* 38:1845–1852

Muzio G, Maggiora M, Paiuzzi E, Oraldi M, Canuto RA (2012) Aldehyde dehydrogenases and cell proliferation. *Free Radic Biol Med* 52:735–746 .

Nakagawa A, Matsumura E, Koyanagi T, Katayama T, Kawano N, Yoshimatsu K, Yamamoto K, Kumagai H, Sato F, Minami H (2016) Total biosynthesis of opiates by stepwise fermentation using engineered *Escherichia coli*. *Nat Commun* 7:10390 .

Nakagawa A, Minami H, Kim J-S, Koyanagi T, Katayama T, Sato F, Kumagai H (2011) A bacterial platform for fermentative production of plant alkaloids. *Nat Commun* 2:326 .

Nakamura CE, Whited GM (2003) Metabolic engineering for the microbial production of 1,3-propanediol. *Curr Opin Biotechnol* 14:454–459 .

Nakano H, Tomita F, Suzuki T (1976) Biosynthesis of Corynecins by *Corynebacterium hydrocarboclastus*: On the Origin of the N-Acyl Group On the Origin of the N-Acyl Group. *Agricultural and biological chemistry,* 40(2):331-336.

Neidhardt FC, Ingraham J, Schaechter M (1992) Physiology of the Bacterial Cell. A Molecular Approach. Wiley-Blackwell, pp 507. ISBN 0-87893-608-4

Nichols BP, Seibold AM, Doktor SZ (1989) para-aminobenzoate synthesis from chorismate occurs in two steps. *J Biol Chem* 264:8597–601

Noda S, Shirai T, Oyama S, Kondo A (2016) Metabolic design of a platform *Escherichia coli* strain producing various chorismate derivatives. *Metab Eng* 33:119–129 .

O'Farrell PH (1975) High resolution two-dimensional electrophoresis of proteins. *Journal of Biological Chemistry* 250, 4007-4021.

Okahashi N, Matsuda F, Yoshikawa K, Shirai T, Matsumoto Y, Wada M, Shimizu H (2017) Metabolic engineering of isopropyl alcohol-producing *Escherichia coli* strains with ^{13} C-metabolic flux analysis. *Biotechnol Bioeng* 114:2782–2793 .

Oldiges M, Kunze M, Degenring D, Sprenger GA, Takors R (2004) Stimulation, Monitoring, and Analysis of Pathway Dynamics by Metabolic Profiling in the Aromatic Amino Acid Pathway. *Biotechnol Prog* 20:1623–1633 .

Olson MM, Templeton LJ, Suh W, Youderian P, Sariaslani FS, Gatenby AA, Van Dyk TK (2007) Production of tyrosine from sucrose or glucose achieved by rapid genetic changes to phenylalanine-producing *Escherichia coli* strains. *Appl Microbiol Biotechnol* 74:1031–1040 .

Onuffer JJ, Ton BT, Klement I, Kirsch JF (1995) The use of natural and unnatural amino acid substrates to define the substrate specificity differences of *Escherichia coli* aspartate and tyrosine aminotransferases. *Protein Sci* 4:1743–1749 .

Paddon CJ, Keasling JD (2014) Semi-synthetic artemisinin: a model for the use of synthetic biology in pharmaceutical development. *Nat Rev Microbiol* 12:355–367 .

Palomares LA, Estrada-Mondaca S, Ramírez OT (2004) Production of Recombinant Proteins: Challenges and Solutions. In: Recombinant Gene Expression. Humana Press, New Jersey, pp 015–052

Pandal N (2014) Global markets for flavors and fragrances. BCC Res Wellesley, MA.

Panula-Perälä J, Šiurkus J, Vasala A, Wilmanowski R, Casteleijn MG, Neubauer P (2008) Enzyme controlled glucose auto-delivery for high cell density cultivations in microplates and shake flasks. *Microb Cell Fact* 7:31 .

Papanikolaou S, Muniglia L, Chevalot I, Aggelis G, Marc I (2002) Yarrowia lipolytica as a potential producer of citric acid from raw glycerol. *J Appl Microbiol* 92:737–44

Park SH, Kim HU, Kim TY, Park JS, Kim S-S, Lee SY (2014) Metabolic engineering of *Corynebacterium glutamicum* for L-arginine production. *Nat Commun* 5:4618 .

Park S, Ryu DDY, Kim JY (1990) Effect of cell growth rate on the performance of a two-stage continuous culture system in a recombinant*Escherichia coli* fermentation. *Biotechnol Bioeng* 36:493–505 .

Parrott S, Jones S, Cooper RA (1987) 2-Phenylethylamine Catabolism by *Escherichia coli* K12. *Microbiology* 133:347–351 .

Partow S (2012) Novel Synthetic Biology Tools for Metabolic Engineering of *Saccharomyces cerevisiae*. Chalmers Univ Technol PhD Dissertation, https://research.chalmers.se/en/publication/162789

Parsons JF, Jensen PY, Pachikara AS, Howard AJ, Eisenstein E, Ladner JE (2002) Structure of Escherichia coli Aminodeoxychorismate Synthase: Architectural Conservation and Diversity in Chorismate-Utilizing Enzymes. *Biochemistry* 41:2198–2208 .

Patnaik R, Spitzer RG, Liao JC (1995) Pathway engineering for production of aromatics inEscherichia coli: Confirmation of stoichiometric analysis by independent modulation of AroG, TktA, and Pps activities. *Biotechnol Bioeng* 46:361–370 .

Patnaik R, Zolandz RR, Green DA, Kraynie DF (2008) L-Tyrosine production by recombinant *Escherichia coli* : Fermentation optimization and recovery. *Biotechnol Bioeng* 99:741–752 .

Pérez JM, Arenas FA, Pradenas GA, Sandoval JM, Vásquez CC (2008) *Escherichia coli* YqhD exhibits aldehyde reductase activity and protects from the harmful effect of lipid peroxidation-derived aldehydes. *J Biol Chem* 283:7346–53 .

Pi J, Wookey PJ, Pittard AJ (1991) Cloning and sequencing of the pheP gene, which encodes the phenylalanine-specific transport system of Escherichia coli. *J Bacteriol* 173:3622–9

Pick A, Rühmann B, Schmid J, Sieber V (2013) Novel CAD-like enzymes from *Escherichia coli* K-12 as additional tools in chemical production. *Appl Microbiol Biotechnol* 97:5815–5824 .

Piraee M, White RL and Vining LC (2004) Biosynthesis of the dichloroacetyl component of chloramphenicol in *Streptomyces venezuelae* ISP5230: genes required for halogenation. Microbiology. 150(Pt 1):85-94.

Pittard J (1996) Biosynthesis of the aromatic amino acids, In: Neidhardt et al.: *Escherichia coli* and Salmonella : cellular and molecular biology, 1st edn. ASM Press, Washington, D.C. :p 2822

Pittard J, Camakaris H, Yang J (2004) The TyrR regulon. *Mol Microbiol* 55:16–26 .

Pittard J, Yang J (2008) Biosynthesis of the Aromatic Amino Acids. *EcoSal Plus*. 3(1).

Pohl M, Lingen B, Müller M (2002) Thiamin-Diphosphate-Dependent Enzymes: New Aspects of Asymmetric C-C Bond Formation. *Chem - A Eur J* 8:5288–5295 .

Pohl M, Sprenger GA, Müller M (2004) A new perspective on thiamine catalysis. Curr Opin Biotechnol 15:335–342 .

Polovnikova ES, McLeish MJ, Sergienko EA, Burgner JT, Anderson NL, Bera AK, Jordan F, Kenyon and GL, Hasson MS (2003) Structural and Kinetic Analysis of Catalysis by a Thiamin Diphosphate-Dependent Enzyme, Benzoylformate Decarboxylase. *Biochemistry* 42:1820–1830 .

Postma PW, Lengeler JW, Jacobson GR (1993) Phosphoenolpyruvate:carbohydrate phosphotransferase systems of bacteria. *Microbiol Rev* 57:543–94

Pratish Gupta (2016) Global Engineering Plastics Market Segmented by Product, Application and Geography (2015-2020). In: Mordor Intell. retrieved. https://www.mordorintelligence.com/industry-reports/global-engineering-plastics-market-industry.

Prieto MA, Perez-Aranda A, and Garci JL (1996) Characterization of an *Escherichia coli* Aromatic Hydroxylase with a Broad Substrate Range. *Journal of Bacteriology*. vol: 178 (1) pp: 111-120.

Pugh S, McKenna R, Halloum I, Nielsen DR (2015) Engineering *Escherichia coli* for renewable benzyl alcohol production. *Metab Eng Commun* 2:39–45 .

Pugh S, McKenna R, Osman M, Thompson B, Nielsen DR (2014) Rational engineering of a novel pathway for producing the aromatic compounds p-hydroxybenzoate, protocatechuate, and catechol in *Escherichia coli*. *Process Biochem* 49:1843–1850 .

Rabinowitz H and Vogel S (2009) Style and Usage for Organic Chemistry. In: The Manual of Scientific Style. Elsevier, pp 399–425

Raederstorff D (2009) Antioxidant Activity of Olive Polyphenols in Humans: a Review. *Int J Vitam Nutr Res* 79:152–165 .

Ramos JL, Duque E, Gallegos M-T, Godoy P, Ramos-González MI, Rojas A, Terán W, Segura A (2002) Mechanisms of Solvent Tolerance in Gram-Negative Bacteria. *Annu Rev Microbiol* 56:743–768 .

Richey DP, Lin EC (1972) Importance of facilitated diffusion for effective utilization of glycerol by Escherichia coli. *J Bacteriol* 112:784–90

Riesenberg D, Schulz V, Knorre WA, Pohl HD, Korz D, Sanders EA, Ross A, Deckwer WD (1991) High cell density cultivation of *Escherichia coli* at controlled specific growth rate. *J Biotechnol* 20:17–27

Righetti PG (1984) Isoelectric focusing : theory, methodology, and applications. *Elsevier Biomedical Press.* ISBN: 9780080858807

Ro D-K, Paradise EM, Ouellet M, Fisher KJ, Newman KL, Ndungu JM, Ho KA, Eachus RA, Ham TS, Kirby J, Chang MCY, Withers ST, Shiba Y, Sarpong R, Keasling JD (2006) Production of the antimalarial drug precursor artemisinic acid in engineered yeast. *Nature* 440:940–943 .

Rodrigues AL, Göcke Y, Bolten C, Brock NL, Dickschat JS, Wittmann C (2012) Microbial production of the drugs violacein and deoxyviolacein: analytical development and strain comparison. *Biotechnol Lett* 34:717–720 .

Rodrigues AL, Trachtmann N, Becker J, Lohanatha AF, Blotenberg J, Bolten CJ, Korneli C, de Souza Lima AO, Porto LM, Sprenger GA, Wittmann C (2013) Systems metabolic engineering of *Escherichia coli* for production of the antitumor drugs violacein and deoxyviolacein. *Metab Eng* 20:29–41 .

Rodriguez A, Martnez JA, Flores N, Escalante A, Gosset G, Bolivar F (2014a) Engineering *Escherichia coli* to overproduce aromatic amino acids and derived compounds. *Microb Cell Fact* 13:126 .

Rodriguez GM, Atsumi S (2014b) Toward aldehyde and alkane production by removing aldehyde reductase activity in Escherichia coli. *Metab Eng* 25:227–237 .

Rodriguez GM, Atsumi S (2012) Isobutyraldehyde production from *Escherichia coli* by removing aldehyde reductase activity. *Microb Cell Fact* 11:90 .

Rodríguez-Morató J, Boronat A, Kotronoulas A, Pujadas M, Pastor A, Olesti E, Pérez-Mañá C, Khymenets O, Fitó M, Farré M, de la Torre R (2016) Metabolic disposition and biological significance of simple phenols of dietary origin: hydroxytyrosol and tyrosol. *Drug Metab Rev* 48:218–236 .

Rüffer N, Heidersdorf U, Kretzers I, Sprenger G a, Raeven L, Takors R (2004) Fully integrated L-phenylalanine separation and concentration using reactive-extraction with liquid-liquid centrifuges in a fed-batch process with *E. coli*. *Bioprocess Biosyst Eng* 26:239–248 .

Sacco E, Bientinesi R (2012) Mirabegron: a review of recent data and its prospects in the management of overactive bladder. *Ther Adv Urol* 4:315–24 .

Sambrook J, Maccallum P and Russell D (2001) Molecular Cloning: A Laboratory Manual. 3rd Edition, Cold Spring Harbor Press, New York, 2344.

Santos CNS, Xiao W, Stephanopoulos G (2012) Rational, combinatorial, and genomic approaches for engineering L-tyrosine production in Escherichia coli. *Proc Natl Acad Sci U S A* 109:13538–43 .

Sariaslani FS (2007) Development of a Combined Biological and Chemical Process for Production of Industrial Aromatics from Renewable Resources. *Annu Rev Microbiol* 61:51–69 .

Sarsero JP, Wookey PJ, Gollnick P, Yanofsky C, Pittard AJ (1991) A new family of integral membrane proteins involved in transport of aromatic amino acids in *Escherichia coli*. *J Bacteriol* 173:3231–4

Satoh Y, Tajima K, Munekata M, Keasling JD, Lee TS (2012a) Engineering of l-tyrosine oxidation in *Escherichia coli* and microbial production of hydroxytyrosol. *Metab Eng* 14:603–610 .

Satoh Y, Tajima K, Munekata M, Keasling JD, Lee TS (2012b) Engineering of a Tyrosol-Producing Pathway, Utilizing Simple Sugar and the Central Metabolic Tyrosine, in *Escherichia coli. J Agric Food Chem* 60:979–984 .

Schaffer JE, Reck MR, Prasad NK, Wencewicz TA (2017) β-Lactone formation during product release from a nonribosomal peptide synthetase. *Nat Chem Biol* 13:737–744 .

Scheidle M, Dittrich B, Klinger J, Ikeda H, Klee D, Büchs J (2011) Controlling pH in shake flasks using polymer-based controlled-release discs with pre-determined release kinetics. *BMC Biotechnol* 11:25.

Scheidle M, Klinger J, Büchs J (2007) Combination of On-line pH and Oxygen Transfer Rate Measurement in Shake Flasks by Fiber Optical Technique and Respiration Activity MOnitoring System (RAMOS). *Sensors (Basel)* 7:3472–3480 .

Schmid A, Dordick JS, Hauer B, Kiener A WM and WB (2001) Industrial biocatalysis today and tomorrow. *Nature* 409:258–270

Schneider J, Niermann K, Wendisch VF (2011) Production of the amino acids l-glutamate, l-lysine, l-ornithine and l-arginine from arabinose by recombinant *Corynebacterium glutamicum*. *J Biotechnol* 154:191–198 .

Schöpp W, Aurich H (1976) Kinetics and reaction mechanism of yeast alcohol dehydrogenase with long-chain primary alcohols. *Biochem J* 157:15–22

Schul'tsev AL (2011) Thermal dehydration of 2-(4-aminophenyl)ethanol. *Russ J Gen Chem* 81:2300–2303 .

Sendovski M, Nir N, Fishman A (2010) Bioproduction of 2-Phenylethanol in a Biphasic Ionic Liquid Aqueous System. *J Agric Food Chem* 58:2260–2265 .

Sentheshanmuganathan S, Elsden SR (1958) The mechanism of the formation of tyrosol by *Saccharomyces cerevisiae*. *Biochem J* 69:210–8

Serra S, Fuganti C, Brenna E (2005) Biocatalytic preparation of natural flavours and fragrances. *Trends Biotechnol* 23:193–198 .

Serrano L (2007) Synthetic biology: promises and challenges. *Mol Syst Biol* 3:158 .

Servili M, Montedoro G (2002) Contribution of phenolic compounds to virgin olive oil quality. *Eur J Lipid Sci Technol* 104:602–613 .

Shi F, Jiang J, Li Y, Li Y, Xie Y (2013) Enhancement of γ-aminobutyric acid production in recombinant Corynebacterium glutamicum by co-expressing two glutamate decarboxylase genes from Lactobacillus brevis. *J Ind Microbiol Biotechnol* 40:1285–1296 .

Shiloach J, Fass R (2005) Growing E. coli to high cell density—A historical perspective on method development. *Biotechnol Adv* 23:345–357 .

Siegert P, McLeish MJ, Baumann M, Iding H, Kneen MM, Kenyon GL, Pohl M (2005) Exchanging the substrate specificities of pyruvate decarboxylase from Zymomonas mobilis and benzoylformate decarboxylase from Pseudomonas putida. *Protein Eng Des Sel* 18:345–57 .

Singh S, Brocker C, Koppaka V, Chen Y, Jackson BC, Matsumoto A, Thompson DC, Vasiliou V (2013) Aldehyde dehydrogenases in cellular responses to oxidative/electrophilic stress. *Free Radic Biol Med* 56:89–101 .

Slock J, Stahly DP, Han CY, Six EW, Crawford IP (1990) An apparent Bacillus subtilis folic acid biosynthetic operon containing pab, an amphibolic *trpG* gene, a third gene required for synthesis of para-aminobenzoic acid, and the dihydropteroate synthase gene. *J Bacteriol* 172:7211–26

Snell K, Draths K, Frost J. (1996) Synthetic Modification of the *Escherichia coli* Chromosome: Enhancing the Biocatalytic Conversion of Glucose into Aromatic Chemicals. *J Am Chem Soc* 118:5605–5614 .

Sørensen HP, Mortensen KK (2005) Soluble expression of recombinant proteins in the cytoplasm of Escherichia coli. *Microb Cell Fact* 4:1 .

Sousa AC, Martins LO, Robalo MP (2013) Laccase-Catalysed Homocoupling of Primary Aromatic Amines towards the Biosynthesis of Dyes. *Adv Synth Catal* 355:2908–2917 .

Souza Cruz R, Peruch G, Santos Pires AC dos (2012) Oxygen Scavengers: An Approach on Food Preservation. In: Structure and Function of Food Engineering. Chapter 2, pp 21-42.

Sprenger GA, Hammer BA, Johnson EA, Lin ECC (1989) Anaerobic Growth of *Escherichia coli* on Glycerol by Importing Genes of the dha Regulon from *Klebsiella pneumoniae. Microbiology* 135:1255–1262 .

Sprenger GA, Schorken U, Sprenger G, Sahm H (1995) Transketolase-A of *Escherichia Coli K12* - Purification and Properties of the Enzyme from Recombinant Strains. *European Journal of Biochemistry* 230, 525-532.

Sprenger GA, Siewe R, Sahm H, Karutz M and Sonke T (1998) Microbial preparation substances from aromatic metabolism/I US Patent 09/298843[6316232 B1].

Sprenger GA, Pohl M (1999) Synthetic potential of thiamin diphosphate-dependent enzymes. *J Mol Catal B Enzym* 6:145–159 .

Sprenger GA (2007a) Aromatic Amino Acids. In: Amino Acid Biosynthesis ~ Pathways, Regulation and Metabolic Engineering. Springer Berlin Heidelberg, Berlin, Heidelberg, pp 93–127

Sprenger GA (2007b) From scratch to value: engineering *Escherichia coli* wild type cells to the production of l-phenylalanine and other fine chemicals derived from chorismate. *Appl Microbiol Biotechnol* 75:739–749 .

Sprenger GA (2017) Glycerol as Carbon Source for Production of Added-Value Compounds, In: Guillermo Gosset (Eds.), Engineering of Microorganisms for the Production of Chemicals and Biofuels from Renewable Resources. pp 93–123.

Stark D, Zala D, Münch T, Sonnleitner B, Marison IW, von Stockar U (2003) Inhibition aspects of the bioconversion of l-phenylalanine to 2-phenylethanol by *Saccharomyces cerevisiae*. *Enzyme Microb Technol* 32:212–223 .

Stellman MJ (1989) "Aromatic Amino Compounds,. In: Encyclopaedia of Occupational Health and Safety, Edn 4th, e. Genewa: International Labour Office.

Stolz M, Peters-Wendisch P, Etterich H, Gerharz T, Faurie R, Sahm H, Fersterra H, Eggeling L (2007) Reduced Folate Supply as a Key to Enhanced L-Serine Production by Corynebacterium glutamicum. *Appl Environ Microbiol* 73:750–755 .

Straathof AJ., Panke S, Schmid A (2002) The production of fine chemicals by biotransformations. *Curr Opin Biotechnol* 13:548–556 .

Su H, Lin J, Wang G (2016) Metabolic engineering of *Corynebacterium crenatium* for enhancing production of higher alcohols. *Sci Rep* 6:39543 .

Su H, Lu Q, Zhao Y, Jiang J, Zhao Z, Wang M (2014) Preliminary investigation of metabolic engineering in a novel host bacterium Corynebacterium crenatum for alcohol biofuel production. *RSC Adv* 4:65021–65030 .

Suástegui M, Shao Z (2016) Yeast factories for the production of aromatic compounds: from building blocks to plant secondary metabolites. *J Ind Microbiol Biotechnol* 43:1611–1624 .

Sun X, Shen X, Jain R, Lin Y, Wang J, Sun J, Wang J, Yan Y, Yuan Q (2015) Synthesis of chemicals by metabolic engineering of microbes. *Chem Soc Rev* 44:3760–85 .

Sun Z, Ning Y, Liu L, Liu Y, Sun B, Jiang W, Yang C, Yang S (2011) Metabolic engineering of the L-phenylalanine pathway in *Escherichia coli* for the production of S- or R-mandelic acid. *Microb Cell Fact* 10:71 .

Suvannasara P, Tateyama S, Miyasato A, Matsumura K, Shimoda T, Ito T, Yamagata Y, Fujita T, Takaya N, Kaneko T (2014) Biobased Polyimides from 4-Aminocinnamic Acid Photodimer. *Macromolecules* 47:1586–1593 .

Swartz JR (1996) *Escherichia coli* recombinant DNA technology. In: Neidhardt FC, Curtiss R, Lin ECC, Low KB, Magasanik B, Reanikoff WS, Riley M, Schaechter M, Umbarger HE, editors. *Escherichia coli and Salmonella*. Vol. 2. Washington D.C: ASM Press; pp. 1693–1712.

Sysolyatin S V, Kryukov YA, Malykhin V V, Muradov KK, Chernysheva GA, Aliev OI, Smol'yakova VI, Anishchenko AM, Sidekhmenova A V, Shamanaev AY, Plotnikov MB (2015) Tyrosol: a new synthetic method and new types of pharmacological activity. *Russ Chem Bull* 64:2210–2214 .

Szlavko CM (1973) Tryptophol, tyrosol and phenylethanol-the aromatic higher alcohols in beer. *J Inst Brew* 79:283–288 .

Takeda Y, Bui VN, Iwasaki K, Kobayashi T, Ogawa H, Imai K (2014) Influence of olive-derived hydroxytyrosol on the toll-like receptor 4-dependent inflammatory response of mouse peritoneal macrophages. *Biochem Biophys Res Commun* 446:1225–1230 .

Tang CT, Ruch FE, Lin CC (1979) Purification and properties of a nicotinamide adenine dinucleotide-linked dehydrogenase that serves an *Escherichia coli* mutant for glycerol catabolism. *J Bacteriol* 140:182–7

Tang X, Tan Y, Zhu H, Zhao K, Shen W (2009) Microbial conversion of glycerol to 1,3-propanediol by an engineered strain of Escherichia coli. *Appl Environ Microbiol* 75:1628–34 .

Tang Y-J, Zhong J-J (2003) Role of oxygen supply in submerged fermentation of Ganoderma lucidum for production of Ganoderma polysaccharide and ganoderic acid. *Enzyme Microb Technol* 32:478–484

Tao J, Xu J-H (2009) Biocatalysis in development of green pharmaceutical processes. *Curr Opin Chem* Biol 13:43–50 .

Tateyama S, Masuo S, Suvannasara P, Oka Y, Miyazato A, Yasaki K, Teerawatananond T, Muangsin N, Zhou S, Kawasaki Y, Zhu L, Zhou Z, Takaya N, Kaneko T (2016) Ultrastrong, Transparent Polytruxillamides Derived from Microbial Photodimers. *Macromolecules* 49:3336–3342 .

Teng CYP, Ganem B, Doktor SZ, Nichols BP, Bhatnagar RK, Vining LC (1985) Total synthesis of (.+-.)-4-amino-4-deoxychorismic acid: a key intermediate in the biosynthesis of p-aminobenzoic acid and L-p-aminophenylalanine. *J Am Chem Soc* 107:5008–5009 .

Thompson B, Machas M, Nielsen DR (2016) Engineering and comparison of non-natural pathways for microbial phenol production. *Biotechnol Bioeng* 113:1745–1754 .

Thomson JM, Gaucher EA, Burgan MF, De Kee DW, Li T, Aris JP, Benner SA (2005) Resurrecting ancestral alcohol dehydrogenases from yeast. *Nat Genet* 37:630–5 .

Thongchuang M, Pongsawasdi P, Chisti Y, Packdibamrung K (2012) Design of a recombinant *Escherichia coli* for producing l-phenylalanine from glycerol. *World J Microbiol Biotechnol* 28:2937–2943 .

Tong IT and Cameron DC (1992). Enhancement of 1,3-propanediol production by cofermentation in *Escherichia coli* expressing *Klebsiella pneumoniae dha* regulon genes. *Appl Biochem Biotechnol*. 34–35: 149–59.

Tieman D, Taylor M, Schauer N, Fernie AR, Hanson AD, Klee HJ (2006) Tomato aromatic amino acid decarboxylases participate in synthesis of the flavor volatiles 2-phenylethanol and 2-phenylacetaldehyde. *Proc Natl Acad Sci* 103:8287–8292 .

Tribe DE, Camakaris H, Pittard J (1976) Constitutive and repressivle enzymes of the common pathway of aromatic biosynthesis in *Escherichia coli* K-12: regulation of enzyme synthesis at different growth rates. *J Bacteriol* 127:1085–97

Tsimidou M, Papadopoulos G, Boskou D (1992) Determination of phenolic compounds in virgin olive oil by reversed-phase HPLC with emphasis on UV detection. *Food Chem* 44:53–60 .

Tsuge Y, Kawaguchi H, Sasaki K, Kondo A (2016) Engineering cell factories for producing building block chemicals for bio-polymer synthesis. *Microb Cell Fact* 15:19 .

Tsuruta H, Paddon CJ, Eng D, Lenihan JR, Horning T, Anthony LC, Regentin R, Keasling JD, Renninger NS, Newman JD (2009) High-Level Production of Amorpha-4,11-Diene, a Precursor of the Antimalarial Agent Artemisinin, in *Escherichia coli*. *PLoS One* 4:e4489 .

Unden G, Bongaerts J (1997) Alternative respiratory pathways of Escherichia coli: energetics and transcriptional regulation in response to electron acceptors. *Biochim Biophys Acta - Bioenerg* 1320:217–234 .

Van Den Hazel, Bart H, Kielland-Brandt MC, Winther JR (1992) Autoactivation of proteinase A initiates activation of yeast vacuolar zymogens. *Eur J Biochem* 207:277–283

Vargas-Tah A, Martínez LM, Hernández-Chávez G, Rocha M, Martínez A, Bolívar F, Gosset G (2015) Production of cinnamic and p-hydroxycinnamic acid from sugar mixtures with engineered Escherichia coli. *Microb Cell Fact* 14:6 .

Varma A, Palsson BO (1994) Stoichiometric flux balance models quantitatively predict growth and metabolic by-product secretion in wild-type *Escherichia coli W3110*. *Appl Environ Microbiol* 60:3724–31

Vasala A, Panula J, Bollók M, Illmann L, Hälsig C, Neubauer P (2006) A new wireless system for decentralised measurement of physiological parameters from shake flasks. *Microb Cell Fact* 5:8 .

Vicente B, Castaño-Cerezo S, Cánovas M (2016) Acetate metabolism regulation in *Escherichia coli*: carbon overflow, pathogenicity, and beyond. *Artic Appl Microbiol Biotechnol*. 100(21):8985-9001.

Viswanathan VK, Green JM, Nichols BP (1995) Kinetic characterization of 4-amino 4-deoxychorismate synthase from Escherichia coli. *J Bacteriol* 177:5918–23

Vuralhan Z, Luttik MAH, Tai SL, Boer VM, Morais MA, Schipper D, Almering MJH, Kotter P, Dickinson JR, Daran J-M, Pronk JT (2005) Physiological Characterization of the ARO10-Dependent, Broad-Substrate-Specificity 2-Oxo Acid Decarboxylase Activity of *Saccharomyces cerevisiae*. *Appl Environ Microbiol* 71:3276–3284 .

Vuralhan Z, Morais MA, Tai S-L, Piper MDW, Pronk JT (2003) Identification and characterization of phenylpyruvate decarboxylase genes in *Saccharomyces cerevisiae*. *Appl Environ Microbiol* 69:4534–41

Wada K, Toya Y, Banno S, Yoshikawa K, Matsuda F, Shimizu H (2017) 13C-metabolic flux analysis for mevalonate-producing strain of Escherichia coli. *J Biosci Bioeng* 123:177–182 .

Walsh CT, Erion MD, Walts AE, Delany JJ, Berchtold GA (1987) Chorismate aminations: partial purification of *Escherichia coli* PABA synthase and mechanistic comparison with anthranilate synthase. *Biochemistry* 26:4734–45

Wang C.T, Sun B.G, Cao Y.P, Wang J ZH (2008) Biosynthesis of natural 2-phenylethanol by yeast cells. *Mod Chem Ind* 28:38–43

Wang CH, Stern I, Gilmour CM, Klungsoyr S, Reed DJ, Bialy JJ, christensen be, cheldelin VH (1958) Comparative study of glucose catabolism by the radiorespirometric method. *J Bacteriol* 76:207–16

Wang J, Cheng L-K, Wang J, Liu Q, Shen T, Chen N (2013) Genetic engineering of *Escherichia coli* to enhance production of l-tryptophan. *Appl Microbiol Biotechnol* 97:7587–7596 .

Wang J, Xiong Z, Zhang S, Wang Y (2014) Engineering MEP pathway in *Escherichia coli* for amorphadiene production and optimizing the bioprocess through glucose feeding control. *Sheng Wu Gong Cheng Xue Bao* 30:64–75

Wang S, Zhang S, Xiao A, Rasmussen M, Skidmore C, Zhan J (2015) Metabolic engineering of *Escherichia coli* for the biosynthesis of various phenylpropanoid derivatives. *Metab Eng* 29:153–159 .

Wang X, Mann CJ, Bai Y, Ni L, Weiner H (1998) Molecular cloning, characterization, and potential roles of cytosolic and mitochondrial aldehyde dehydrogenases in ethanol metabolism in *Saccharomyces cerevisiae*. *J Bacteriol* 180:822–30

Wang Z-J, Wang H-Y, Li Y-L, Chu J, Huang M-Z, Zhuang Y-P, Zhang S-L (2010) Improved vitamin B12 production by step-wise reduction of oxygen uptake rate under dissolved oxygen limiting level during fermentation process. *Bioresour Technol* 101:2845–2852 .

Webb AD, Ingraham JL (1963) Fusel Oil. *Adv Appl Microbiol* 5:317–353 .

Weber J, Leung J, Swanson S, Idler K, McAlpine J (1991) An erythromycin derivative produced by targeted gene disruption in Saccharopolyspora erythraea. *Science* (80-) 252:114–117 .

Weiner JH, Heppel LA (1972) Purification of the membrane-bound and pyridine nucleotide-independent L-glycerol 3-phosphate dehydrogenase from *Escherichia coli*. *Biochem Biophys Res Commun* 47:1360–1365 .

Weiner M, Albermann C, Gottlieb K, Sprenger GA, Weuster-Botz D (2014) Fed-batch production of l-phenylalanine from glycerol and ammonia with recombinant *Escherichia coli. Biochem Eng J* 83:62–69 .

Weiner M, Tröndle J, Albermann C, Sprenger GA, Weuster-Botz D (2015) Perturbation Experiments: Approaches for Metabolic Pathway Analysis in Bioreactors. Springer, Berlin, Heidelberg, pp 91–136

Whipp MJ, Pittard AJ (1977) Regulation of Aromatic Amino Acid Transport Systems in *Escherichia coli* K-12. *J Bacteriol* 132:453–461

White WH, Skatrud PL, Xue Z, Toyn JH (2003) Specialization of function among aldehyde dehydrogenases: the ALD2 and ALD3 genes are required for beta-alanine biosynthesis in *Saccharomyces cerevisiae*. *Genetics* 163:69–77

Winkler K, Socher ML (2014) Shake Flask Technology. In: Encyclopedia of Industrial Biotechnology. John Wiley & Sons, Inc., Hoboken, NJ, USA, pp 1–16

Wittmann C, Hans M, Bluemke W (2002) Metabolic physiology of aroma-producingKluyveromyces marxianus. *Yeast* 19:1351–1363 .

Witze A (2013) Light in the dark: Factory of life: Synthetic biologists reinvent nature with parts, circuits. *Sci. News* 183, 22–28.

Woodruff LBA, May BL, Warner JR, Gill RT (2013) Towards a metabolic engineering strain "commons": An *Escherichia coli* platform strain for ethanol production. *Biotechnol Bioeng* 110:1520–1526 .

Wubbolts MG, Bongaerts JJ, Bovenberg RAL, Kozak S, Sprenger G, Müller M. Biosynthetic production of 4-amino-4-deoxychorismate (ADC) and [3R,4R]-amino-3-hydroxycyclohexa-1,5-diene-1-carboxylic acid (3,4-CHA). European patent application EP 1602730A2 (2005).

Wookey PJ, Pittard AJ (1988) DNA sequence of the gene (tyrP) encoding the tyrosine-specific transport system of Escherichia coli. *J Bacteriol* 170:4946–9.

Wright F, Bibb MJ (1992) Codon usage in the G+C-rich *Streptomyces* genome. *Gene* 113:55–65 .

Xu H, Dou W, Xu H, Zhang X, Rao Z, Shi Z, Xu Z (2009) A two-stage oxygen supply strategy for enhanced l-arginine production by *Corynebacterium crenatum* based on metabolic fluxes analysis. *Biochem Eng J* 43:41–51.

Xu P, Hua D, Ma C (2007) Microbial transformation of propenylbenzenes for natural flavour production. *Trends Biotechnol* 25:571–576

Xu Z, Wang S, Wang L, Fang Z, Wang X (2008) Preparation and Pyroelectric Properties of Poly(pentafluorostyrene)-r-Poly(4-vinylaniline) Copolymer Films. *Macromol Symp* 261:144–147 .

Xue Y, Chen X, Yang C, Chang J, Shen W, Fan Y (2017) Engineering *Eschericha coli* for Enhanced Tyrosol Production. *J Agric Food Chem* 65:4708–4714 .

Yadav SK, Cho JW (2013) Functionalized graphene nanoplatelets for enhanced mechanical and thermal properties of polyurethane nanocomposites. *Appl Surf Sci* 266:360–367 .

Yakandawala N, Romeo T, Friesen AD, Madhyastha S (2008) Metabolic engineering of *Escherichia coli* to enhance phenylalanine production. *Appl Microbiol Biotechnol* 78:283–291 .

Yamaguchi M, Saito R, Utsumi K, Ochiai A, Kawashima N, Tokuoka Y, Katoh A (2007) The nicotinic acid-p-aminophenylalanine-hydroxybenzoic acid triads induce apoptosis in human leukemia U937 cells. *Heterocycles* 71:1503–1508

Yamanè T, Shimizu S (1984) Fed-batch techniques in microbial processes. In: Bioprocess Parameter Control. Springer-Verlag, Berlin/Heidelberg, pp 147–194.

Yanai K, Sumida N, Okakura K, Moriya T, Watanabe M, Murakami T (2004) Para-position derivatives of fungal anthelmintic cyclodepsipeptides engineered with *Streptomyces venezuelae* antibiotic biosynthetic genes. *Nat Biotechnol* 22:848–855 .

Yang F, Hanna MA, Sun R (2012) Value-added uses for crude glycerol--a byproduct of biodiesel production. *Biotechnol Biofuels* 5:13 .

Yao YF, Wang CS, Qiao J, Zhao GR (2013) Metabolic engineering of *Escherichia coli* for production of salvianic acid A via an artificial biosynthetic pathway. *Metab Eng* 19:79–87 .

Yazdani SS, Gonzalez R (2007) Anaerobic fermentation of glycerol: a path to economic viability for the biofuels industry. *Curr Opin Biotechnol* 18:213–219 .

Ye Q-Z, Liu J, Walsh CT (1990) p-Aminobenzoate synthesis in Escherichia coli: Purification and characterization of PabB as aminodeoxychorismate synthase and enzyme X as aminodeoxychorismate Iyase. *Biochemistry* 87:9391–9395

Yeh BJ, Lim WA (2007) Synthetic biology: lessons from the history of synthetic organic chemistry. *Nat Chem Biol* 3:521–525 .

Yep A, Kenyon GL, McLeish MJ (2008) Saturation mutagenesis of putative catalytic residues of benzoylformate decarboxylase provides a challenge to the accepted mechanism. *Proc Natl Acad Sci* 105:5733–5738 .

Yep A, Kenyon GL, McLeish MJ (2006) Determinants of substrate specificity in KdcA, a thiamin diphosphate-dependent decarboxylase. *Bioorg Chem* 34:325–336 .

Yi J, Li K, Draths KM, Frost JW (2002) Modulation of Phosphoenolpyruvate Synthase Expression Increases Shikimate Pathway Product Yields in E. coli. *Biotechnol Prog* 18:1141–1148 .

Yim H, Haselbeck R, Niu W, Pujol-Baxley C, Burgard A, Boldt J, Khandurina J, Trawick JD, Osterhout RE, Stephen R, Estadilla J, Teisan S, Schreyer HB, Andrae S, Yang TH, Lee SY, Burk MJ, Van Dien S (2011) Metabolic engineering of *Escherichia coli* for direct production of 1,4-butanediol. *Nat Chem Biol* 7:445–452 .

Yin S, Zhou H, Xiao X, Lang T, Liang J, Wang C (2015) Improving 2-Phenylethanol Production via Ehrlich Pathway Using Genetic Engineered *Saccharomyces cerevisiae* Strains. *Curr Microbiol* 70:762–767 .

Yoo S (1982) Antihypertensive polyhalohydroxyisopropyl phenylalka(e)noic acid esters of alkylaminohydroxypropyloxyphenylalkyl alcohols. US Pat. 4727180.

Zhang H, Cao M, Jiang X, Zou H, Wang C, Xu X, Xian M (2014) De-novo synthesis of 2-phenylethanol by Enterobacter sp. CGMCC 5087. *BMC Biotechnol* 14:30 .

Zhang L, Liu Q, Pan H, Li X, Guo D (2017) Metabolic engineering of *Escherichia coli* to high efficient synthesis phenylacetic acid from phenylalanine. *AMB Express* 7:105 .

Zhao Z-J, Zou C, Zhu Y-X, Dai J, Chen S, Wu D, Wu J, Chen J (2011) Development of l-tryptophan production strains by defined genetic modification in *Escherichia coli. J Ind Microbiol Biotechnol* 38:1921–1929 .

Zhou L, Ding Q, Jiang G, Liu Z, Wang H, Zhao G (2017) Chromosome engineering of *Escherichia coli* for constitutive production of salvianic acid A. *Microb Cell Fact* 16:1.

Zhu J, Shimizu K (2005) Effect of a single-gene knockout on the metabolic regulation in *Escherichia coli* for D-lactate production under microaerobic condition. *Metab Eng* 7:104–115 .

Zwaig N, Kistler WS, Lin EC (1970) Glycerol kinase, the pacemaker for the dissimilation of glycerol in Escherichia coli. *J Bacteriol* 102:753–9